PAGES 831–932

ISSN 0003–2654

The Analyst

A monthly international journal dealing with all branches of the theory and practice of analytical chemistry, including instrumentation and sensors, and physical, biochemical, clinical, pharmaceutical, biological, environmental, automatic and computer-based metho

Vol.117 No.5 May 1992

The Analyst

The Analytical Journal of The Royal Society of Chemistry

Editorial Manager, Analytical Journals: Judith Egan

Editor, *The Analyst*
Harpal S. Minhas
The Royal Society of Chemistry,
Thomas Graham House, Science Park,
Milton Road, Cambridge CB4 4WF, UK
Telephone 0223 420066.
Fax 0223 423623. Telex No. 818293 ROYAL.

US Associate Editor, *The Analyst*
Dr J. F. Tyson
Department of Chemistry,
University of Massachusetts,
Amherst MA 01003, USA
Telephone 413 545 0195
Fax 413 545 4490

Senior Assistant Editor
Paul Delaney

Assistant Editors
Brenda Holliday, Paula O'Riordan, Sheryl Whitewood

Editorial Secretary: Claire Harris

Advertisements: Advertisement Department, The Royal Society of Chemistry, Burlington House, Piccadilly, London, W1V 0BN. Telephone 071-437 8656. Telex No. 268001. Fax 071-437 8883.

The Analyst (ISSN 0003–2654) is published monthly by The Royal Society of Chemistry, Thomas Graham House, Science Park, Milton Road, Cambridge CB4 4WF, UK. All orders, accompanied with payment by cheque in sterling, payable on a UK clearing bank or in US dollars payable on a US clearing bank, should be sent directly to The Royal Society of Chemistry, Turpin Distribution Services Ltd., Blackhorse Road, Letchworth, Herts SG6 1HN, United Kingdom. Turpin Distribution Services Ltd., is wholly owned by the Royal Society of Chemistry. 1992 Annual subscription rate EC £276.00, USA $589, Rest of World £310.00. Purchased with *Analytical Abstracts* EC £604.00, USA $1299.00, Rest of World £669.00. Purchased with *Analytical Abstracts* plus *Analytical Proceedings* EC £712.00, USA $1527.00, Rest of World £791.00. Purchased with *Analytical Proceedings* EC £351.00, USA $749.00, Rest of World £395.00. Air freight and mailing in the USA by Publications Expediting Inc., 200 Meacham Avenue, Elmont, NY 11003.

USA Postmaster: Send address changes to: *The Analyst,* Publications Expediting Inc., 200 Meacham Avenue, Elmont, NY 11003. Second class postage paid at Jamaica, NY 11431. All other despatches outside the UK by Bulk Airmail within Europe, Accelerated Surface Post outside Europe. PRINTED IN THE UK.

Information for Authors

Full details of how to submit material for publication in *The Analyst* are given in the Instructions to Authors in the January issue. Separate copies are available on request.

The Analyst publishes papers on all aspects of the theory and practice of analytical chemistry, fundamental and applied, inorganic and organic, including chemical, physical, biochemical, clinical, pharmaceutical, biological, environmental, automatic and computer-based methods. Papers on new approaches to existing methods, new techniques and instrumentation, detectors and sensors, and new areas of application with due attention to overcoming limitations and to underlying principles are all equally welcome. There is no page charge.

The following types of papers will be considered:

Full research papers.

Communications, which must be on an urgent matter and be of obvious scientific importance. Rapidity of publication is enhanced if diagrams are omitted, but tables and formulae can be included. Communications receive priority and are usually published within 5–8 weeks of receipt. They are intended for brief descriptions of work that has progressed to a stage at which it is likely to be valuable to workers faced with similar problems. A fuller paper may be offered subsequently, if justified by later work. Although publication is at the discretion of the Editor, communications will be examined by at least one referee.

Reviews, which must be a critical evaluation of the existing state of knowledge on a particular facet of analytical chemistry.

Every paper (except Communications) will be submitted to at least two referees, by whose advice the Editorial Board of *The Analyst* will be guided as to its acceptance or rejection. Papers that are accepted must not be published elsewhere except by permission. Submission of a manuscript will be regarded as an undertaking that the same material is not being considered for publication by another journal.

Regional Advisory Editors. For the benefit of potential contributors outside the United Kingdom and North America, a Group of Regional Advisory Editors exists. Requests for help or advice on any matter related to the preparation of papers and their submission for publication in *The Analyst* can be sent to the nearest member of the Group. Currently serving Regional Advisory Editors are listed in each issue of *The Analyst.*

Manuscripts (four copies typed in double spacing) should be addressed to:

Harpal S. Minhas, Editor, *The Analyst,*
Royal Society of Chemistry,
Thomas Graham House,
Science Park, Milton Road,
CAMBRIDGE CB4 4WF, UK *or*:

Dr. J. F. Tyson
US Associate Editor, *The Analyst*
Department of Chemistry
University of Massachusetts
Amherst MA 01003, USA

Particular attention should be paid to the use of standard methods of literature citation, including the journal abbreviations defined in Chemical Abstracts Service Source Index. Wherever possible, the nomenclature employed should follow IUPAC recommendations, and units and symbols should be those associated with SI.

All queries relating to the presentation and submission of papers, and any correspondence regarding accepted papers and proofs, should be directed either to the Editor, or Associate Editor, *The Analyst* (addresses as above). Members of the Analytical Editorial Board (who may be contacted directly or via the Editorial Office) would welcome comments, suggestions and advice on general policy matters concerning *The Analyst.*

Fifty reprints are supplied free of charge.

Solute–Mobile Phase and Solute–Stationary Phase Interactions in Micellar Liquid Chromatography

A Review

María José Medina Hernández and María Celia García Alvarez-Coque*
Departamento de Química Analítica, Facultad de Química, Universidad de Valencia, 46100 Burjassot, Valencia, Spain

Summary of Contents

Keywords: *Review; reversed-phase liquid chromatography; micellar eluents; solute interactions; solvent strength; efficiency*

Introduction

Micellar liquid chromatography (MLC) with normal micelles is an alternative to conventional reversed-phase liquid chromatography (RP-LC), which uses a surfactant solution above the critical micellization concentration (c.m.c.) as the mobile phase, instead of hydro-organic mixtures.[1–4]

Micelles are not static, but exist in equilibrium with surfactant monomers above the c.m.c. Adsorption of these monomers on alkyl-bonded stationary phases (*e.g.*, C_1, C_8 and C_{18}) could occur in at least two ways:[5] (*a*) hydrophobic adsorption, where the alkyl tail of the surfactant would be adsorbed and the ionic head group would then be in contact with the polar solution, giving the stationary phase some ion-exchange capacity with charged solutes; and (*b*) sylanophilic adsorption, where the ionic head group of the surfactant would be adsorbed, the stationary phase becoming more hydrophobic. For most surfactants and stationary phases, the amount of surfactant adsorbed on the stationary phase remains constant after equilibration once the concentration of surfactant is above the c.m.c.[6,7]

The complexity of MLC is much greater than conventional RP-LC with hydro-organic solvents, owing to the large number of possible interactions (electrostatic, hydrophobic and steric) with the micellar mobile phase and with the modified stationary phase (Fig. 1). None of these interactions can occur for a hydro-organic system.[8]

Almost any compound can be determined by MLC. The separation of inorganic anions[9] and of dithiocarbamates[10,11] with a micellar mobile phase of hexadecyltrimethylammonium chloride (CTAC) and bromide (CTAB), respectively, has been reported. Complete resolution of the *cis* and *trans* isomers of anionic cobalt(III)–iminodiacetate was achieved with CTAB, and neutral 4,4′-ethylenedinitrilobispentan-2-one complexes of copper(II) and nickel(II) were separated with a sodium dodecyl sulfate (SDS) micellar mobile phase.[12]

A concentrated micellar solution of Brij 35 has been used to extract aldehydes from tobacco samples, which were separated chromatographically with a more dilute solution of the same surfactant.[13] The activity of folylpolyglutamate hydrolase in crude tissue extracts was determined after denaturation of the enzyme in SDS, which subsequently served as the micellar solvent system for the chromatographic separation of substrate from reaction products.[14] Excellent correlations have been found between capacity factors with a tetradecyltrimethylammonium bromide mobile phase and the bioactivity of 26 *para*-substituted phenols,[15] and between capacity factors with a 0.03 mol dm^{-3} SDS mobile phase and the site of action of diuretics along the nephron.[16]

One of the most interesting applications of MLC is the possibility of determining drugs in biological fluids without previous separation of proteins.[17–26] Micellar solutions of SDS or Brij-35 solubilize the proteins in the biological sample and cause them to be eluted at the front of the chromatogram (Fig. 2).

Partition Behaviour

Armstrong and Nome[27] proposed a three-phase model (stationary phase, and bulk aqueous and micellar pseudo-phases) to explain the chromatographic behaviour of a solute eluted with an aqueous micellar mobile phase containing a surfactant. The solutes partition not only between water and the stationary phase, but also inside the mobile phase, between water and the micelle. Hence, elution of a solute in MLC depends on three partition coefficients: that between the stationary phase and water (P_{SW}), between the stationary phase and the micelle (P_{SM}), and between the micelle and water (P_{MW}).

First, Armstrong and Nome,[27] and later Arunyanart and Cline Love,[28] proposed different models to describe the change in retention of solutes at various micelle concentrations. The equations can be rewritten as:

$$\frac{1}{k'} = \frac{K_{AM}}{\Phi P_{SW}}[M] + \frac{1}{\Phi P_{SW}} \quad (1)$$

* To whom correspondence should be addressed.

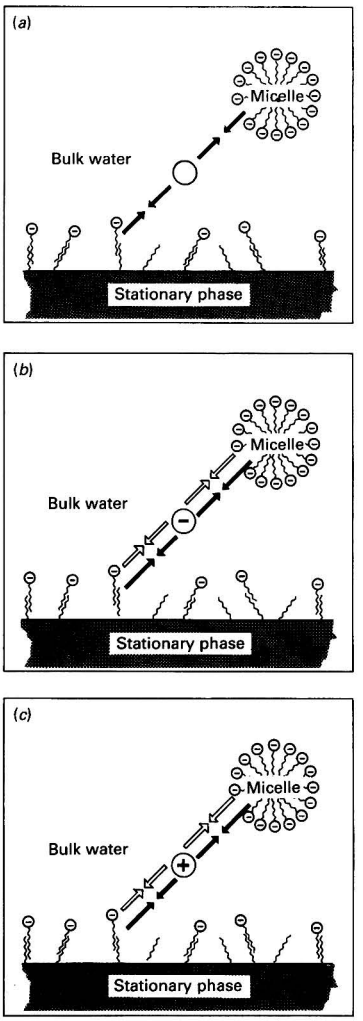

Fig. 1 Solute–micelle and solute–stationary phase hydrophobic (⟶) and electrostatic interactions (⟿) with an anionic surfactant: (*a*) apolar solute; (*b*) anionic solute; and (*c*) cationic solute

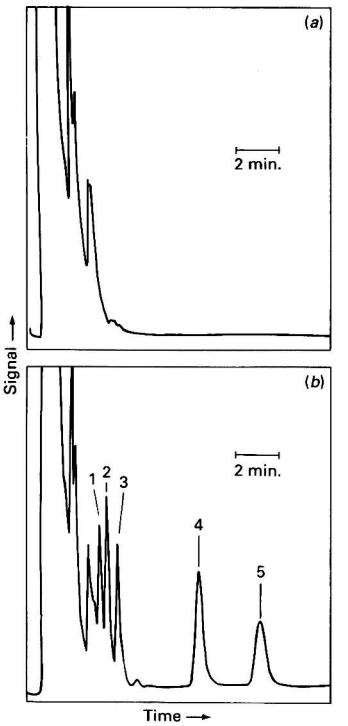

Fig. 2 (*a*) Chromatogram of urine. (*b*) Chromatogram of urine spiked with: 1, 30 μg ml^{-1} of amiloride; 2, 5 μg ml^{-1} of spironolactone; 3, 1.2 μg ml^{-1} of metandienone; 4, 56 μg ml^{-1} of amino(phenyl)-propanol; and 5, 30 μg ml^{-1} of clostebol. Mobile phase, 0.1 mol dm^{-3} SDS solution with 3% pentan-1-ol; column temperature, 60 °C; flow rate, 1 ml min^{-1}; UV detection, 260 nm. Reprinted, with permission, from ref. 26

where k' is the capacity factor, [M] is the total concentration of surfactant in the mobile phase minus the c.m.c., Φ is the ratio of the volume of the stationary phase, V_S, to the volume of the mobile phase, V_M, in the column, and K_{AM} is the solute–micelle binding constant. By plotting $1/k'$ *versus* [M] one should obtain a straight line. The values of P_{SW} and K_{AM} are given by the slope and intercept of the plot, respectively.

The calculation of P_{SW} requires knowledge of V_S, which cannot easily be determined. Usually, the difference between the empty column volume and the packed column void volume is taken as V_S. This difference gives an overestimation of V_S because it includes the entire volume occupied by the silica solid support particles rather than just the true stationary phase. The use of such a V_S value can be expected to result in a P_{SW} coefficient that is significantly in error. An approach that completely excludes any volume associated with the base silica material should be used.[29]

Eqn. (1) can be used to describe the retention of apolar, polar, and even ionic solutes, chromatographed with anionic, cationic and non-ionic surfactants.[8,13] For high relative molecular mass solutes, intercepts are nearly zero in the $1/k'$ *versus* [M] plot. A zero intercept requires either that the reciprocal of the phase ratio must be zero, which is not physically possible, or that P_{SW} is extremely large. This is not only physically possible but also consistent with solubility data for compounds that show this behaviour (*e.g.*, alkylbenzene homologues beyond butylbenzene are insoluble in water). The direct transfer of these compounds from the micellar pseudo-phase to the surfactant-modified stationary phase, *via* reversible sorption of the solute-occupied micelle onto the 'hemimicellar' surfactant-modified stationary phase, has been suggested.[29]

Electrostatic and Hydrophobic Interactions

The non-homogeneous nature of micelles creates a unique situation in which different solutes can experience various micro-environment polarities in a given mobile phase. Retention of a solute will depend on the type of interaction with the micelle and the surfactant-modified stationary phase. Non-polar solutes, such as benzene and toluene, should only be affected by hydrophobic interactions [Fig. 1(*a*)], but for solutes that are charged, two distinct situations can be considered: (*i*) the charge on the solute and surfactant has the same sign [Fig. 1(*b*)]; or (*ii*) the charge on the solute and surfactant has the opposite sign [Fig. 1(*c*)].[30]

The first situation is encountered when an anionic solute is chromatographed with an anionic surfactant or a cationic solute with a cationic surfactant [*e.g.*, dissociated phenol and 2-naphthol with SDS, and protonated benzylamine with dodecyltrimethylammonium bromide (DTAB) on a C_{18} column].[31] Electrostatic repulsion from the micelle should not

affect retention as the solute would still reside in the bulk mobile phase and, therefore, still move down the column. In contrast, repulsion from the surfactant-modified stationary phase should cause a decrease in retention. Solutes may be eluted in the void volume. However, they may also be retained if hydrophobic interaction with the stationary phase exists. Because of the different hydrophobic interaction, dissociated phenol and 2-naphthol are well separated with SDS.

The second situation appears when a solute is chromatographed with an oppositely charged surfactant, where electrostatic attraction occurs between both species. If the electrostatic attraction with the micelle is complemented by a hydrophobic interaction, the solutes will remain in the mobile phase for a longer period of time, and retention will decrease. However, electrostatic and hydrophobic interactions with the stationary phase may be sufficiently large to offset the increase in micellar attraction and would increase retention. Dissociated phenol and 2-naphthol are retained to a greater extent with DTAB than with SDS on a C_{18} column.[31]

With an appropriate surfactant, mixtures of polar and apolar solutes can be resolved adequately.[32] For example, dissociated phenol and benzene are not well resolved with DTAB, but are completely resolved with SDS. In contrast, *p*-nitrophenol and *p*-nitroaniline are not separated with SDS, but are well resolved with DTAB.[31]

Binding, Non-binding and Antibinding Solutes

The function of the micellar pseudo-phase in MLC has been compared with that of the organic modifier in traditional RP-LC, as for many solutes, an increase in the concentration of surfactant in the mobile phase results in a decrease in the retention of the solutes being separated. However, the eluent strength increases with micelle concentration only if the solute interacts with the micelle in the mobile phase.

Armstrong and Stine[33] proposed a classification of the solutes into three groups according to their chromatographic properties with a micellar mobile phase: (*i*) solutes binding to micelles; (*ii*) non-binding solutes; and (*iii*) antibinding solutes. Compounds that associate or bind to micelles show decreased retention when the concentration of micelles in the mobile phase is increased ($K_{AM} > 0$).[34] For compounds that do not associate with micelles, retention can remain unaltered by the micelle content of the mobile phase (non-binding, $K_{AM} = 0$) or their retention can increase with increasing micelle concentration (antibinding, $K_{AM} < 0$). Antibinding results from a compound being strongly excluded or repelled from the micelle.

High positive values of K_{AM} have been observed with solutes showing electrostatic interactions (*e.g.*, benzyltrimethylammonium bromide with SDS micelles, and benzoic acid with CTAB micelles), or with co-micellization [*e.g.*, sodium octylbenzenesulfonate with SDS, and cetylpyridinium chloride (CPC) with CTAB].[8] The similar K_{AM} values for CPC and benzoic acid in CTAB micellar phases explain the similar retention observed for both solutes; however, the location of the solute in the micelle is very different: benzoic acid is bound onto the micelle surface, in the Stern layer, whereas CPC occupies the same site as a CTAB molecule in the micelle, the alkyl tail being in the micellar core and the polar head in the Stern layer.

Negative K_{AM} values apparently have no meaning. However, just as compounds that bind to micelles each have a characteristic positive constant, compounds that are excluded from the micelle may have a characteristic negative constant.[33] Most non-binding compounds with anionic micelles are negatively charged and with cationic micelles are positively charged. It is apparent that electrostatic repulsion is an important factor in antibinding behaviour. However, there are also many positively charged compounds that bind to cationic micelles in addition to negatively charged compounds that bind to anionic micelles. It is, therefore, sometimes difficult to predict the exact retention behaviour of an organic ion. Antibinding has never been observed between a charged solute and an oppositely charged micelle.[33]

These effects cannot be observed by using stationary phases that adsorb an appreciable amount of surfactant, *i.e.*, C_8- or C_{18}-bonded phases.[33] For these phases, when the stationary phase acquires the same charge as the micelle, and no hydrophobic interaction occurs, similarly charged solutes tend to elute in the void volume of the column. When using a C_1 or preferably a cyano-bonded phase, however, one can observe increased retention when eluting.

The antibinding phenomenon is useful in MLC because it produces unusual selectivities.[35] On a cyano column and with SDS in the mobile phase, neutral phenol behaves as a binding compound, whereas the anionic naphthalene-2-sulfonate behaves as an antibinding compound because electrostatic repulsion is stronger than hydrophobic interaction. In contrast, for pyrene-1-sulfonate, with a binding behaviour, the larger pyrene moiety should produce a counterbalancing of the electrostatic repulsion and associate more strongly with the micelle. By using a C_{18} column, where negatively charged surfactant monomers are adsorbed, the elution behaviour of phenol and pyrene-1-sulfonate, where hydrophobic effects would dominate, is very similar to that obtained using cyano columns. The less hydrophobic and negatively charged naphthalene-2-sulfonate elutes very rapidly because of repulsion from both the micelle and the negatively charged modified stationary phase.

Influence of pH

Retention of weak organic acids and bases is affected by the pH of the micellar mobile phase. Solute–micelle partition coefficients of the dissociated and undissociated forms are different. Small changes in pH can significantly alter chromatographic retention, particularly when the mobile phase pH is close to the pK_a value.[23,25,36] Therefore, the pH of the micellar mobile phase must be specified when retention data are reported. With anionic or cationic surfactants in the mobile phase, retention can be modified appropriately by working at a pH value where some compounds are ionized.

Cyano-bonded and C_{18} columns interact very differently with surfactant monomers, resulting in a different elution behaviour of organic acids and bases as a function of the micelle concentration in the mobile phase and pH.[35] Ionizable compounds on a cyano packing show a different behaviour depending on pH, that is, the slope of the $1/k'$ *versus* [M] plot can be positive, negative or zero. Hence, for benzoic acid, at $pH \ll 4$, k' values decrease, and at $pH \gg 4$, k' values increase with increasing SDS concentration. In the intermediate range of pH values, there is an isoeluting point where k' is completely independent of SDS concentration. This is the pH value at which two species, acid and base, in equilibrium with each other, have the same k' value. This is analogous to the isosbestic point in spectroscopy and would be expected to give the acid dissociation constant in the micellar medium.

For weak acids, such as Bromocresol Green, using a C_{18} column and increasing SDS concentration in the mobile phase, k' values decrease in acidic solution where the neutral form is present and remain constant in more basic solution where the anionic acid form is present, electrostatically repulsed by both the negative micelle and stationary phase.[35]

The elution behaviour *versus* pH of protonated bases on C_{18} columns will be the opposite of that observed on cyano columns. Adsorption of anionic surfactant monomers on the surface of the C_{18} stationary phase causes protonated organic bases, such as aniline, to be retained for a longer period of time than the neutral free-base form because of electrostatic attraction. In contrast, for weak bases using cyano columns, it

is found that the largest k' values occur in more basic solution where the neutral, free-base form is present and are smallest in acidic solution where the protonated positively charged form exists, which has favourable electrostatic attraction to the negatively charged micelles.[35]

Dependence of k' on pH at a constant value of [M] is sigmoidal if there is no electrostatic repulsion between any of the two acid–base forms and surfactant molecules.[35] For example, for 6-thioguanine, a plot of k' *versus* pH at various concentrations of SDS on a C_{18} column reveals that the largest k' values occur in acidic solution, where the protonated form of the drug is present, and the smallest values occur in more alkaline solutions, where its neutral form is present. The observed increase in retention could be ascribed to the fact that electrostatic attractions of the solute with the surface of the surfactant-modified stationary phase are stronger than those with the micelles.[22]

Ionic Strength

If antibinding is chiefly an electrostatic phenomenon, one would expect to see definite salt effects on the magnitude of K_{AM}. The solute is not only excluded from the micelle but also from the double layer around the micelle. The thickness of the electrical double layer decreases with increasing ionic strength, thus allowing hydrophobic interaction of the solute with the micelle.[37]

Modification of ionic strength might be sufficient to change completely from an antibinding to a binding type behaviour. In the absence of salt, Bromophenol Blue is an antibinding compound, whereas in the presence of as little as 0.02 mol dm^{-3} NaCl, it appears to be non-binding. At slightly higher salt concentrations, the compound binds strongly to SDS micelles. The binding to SDS micelles increases substantially with the concentration of NaCl.[37]

For most antibinding solutes the value of K_{AM} becomes less negative with increasing ionic strength, although not all compounds show this type of behaviour. For example, the interaction of Naphthol Green B with SDS micelles appears to be largely unaffected by the addition of salt. Conversely, K_{AM} for thiocyanate ion becomes even more negative with increasing NaCl concentration.[37]

In order for the transition from antibinding to non-binding to binding to occur, the solute ion must have sufficient hydrophobic character to associate with the non-polar portion of the micelle, once electrostatic repulsions have been minimized. The behaviour of thiocyanate is difficult to explain in terms of electrostatic criteria. However, it may be possible to rationalize such behaviour by considering the negligible hydrophobic character of this ion.

Selectivity With Purely Micellar Eluents

A study of the chromatographic behaviour of a homologous series of compounds provides important information that can be used to distinguish retention and selectivity between conventional RP-LC and MLC.[38] With hydro-organic mobile phases the logarithm of k' is linearly related to the number of carbons, n_C, in a homologous series in the following form:[39]

$$\log k' = \log \alpha(CH_2)\, n_C + \log \beta \qquad (2)$$

where $\alpha(CH_2) = k'_{n+1}/k'_n$ is the hydrophobic or methylene selectivity, that is, the ratio of the retention factors of two solutes that differ from each other by a methylene group, and $\log \beta$ reflects the specific interactions between the functional group of the molecule and the mobile and stationary phases.

The retention behaviour of a homologous series in MLC is, however, very different and k' is linearly dependent on n_C:[40]

$$k' = Bn_C + A \qquad (3)$$

where A and B are the intercept and slope, respectively, of the straight line. A plot of $\log k'$ *versus* n_C for these systems has a clear curvature (Fig. 3). This is probably due to different solute locations in the micelles for different members of a homologous series, which will experience different polarities. This behaviour has been observed with non-ionic, anionic and cationic surfactants.[29]

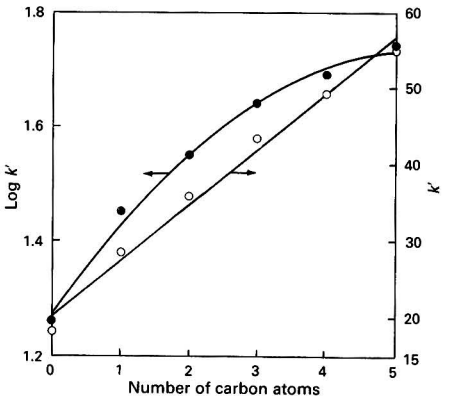

Fig. 3 Log k' and k' *versus* number of carbons for alkylbenzenes with a 0.072 mol dm^{-3} CTAB micellar mobile phase[38]

For hydro-organic mobile phases, $\alpha(CH_2)$ is independent of the type of homologous series for a given mobile and stationary phase system. In contrast, with micelles the $\alpha(CH_2)$ values for alkylphenones are larger than those observed for alkylbenzenes. A methylene group of an alkylphenone undergoes a larger change in its microenvironment polarity as it is transferred from micellar eluents to the stationary phase.[38]

In conventional RP-LC systems, $\alpha(CH_2)$ decreases with an increase in modifier concentration in the aqueous mobile phase. For a purely aqueous mobile phase, $\alpha(CH_2) \approx 4$ and for 100% methanol it is about 1.1–1.2. With micellar eluents, the over-all $\alpha(CH_2)$ values are much smaller and the variation with micelle concentration is fairly small. Typical selectivities for alkylphenones range from 1.6 to 1.1 for SDS concentrations between 0.06 and 0.5 mol dm^{-3}. The net free energy of transfer of a methylene group from the mobile phase to the stationary phase is the difference in the free energy of transfer from the bulk solvent to the stationary phase and from the bulk solvent to the micelle. Micelles and surfactant-modified phases have a similar molecular organization, which leads to low selectivity.[38]

Functional group selectivity is defined as the ratio of the value of k' of a compound with a substituent to that of the parent compound [*e.g.*, $\alpha(R) = k'(Bz–R)/k'(Bz)$ for substituted benzenes]. For a large group of compounds, particularly non-ionic compounds, hydrophobic interactions play a major role; an alkyl-bonded stationary phase modified with surfactant monomers makes the environment of the stationary phase similar to that of the micelles. A decrease in functional group selectivity was observed with increasing micelle concentration.[41]

In general, the change in selectivity with micellar eluents is evident when $\log k'$ for different compounds is plotted against log[surfactant].[31] Frequently, the linear plots are not parallel but intersect each other (Fig. 4). Reversal of elution order indicates the occurrence of two competing equilibria: solute–micelle association and solute–stationary phase interaction. The parameters P_{SW} and K_{AM} have opposing effects on retention. As P_{SW} increases, retention increases, whereas as K_{AM} increases, retention decreases. At a low micelle concentration, the system resembles conventional RP-LC and P_{SW} controls retention. However, as the concentration of surfactant is increased, K_{AM} has an increasing effect owing to the larger number of micelles present in the mobile phase. The

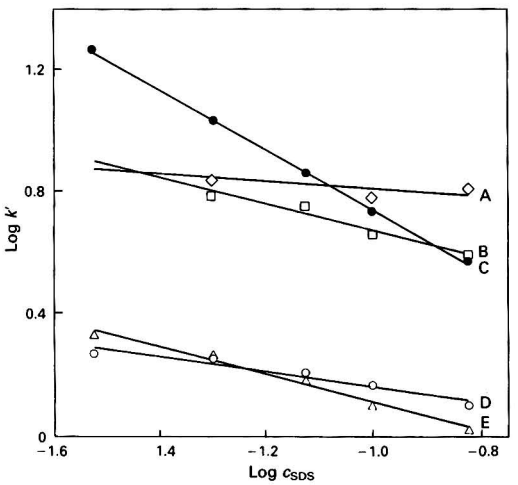

Fig. 4 Log *k' versus* log total SDS concentration in the mobile phase for several diuretics: A, probenecid; B, ethacrynic acid; C, chlorthalidone; D, acetazolamide; and E, hydrochlorothiazide[42]

difference in K_{AM} values among the solutes is sometimes so large that the elution order is reversed.

When comparing the elution of any two solutes, selectivity might increase or decrease with micelle concentration depending on the contribution of electrostatic and hydrophobic interactions, which in turn depend on the structure of the compounds. Selectivity also depends on the type of surfactant. This is true for diverse pairs of zwitterionic amino acids and peptides.[41]

Addition of Modifiers to Micellar Eluents

The predominant factor influencing band broadening in MLC appears to be stationary phase mass transfer. The thickness of the stationary phase layer and its viscosity are significantly increased by surfactant adsorption.[13] In conventional RP-LC, for well-designed column packings, this term is considered to be negligible. However, it becomes significant for column packings that have a thick stationary phase or poor stationary-phase diffusion, such as some of the original bonded-phase materials that had thick polymeric layers of stationary phase.[43] The surfactant-coated column is analogous to those packing materials.

The addition of small percentages of propan-1-ol to micellar mobile phases was recommended by Dorsey *et al.*[44] to enhance chromatographic efficiency and to decrease the asymmetry of the chromatographic peaks. Since then other organic solvents have been studied as modifiers in MLC.[45] Of these, short-chain alcohols have usually been demonstrated to be the most suitable.[46–48] The term hybrid is used for ternary eluents of water–organic solvent–micelles.

The general pore shapes of the parent C_{18} material appear to be retained in a surfactant-modified stationary phase, indicating that the surfactant produces a thick film on the interior walls of the capillaries, rather than completely filling the pore. Alcohol modifiers reduce the amount of surfactant sorbed on the stationary phase, and the effect is larger with increasing concentration and hydrophobicity of the modifier.[48]

In addition to reducing the carbon loading and film thickness, the addition of an alcohol is also expected to influence the fluidity/rigidity of the surfactant–C_{18}-bonded ligand structure on the stationary phase, just as its presence alters the fluidity of the micellar aggregate structure. The solute–stationary phase diffusion coefficient should increase as the microviscosity of the phase decreases.[45]

At a fixed modifier concentration, the efficiency was observed to decrease as the surfactant concentration in the mobile phase was increased, as in the absence of a modifier. Addition of increasing amounts of alcohol at a fixed surfactant concentration increased the efficiency. Therefore, the additive to surfactant concentration ratio is the dominant factor influencing chromatographic efficiency.[45]

For example, after addition of 5 or 10% methanol to a 0.02 mol dm^{-3} SDS mobile phase, the number of theoretical plates, n, increased from 300 to 750 and 1120, respectively, for acetone,[44] and after addition of 5% pentan-1-ol to a 0.28 mol dm^{-3} SDS mobile phase, n increased from 1530 to 3570, and from 50 to 950 for benzene and 2-ethylanthraquinone, respectively,[45] even though the relative microviscosity of the micellar mobile phase had increased due to the added alcohol. The low efficiency observed for 2-ethylanthraquinone with SDS and without modifier is due to its low solubility in water. The compound can only partition between the micelle in the mobile phase and the surfactant-coated stationary phase. Consequently, in order to desorb/exit the stationary phase or micelle in the mobile phase, for both of which this compound has a great affinity, the ionic micelle should be located close to the surfactant-modified stationary phase. However, both are similarly charged. Hence, an electrostatic repulsive barrier to the direct merger of the micellar entity with the surfactant-coated stationary phase will exist, which will impede solute mass transfer across this interface. The greater the fraction of partitioning that must occur *via* the direct transfer mode, the poorer will be the observed chromatographic efficiency.

It should be noted that another reason why alcohols improve the efficiency in MLC, with ionic surfactant micelles, may be because their presence can reduce the net electrical charge density of the ionic micellar surface.[45] This would be expected to diminish the repulsive barrier. The presence of alkane additives does not affect the surface charge density; hence, these types of additive do not improve efficiency for very hydrophobic solutes, even though they reduce the extent of surfactant coverage of the stationary phase.

This also explains why alcohol additives do not enhance the efficiency in MLC with non-ionic micellar mobile phases.[45] Non-ionic micellar surfactants are long-chain tensioactive alcohols themselves and C_1–C_5 alcohols are not very effective in desorbing these non-ionic surfactants from the surfactant-modified C_{18} stationary phase. Such non-ionic surfactants also have no charge and, therefore, no electrostatic charge barrier is encountered in the direct transfer process envisaged for water-insoluble solutes. In fact, the efficiency achieved in very hydrophobic test solutes with a Brij 35 micellar mobile phase is better than that which can be obtained with any ionic micelles.

Solvent Strength

One of the main disadvantages of purely micellar eluents is their weak solvent strength. The solvent strength can be increased by addition of an alcohol. This significantly alters the equilibrium of the solute away from the micelle towards the bulk aqueous phase, which becomes more non-polar.[49]

The addition of alcohols to micellar mobile phases would cause changes in certain micellar properties, such as the aggregation number and the c.m.c of the surfactant. However, the observed changes in retention and selectivity in hybrid systems are too large to be explained in terms of changes in micellar properties. The changes might be explained by modification of the micro-environment of the micelles and the stationary phase.

Large concentrations of the organic solvent can totally disrupt the micelle structure; hence, the use of alcohols in MLC has been questioned. Some workers have argued that when organic modifiers are used this type of chromatography loses some of its appeal.[46]

It may seem logical to assume that the separation mechanism with a hybrid mobile phase is similar to that with traditional hydro-organic solvents, rather than to that with a purely aqueous surfactant mobile phase. Addition of an organic solvent might reduce the role of micelles and would create a system that is closer to hydro-organic eluents. However, as long as the integrity of the micelles is maintained, addition of an alcohol to a micellar mobile phase will not create a hydro-organic system, even though in hybrid systems interactions are reduced by the presence of an alcohol and the stationary phase is more similar to that in a conventional hydro-organic system. Interestingly, the non-logarithmic behaviour of k' *versus* n_C for a homologous series is also observed with hybrid micellar systems. This shows that it is micelles that influence the role of an organic co-solvent in the mobile phase.[38]

With hybrid eluents, solute binding constants to micelles, K_{AM}, and their partitioning into the stationary phase, P_{SW}, both decrease as a result of the addition of an alcohol and, therefore, the eluting power of the mobile phase increases. Binding constants of hydrophobic solutes decrease more than those of hydrophilic solutes with an increasing alcohol concentration. Hence, selectivity is modified. The decrease in P_{SW} may be associated with an alteration of the stationary phase.[49,50]

In traditional RP-LC with a binary hydro-organic mobile phase, the effect of the organic modifier concentration, θ, on retention is often expressed as

$$\log k' = -S\theta + \log k'_0 \qquad (4)$$

where S is the solvent strength parameter.[51] [The intercept log k'_0 is the logarithm of the capacity factor in a purely aqueous mobile phase (in hydro-organic systems) or at a given micelle concentration without modifier.] This equation is valid only for a small range of concentrations for hydro-organic eluents. In contrast, excellent linearity was observed between log k' and θ even for water-rich eluents.[40]

The over-all S values for micellar hybrid eluents can be ranked as $S_{\text{pentan-1-ol}} > S_{\text{butan-1-ol}} > S_{\text{propan-1-ol}} > S_{\text{methanol}}$, which is similar, for the last three solvents, to conventional hydro-organic systems.[41,42] The larger S value for pentan-1-ol and butan-1-ol indicates that these solvents interact to a greater extent with micelles. However, the over-all S values for hybrid systems are still smaller than in the absence of a micelle.

The S values for a hydro-organic mobile phase change markedly with solute size in a homologous series. Variation in solvent strength with increasing solute size is minimized in the presence of micelles.[40] For a hybrid mobile phase, the solvent strength values are almost constant for a group of homologous compounds. The constancy of solvent strength with the variation in solute size is due to localization of solutes in the micelle environments, which reduces the size factor as far as the solvation of the solute by an alcohol is concerned.

Selectivity With Hybrid Micellar Eluents

In conventional hydro-organic systems, the same ranking of S values for different solutes with butan-1-ol, propan-1-ol and methanol is observed, because the three solvents belong to the same selectivity group. In the presence of micelles, this may not be the situation, because these solvents interact differently with micelles. The selectivity of different organic solvents in the presence of micelles might change.[41,42] This extends the possibilities for chromatographic separations.

In conventional RP-LC a systematic decrease in selectivity occurs as a result of an increase in the volume fraction of the organic modifier, *i.e.*, solvent strength. In the presence of micelles, selectivity may increase, decrease or remain unchanged with solvent strength. In hybrid systems, solvent strength may be enhanced without sacrificing the selectivity. As occurs with purely micellar systems, both the alkyl-bonded phase and the micelles are solvated by an alcohol to a similar extent, so that the methylene groups still find the same difference in their micro-environment polarities on transferrence to the stationary phase. Addition of up to 20% propan-1-ol to a micellar mobile phase of SDS or CTAB has a negligible effect on the hydrophobic selectivity.[41]

It is not surprising that peculiar behaviour might be observed as different solutes experience different polarities in their immediate vicinities. For example, the carbonyl-group selectivity, $\alpha(CO)$, defined as $k'[C_6H_5CO(CH_2)_nCH_3]/k'[C_6H_5(CH_2)_nCH_3]$, changes with the hydrophobicity (or number of carbon atoms in the side-chain) of two homologous pairs for a micellar eluent.[41] In this instance, the selectivity decreases with hydrophobicity, approaching unity, whereas it is independent of solute type for a hydro-organic eluent. This can be attributed to the fact that the more hydrophobic pairs are located in the more hydrophobic environment of the micelles and, therefore, experience a smaller change in their micro-environment polarities on being transferred from the mobile to the stationary phase. The $\alpha(CO)$ selectivity increases on addition of an alcohol to the micellar mobile phase, but decreases with an increase in micelle concentration.

The selectivity for a group of peptides and amino acids increases systematically on addition of an organic modifier. Similar behaviour is observed for some of the substituted benzenes, whereas for others, functional group selectivity decreases with increasing solvent strength. For the latter, the largest positive changes of selectivity are observed for compounds that are more hydrophilic or retained to a lesser extent than benzene (*e.g.*, benzyl alcohol, acetanilide, phenol), whereas for compounds that are more hydrophobic or retained to a greater extent than benzene, selectivity decreases with increasing solvent strength (*e.g.*, anthracene, naphthalene, butyrophenone).[41]

Although the solvent strength can be increased adequately in certain instances by increasing the micelle concentration, chromatographic efficiency in MLC usually deteriorates at higher micelle concentrations. Addition of an organic solvent to the micellar eluent may give an adequate eluent strength; it also improves the chromatographic efficiency, and in many instances can lead to an enhancement of separation selectivity. However, use of organic modifiers is not always appropriate. In certain instances selectivity enhancement might not lead to an improvement in resolution if retention falls below the optimum k' range as a result of an increase in eluent strength.[52] In other instances, the addition of an organic solvent to micellar eluents may have a beneficial effect on retention, but the efficiency may remain low.

Use of Reversed Micelles in Liquid Chromatography

In conventional normal-phase high-performance liquid chromatography a problem exists with reproducibility over time because of the variation in the water content of the mobile phase. The use of reversed micelle mobile phases [*e.g.*, sodium bis(2-ethylhexyl)sulfosuccinate, known as Aerosol OT, AOT] offers a unique solution to this problem owing to the ability to solubilize water in the interior of the micelle structure.[53] However, the presence of a surfactant leads to a loss of efficiency, probably because of the localization of polar solutes in the hydrophilic core with a slow transfer step out of the micelle.

The use of reversed micelles in supercritical fluid chromatography (SFC) provides another way of modifying the mobile phase, and is an alternative to polar and modified fluids.[54,55] In SFC, solubilization of large polar molecules is possible and the behaviour of the micellar mobile phase may be changed by control of temperature and pressure. Retention times of polar solutes are substantially reduced with a reversed micellar

mobile phase and solutes that are more polar can be separated. Reversed micelle chromatography may be better adapted to supercritical fluids owing to the gain in efficiency at higher temperatures. The higher diffusion rates and lower viscosities of supercritical fluids, compared with those of liquids at the same temperature, may enhance micelle diffusion rates, leading to an increased over-all efficiency.

This work was supported by the CICYT Project DEP89-0429.

References

1 Hinze, W. L., in *Ordered Media in Chemical Separations*, eds. Hinze, W. L., and Armstrong, D. W., ACS Symposium Series, American Chemical Society, Washington, DC, 1987, vol. 342, p. 2.
2 Dorsey, J. G., *Adv. Chromatogr.*, 1987, **27**, 167.
3 Berthod, A., and Dorsey, J. G., *Analusis*, 1988, **16**, 75.
4 Khaledi, M. G., *BioChromatography*, 1988, **3**, 20.
5 Berthod, A., Girard, I., and Gonnet, C., in *Ordered Media in Chemical Separations*, eds. Hinze, W. L., and Armstrong, D. W., ACS Symposium Series, American Chemical Society, Washington, DC, 1987, vol. 342, p. 130.
6 Dorsey, J. G., Khaledi, M. G., Landy, J. S., and Lin, J.-L., *J. Chromatogr.*, 1984, **316**, 183.
7 Berthod, A., Girard, I., and Gonnet, C., *Anal. Chem.*, 1986, **58**, 1356.
8 Berthod, A., Girard, I., and Gonnet, C., *Anal. Chem.*, 1986, **58**, 1359.
9 Mullins, F. G. P., and Kirkbright, G. F., *Analyst*, 1984, **109**, 1217.
10 Kirkbright, G. F., and Mullins, F. G. P., *Analyst*, 1984, **109**, 493.
11 Mullins, F. G. P., and Kirkbright, G. F., *Analyst*, 1986, **111**, 1273.
12 Kirkman, Ch. M., Zu-Ben, Ch., Uden, P. C., Stratton, W. J., and Henderson, D. E., *J. Chromatogr.*, 1984, **317**, 569.
13 Borgerding, M. F., and Hinze, W. L., *Anal. Chem.*, 1985, **57**, 2183.
14 Stratton, L. P., Hynes, J. B., Priest, D. G., Doig, M. T., Barron, D. A., and Asleson, G. L., *J. Chromatogr.*, 1986, **357**, 183.
15 Breyer, E. D., Strasters, J. K., and Khaledi, M. G., *Anal. Chem.*, 1991, **63**, 828.
16 Medina Hernández, M. J., Bonet Domingo, E., Ramis Ramos, G., and García Alvarez-Coque, M. C., unpublished work.
17 DeLuccia, F. J., Arunyanart, M., and Cline Love, L. J., *Anal. Chem.*, 1985, **57**, 1564.
18 Arunyanart, M., and Cline Love, L. J., *J. Chromatogr.*, 1985, **342**, 293.
19 Cline Love, L. J., Zibas, S., Noroski, J., and Arunyanart, M., *J. Pharm. Biomed. Anal.*, 1985, **3**, 511.
20 Haginaka, J., Wakai, J., and Yasuda, H., *Anal. Chem.*, 1987, **59**, 2732.
21 Kim, Y.-N., and Brown, P. R., *J. Chromatogr.*, 1987, **384**, 209.
22 Menéndez Fraga, P., Blanco González, E., and Sanz-Medel, A., *Anal. Chim. Acta*, 1988, **212**, 181.
23 Palmisano, F., Guerrieri, A., Zambonin, P. G., and Cataldi, T. R. I., *Anal. Chem.*, 1989, **61**, 946.
24 Sentell, K. B., Clos, J. P., and Dorsey, J. G., *BioChromatography*, 1989, **4**, 35.
25 Cline Love, L. J., and Fett, J., *J. Pharm. Biomed. Anal.*, 1991, **9**, 323.
26 Carretero, I., Maldonado, M., Laserna, J. J., Bonet, E., and Ramis Ramos, G., *Anal. Chim. Acta*, in the press.
27 Armstrong, D. W., and Nome, F., *Anal. Chem.*, 1981, **53**, 1662.
28 Arunyanart, M., and Cline Love, L. J., *Anal. Chem.*, 1984, **56**, 1557.
29 Borgerding, M. F., Quina, F. H., Hinze, W. L., Bowermaster, J., and McNair, H. M., *Anal. Chem.*, 1988, **60**, 2520.
30 Cline Love, L. J., Weinberger, R., and Yarmchuk, P., in *Surfactants in Solution*, eds. Mittal, K. L., and Lindman, B., Plenum Press, New York, 1984, vol. 2, pp. 1139–1158.
31 Yarmchuk, P., Weinberger, R., Hirsch, R. F., and Cline Love, L. J., *Anal. Chem.*, 1982, **54**, 2233.
32 Landy, J. S., and Dorsey, J. G., *Anal. Chim. Acta*, 1985, **178**, 179.
33 Armstrong, D. W., and Stine, G. Y., *Anal. Chem.*, 1983, **55**, 2317.
34 Pramauro, E., and Pelizzetti, E., *Anal. Chim. Acta*, 1983, **154**, 153.
35 Arunyanart, M., and Cline Love, L. J., *Anal. Chem.*, 1985, **57**, 2837.
36 Haginaka, J., Wakai, J., and Yasuda, H., *J. Chromatogr.*, 1989, **488**, 341.
37 Armstrong, D. W., and Stine, G. Y., *J. Am. Chem. Soc.*, 1983, **105**, 6220.
38 Khaledi, M. G., *Anal. Chem.*, 1988, **60**, 876.
39 Colin, H., Guiochon, G., Yun, Z., Díez-Masa, J. C., and Jandera, P., *J. Chromatogr. Sci.*, 1983, **21**, 179.
40 Khaledi, M. G., Peuler, E., and Ngeh-Ngwainbi, J., *Anal. Chem.*, 1987, **59**, 2738.
41 Khaledi, M. G., Strasters, J. K., Rodgers, A. H., and Breyer, E. D., *Anal. Chem.*, 1990, **62**, 130.
42 Bonet Domingo, E., Medina Hernández, M. J., Ramis Ramos, G., and García Alvarez-Coque, M. C., *Analyst*, 1992, **117**, 843.
43 Snyder, L. R., and Kirkland, J. J., *Introduction to Modern Liquid Chromatography*, Wiley, New York, 1979, ch. 5.
44 Dorsey, J. G., De Echegaray, M. T., and Landy, J. S., *Anal. Chem.*, 1983, **55**, 924.
45 Borgerding, M. F., Williams, R. L., Jr., Hinze, W. L., and Quina, F. H., *J. Liq. Chromatogr.*, 1989, **12**, 1367.
46 Yarmchuk, P., Weinberger, R., Hirsch, R. F., and Cline Love, L. J., *J. Chromatogr.*, 1984, **283**, 47.
47 Berthod, A., and Roussel, A., *J. Chromatogr.*, 1988, **449**, 349.
48 Borgerding, M. F., Hinze, W. L., Stafford, L. D., Fulp, G. W., Jr., and Hamlin, W. C., Jr., *Anal. Chem.*, 1989, **61**, 1353.
49 Tomasella, F. P., Fett, J., and Cline Love, L. J., *Anal. Chem.*, 1991, **63**, 474.
50 Berthod, A., Girard, I., and Gonnet, C., *Anal. Chem.*, 1986, **58**, 1362.
51 Snyder, L. R., Dolan, J. W., and Gant, J. R., *J. Chromatogr.*, 1979, **165**, 3.
52 Foley, J. P., *Anal. Chim. Acta*, 1990, **231**, 237.
53 Hernández Torres, M. A., Landy, J. S., and Dorsey, J. G., *Anal. Chem.*, 1986, **58**, 744.
54 Gale, R. W., Fulton, J. L., and Smith, R. D., *Anal. Chem.*, 1987, **59**, 1977.
55 Veuthey, J. L., Caude, M., and Rosset, R., *Analusis*, 1988, **16**, 466.

Paper 1/05258F
Received October 16, 1991
Accepted December 13, 1991

Determination of Parabens in Cosmetic Products by Supercritical Fluid Extraction and High-performance Liquid Chromatography

Santo Scalia* and David E. Games
Mass Spectrometry Research Unit, Department of Chemistry, University College of Swansea, Singleton Park, Swansea SA2 8PP, UK

A rapid and simple supercritical fluid extraction (SFE) procedure has been developed for the isolation of paraben preservatives from cosmetic matrices. Method optimization indicates that recovery is affected most by extraction temperature and time. The parabens were assayed by high-performance liquid chromatography after extraction of the cosmetic preparations with supercritical carbon dioxide at 60 °C and at a density of 0.85 g ml^{-1}. Quantitative recoveries of parabens were obtained with two sequential 7 min extraction steps. Supercritical fluid extraction of cosmetic samples gave better recovery for parabens than conventional liquid extraction techniques within a shorter period of time. Moreover, the automated SFE system used minimized sample manipulation and allowed stand-alone operations. The SFE method is simple to perform, accurate, reproducible and suitable for routine analyses of commercial cosmetic products.

Keywords: *Supercritical fluid extraction; high-performance liquid chromatography; paraben preservatives; cosmetic product*

Preservatives are commonly contained in cosmetic preparations for the primary purpose of inhibiting the development of micro-organisms. However, all the preservatives can be harmful to the consumer by their potency to induce allergic contact dermatitis.[1] The European Economic Community (EEC) Directive on cosmetics[2] includes a list of preservatives authorized as cosmetic additives and their allowed maximum concentrations. Hence, the assay of these substances in cosmetic products is important for checking compliance with the EEC legislation.

The *p*-hydroxybenzoic acid esters or parabens are the most widely used antimicrobial agents in cosmetics,[3] the most important ones being the methyl, ethyl, propyl and butyl esters.[1] Combinations of two or more parabens are often used to increase the ability of the system to withstand microbial contaminations.[4] Published methods for the determination of these preservatives in cosmetic preparations are based on gas chromatography (GC)[5] and high-performance liquid chromatography (HPLC).[6–8] The latter technique offers distinct advantages over GC such as simpler purification procedures and the lack of derivatization steps. However, solid and semi-solid samples which are often encountered in the analysis of cosmetics must first be put into a liquid form before HPLC analyses. This requires several sample manipulations[7,8] (*e.g.*, solvent extraction, mixing, sonication, heating, addition of acids and centrifugation), which represent a source of possible errors. Moreover, the organic solvents used must be pure and eventually be disposed of.

Supercritical fluid extraction (SFE) is emerging as a valuable technique[9,10] for the isolation of solutes from solid samples, using supercritical fluids as the extraction media. While supercritical fluids exhibit solvation powers approaching those of liquids, they have both lower viscosities and higher diffusivities,[11] which lead to more rapid and efficient extractions of analytes. Moreover, the solvent strength of a supercritical fluid increases with increasing density, allowing modifications of the extraction selectivity simply by changing the pressure or the temperature. Finally, carbon dioxide, the supercritical fluid most frequently used in SFE, is non-flammable, non-toxic and available in a pure form at a reasonable cost. Hence, it represents an excellent alternative to the potentially hazardous solvents currently used in sample preparation.

This paper describes the development of an SFE procedure, performed with a commercially available system, for the rapid and efficient purification of the complex cosmetic matrices before assay of paraben preservatives by HPLC. The application of the method to the determination of parabens in commercial cosmetic products is also reported.

Experimental

Materials

Instrument-grade liquid carbon dioxide supplied in cylinders with a dip tube was obtained from BOC (London, UK). Methanol, acetonitrile and water of HPLC-grade were supplied by Fisons (Ipswich, UK). Methyl, ethyl, propyl and butyl parabens were purchased from Sigma (St. Louis, MO, USA). Their purity was checked by HPLC prior to use. All other chemicals were of analytical-reagent grade (Sigma). Commercial cosmetics were from retail stores.

Chromatography

The HPLC apparatus consisted of a Hewlett-Packard 1084B high-performance liquid chromatograph (Hewlett-Packard, Avondale, PA, USA) linked to an injection valve with a 10 μl sample loop (Rheodyne, Cotati, CA, USA). The column effluent was monitored by the built-in multiple wavelength ultraviolet/visible detector set at a wavelength of 254 nm and 0.38 a.u.f.s. Separations were performed on a Spherisorb ODS column (particle diameter 5 μm, 100 × 4.6 mm i.d.; Jones Chromatography, Hengoed, Mid-Glamorgan, UK) under gradient conditions at a flow rate of 1.0 ml min^{-1}. Solvent A and solvent B were 20 and 80% v/v acetonitrile in water, respectively. The elution programme was as follows: isocratic elution with 40% solvent B–60% solvent A for 6.5 min, then a 1 min linear gradient to 100% solvent B. The mobile phase was filtered through HVLP-type 0.45 μm filters. Chromatography was carried out at ambient temperature.

The identity of the separated compounds was assigned by co-chromatography with the authentic substances. Peak areas were used for calculations.

* On leave from the Dipartimento di Scienze Farmaceutiche, Università di Ferrara, via Scandiana 21, 44100 Ferrara, Italy.

Table 1 SFE parameters

Extraction fluid density	0.85 g ml^{-1}
Extraction fluid flow rate	2 ml min^{-1}
Extraction temperature	60 °C
Equilibration time	2 min
Extraction time	7 min
Restrictor temperature	60 °C extraction/50 °C rinse
Trap temperature	30 °C extraction/50 °C rinse
Rinse solvent	Methanol
Rinse volume	1.2 ml
Rinse rate	1.0 ml min^{-1}

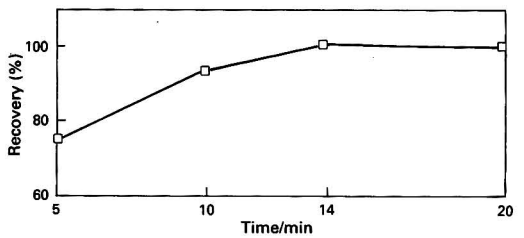

Fig. 1 Influence of the extraction time on the average recovery of a mixture of methyl, ethyl, propyl and butyl parabens from a hand cream. Other SFE conditions as in Table 1. Values plotted are means of triplicate experiments

Sample Extraction

Supercritical fluid extractions were performed with a computer-controlled HP 7680A SFE system (Hewlett-Packard). The cosmetic product (0.2–0.3 g) was accurately weighed on a piece of filter-paper which was rolled and inserted into the extraction cell. After initiation of the extraction programme, the supercritical carbon dioxide flows through the extraction cell and then through the restrictor into the analyte trap. The sudden pressure drop at the restrictor causes the supercritical fluid to evaporate depositing the analytes on an internal trap packed with small (diameter 0.36–0.43 mm) stainless-steel balls. Finally, the trap is rinsed with methanol and the rinse solvent collected in sample vials. The contents of the vials were made up to volume (3 ml), filtered if necessary and analysed directly by HPLC. Extraction density and time, cell temperature, supercritical carbon dioxide flow rate, trap temperature and amount of rinse solvent were controlled by the software program in the personal computer. The specific extraction conditions used are reported in Table 1.

Recovery and Reproducibility

'Spiked' solutions were obtained by dissolving weighed amounts of parabens in methanol. The test samples were prepared by adding 50 μl aliquots of the spiked solutions, corresponding to 0.04% m/m of each single paraben, to the cosmetic products (0.2 g) and mixing them thoroughly. The percentage recovery was determined by comparing the peak areas of the parabens extracted from the samples with those obtained by direct injections of the standard solutions.

The intra-assay reproducibility was tested by analysing, on ten different days, 10 μl of the same stock sample solution from a suncream. The inter-assay variability was evaluated by replicate (n = 10) extractions of the same suncream product.

Results and Discussion

A hand cream product, containing no detectable parabens, was spiked with methyl, ethyl, propyl and butyl parabens at 0.04% m/m and extracted for 10 min with supercritical carbon dioxide at 40 °C and at a density of 0.95 g ml^{-1}. In order to prevent the matrix from being swept out of the extraction cell, the sample was smeared on filter-paper. In spite of the high value of the fluid density used (at the limit of the operating range of the instrument), low recoveries (19.8–22.5%) were observed for all the compounds investigated. Increasing the extraction temperature from 40 to 60 °C produced higher recoveries (65.4–67.0%) even though the carbon dioxide density, and hence its solvating power, had to be reduced (0.85 g ml^{-1} was the maximum density achieved with the SFE system at 60 °C). A second extraction of the same sample was found to recover all the compounds quantitatively. Although the density is generally the most important parameter that influences the extraction efficiency in SFE, for the parabens the temperature has a dominant role. The improved recoveries obtained at higher temperature are due to increased solute solubility and also to sample matrix modifications (such as swelling) and enhanced diffusivity. The influence of the extraction time on the recovery of the parabens from the cosmetic matrix was also investigated. As illustrated in Fig. 1, the extraction is complete after 14 min. The optimized SFE procedure consists of two 7 min extraction steps performed under identical conditions (Table 1) and preceded by a static equilibration of 2 min.

Three different cosmetic preparations, containing no detectable parabens, were spiked with each preservative at a concentration of 0.04% m/m and subjected to the SFE method outlined above. The average recoveries ± the standard deviations for the four parabens from a hand cream, a

Table 2 Comparison of total concentrations of parabens in cosmetic products purified by SFE or liquid extraction[7]

	Concentration* (% m/m)	
Sample	SFE	Liquid extraction
Suncream	0.164	0.150
Moisturising lotion	0.179	0.169
Cleansing milk	0.207	0.197
Skin cream	0.237	0.219
Day cream	0.058	0.052

* Mean value of three determinations.

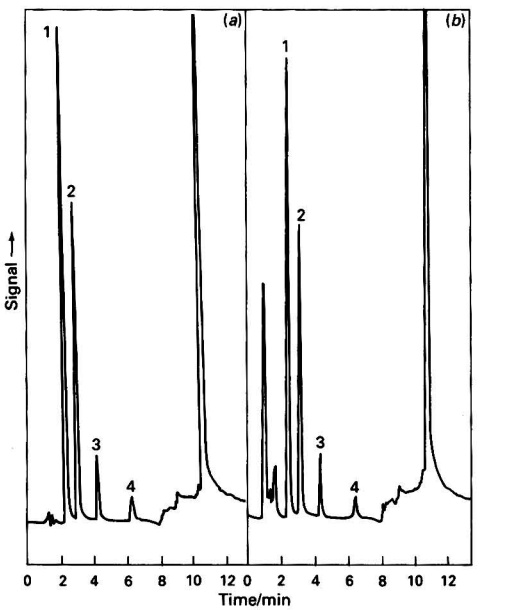

Fig. 2 HPLC trace of a suncream product purified by (*a*) SFE or (*b*) by the method reported in the literature.[7] 1, Methyl paraben; 2, ethyl paraben; 3, propyl paraben; and 4, butyl paraben. Operating conditions as described under Experimental

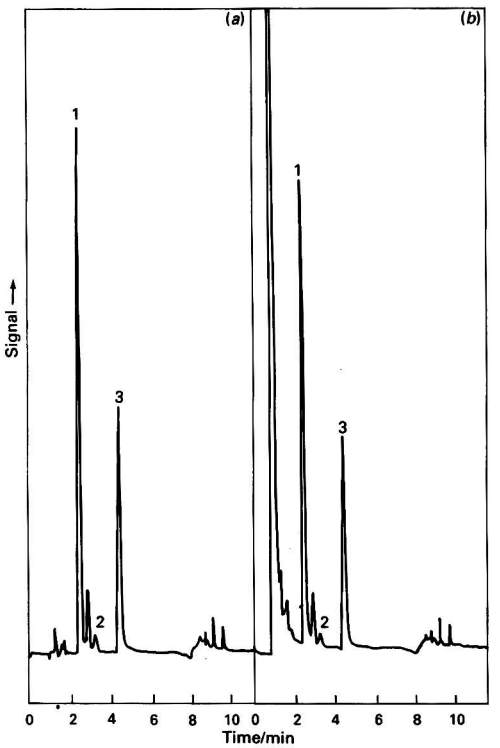

Fig. 3 HPLC trace of a day cream preparation purified by (*a*) SFE or (*b*) by the method reported in the literature.[7] Sensitivity, 0.19 a.u.f.s. Other operating conditions as described under Experimental and peak identification as in Fig. 2

sunscreen lotion and a shampoo were 100.3 ± 1.7% (n = 6), 96.7 ± 1.4% (n = 6) and 99.5 ± 2.3% (n = 6), respectively.

Calibration graphs were linear in the range 0.004–0.4% m/m with correlation coefficients greater than 0.998. In none of the graphs was the intercept with the y-axis significantly different from zero at the 95% confidence interval. The minimum quantifiable amounts were at least ten times below the levels normally used in the formulation of cosmetics.[6,8]

Applying the SFE procedure to a commercial suncream product, the total concentration of parabens (0.164% m/m) was determined with a relative standard deviation of 1.3% (n = 10) for the intra-assay reproducibility and 1.6% (n = 10) for the inter-assay reproducibility. The good precision achieved can be traced to the automated extraction process, which minimizes the sample handling steps.

As spiked samples do not really simulate real samples, the SFE method developed in this study was further validated by comparison with the previously adopted liquid extraction procedure[7] on the same cosmetic preparations known to contain parabens. Five different commercial products were assayed. The levels measured (Table 2) conform to the EEC legislation[2] (limiting value, 0.8% m/m for mixtures of parabens) and indicate that the recoveries of these preservatives with SFE are higher than those obtained with the liquid extraction technique currently used.[7,8] Moreover, the purification based on SFE is more rapid (taking less than 40 min to perform) and less labour-intensive than others reported in the literature.[7,8] Faster sample preparation has been attained by other workers;[6] however the recoveries of the parabens were not evaluated. Further, rapid column deterioration is a disadvantage of this method as the cosmetic preparation after solubilization is injected directly onto the HPLC column without any sample clean-up. Representative chromatograms of a suncream preparation and of a day cream product, extracted by the SFE procedure described here (*a*) or by the method reported in the literature[7] (*b*), are shown in Figs. 2 and 3, respectively. In addition to improved recoveries (Table 2), the SFE method [Figs. 2(*a*) and 3(*a*)] affords a more effective purification of the cosmetic matrices compared with the classical liquid extraction technique [Figs. 2(*b*) and 3(*b*)], as is evident by the absence in the HPLC traces of large peaks close to the void volume.

Conclusions

An SFE procedure for the rapid isolation of the paraben preservatives from cosmetics has been developed. The proposed method is less laborious than others reported in the literature, as sample pre-treatment simply involves weighing the cosmetic product and inserting it into the extraction cell. Moreover, because SFE allows the automation of various processes, method development is faster than with the traditional manual sample preparation. The rapidity, simplicity, good accuracy and reproducibility of the SFE procedure make it suitable for routine quality control analyses of parabens in cosmetics, particularly to verify their conformance to the EEC legislation. Work is in progress in this laboratory to investigate the effectiveness of SFE as a generally applicable procedure for extracting a variety of additives from cosmetic matrices.

The authors thank the SERC for assistance in the purchase of some of the equipment used in these studies. S. S. thanks the CNR for financial support. Provision of the SFE system by Hewlett-Packard is gratefully acknowledged.

References

1 Schopf, E., and Baumgartner, A., *J. Appl. Cosmetol.*, 1990, **8**, 39.
2 European Economic Community Council Directive 76/768/EEC, Appendix VI, 1976.
3 Wallhausser, K. H., in *Surfactants in Cosmetics*, ed. Rieger, M. M., Marcel Dekker, New York, 1985, p.225.
4 Parker, M. S., in *Cosmetic and Drug Preservation*, ed. Kabara, J. J., Marcel Dekker, New York, 1984, p. 389.
5 Geahchan, A., Pierson, M., and Chambon, P., *J. Chromatogr.*, 1979, **176**, 123.
6 Dong, M. W., and DiCesare, J. L., *J. Chromatogr. Sci.*, 1982, **20**, 49.
7 Gagliardi, L., Amato, A., Basili, A., Cavazzutti, G., Gattavecchia, E., and Tonelli, D., *J. Chromatogr.*, 1984, **315**, 465.
8 de Kruijf, N., Schouten, A., Rijk, M. A., and Pranoto-Soetardhi, L. A., *J. Chromatogr.*, 1989, **469**, 317.
9 Lee, M. L., and Markides, K. E., in *Analytical Supercritical Fluid Chromatography and Extraction*, eds. Lee, M. L., and Markides, K. E., Chromatography Conferences, Provo, UT, 1990, pp. 313–352.
10 Hawthorne, S. B., *Anal. Chem.*, 1990, **62**, 633A.
11 Games, D. E., Berry, A. J., Mylchreest, I. C., Perkins, J. R., and Pleasance, S., in *Supercritical Fluid Chromatography*, ed. Smith, R. M., Royal Society of Chemistry, London, 1988, p. 159.

Paper 1/05583F
Received November 4, 1991
Accepted December 6, 1991

Evaluation of Diuretics in Pharmaceuticals by High-performance Liquid Chromatography With a 0.05 mol dm^{-3} Sodium Dodecyl Sulfate–3% Propanol Mobile Phase

Emilio Bonet Domingo, María José Medina Hernández, Guillermo Ramis Ramos and María Celia García Alvarez-Coque*

Departamento de Química Analítica, Facultad de Química, Universidad de Valencia, Burjassot, Valencia, Spain

The use of micellar liquid chromatography for the determination of diuretics in pharmaceutical preparations is studied. Micellar mobile phases containing sodium dodecyl sulfate (SDS), with and without different alcohols, are considered in order to determine the most appropriate combination. The elution behaviour of each diuretic in an unmodified micellar mobile phase is related to the solute–micelle association constants and the stationary phase-water partition coefficients. Diuretics of high, intermediate and low efficacy, contained in several pharmaceutical preparations, are determined using a 0.05 mol dm^{-3} SDS–3% propanol micellar mobile phase and a C_{18} column.

Keywords: *Diuretic; pharmaceutical analysis; sodium dodecyl sulfate; high-performance liquid chromatography; micellar mobile phase*

Diuretics enhance renal excretion of water and electrolytes and are among the most extensively used drugs. The action of diuretics is based on interference with the mechanism of ionic transport along the complete length of the nephron. According to their action diuretics are classified as having high, intermediate or low efficacy.

Numerous procedures have been described for the control of the content of diuretics in pharmaceutical formulations using reversed-phase liquid chromatography with hydro-organic mobile phases.[1–12] Most of the reports consider the determination of one or two diuretics. For these analyses, a C_{18} stationary phase, with methanol–water and acetonitrile–water mobile phases and acetate and phosphate buffers were usually used. Detection was performed in the ultraviolet (UV) region and recoveries and reproducibility were usually high.

In the last 5–10 years, reported applications of micellar liquid chromatography have increased. Micellar liquid chromatography, which employs solutions of surfactants as the mobile phases, is a mode of liquid chromatography that can be considered as an alternative to classical partition chromatography. Some advantages of the technique are the low cost and the non-flammability, non-toxicity and easy disposal of the solvent. Difficult separations of hydrophobic and hydrophilic compounds have been achieved as a result of the large number of interactions of the solutes with the stationary and mobile phases.

First, micellar mobile phases without the addition of modifiers were used, however, it was demonstrated that the presence in the mobile phase of a small amount of alcohol, giving rise to the so-called 'hybrid' mobile phases, enhances the efficiency of the separation and improves the retention control.[13–15] Khaledi *et al.*[16,17] demonstrated that the mechanism of separation with hybrid micellar eluents more closely resembles that in a purely micellar phase than that in conventional hydro-organic phases, as long as the integrity of the micelles is maintained.

In this work, the use of micellar liquid chromatography for the determination of diuretics in pharmaceutical preparations was studied. Different micellar mobile phases were considered in order to determine the most appropriate. A sodium dodecyl sulfate (SDS) micellar solution of increasing concentration, without any modifier, was first used. Next, the addition of several alcohols to the micellar mobile phase was studied. Nine diuretics, present in several different pharmaceutical preparations commercially available in Spain, were determined using a 0.05 mol dm^{-3} SDS–3% propanol micellar mobile phase and a C_{18} column.

Experimental

Reagents

Aqueous SDS (99%, Merck, Darmstadt, Germany) solutions were used as the mobile phases. Micellar mobile phases with modifier were prepared by mixing the surfactant solution with a small amount of the alcohol to obtain the working concentration (v/v). Methanol [for high-performance liquid chromatography (HPLC)] and propanol (analytical-reagent grade) were from Panreac (Barcelona, Spain), and pentan-1-ol (analytical-reagent grade) was from Merck. Nanopure de-ionized water (Barnstead Sybron, MA, USA) was used throughout. The mobile phases were vacuum-filtered through 0.47 μm nylon membranes from Micron-Scharlau (Barcelona, Spain).

Stock solutions of 100 μg ml^{-1} of the diuretics were prepared. Most of the compounds were soluble in 0.1 mol dm^{-3} SDS, but for some it was necessary to dissolve them in a small volume of methanol prior to the addition of the SDS solution. Most of the compounds were kindly donated by several Spanish pharmaceutical laboratories: acetazolamide (Lederle, Madrid, Spain), amiloride and atenolol (ICI Farma, Madrid, Spain), bendrofluazide (Davur, Madrid, Spain), bumetanide (Boehringer Ingelheim, Barcelona, Spain), chlorthalidone (Ciba-Geigy, Barcelona, Spain), ethacrynic acid (Merck Sharp and Dohme, Madrid, Spain), frusemide (Lasa, Barcelona, Spain), hydrochlorothiazide (Galloso Wellcome, Madrid, Spain), spironolactone (Searle, Madrid, Spain), and xipamide (Lacer, Barcelona, Spain). Probenecid and triamterene were purchased from Sigma (Buchs, Switzerland).

No decomposition was observed in the diuretic stock solutions for between 15 d and 1 month; except for bendrofluazide, which should be prepared every 2–3 d. The decomposition was evident by the appearance of a peak during the dead volume of the chromatographic column and another with a retention time shorter than that of bendrofluazide, which increased with the age of the solution.

* To whom correspondence should be addressed.

Table 1 Influence of the concentration of SDS in the mobile phase on the values of capacity factor, k', efficiency, N, and asymmetry, B/A, of the peaks*

	[SDS]/mol dm^{-3}														
	0.03			0.05			0.075			0.1			0.15		
Diuretic	k'	N	B/A	k'	N	B/A	k'	N	B/A	k'	N	B/A	k'	N	B/A
Acetazolamide	1.9	1315	1.10	1.8	920	1.43	1.6	995	1.50	1.5	838	1.56	1.3	772	1.50
Amiloride	67.6	—	—	33.7	111	3.69	20.8	131	3.77	14.1	201	3.25	9.6	147	3.20
Bendrofluazide	28.3	1780	1.09	15.4	978	1.36	9.9	798	1.40	7.3	844	0.95	4.9	605	1.21
Chlorthalidone	18.1	1688	1.21	10.7	1287	1.00	7.1	920	1.27	5.3	812	1.30	3.7	555	1.17
Ethacrynic acid	4.1	204	3.00	6.2	65	4.43	5.6	115	3.67	4.6	102	2.90	3.9	139	2.82
Frusemide	2.0	600	0.92	3.0	147	2.17	2.9	460	0.67	2.5	739	0.43	2.5	494	1.22
Hydrochlorothiazide	2.2	632	1.89	1.8	1100	1.20	1.5	1019	1.31	1.3	865	1.22	1.0	792	1.45
Probenecid	5.2	42	4.70	6.9	52	3.90	7.1	59	3.80	6.0	41	3.30	6.2	85	2.90
Triamterene	149	—	—	78.0	—	—	44.9	96	3.47	30.4	123	2.41	21.2	50	3.29
Xipamide	38.0	96	2.14	40.6	677	1.00	12.5	148	2.93	20.7	879	0.71	9.6	273	2.00
Spironolactone	>150	—	—	>80	—	—	>50	—	—	>35	—	—	>25	—	—

* Asymmetry factors.[18]

Apparatus

Absorption spectra were obtained using a Hewlett-Packard 8452A diode-array spectrophotometer (Avondale, PA, USA). The HPLC system consisted of a Hewlett-Packard HP 1050 chromatograph, with an isocratic pump, a programmable UV visible detector and an HP 3396A integrator. The sample was injected through a Rheodyne valve (Cotati, CA, USA), with a 20 μl loop. A Spherisorb octadecyl-silane (ODS)-2 C_{18} analytical column (5 μm particle size, 12.5 cm × 4 mm) and a C_{18} pre-column of similar characteristics (2 cm × 4 mm) both from Hewlett-Packard were used.

The dead volume (t_M = 0.77 min) was determined from 10 replicate injections of an aqueous solution of potassium iodide and measurement of the absorbance at 254 nm. Efficiencies were calculated as theoretical plates, according to the equation of Foley and Dorsey[18] for skewed peaks.

Analysis of Pharmaceutical Formulations

The pharmaceuticals analysed in this work were presented as tablets, except one containing probenecid, which was a powder for oral suspensions. In order to perform the determinations, the tablets were pulverized and an adequate amount weighed out. A 0.05 mol dm^{-3} SDS solution was added and the sample immersed for 5 min in an ultrasonic bath to facilitate dissolution. Dilutions were made with 0.05 mol dm^{-3} SDS. It was unnecessary to add methanol for solution. In order to eliminate any solid particles the sample was filtered through sintered glass and vacuum-filtered through the 0.47 μm membrane.

Results and Discussion

Mobile Phases Without Modifier

Table 1 shows capacity factors, k', and efficiencies, N, for various SDS concentrations, together with the asymmetry factors of the chromatographic peaks. Detection was carried out at 254 nm. As observed, the capacity factors usually decreased at increasing SDS concentrations. In 0.03 and 0.05 mol dm^{-3} SDS, retention of acetazolamide, ethacrynic acid, frusemide, hydrochlorothiazide and probenecid was in the $1 < k' < 10$ range. For the other diuretics, $k' > 10$. At larger SDS concentrations, the k' value of more diuretics is in the $1 < k' < 10$ range. However, the value of k' for triamterene was still too large even in 0.15 mol dm^{-3} SDS; retention of spironolactone was even longer.

At increasing SDS concentrations, a decrease in efficiency was observed for acetazolamide, bendrofluazide and chlorthalidone. For the other compounds, efficiency did not show a clear trend, although for hydrochlorothiazide and xipamide an important increase in efficiency was observed in 0.05 mol dm^{-3} SDS compared with the 0.03 mol dm^{-3} mobile phase. Efficiencies were extremely low in all the unmodified SDS mobile phases for amiloride, ethacrynic acid, probenecid and triamterene. There was no clear trend in the values of the asymmetry factors either. Very asymmetric peaks were obtained for amiloride, ethacrynic acid, probenecid, triamterene and xipamide.

These results indicated that an aqueous micellar mobile phase of SDS is not appropriate for the chromatographic determination of diuretics, partially due to the poor efficiencies obtained.

Partitioning Behaviour of the Diuretics

Armstrong and Nome[19] and Arunyanart and Cline Love[20] proposed equivalent equations to describe the behaviour of a solute in micellar liquid chromatography as the micelle concentration is changed. The equations can be re-written as:

$$\frac{1}{k'} = \frac{K_{AM}}{\phi P_{SW}}[M] + \frac{1}{\phi P_{SW}} \quad (1)$$

where K_{AM} is the solute–micelle association constant; [M] is the micelle concentration, *i.e.*, the surfactant concentration minus the critical micellization concentration (c.m.c.); and ϕP_{SW} is the stationary phase–water partition coefficient multiplied by the phase ratio, ϕ, where $\phi = (V_S/V_M)$ and V_S is the volume of the stationary phase and V_M the volume of the mobile phase. The value of P_{SW} was not calculated because of the difficulty in determining the volume of the stationary phase.

Table 2 shows the values of ϕP_{SW} and K_{AM}, calculated from eqn. (1), for several diuretics. For the most retained of the diuretics, the intercepts ($1/\phi P_{SW}$) were almost zero (amiloride, -1.2×10^{-3}; bendrofluazide, 5.7×10^{-3}; and triamterene, -7.2×10^{-4}). Borgerding *et al.*[21] indicated that a zero intercept requires the reciprocal of the phase ratio to be zero, which is not physically possible, or that P_{SW} must be very large. This behaviour has been observed with sparingly soluble solutes. Bendrofluazide and triamterene were not soluble in water, but amiloride was soluble.

On the other hand, as expected, for diuretics with low values of ϕP_{SW} (acetazolamide, frusemide and hydrochlorothiazide), retention times were very short. Retention of probenecid was not appreciably modifed by varying the SDS concentration and should be considered as a non-binding

Table 2 Values of ϕP_{SW} and K_{AM} for some diuretics obtained from the $1/k'$ *versus* c_{SDS} – c.m.c. linear plots [eqn. (1)]

Diuretic	ϕP_{SW}	K_{AM}
Acetazolamide	2.1	4.5
Bendrofluazide	177	249
Chlorthalidone	56	101
Ethacrynic acid	8.2	7.9
Frusemide	3.9	5.8
Hydrochlorothiazide	2.6	10.8

solute[22] (K_{AM} being close to zero). Xipamide had a variable behaviour when any condition was changed.

Order of Elution

It is of interest to relate the elution behaviour of each diuretic to the parameters obtained from eqn. (1), K_{AM} and ϕP_{SW}. At a low micelle concentration, the system resembles conventional reversed-phase chromatography. If the compounds are ordered according to their elution with a 0.03 mol dm^{-3} SDS mobile phase, it is observed that P_{SW} controls the retention: the less retained solutes had lower ϕP_{SW} values and the most retained had the largest (*e.g.*, acetazolamide, 2.1; hydrochlorothiazide, 2.6; frusemide, 3.9; ethacrynic acid, 8.2; chlorthalidone, 56; and bendrofluazide, 177). The values of ϕP_{SW} for amiloride, triamterene and xipamide were also large.

In micellar liquid chromatography, when log k' is plotted *versus* log c_{SDS} (surfactant concentration), for solutes of different character, the linear plots intersect one another, which leads to a reversal in the elution order.[23] This occurs as a result of the concurrence of two competitive equilibria: solute–micelle association and solute–stationary phase interaction. An increasing micellar concentration brings the solute into the micellar phase, whereas it has no effect, or a small effect on the stationary phase equilibria. For solutes with high K_{AM} values, the modification in surfactant concentration leads to important changes in retention, and the elution order is altered.

Such elution order reversals were also observed for diuretics. The following compounds altered their elution order at the SDS concentration indicated: probenecid–ethacrynic acid, 0.03; acetazolamide–hydrochlorothiazide, 0.06; probenecid–chlorthalidone, 0.08; xipamide–amiloride, 0.09; bendrofluazide–probenecid, 0.1; and chlorthalidone–ethacrynic acid, 0.13 mol dm^{-3}.

Table 3 shows that the diuretics with the largest changes in capacity factors (the slope of the log k' *versus* log c_{SDS} plot was larger) were triamterene, amiloride, bendrofluazide, and chlorthalidone. The latter three reversed their elution order. Triamterene, because of its long retention, although being affected, did not produce any reversal.

If the diuretics are ordered according to the value of K_{AM}, the order in Table 3 is observed: bendrofluazide, 249; chlorthalidone, 101; hydrochlorothiazide, 10.8; ethacrynic acid, 7.9; frusemide, 5.8; and acetazolamide, 4.5. Elution order reversals occurred between diuretics with sufficiently different K_{AM} values, such as bendrofluazide and probenecid, chlorthalidone and probenecid, and ethacrynic acid and chlorthalidone.

Addition of Modifiers to the Micellar Mobile Phase

The addition of short-chained alcohols to the micellar mobile phase reduces the thickness of the film of surfactant molecules covering the stationary phase and thus, produces an enhancement in efficiency.[21] The presence of the alcohol in the micellar mobile phase also alters the retention mechanism by shifting the equilibria of the solutes from the stationary phase and the micelle toward the bulk aqueous phase. This leads to a reduction in the capacity factors.[16,17]

Table 3 Regression line for the log k' *versus* log c_{SDS} plot

Diuretic	Slope	Intercept	Coefficient of regression (r)
Triamterene	−1.2	0.29	0.997
Amiloride	−1.2	−0.05	0.998
Bendrofluazide	−1.1	−0.22	0.999
Chlorthalidone	−1.0	−0.26	0.9995
Hydrochlorothiazide	−0.45	−0.34	0.994
Ethacrynic acid	−0.43	0.24	0.986
Acetazolamide	−0.25	−0.09	0.981
Frusemide	−0.22	0.20	0.913

Table 4 Influence of the modifier on the values of capacity factor, k', efficiency, N, and asymmetry, B/A, of the peaks

	5% methanol			3% propanol			1% pentanol		
Diuretic	k'	N	B/A	k'	N	B/A	k'	N	B/A
Acetazolamide	1.3	1302	1.46	1.1	—	—	0.8	1654	1.13
Amiloride	29.5	237	3.74	22.4	241	4.76	5.7	207	3.40
Bendrofluazide	12.5	780	2.57	9.9	2552	0.87	4.0	983	0.68
Bumetanide	—	—	—	1.4	939	1.10	2.0	1080	1.00
Chlorthalidone	8.7	2145	1.07	6.0	2240	1.00	2.2	1345	1.13
Ethacrynic acid	2.9	270	2.92	1.4	1240	1.12	1.2	593	1.54
Frusemide	1.5	1165	1.83	0.6	475	0.75	0.4	1740	0.67
Hydrochlorothiazide	1.3	1136	1.67	1.1	380	4.83	0.8	1093	1.28
Probenecid	3.4	59	—	0.4	896	1.75	1.1	320	1.46
Spironolactone	—	—	—	55.5	—	—	10.8	—	—
Triamterene	60.0	—	—	37.1	336	2.05	9.9	452	0.94
Xipamide	18.9	94	3.52	1.1	36	3.25	3.8	220	3.00

A comparative study was performed to observe the effect of different alcohols added to the SDS micellar mobile phase, on the retention of the diuretics, and on the efficiency and asymmetry of the chromatographic peaks. For the preparation of these mobile phases a 0.05 mol dm^{-3} SDS solution was selected. This concentration is not high and the values for efficiency were large compared with other SDS concentrations. The alcohols used were 5% methanol, 3% propanol and 1% pentanol.

Table 4 gives the chromatographic parameters. Addition of 5% methanol produced the smallest modifications of the capacity factors; all were lower than with a 0.05 mol dm^{-3} SDS mobile phase without modifier. However, only acetazolamide, ethacrynic acid, frusemide, hydrochlorothiazide and probenecid shifted to shorter retention times as compared with a 0.075 mol dm^{-3} SDS phase. When compared with a 0.15 mol dm^{-3} SDS phase, only ethacrynic acid, frusemide and probenecid were less retained in a 0.05 mol dm^{-3} + 5% methanol mobile phase.

The addition of 3% propanol to a 0.05 mol dm^{-3} SDS mobile phase had a similar effect. Compared with a 0.15 mol dm^{-3} SDS mobile phase, acetazolamide, ethacrynic acid, frusemide, probenecid and xipamide were less retained. A 0.05 mol dm^{-3} SDS + 1% pentanol mobile phase gave the largest eluent strength, and with the elution being largely enhanced compared with the 0.15 mol dm^{-3} SDS mobile phase.

The behaviour of bumetanide, probenecid and xipamide was different, as retention was decreased when propanol was used as modifier compared with pentanol as modifier. Spironolactone underwent important changes in retention: with a 0.05 mol dm^{-3} SDS mobile phase without an alcohol modifier, and with a 5% methanol modifier, its retention time was >60 min, whereas with a 3% propanol modifier it was reduced to 43.5 min and with 1% pentanol it was 9 min. Other diuretics for which the retention times suffered an important diminution when using a 1% pentanol modifier in the mobile

Table 5 Detection wavelength and limits of detection (LOD] for use with a 0.05 mol dm^{-3} SDS–3% propanol mobile phase

Compound	λ/nm	LOD/μg ml^{-1}
Acetazolamide	224	0.037
Amiloride	220	0.057
Atenolol	220	0.59
Bendrofluazide	274	0.019
Bumetanide	224	0.0032
Chlorthalidone	274	0.0052
Frusemide	224	0.0029
Hydrochlorothiazide	224	0.0036
Probenecid	224	0.0051
Spironolactone	242	0.55
Triamterene	242	0.10
Xipamide	224	0.0040

Table 6 Nominal contents, recoveries and reproducibility for the drugs in the pharmaceuticals

Pharmaceutical	Content	Recovery (%)	RSD (%)
Aldactone-A (Searle)	25 mg spironolactone	102.5	4.2
Blénox (Farma)	1 g probenecid 2.5 g amoxycillin 40 mg sodic saccharin	96.1	2.8
Diamox (Cyanamid Ibérica)	250 mg acetazolamide	117.0	2.6
Diurex (Lacer)	20 mg xipamide lactose	98.3	0.8
Fordiuran (Boehringer Ingelheim)	1 mg bumetanide lactose	103.7	0.5
Hidrosaluretil (Gayoso Wellcome)	50 mg hydrochlorothiazide	104.4	0.5
Triniagar (Farmasines)	50 mg triamterene 50 mg mebuticine lactose	100.2	3.6
Aldoleo (Leo)	50 mg chlorthalidone 50 mg spironolactone	97.5 99.8	4.3 6.8
Ameride (Merck Sharp & Dohme)	50 mg hydrochlorothiazide 5 mg amiloride chlorhydrate lactose	100.7	0.3
Neatenol (Fides)	5 mg bendrofluazide 100 mg atenolol	101.4 107.5	1.5 1.4
Normopresil (Semar)	25 mg chlorthalidone 100 mg atenolol	102.9 108.0	4.5 2.1
Spirometón (Davur)	2.5 mg bendrofluazide 50 mg spironolactone	103.2 99.4	0.4 2.8

phase were amiloride, bendrofluazide, chlorthalidone, triamterene and xipamide. When elution was performed with 1% pentanol in the mobile phase, $k' < 10$ for all diuretics, except spironolactone.

With respect to the efficiencies, the behaviour was variable, but frequently the best efficiencies corresponded to a micellar mobile phase with 3% propanol, as has been indicated by other workers.[24,25] The improvement was most marked for bendrofluazide, ethacrynic acid and probenecid. However, with the 3% propanol in the mobile phase, efficiency was decreased compared with the other two mobile phases for frusemide, hydrochlorothiazide and xipamide. When retention times were either extremely short (acetazolamide) or extremely long (triamterene and spironolactone), background noise was excessive and sometimes the efficiencies could not be calculated, as the peak width at 1/10 peak height, $W_{0.1}$, was needed. For many diuretics, the most symmetrical peaks were obtained with a 'hybrid' 1% pentanol mobile phase.

In conventional liquid chromatography with hydro-organic mobile phases, as the elution strength of the solvent increases there is a systematic decrease in selectivity, expressed as $\alpha = (k'_2/k'_1)$ (k'_1 and k'_2 are the capacity factors of two solutes, with $k'_2 > k'_1$).[17] In contrast, in micellar liquid chromatography, selectivity might increase or decrease with micelle concentration depending on the nature of the compounds, that is, on the electrostatic and hydrophobic interactions with micelles.

Selectivity modifications were observed with different pairs of diuretics eluting close together. Elution order reversals occur when the mobile phase is changed. Thus, in order to compare selectivity among different mobile phases, a set order of elution should be taken to obtain the selectivity factors, such as the order of elution in 0.05 mol dm^{-3} SDS solution, in the absence of modifier. With the values of k' given in Tables 1 and 4, it can be calculated whether the selectivity increases or decreases for different pairs of compounds.

Analysis of Pharmaceutical Formulations

Retention of diuretics in a purely SDS micellar mobile phase should be decreased in order to perform the analyses. With methanol as modifier, elution was still too slow, however, when using pentanol, elution of the diuretics appearing at the beginning of the chromatogram was markedly accelerated and resolution deteriorated. Propanol showed an intermediate behaviour and sometimes gave the best efficiencies. Therefore, a 0.05 mol dm^{-3} SDS–3% propanol mobile phase was chosen.

Table 5 indicates the wavelengths of detection used for each diuretic, which was close to a maximum wavelength. A calibration curve was obtained for each diuretic with five 0.05 mol dm^{-3} SDS solutions at different concentrations. Usually, the coefficients of regression were >0.99. The highest sensitivities corresponded to bumetanide, frusemide, hydrochlorothiazide, probenecid and xipamide. The limits of detection were calculated from the background noise in the nearest of the chromatographic peaks (3σ criterion, 10 replicates). The lowest limits of detection corresponded to bumetanide, frusemide, hydrochlorothiazide and xipamide (Table 5), *i.e.*, the diuretics showing the highest sensitivity. The poorest limits of detection corresponded to spironolactone and triamterene, owing to their long retention times.

Table 6 shows the pharmaceuticals analysed that contained one or two diuretics; when two diuretics were together, one was of high or intermediate efficacy and the other of low efficacy. The peaks were always well resolved. Some preparations also contained another drug, such as a β-blocker or a stimulant, which did not interfere with the analyses. The determination of atenolol was also considered. When the solutions of the preparations were injected into the column, a peak was always observed in the dead volume of the system, which probably corresponded to the excipient.

Amiloride, triamterene, spironolactone and atenolol had long retention times. The determination of these compounds is more appropriate with a mobile phase of high eluent strength, *e.g.*, with an SDS–pentanol mobile phase. The determination of some of these compounds with the SDS–propanol mobile phase was also examined.

Table 6 also shows the recoveries with respect to the composition given by the manufacturers. These were usually in the 96–104% range. Relative standard deviations (RSDs) of five replicate injections were usually in the 0.3–4.2% range. The results indicate that micellar liquid chromatography is adequate for the determination of diuretics in pharmaceutical preparations.

This work was supported by the Comisión Interministerial de Ciencia y Technologia (CICyT), Project DEP89-0429.

References

1 Honigberg, I. L., Stewart, J. T., Smith, A. P., and Hester, D. W., *J. Pharm. Sci.*, 1975, **64**, 1201.
2 Menon, G. N., and White, L. B., *J. Pharm. Sci.*, 1981, **70**, 1083.

3 Roth, J., Rapaka, R. S., and Prasad, V. K., *Anal. Lett.*, 1981, **14**, 1013.
4 Walters, S. M., and Stonys, D. B., *J. Chromatogr. Sci.*, 1983, **21**, 43.
5 de Croo, F., van den Bossche, W., and de Moerloose, P., *Chromatographia*, 1985, **20**, 477.
6 Fogel, J., Sisco, J., and Hess, F., *J. Assoc. Off. Anal. Chem.*, 1985, **68**, 96.
7 de Croo, F., van den Bossche, W., and de Moerloose, P., *J. Chromatogr.*, 1985, **329**, 422.
8 Yarwood, R. J., Moore, W. D., and Collett, J. H., *J. Pharm. Sci.*, 1985, **74**, 220.
9 Sane, R. T., Sadana, G. S., Bhounsule, G. J., Gaonkar, M. V., Nadkarni, A. D., and Nayak, G., *J. Chromatogr.*, 1986, **356**, 468.
10 de Croo, F., van den Bossche, W., and de Moerloose, P., *J. Chromatogr.*, 1986, **354**, 367.
11 Hitscherich, M. E., Rydberg, E. M., Tsilifonis, D. C., and Daly, R. E., *J. Liq. Chromatogr.*, 1987, **10**, 1011.
12 Bachman, W. J., and Stewart, J. T., *J. Chromatogr. Sci.*, 1990, **28**, 123.
13 Dorsey, J., Khaledi, M. G., Landy, J. S., and Lin, J.-L., *J. Chromatogr.*, 1984, **316**, 183.
14 Borgerding, M. F., Hinze, W. L., Stafford, L. D., Fulp, G. W., Jr., and Hamlin, W. C., Jr., *Anal. Chem.*, 1989, **61**, 1353.
15 Berthod, A., Girard, I., and Gonnet, C., *Anal. Chem.*, 1986, **58**, 1362.
16 Khaledi, M. G., *Anal. Chem.*, 1988, **60**, 876.
17 Khaledi, M. G., Strasters, J. K., Rodgers, A. H., and Breyer, E. D., *Anal. Chem.*, 1990, **62**, 130.
18 Foley, J. P., and Dorsey, J. G., *Anal. Chem.*, 1983, **55**, 730.
19 Armstrong, D. W., and Nome, F., *Anal. Chem.*, 1981, **53**, 1662.
20 Arunyanart, M., and Cline Love, L. J., *Anal. Chem.*, 1984, **56**, 1557.
21 Borgerding, M. F., Quina, F. H., Hinze, W. L., Bowermaster, J., and McNair, H. M., *Anal. Chem.*, 1988, **60**, 2520.
22 Armstrong, D. W., and Stine, G. Y., *Anal. Chem.*, 1983, **55**, 2317.
23 Yarmchuk, P., Weinberger, R., Hirsch, R. F., and Cline Love, L. J., *Anal. Chem.*, 1982, **54**, 2233.
24 Dorsey, J. G., DeEchegaray, M. T., and Landy, J. S., *Anal. Chem.*, 1983, **55**, 924.
25 Berthod, A., and Roussel, A., *J. Chromatogr.*, 1988, **449**, 349.

Paper 1/04774D
Received September 16, 1991
Accepted November 11, 1991

Determination of Neutral Sizing Agents in Paper by Pyrolysis–Gas Chromatography

Tatsuya Yano,* Hajime Ohtani and Shin Tsuget
Department of Applied Chemistry, Faculty of Engineering, Nagoya University, Furo-cho, Chikusa, Nagoya, 464-01, Japan
Takao Obokata
DIC-Hercules Chemicals Inc., Ichihara 290, Japan

Neutral sizing agents, *viz.*, alkylketene dimers (AKDs) and alkenylsuccinic anhydride (ASA), in paper were determined by pyrolysis–gas chromatography, including those that reacted chemically with the paper. The peaks of intact AKDs and related ketones in the pyrograms were used as the key peaks for the determination of AKDs in paper samples containing between 0.025 and 1.0% of AKDs. The results obtained suggest that almost 75% of the AKDs added are retained in all the paper samples. Further, the relationship between the AKD content and the degree of sizing is interpreted in terms of the possible paper sizing mechanisms. The ASA content in paper was also determined in essentially the same way as for the AKDs, and is discussed in relation to the degree of sizing.

Keywords: *Pyrolysis–gas chromatography; neutral sizing agent; paper; alkylketene dimer; alkenylsuccinic anhydride*

As paper is composed of hydrophilic cellulose fibres, it tends to absorb aqueous liquids by capillary action of the inter- and intra-fibre voids. Although this property is useful for filter and blotting paper, printing and writing paper has to be resistant to the blotting of ink to some extent. Therefore, sizing agents are often added to the pulp slurry or applied to the surface of the paper in order to improve the printing and writing qualities by developing resistance to penetration by aqueous liquids. Rosin–alum is one of the most popular and traditional sizing agents. However, it is difficult to preserve paper sized with rosin–alum for long periods of time because of the acidic nature of alum (aluminium sulfate).

On the other hand, sizing agents such as alkylketene dimers (AKDs) and alkenylsuccinic anhydride (ASA) react covalently with the hydroxy groups of cellulose to form ester linkages under neutral or alkaline conditions.[1,2] Therefore, small amounts of AKDs and ASA can provide strong sizing effects for prolonged periods without destroying the paper matrix.

These sizing agents are generally added to the pulp slurry and are partly lost with wasted white water. Moreover, the AKDs retained in the paper are known to have at least three different forms:[1]

(*a*) intact AKDs physically adsorbed with cellulose

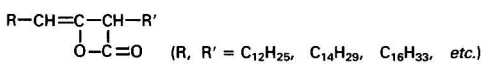

(*b*) ketones formed by hydrolysis

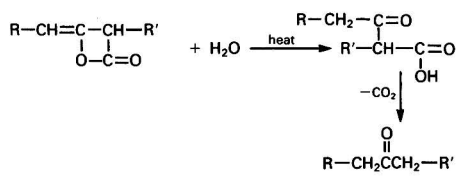

(*c*) β-keto esters formed by reaction with the hydroxy groups of cellulose

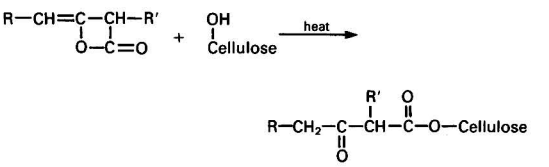

By analogy with AKDs, ASA in paper could have three possible forms:

(*a*) intact ASA

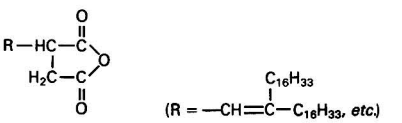

(*b*) di-acids formed by hydrolysis

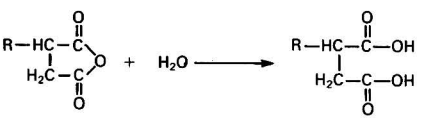

(*c*) The ester acids formed by reaction with the hydroxy groups of cellulose

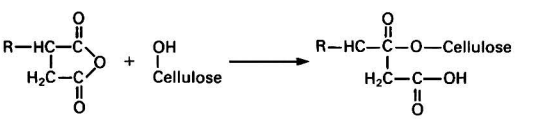

By examining ASA in paper with infrared spectroscopy, McCarthy and Stratton[2] reported that the esterification of ASA with the hydroxy groups of cellulose and the resulting sizing effect were strongly influenced by the drying conditions.

Therefore, the discriminative determination of each form of AKD or ASA would be highly desirable in the field of paper manufacture. In order to study the mechanism of neutral

* Present address: DIC-Hercules Chemicals Inc., Ichihara 290, Japan.

† To whom correspondence should be addressed.

sizing, Roberts and Garner[1] determined the content of AKDs in papers by using ^{14}C-labelled reagents. The radioactivity of the paper samples before and after extraction with chloroform was measured in order to distinguish between the reagents that had reacted with cellulose and those that had not. Pan *et al.*[3] reported that ultrasonic attenuation by paper in water corresponded to the amount of AKDs in a paper sheet.

Recently, Dart and McCalley[4] determined the content of AKDs in paper by capillary gas chromatography–mass spectrometry (GC–MS) based on hydrolytic extraction followed by quantification of the resulting long-chain ketones. However, the recovery of the AKDs was not quantitative because they reacted with the hydroxy groups of cellulose still present in the paper even after the extraction.

In recent work, pyrolysis–gas chromatography (GC) was successfully applied to the determination of small amounts of a polyamide–epichlorohydrin wet-strength resin added to paper.[5] In the present work, AKDs and ASA in paper, including those that cannot be extracted with a solvent, were determined by using essentially the same technique. The results obtained are interpreted in terms of the possible mechanisms of sizing.

Experimental

Materials

The AKD emulsion (Aqapel 12), which contains a solid fraction (20%) including AKDs (86%), produced by DIC-Hercules Chemicals, was added to the pulp slurry at pH 8.0 in order to prepare the paper samples. The samples were then dried with a drum dryer at 100 °C for 50 s. The eight paper samples containing various amounts of AKDs are listed in Table 1 together with their Stoeckigt degrees of sizing.[6] All the samples contained 0.5% of polyamide–epichlorohydrin resin.

The ASA (hexadecenylsuccinic anhydride containing 16% octadecenylsuccinic anhydride) produced by the Dixie Chemical Co. was also added to the pulp slurry at pH 7.5 to prepare the other two paper samples containing 0.12% of ASA. These samples also contained 20% of $CaCO_3$, 0.75% of cationic starch, 0.5% of $Al_2(SO_4)_3 \cdot 14H_2O$ and 0.02% of polyacrylamide.

In addition, standard paper samples containing known amounts of AKDs or ASA were also prepared for calibration. A prescribed amount of the AKD emulsion was added to two sheets of filter-paper (Advantec Toyo No. 6, 90 mm diameter) and then dried at 105 °C. Seven types of standard paper samples with AKD concentrations ranging from 0.004 to 2.3% were prepared. The standard paper samples containing ASA were also prepared in essentially the same manner.

All the paper samples were cryo-milled into a fine powder by a freeze/mill (Spex 6700) prior to pyrolysis–GC measurements in order to homogenize the samples.

Conditions for Pyrolysis–GC

The high-resolution pyrolysis–GC system utilized in this work was essentially the same as that described previously.[7] A vertical microfurnace-type pyrolyser (Yanagimoto GP-1018) was directly attached to a gas chromatograph (Shimadzu GC-9A) equipped with a flame-ionization detector. About 0.5 mg of the milled paper sample, 0.1 mg of the AKD sample or 0.02 mg of the ASA sample was placed in a platinum sample cup and then pyrolysed under a flow of nitrogen carrier gas. The pyrolysis temperature was set empirically at 500 °C, which was sufficiently high to attain almost complete thermal degradation of the main cellulose matrix of the paper and to achieve thermal desorption of the various reagents added to the paper sample. A fused silica capillary column (30 m × 0.25 mm i.d.) coated with dimethylsiloxane or 5% phenylmethylsiloxane (0.25 μm thick), immobilized by chemical cross-linking, was used. The 50 ml min^{-1} carrier gas flow rate at the pyrolyser was reduced to 1.0 ml min^{-1} at the capillary column by means of a splitter. The column temperature was initially set at 50 °C and then programmed to increase to 300 °C at a rate of 5 °C min^{-1}. Identification of the peaks on the pyrograms was mainly carried out using a GC–MS system (Shimadzu QP-1000) with an electron impact ionization source to which the pyrolyser was also directly attached.

Table 1 Paper samples containing AKDs

Sample No.	AKD dosage (%)	Stoeckigt degree of sizing/s
1	0	0.1
2	0.025	4.6
3	0.05	21.9
4	0.075	32.0
5	0.1	44.7
6	0.2	91.8
7	0.5	125.0
8	1.0	162.0

Results and Discussion

Determination of Retained AKDs

The pyrogram of the AKD sample at 500 °C is shown in Fig. 1(*a*). The peaks in the pyrogram are summarized in Table 2. The main products are intact AKDs and their hydrolysis products (ketones), which are observed in the latter part of the pyrogram. As the AKD sample utilized consists of a mixture of various ketene dimers mainly with C_{12}- and C_{14}-, C_{14}- and C_{14}-, C_{14}- and C_{16}-, and C_{16}, and C_{16}-alkyl chains, the main peaks in the latter part of the pyrogram are assigned to the corresponding four AKDs and the four associated ketones.

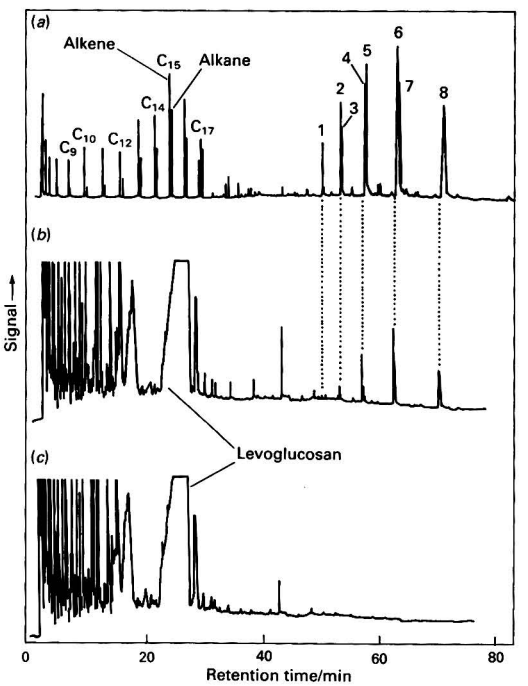

Fig. 1 Pyrograms of a paper sample containing AKDs and pure AKDs at 500 °C. (*a*) Pure AKDs; (*b*) paper with 1.0% of AKDs added; and (*c*) control paper. Peak numbers correspond to those in Table 2

Table 2 Assignment of the main peaks derived from AKDs

Peak No.	Compound	Structure of alkyl chains, R,R'* Total number of carbon atoms	Combination
1	Ketone	26	$C_{12}H_{26}$ and $C_{14}H_{30}$
2	AKD	26	$C_{12}H_{26}$ and $C_{14}H_{30}$
3	Ketone	28	$C_{14}H_{30}$ and $C_{14}H_{30}$
4	AKD	28	$C_{14}H_{30}$ and $C_{14}H_{30}$
5	Ketone	30	$C_{14}H_{30}$ and $C_{16}H_{34}$
6	AKD	30	$C_{14}H_{30}$ and $C_{16}H_{34}$
7	Ketone	32	$C_{16}H_{34}$ and $C_{16}H_{34}$
8	AKD	32	$C_{16}H_{34}$ and $C_{16}H_{34}$

* Ketone, $R-CH_2\overset{O}{\overset{\|}{C}}CH_2-R'$ AKD, $R-CH=\underset{O-C=O}{\overset{}{C}}-CH-R'$

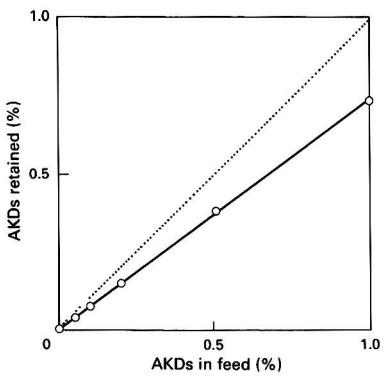

Fig. 2 Relationship between feed of AKDs into the pulp slurry and AKDs retained in a paper sample, estimated by pyrolysis–GC. Solid line: observed relationship. Broken line: hypothetical relationship for complete retention (100%)

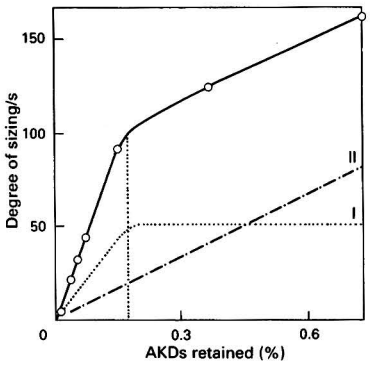

Fig. 3 Relationship between AKD content determined by pyrolysis–GC and degree of sizing of paper samples. For details, see text

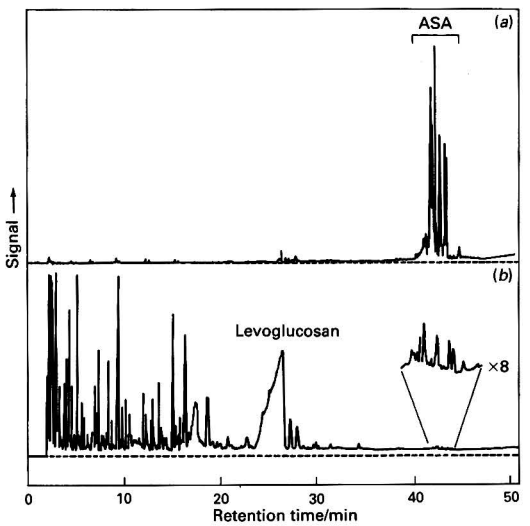

Fig. 4 Pyrograms of a paper sample containing ASA and pure ASA at 500 °C. (*a*) Pure ASA and (*b*) paper with 1.2% of ASA added

About 70% of the weighed AKD sample was recovered as the intact AKDs and the associated ketones in the pyrogram under the pyrolysis conditions used, whereas the remaining 30% was mostly degraded to a series of hydrocarbons (up to C_{17}), which were observed in the early part of the pyrogram, each of which mainly consisted of a doublet corresponding to an alk-1-ene and an *n*-alkane formed from the alkyl groups in the AKDs.

The pyrogram of the paper prepared by feeding 1.0% of AKD into the pulp slurry is shown in Fig. 1(*b*). Although the region for the peaks of the hydrocarbons from AKD overlaps that for the pyrolysates from cellulose, the eight major peaks of the ketones and AKDs are clearly observed in the pyrogram after a large number of polar pyrolysates such as levoglucosan, formed from cellulose, have been eluted. On the other hand, no significant peaks are observed in the latter part of the pyrogram of the paper containing no additives [Fig. 1(*c*)]. Therefore, the AKDs and the ketones can be used as the key peaks for the determination of AKDs.

Here, the AKD content in a given paper sample was calculated on the basis of the total intensities of the eight major peaks (1–8) observed in the pyrogram. Firstly, the relationship between the AKD content and the total intensities of the eight peaks relative to the sample mass was established by using the seven standard samples with AKD concentrations ranging from 0.004 to 2.3%. The correlation coefficient for the seven calibration points was 0.999. Then, the peak intensities in the pyrogram of a weighed unknown sample were correlated to the calibration graph thus prepared. The contents determined in this manner must be the total amounts of AKDs in the paper, including those AKDs that have reacted chemically with the hydroxy groups of cellulose and those that have been physically adsorbed, because the cellulose matrix is completely degraded to volatile products under the pyrolysis conditions used. This method was successfully applied to the analysis of a sample containing only 0.001% of AKDs. The observed reproducibility was within 4% of the relative standard deviation for five repetitive runs with the same sample (sample No. 3).

Table 3 ASA contents determined by pyrolysis–GC and degree of sizing of paper samples prepared in the presence of 0.12% of ASA

Sample No.	ASA in paper (%)	ASA retained (%)	Stoeckigt degree of sizing/s
1	0.056	47	27.8
2	0.077	64	38.5

As shown in Fig. 2, an almost linear relationship holds between the amounts of AKDs fed into the pulp slurry and the amounts retained in the paper as calculated by pyrolysis–GC. The broken line refers to the hypothetical relationship for complete retention (100%). The results obtained suggest that

almost the same fraction (about 75%) of AKDs added is retained in the paper samples prepared by adding AKD at concentrations of between 0.025 and 1.0%. On the other hand, as shown in Fig. 3, the relationship between the AKD contents determined by pyrolysis–GC and the degree of sizing of the paper samples does not exhibit a simple linear tendency. The degree of sizing is approximately proportional to the AKD content up to about 0.15%, whereas the slope of the graph rapidly deviates from linearity at higher contents. Although initially (<0.15% AKDs retained), both the chemical reaction to the AKDs with the hydroxy groups of cellulose (I) and their physical adsorption onto cellulose (II) might lead to an almost linear increase in the degree of sizing, the chemical reaction would eventually be fully completed at a certain amount of retained AKDs (about 0.15%) when the available hydroxy groups of cellulose on the surface of the paper matrix had been consumed. On the other hand, physical adsorption can still proceed at the higher concentrations of AKDs added, so that the degree of sizing might then be increased mostly by the physically adsorbed AKDs. The ratio of the increase in the degree of sizing in the first stage to that in the second stage (see Fig. 3) is about 1 : 5. This result suggests that the chemically reacted AKDs might be about four times as effective as the physically adsorbed AKDs for the development of sizing.

Determination of Retained ASA

The pyrograms at 500 °C for ASA and the paper to which 0.12% of ASA has been added are shown in Fig. 4. The main peaks observed in Fig. 4(*a*) are due to intact ASA together with minor pyrolysis products such as alkanes and alkenes formed from the alkyl groups of the ASA. As the ASA generally consists of a complex mixture of various homologues and isomers with alkyl groups of different chain length and/or structure, the resulting chromatogram is very complex. As the small peaks of vaporized ASA are also clearly observed in Fig. 4(*b*), the ASA content in the paper samples can also be calculated from the intensity in a similar manner to that for the AKDs.

The ASA contents determined by pyrolysis–GC, and the Stoeckigt degrees of sizing for the two paper samples prepared from the same pulp slurry containing 0.12% of ASA, are shown in Table 3. However, the degree of sizing of the two paper samples is different, in spite of the fact that the initial ASA dose was the same in both instances. The amounts of ASA retained in the paper, as determined by pyrolysis–GC, are consistent with the degree of sizing of the paper. These results demonstrate that pyrolysis–GC can be used to determine trace amounts of neutral sizing agents in paper.

References

1 Roberts, J. C., and Garner, D. N., *Tappi J.*, 1985, **68**, 118.
2 McCarthy, W. R., and Stratton, R. A., *Tappi J.*, 1987, **70**, 117.
3 Pan, Y. I., Kuga, S., Usuda, M., and Kadoya, T., *Tappi J.*, 1985, **68**, 98.
4 Dart, P. J., and McCalley, D. V., *Analyst*, 1990, **115**, 13.
5 Yano, T., Ohtani, H., Tsuge, S., and Obokata, T., *Tappi J.*, 1991, **74**, 197.
6 JIS P 8122, *Testing Method for Stoeckigt Sizing Degree of Paper*, Japanese Industrial Standards Committee, Tokyo, 1976.
7 Ohtani, H., Kimura, T., and Tsuge, S., *Anal. Sci.*, 1986, **2**, 179.

Paper 1/03409J
Received July 8, 1991
Accepted November 18, 1991

trans-Cyclohexano Crown Ethers as Ion Sensors in Cation-selective Electrodes

R. D. Tsingarelli, L. K. Shpigun,* V. V. Samoshin, O. A. Zelyonkina, M. E. Zapolsky, N. S. Zefirov and Yu. A. Zolotov

N.S.Kurnakov Institute of General and Inorganic Chemistry, USSR Academy of Sciences, Leninsky Prospect 31, Moscow 117907, Russia

Several *trans*-cyclohexano crown ethers have been synthesized and studied as sensor materials for different metal cations in PVC-matrix membranes of ion-selective electrodes. The potentiometric selectivity of the membranes has been found to correlate with the chemical structure peculiarities of the incorporated compound and can be changed by variation of the substituent attached to the cyclohexane fragment. Some of the compounds show superior selectivity for potassium over many other metal cations.

Keywords: *Ion-selective electrode; macrocyclic crown ether; sensor material*

Ion-selective electrodes (ISEs) with liquid membranes containing electrically neutral lipophilic macrocyclic or non-cyclic ion carriers are widely used for the determination of different metal ions in various samples.[1-3] The significance of macrocyclic compounds as cation-sensor materials in ISEs has been recognized, and increasing interest has been focused on the molecular design of these structures. This has resulted in the development of ISEs based on synthesized ionophores.[4] The function mechanism of such sensors is based on a cation-transfer reaction at the membrane interface (or at the aqueous solution–organic phase boundary) by means of reversible complexation of the cation by the neutral carrier introduced into the membrane.[5] In fact, the potentiometric selectivity of these compounds for various equally charged metal cations is related to the ratio of their corresponding complex stability constants,[6] and has been found to correlate with their extraction constants.[7] Although a number of compounds have been synthesized, the molecular design of a sensor with given analytically relevant ion selectivity still remains empirical.[8,9] Hence, some specifically complexing macro-heterocyclic compounds, *e.g.*, some crown ethers,[5,10] either do not act as ionophores in membranes or do not reveal an electrode activity[11,12]

The present paper describes a comparative study on the potentiometric selectivity of a series of solvent polymeric membranes, containing a number of *trans*-cyclohexano crown ethers (*trans*-CCEs) and their 4-alkyl derivatives as the sensor material, in ISEs. The results are discussed in terms of the chemical structure peculiarities and of the possibility of complex formation between these compounds and alkali or alkaline earth metal cations.

Experimental

Reagents

All the crown compounds investigated were obtained from appropriate cyclohexano glycols and oligoethylene glycol ditosylates by well-known cyclization procedures[13] (Fig. 1). Cyclohexano glycols in turn were prepared by the acid-catalysed reaction of the corresponding epoxides with oligoethylene glycols.[14,15] The wide variety of potential reactants makes this approach to the synthesis of *trans*-CCEs flexible and highly promising.

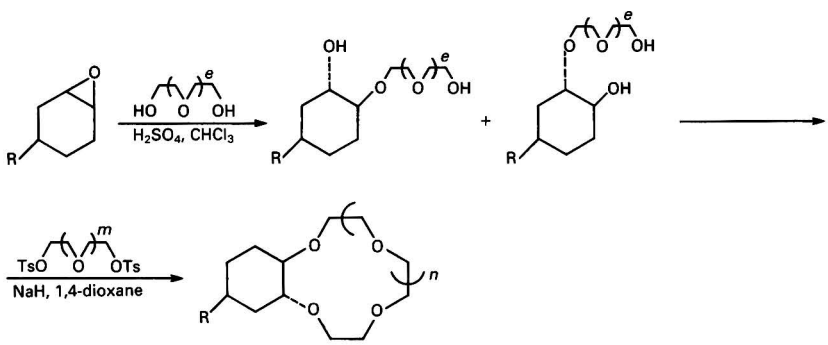

I: $n = 2$, R = H	VI: $n = 2$, R = CH_3	XI: $n = 2$, R = $(CH_3)_3C$
II: $n = 3$, R = H	VII: $n = 3$, R = CH_3	XII: $n = 3$, R = $(CH_3)_3C$
III: $n = 4$, R = H	VIII: $n = 4$, R = CH_3	XIII: $n = 4$, R = $(CH_3)_3C$
IV: $n = 5$, R = H	IX: $n = 5$, R = CH_3	XIV: $n = 5$, R = $(CH_3)_3C$
V: $n = 6$, R = H	X: $n = 6$, R = CH_3	XV: $n = 6$, R = $(CH_3)_3C$

Fig. 1 Synthesis of the crown compounds investigated

* To whom correspondence should be addressed

Table 1 Potentiometric selectivity coefficients of various membranes containing *trans*-cyclohexano crown ethers

	$-\log k^{pot}_{K^+,M^{n+}}$ ($n = 5$; $P = 0.95$)							
trans-CCE	Li^+	Na^+	Rb^+	Cs^+	Mg^{2+}	Ca^{2+}	Sr^{2+}	Ba^{2+}
H-CCE—								
15C5 (I)	2.18	0.50	0.17	0.45	2.23	2.18	2.86	2.05
18C6 (II)	1.80	0.73	0.03	0.15	2.57	2.86	2.68	2.05
21C7 (III)	2.37	0.94	0.26	0.31	2.08	3.14	2.76	2.24
24C8 (IV)	2.36	0.86	0.18	0.50	2.50	2.68	3.08	1.55
27C9 (V)	1.68	0.69	0.26	0.77	1.80	1.77	2.09	0.99
CH_3-CCE—								
15C5 (VI)	1.20	0.00	−0.13	0.70	1.90	2.20	1.50	1.00
18C6 (VII)	2.30	1.20	0.10	0.60	2.80	2.84	2.80	2.04
21C7 (VIII)	2.07	1.01	0.00	0.15	2.17	2.68	2.41	1.56
24C8 (IX)	2.19	0.31	0.18	0.36	2.26	2.82	2.58	1.69
27C9 (X)	1.00	0.29	0.19	0.43	0.88	1.72	1.22	0.76
$C(CH_3)_3$-CCE—								
15C5 (XI)	1.80	0.05	0.25	0.68	1.43	1.34	1.36	0.75
18C6 (XII)	2.40	1.30	0.45	1.00	2.61	3.15	2.88	2.35
21C7 (XIII)	1.43	0.95	0.00	0.20	2.29	1.80	2.44	1.96
24C8 (XIV)	2.51	1.06	0.08	0.30	2.67	3.20	3.20	2.29
27C9 (XV)	2.03	1.10	0.05	0.21	2.41	2.53	2.09	1.24

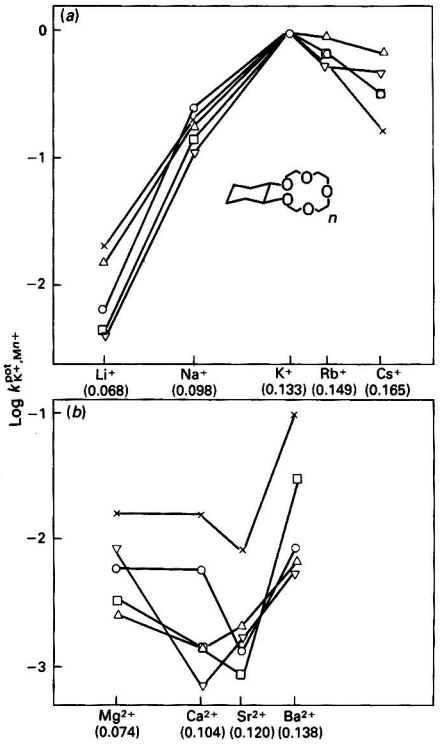

Fig. 2 Dependence of the potentiometric selectivity coefficients (log k) on the cationic radius (r) for (*a*) alkali metal cations and (*b*) alkaline earth metal cations. The values in parentheses on the abscissa are the cationic radii of the metal ions in nanometres. ○, $n = 1$; △, $n = 2$; ▽, $n = 3$; □, $n = 4$; and ×, $n = 5$

Membranes

The plasticized polymer membranes containing the above-mentioned macrocycles were prepared by a known procedure.[16] the membranes included (mass ratio in percentages): macrocycle, 1.0; poly(vinyl chloride) (PVC), 33.0; and *o*-nitrophenyl octyl ether, 66.0. Reference PVC membranes, which did not contain macrocycles, were also prepared. The thickness of the membrane thus obtained was 0.1–0.2 mm. All the membranes were conditioned before use by soaking for 24 h in 0.02 mol dm^{-3} potassium chloride.

Electrode System and e.m.f. Measurements

The membranes were studied with use of electrochemical cells of the following type:

Ag–AgCl|KCl(0.1 mol dm^{-3})| Bridge electrolyte |Sample |Membrane‖KCl(0.1 mol dm^{-3})AgCl–Ag

The conditioned membrane discs (10 mm in diameter) were assembled in a commercial electrode body (NPO Analit Pribor, Tbilisi). A double-junction reference electrode was also used (Model 90-02: Orion Research, Cambridge, MA, USA) and the outer filling solution was 0.1 mol dm^{-3} ammonium nitrate.

The e.m.f. measurements were carried out at 295 ± 2 K, with use of a digital Radelkis (Budapest, Hungary) OP-208 pH meter. Potentiometric selectivity coefficients for different metal cations relative to potassium ions ($k^{pot}_{K^+,M^{n+}}$) were determined by the separate-solution method with the 0.1 mol dm^{-3} respective metal ion solutions.[17]

Results and Discussion

The membrane potentiometric selectivity for alkali and alkaline earth metal cations, referred to K^+, was studied. Table 1 lists the selectivity coefficients obtained. It is shown that the values $-\log k^{pot}_{K^+,M^{n+}}$ ($n = 1,2$) for each metal cation depend significantly both on the size of the ring and on the nature of the substituent R in the cyclohexane fragment. All the *trans*-CCEs studied reveal selectivity towards alkali metal cations, especially K^+ and Rb^+.

Fig. 2(*a*) shows that the dependence of $-\log k^{pot}_{K^+,M^+}$ on the cationic radius for alkali metals has a maximum at 0.133 nm, irrespective of the size of the crown ether ring (when R = H). The order of selectivity is as follows: K^+, Rb^+, Cs^+, Na^+, Li^+. The values of $-\log k^{pot}_{K^+,Li^+}$ are 1.0–2.5 orders of magnitude lower than those for other alkali metals. It is interesting to note that the above-mentioned experimental results, especially the highest potentiometric selectivity towards K^+, are in agreement with those for the crown ethers not containing the cyclohexane fragment.[18]

On the other hand, for alkaline earth metal cations, the analogous curves have minima at 0.098–0.113 nm [Fig. 2(*b*)]. The order of the selectivity in this instance is different for each macrocycle, but all $\log k^{pot}_{K^+,M^{2+}}$ values are essentially lower than those for alkali metals, except Li^+. This indicates that the known hole-size concept[19,20] cannot be used to predict the potentiometric selectivity of membrane electrode systems.

Fig. 3 shows the dependence of $k^{pot}_{K^+,M^{n+}}$ on the size of the macrocycle. These curves are non-monotonic for all metal ions, especially for the alkyl derivatives of *trans*-CCEs. Hence, for *tert*-butyl derivatives (**XI–XV**), there are two distinct minima at 18-crown-6 (18C6) and 24-crown-8 (24C8) ($n = 3$ and 5), which alternate with three maxima at 15-crown-5 (15C5), 21-crown-7 (21C7) and 27-crown-9 (27C9) ($n = 2$, 4 and 6). The highest selectivity for K^+ compared with alkaline earth metal cations and Li^+ is observed for membranes containing *tert*-butyl-*trans*-cyclohexano-18-crown-6 (**XII**) and *tert*-butyl-*trans*-cyclohexano-24-crown-8 (**XIV**). The influence of other alkali metal cations is relatively low only for compound **XII**. The membranes containing methyl-*trans*-cyclohexano-15-crown-5 (**XI**) are sensitive to the cations Rb^+, Na^+ and K^+.

Hence, the introduction of a fairly well-branched alkyl substituent into the cyclohexane fragment results in a significant change in the cation selectivity of the membrane.

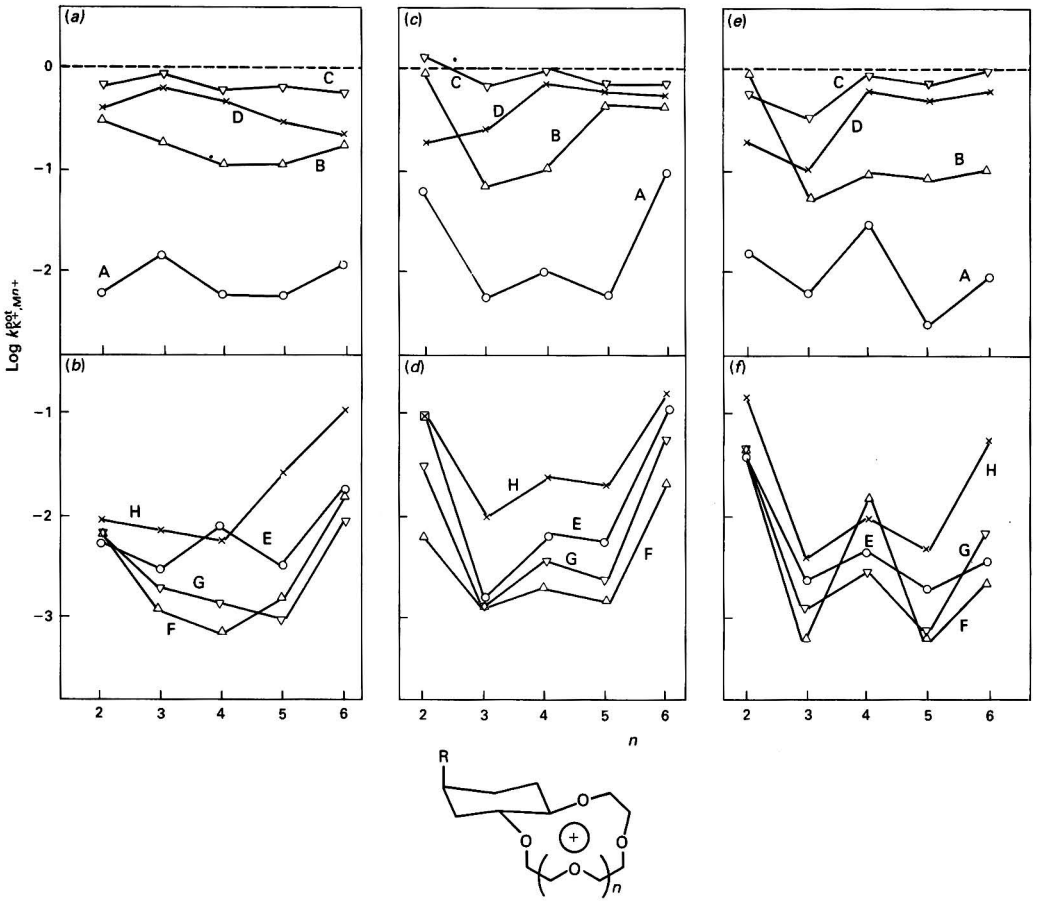

Fig. 3 Dependence of the potentiometric selectivity coefficients (log $k^{pot}_{K^+,M^{n+}}$) on the number (n) of binding-site atoms in the macrocyclic ring. (a) and (b): R = H; (c) and (d): R = CH_3; (e) and (f): R = $C(CH_3)_3$. A, Li^+; B, Na^+; C, Rb^+; D, Cs^+; E, Mg^{2+}; F, Ca^{2+}; G, Sr^{2+}; and H, Ba^{2+}

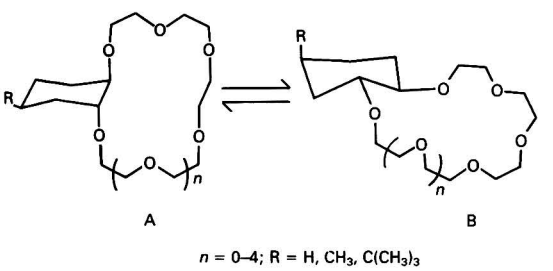

Fig. 4 Two chair conformations of the six-membered ring in *trans*-CCEs

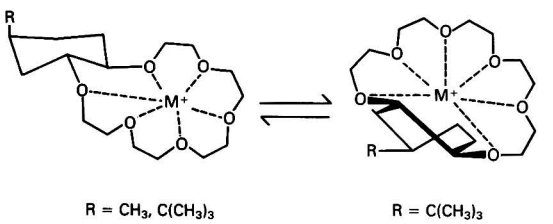

Fig. 5 Two interconverting forms of the complexes for *tert*-butyl derivatives of the *trans*-CCEs

Some of the features of *trans*-CCE membrane activity can be explained in terms of the conformational properties of these compounds. A six-membered ring in a *trans*-CCE can adopt two chair conformations, which differ in substituent orientation (Fig. 4): C–O bonds are axial in conformation A and equatorial in conformation B. Nuclear magnetic resonance (NMR) studies of the equilibrium (A $\rightleftharpoons$ B) have shown that it is strongly shifted to the conformation B (>90%) when R = H.[14,21–23] When R = CH_3, conformation A is predominant to nearly the same extent, and when R = $C(CH_3)_3$, conformation A becomes virtually the sole conformation. This regularity is in accord with conformational properties of R-substituted cyclohexanes; *i.e.*, the destabilization of the axial position of the alkyl group (B) increases with an increase in its volume.[24]

An interesting conformational feature of *trans*-CCEs is the alteration of the proportion of conformers with the increasing size of the macrocycle: the population of conformers (A) decreases on passing from *trans*-cyclohexano-15-crown-5 (**I**) to *trans*-cyclohexano-18-crown-6 (**II**), and increases again on passing from **II** to *trans*-cyclohexano-21-crown-7 (**III**).[14,21–23] Apparently, this is a related peculiarity of macrocycles.

Owing to the ring *trans* fusion, the chair–chair interconversion of the six-membered ring is accompanied by a marked change in the conformation of the macrocycle. The macrocycle in conformer A has on oval form resulting from *trans* diaxial orientation of the bridge fragment O–C–C–O. It is

known that 18-crown-6 has an analogous oval form (with symmetry C) in the crystalline state or in a non-polar solvent.[22–27] In the complexes of 18-crown-6, with most metal cations this macrocycle adopts a ring-shaped conformation (with symmetry D), and all the fragments O–C–C–O have a *gauche* conformation (dihedral angle about 60°).[13,28] For *trans*-CCE, such a conformation of the macrocycle is attainable only in conformer B. Indeed, it has been shown that the crown ether **VII** in complexes with inorganic salts adopts conformation B[14,15] in spite of destabilization by the axial methyl group. The conformational energy of the *tert*-butyl group (23 kJ mol^{-1})[24] is comparable to the energy difference between the chair and twist conformations of the cyclohexane ring (22 kJ mol^{-1}).[23] Therefore, one can expect two interconverting forms of complexes for the *tert*-butyl derivatives (Fig. 5).

The axial substituent R destabilizes the complexes of compounds **VI–XV** compared with complexes of unsubstituted compounds **I–V**. As the ionophore properties of neutral carriers are determined mainly by the stability of their complexes,[5,29] so it is believed that the change in complex-formation ability, with the introduction of a substituent R, is the result of conformational perturbation. The destabilization of complexes makes the substituted *trans*-CCE more sensitive to conformational features of the macrocycle, *e.g.*, to the alteration of conformer population with an increase in the size of the macrocycle (see above). This results in an alteration of the selectivity coefficients, which increase with an increase in the size of the substituent R.

Conclusion

The potentiometric selectivity of some synthesized *trans*-CCEs as sensor materials in PVC-matrix membrane electrodes has been studied. The selectivity for potassium by some compounds is close to that of electrodes based on valinomycin. It was observed that the properties of *trans*-CCEs as ion carriers can be modified *via* conformational change caused by variation of substituents attached to the cyclohexane fragment. This offers the possibility of purely conformational control of crown ether complexation.

References

1 Oggeneuss, P., Morf, W. E., Oesch, U., Amman, D., Pretsch, E., and Simon, W., *Anal. Chim. Acta*, 1986, **180**, 155.
2 Koryta, J., *Anal. Chim. Acta*, 1986, **183**, 1.
3 Koryta, J., *Anal. Chim. Acta*, 1988, **206**, 1.
4 Amman, D., Morf, W. E., Anker, P., Meier, P. C., Pretsch, E., and Simon, W., *Ion Sel. Electrode Rev.*, 1983, **5**, 37.
5 Morf, W. E., in *The Principles of Ion-Selective Electrodes and of Membrane Transport*, ed. Pungor, E., Akadémiai Kiadó, Budapest, 1981, p. 181.
6 Lamb, J. D., Christensen, J. J., Ocarson, J. L., Nielsen, B. L., Asay, B. W., and Izatt, R. M., *J. Am. Chem. Soc.*, 1980, **102**, 6820.
7 Yamauchi, M., Imato, T., Katahira, M., Inudo, Y., and Ishibashi, N., *Anal. Chim. Acta*, 1985, **169**, 59.
8 Amman, D., Bissig, R., Guggi, M., Pretsch, W., Simon, W., Borowith, J. J., and Weis, L., *Helv. Chim. Acta*, 1975, **58**, 1535.
9 Hara, H., and Okazaki, S., *Analyst*, 1985, **110**, 11.
10 Yoshio, M., and Noguchi, H., *Anal. Lett.*, 1982, **15**, 1197.
11 Lamb, J. D., Izatt, R. M., Raberleen, P. A., and Christensen, J. J., *J. Am. Chem. Soc.*, 1980, **102**, 2452.
12 Shpigun, L. K., Novikov, E. A., and Zolotov, Yu. A., *Zh. Anal. Khim.*, 1986, **41**, 617.
13 Hiraoka, M., in *Crown Compounds*, ed. Emanuel, N. M., Mir, Moscow, 1982, p. 266.
14 Zelenkina, O. A., Avtoreferaz Dissertation, Moscow State University, Moscow, 1987.
15 Samoschin, V. V., Zelenkina, O. A., Subbotin, O. A., Sergeev, N. M., and Zefirov, N. S., *Zh. Org. Khim.*, 1988, **24**, 265.
16 Moody, G. J., and Thomas, J. D. R., in *Ion-Selective Electrodes in Analytical Chemistry*, ed. Freiser, H., Plenum Press, New York, 1978, p. 287.
17 Camman, K., in *Rabota s Ionoselectivnimi Electrodami*, ed. Petruchin, O. M., Mir, Moscow, 1980, p. 71.
18 Mascini, M., and Pallozzi, F., *Anal. Chim. Acta*, 1974, **73**, 375.
19 Lamb, Y. Y., Izatt, R. M., Garrick, D. G., Bradshow, J. S., and Christensen, Y. Y., *J. Membr. Sci.*, 1981, **9**, 83.
20 Izatt, R. M., Bradshow, J. S., Nielsen, S. A., Lamb, J. D., and Christensen, J. J., *Chem. Rev.*, 1985, **85**, 271.
21 Samoshin, V. V., Sybbotin, O. A., Zelyonkina, O. A., and Zefirov, N. S., *Zh. Org. Khim.*, 1986, **22**, 2231.
22 Samoshin, V. V., Zelyonkina, O. A., Yartseva, I. V., and Zefirov, N. S., *Zh. Org. Khim.*, 1987, **23**, 2244.
23 Samoshin, V. V., Zelyonkina, O. A., Yartseva, I. V., Sybbotin, O. A., and Zefirov, N. S., *Zh. Org. Khim.*, 1988, **24**, 2458.
24 Potupov, V. M., *Stereokhimia*, Khimia, Moscow, 1976, p. 339.
25 Wipff, G., Weiner, P., and Kollman, P., *J. Am. Chem. Soc.*, 1982, **104**, 3249.
26 Ronghino, G., Romano, S., Lehn, T. M., and Wipff, G., *J. Am. Chem. Soc.*, 1985, **107**, 7873.
27 Takenchi, H., Arai, T., and Horada, I., *J. Mol. Struct.*, 1986, **146**, 197.
28 Spuillacote, M., Sheridan, R. S., Chapman, O. L., and Anet, F. A., *J. Am. Chem. Soc.*, 1975, **97**, 3244.
29 Moody, G. J., and Thomas, J. D. R., *Chem. Ind. (London)*, 1975, 644.

Paper 1/00922B
Received February 26, 1991
Accepted November 6, 1991

Simple Voltammetric Method for the Determination of β-Carotene in Brine and Soya Oil Samples at Mercury and Glassy Carbon Electrodes

B. Valentin Pfund and Alan M. Bond
Department of Chemistry, La Trobe University, Bundoora, 3083, Victoria, Australia
Terence C. Hughes*
Denehurst Ltd., 961 Glenhuntly Road, Caulfield South, 3162, Victoria, Australia

β-Carotene is a naturally occurring yellow–orange pigment, which can be derived from saline micro-algae marine phytoplankton and some plant-derived natural oils. In this work, a simple method for the determination of β-carotene, involving only solvent extraction from brine (or soya oil) samples into dichloromethane, followed by addition of electrolyte and direct measurement of the differential-pulse polarogram at mercury electrodes or differential-pulse voltammograms at a glassy carbon electrode, is described, based on the extremely well-defined two-electron oxidation process that occurs in non-aqueous solvents. The method has been applied to soya oil and brine reference concentrates and to feed and effluent samples associated with the production of β-carotene *via* marine micro-algae. Excellent agreement with a well-established spectrophotometric method has been obtained, confirming that the simple voltammetric method should be a useful addition to the analytical methodology available for monitoring the production of β-carotene concentrates.

Keywords: *Voltammetry; analytical determination; β-carotene*

β-Carotene is a precursor of vitamin A and contributes to the colour of many plants. It is particularly well known as a yellow–orange pigment found in carrots. β-Carotene contains 11 carbon–carbon double bonds in conjugation (Fig. 1) and owes its colour to absorption at the violet end of the visible spectrum (λ = 451 nm).[1] In view of its colour, it is not surprising that spectrophotometric methods for the determination of β-carotene have been widely used.[2]

In addition to being present in many plants, carotenoids, including β-carotene, are present at relatively high concentrations in saline micro-algae marine phytoplankton and other marine matter. For the determination of β-carotene in marine samples, high-performance liquid chromatographic separation procedures, coupled with spectrophotometric detection[3,4] and a very sensitive and specific resonance Raman method, have been described.[5,6]

In view of the presence of β-carotene in many natural products, it is not surprising that commercial products are usually derived from sources such as micro-algae. In the production of β-carotene from natural sources, it is necessary to have quality control at every stage of the plant production process. Simple methods for the rapid determination of β-carotene are, therefore, required as an alternative or in addition to the commonly used spectrophotometric methods,[2–6] which generally require relatively time-consuming separation procedures to achieve adequate selectivity.

Despite the fact that the extensive series of conjugated double bonds that are present in the structure of β-carotene should indicate that carotene is likely to be electroactive, the analytical use of voltammetric oxidation and/or reduction processes, known to occur on a range of electrode surfaces,[7–13] has been rather limited. However, the amperometric detection of β-carotene in irradiated fruits after chromatographic separation has been described in detail.[14] In this method, carotene esters and other carotene compounds are hydrolysed by addition of KOH, mixed with ethanol containing pyrogallate and extracted into light petroleum for injection on to the chromatographic column. This application refers to the determination at naturally occurring trace levels, where interference from many other related electroactive compounds is expected to occur without inclusion of a chromatographic or other form of separation into the analytical methodology. In this work, we have investigated the possibility of developing a more direct voltammetric method in which the β-carotene present in relatively high concentrations in the commercial concentrate is simply extracted into dichloromethane containing an electrolyte, and a direct voltammetric determination is then undertaken in the non-aqueous solvent. Results from this very simple procedure are then compared with a spectrophotometric method to confirm the validity of the voltammetric method.

Experimental

A 30% β-carotene sample (Hoffman-La Roche, Basle, Switzerland) was used to prepare a 10^{-2} mol dm^{-3} standard solution in dichloromethane (electrolyte). The reference material samples (technical-grade quality), provided by Betatene (Melbourne, Australia), were as follows: (*i*) 30% β-carotene in soya oil, and (*ii*) 1.5% β-carotene in brine. Samples obtained from various stages of the production of β-carotene, and examined in this work, were also supplied by

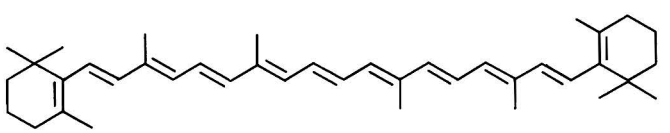

Fig. 1 Structure of β-carotene

* Present address: Unichema Australia Pty Ltd., 164 Ingles Street, Port Melbourne, 3207, Victoria, Australia.

Betatene. The reference method for the determination of β-carotene was a spectrophotometric procedure, which is approved by the AOAC.[15] It consists of a sample homogenization step, separation and purification of the β-carotene by quantitative solvent extraction into hexane, and a spectrophotometric determination under standardized conditions at 436 nm.

Before use, analytical-reagent grade dichloromethane was distilled with use of a 30 cm Vigreux column. The electrolytes were electrometric grade (G. Frederick Smith Chemicals, Columbus, OH) tetrabutylammonium perchlorate (Bu_4NClO_4) or tetrabutylammonium tetrafluoroborate (Bu_4NBF_4), used at a concentration of 0.1 mol dm^{-3} in distilled dichloromethane.

Initial voltammetric (polarographic) investigations to confirm the mechanism of the electrode processes and to establish optimal conditions for the analytical procedures were undertaken with a PAR Model 174A polarographic analyser, equipped with a dropping-mercury or platinum-disc working electrode, a platinum-wire auxiliary electrode and an Ag–AgCl (dichloromethane; saturated LiCl) reference electrode.

Analytical determinations of β-carotene were carried out with a Metrohm Model 646 VA processor and Model 647 VA stand, with use of a multi-mode mercury working electrode operated in the dropping-mercury mode, or a glassy carbon working electrode, with a glassy carbon auxiliary electrode and the same Ag–AgCl reference electrode as above.

All experiments were undertaken at 20 ± 1 °C and where necessary (for reduction studies) solutions were de-gassed with high-purity nitrogen to remove oxygen before commencing a voltammetric experiment.

Results and Discussion

Details of the Electrode Processes in Dichloromethane

Fig. 2 shows a differential-pulse polarogram for a 1 mmol dm^{-3} solution of β-carotene in dichloromethane (0.1 mol dm^{-3} Bu_4NClO_4). At a (peak) potential (E_p) of −1.70 V *versus* the Ag–AgCl, a well-defined reduction wave is observed, and at +0.59 V *versus* the Ag–AgCl, a narrower and larger oxidation process is observed. As also shown in Fig. 2, the reference compound ferrocene (Fc) exhibits a reversible one-electron oxidation process ($Fc \rightleftarrows Fc^+ + e^-$) with a peak potential of 0.50 V *versus* the Ag–AgCl under the same conditions. At a mercury electrode, no other waves were observed prior to the solvent limit (negative potential limit) or mercury electrode oxidation (positive potential limit).

Mairanovsky *et al.*[13] report a reversible one-electron reduction with a half-wave potential ($E_{\frac{1}{2}}$ value) of −1.68 V *versus* the SCE in non-aqueous solvents to produce a moderately stable anion radical (and other reduction processes at a more negative potential, which are outside the dichloromethane solvent range) and a two-electron oxidation process with an $E_{\frac{1}{2}}$ value of +0.61 V *versus* SCE. The oxidation process is a reversible two-electron charge transfer with an irreversible chemical step, following charge transfer being observed with long-term domain experiments. The separation between the E_p-values in this work and the $E_{\frac{1}{2}}$ values reported in ref. 13 agree completely, confirming that the solvent is not particularly important in determining the potential for reduction or oxidation nor probably the mechanism for either process. In agreement with Mairanovsky *et al.*, we find that the reduction process is a one-electron step and the oxidation a two-electron step, which disagrees with Takakachi and Tachi,[8,9] who described the reduction as a four-electron process.

The reduction process is chemically and electrochemically reversible in dichloromethane under conditions of cyclic voltammetry in the sense that it has a ΔE_p value at both platinum and mercury electrodes for separation of reduction and oxidation components identical to that obtained for the known reversible one-electron oxidation of Fc. The product of the reduction in dichloromethane can, therefore, be postulated to be the anion radical as is the case in other non-aqueous solvents.[13] As required for the proposed mechanism, the direct-current polarographic limiting current for the reduction step is one-half that of the oxidation process (ignoring sign differences), and, in agreement with Mairanovsky *et al.*,[13] the oxidation process, while having electrochemically reversible two-electron characteristics with respect to charge transfer, exhibits some degree of chemical irreversibility at both platinum and mercury electrodes at a scan rate of 500 mV s^{-1} (Fig. 3). Oxidation processes at more positive potentials are not discussed in this paper.

The mechanism for oxidation proposed by Mairanovsky *et al.*[13] involves the initial formation of a dication by a two-electron charge transfer process followed, in longer time domain experiments, by proton loss to form a monocation and the one-electron reduction of the monocation to a neutral, but unstable, radical is then detected on the reverse scan of cyclic voltammograms (Fig. 3). The oxidation mechanism in dichloromethane, while not studied in detail in this work, therefore appears to be the same as in other solvents examined by Mairanovsky *et al.*[13]

In dichloromethane, the above data demonstrate that, in principle, either of two processes could be used for analytical purposes. However, the oxidation process is a more sensitive two-electron step, has a narrower half-width, is better resolved from the solvent limit process, and because it is an

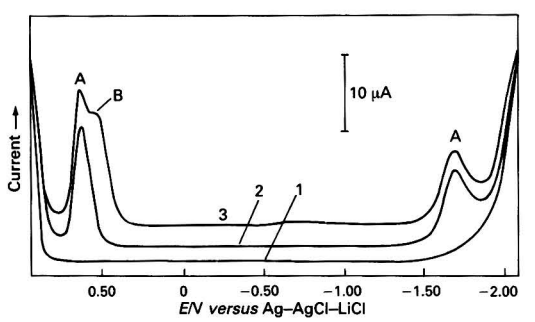

Fig. 2 Differential-pulse polarogram (drop time = 1 s, pulse amplitude = 50 mV) for reduction and oxidation of β-carotene in dichloromethane (0.1 mol dm^{-3} Bu_4NClO_4). 1, Solvent (baseline); 2, solvent and 1 × 10^{-3} mol dm^{-3} β-carotene; and 3, solvent with 1 × 10^{-3} mol dm^{-3} β-carotene and 1 × 10^{-3} mol dm^{-3} ferrocene. A, β-Carotene and B, ferrocene

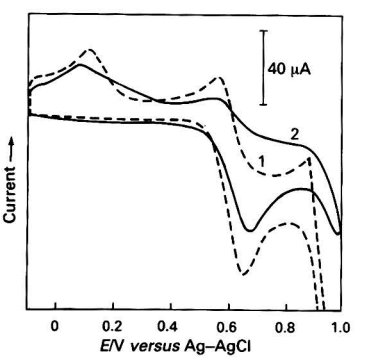

Fig. 3 Cyclic voltammograms (scan rate = 500 mV s^{-1}) obtained at 1, a slowly growing mercury electrode and 2, at a platinum disc electrode for oxidation of 1 × 10^{-3} mol dm^{-3} β-carotene in dichloromethane (0.1 mol dm^{-3} Bu_4NClO_4)

oxidation occurring at relatively positive potentials, rather than a reduction step, its use does not require the removal of oxygen. This process was, therefore, employed in subsequent analytical studies.

Differential-pulse Polarography at the Dropping-mercury Electrode

Calibration

With a drop time of 1.0 s and a pulse amplitude of 50 mV, a plot of differential-pulse peak height for the oxidation of β-carotene in dichloromethane (0.1 mol dm^{-3} Bu_4NClO_4) was linear over the concentration range of 2×10^{-5} to 10^{-3} mol dm^{-3} with a correlation coefficient of 0.9997 (slope 27.5 μA/μmol dm^{-3}, intercept 0.006 μA). At concentrations above 2×10^{-3} mol dm^{-3}, non-linearity was observed in the calibration curve, which may have been a result of Ohmic *iR* drop. Consequently, determinations were confined to concentrations up to 10^{-3} mol dm^{-3} and were undertaken by the method of standard additions to avoid matrix effects.

Determination of β-carotene in a reference soya oil sample

A 100 mg sample of β-carotene in soya oil (30%) (Betatene) was weighed into a 100 ml calibrated flask containing distilled dichloromethane (0.1 mol dm^{-3} Bu_4NClO_4). After dilution to 100 ml with dichloromethane, the differential-pulse polarogram (drop time = 1.0 s, ΔE = 50 mV) was recorded for the solution over the range +0.20 to +0.85 V *versus* the Ag–AgCl. A well-defined differential-pulse peak corresponding to oxidation of β-carotene was observed at +0.55 V *versus* the Ag–AgCl [Fig.4(*a*)]. The standard-additions method was used to determine the β-carotene in the sample with a value of 34.7 ± 0.8% of β-carotene being obtained from four determinations, which is in satisfactory agreement with the manufacturer's nominal value of 30%. Recoveries of 100 ± 3% were obtained for soya oil samples spiked with known amounts of β-carotene, which also suggests that a valid procedure has been developed for the voltammetric determination of β-carotene in soya oil.

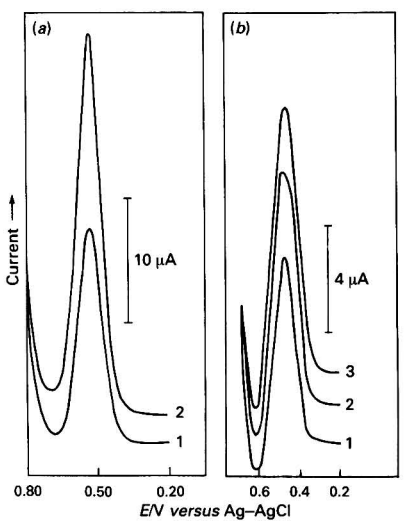

Fig. 4 Differential-pulse polarograms (drop time = 1 s, pulse amplitude = 50 mV) obtained for the determination of β-carotene in (*a*) soya oil reference sample: 1, sample; 2, after addition of 5×10^{-4} mol dm^{-3} β-carotene; and (*b*) brine reference sample: 1, sample; 2, after addition of 5×10^{-4} mol dm^{-3} β-carotene; and 3, after addition of 1×10^{-3} mol dm^{-3} β-carotene. For details see text

Determination of β-carotene in brine

A 2.50 mg sample of β-carotene concentrate in brine (1.5%) (Betatene) was extracted with distilled dichloromethane (4 × 10 ml) and, after addition of 3.4 g of Bu_4NClO_4, the extract was diluted to 100 ml with distilled dichloromethane. Differential-pulse polarograms [Fig. 4(*b*)] obtained for the solution and analysed by the standard-additions method, as for the soya oil sample, gave a value of 1.9 ± 0.1% of β-carotene, based on four determinations, which again is in satisfactory agreement with the manufacturer's nominal value of 1.5%. As was the case with the soya oil sample, recoveries of 100 ± 3% were obtained for samples of brine spiked with known amounts of β-carotene.

Table 1 Data for the differential-pulse polarographic determination of β-carotene in brine samples obtained at various stages of production from marine micro-algae (details of the method used are given in the text)

		Results (β-carotene concentration)	
Sample origin	Mass used/g	Voltammetry (n = 4)	Spectrophotometry (n = 2)
Product 2	0.625	3.06 ± 0.07 (g kg^{-1})	3.06 ± 0.07 (g kg^{-1})
Product 3	50.0	37 ± 3 (mg kg^{-1})	37 ± 4 (mg kg^{-1})
Product 1	510	1.47 ± 0.02 (mg kg^{-1})	1.61 ± 0.02 (mg kg^{-1})
Effluent 1	461	0.06 ± 0.02 (mg kg^{-1})	0.07 ± 0.02 (mg kg^{-1})
Effluent 2	509	<0.05 (mg kg^{-1})	<0.1 (mg kg^{-1})

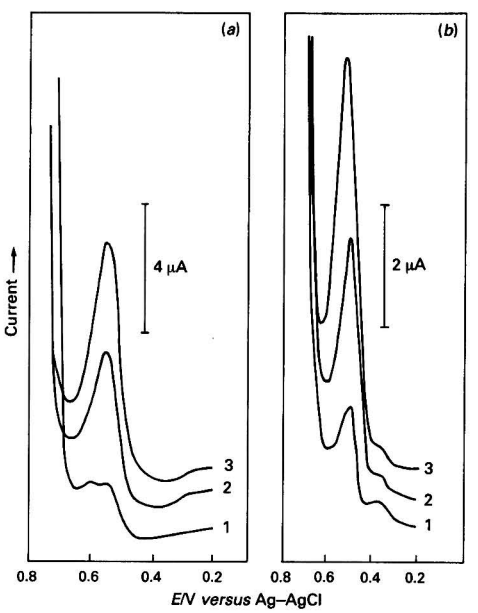

Fig. 5 Differential-pulse polarograms (drop time = 1 s, pulse amplitude = 50 mV) for the determination of β-carotene in brine plant feed samples, (*a*) product 2 sample: 1, sample; 2, sample plus 200 μl of 1×10^{-2} mol dm^{-3} β-carotene standard; 3, sample plus 400 μl of 1×10^{-2} mol dm^{-3} β-carotene standard; (*b*) product 1 sample: 1, sample; 2, sample plus 100 μl of 1×10^{-2} mol dm^{-3} β-carotene standard; 3, sample plus 200 μl of 1×10^{-2} mol dm^{-3} β-carotene standard. For details see Table 1 and text

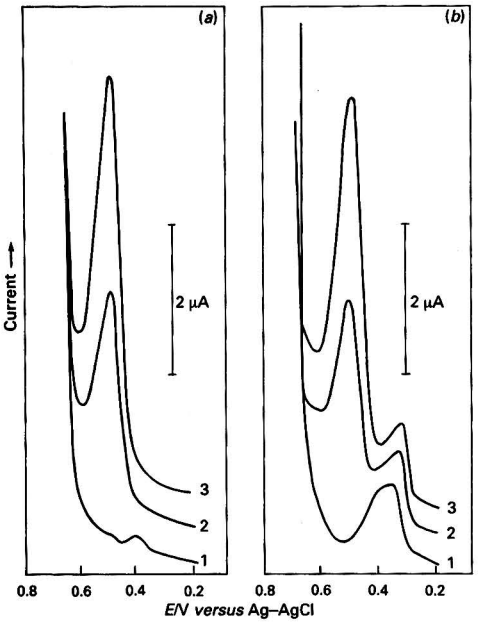

Fig. 6 Differential-pulse polarogram for the determination of β-carotene in brine plant effluent samples. (*a*) Effluent 1 sample; (*b*) Effluent 2 sample. Curve 1 is the sample and curves 2 and 3 correspond to addition of 100 and 200 μl of 1×10^{-2} mol dm^{-3} β-carotene standard, respectively. For details see Table 1 and text

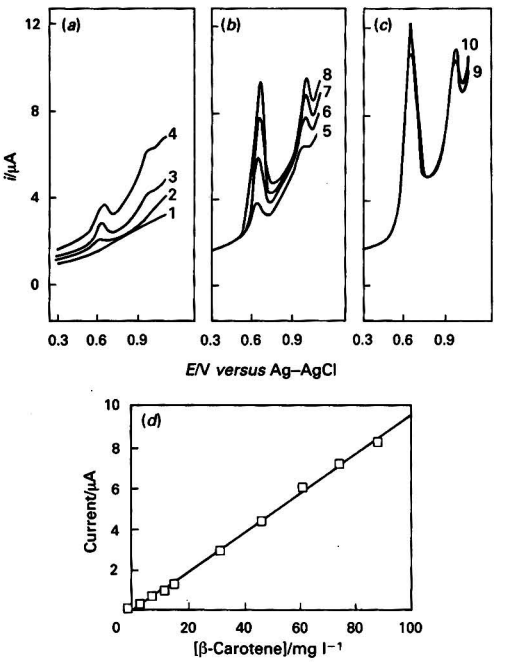

Fig. 7 (*a*)–(*c*) Differential-pulse voltammograms and (*d*) calibration graph for oxidation of β-carotene at a glassy carbon electrode in 25 ml of dichloromethane (0.1 mol dm^{-3} Bu_4NClO_4) after addition of an aliquot of a 1.00 g l^{-1} β-carotene standard solution. Curve 1 is for a sample containing no β-carotene, curves 2–5 are for samples containing 4×100 μl additions of the β-carotene standard, and curves 6–10 are for samples containing 5×400 μl additions of the β-carotene standard. Duration between pulses = 0.8 s. Pulse amplitude = 50 mV. For details see text

Determination of β-carotene in brine during various stages of production

In the commercial production of β-carotene from marine micro-algae, a substantial number of determinations are required at each of various stages of the manufacturing process. Results for the determination of β-carotene in the production samples and effluent samples are in excellent agreement with values determined spectrophotometrically, as indicated in Table 1.

For the brine samples cited in Table 1, an aliquot of each sample was extracted with distilled dichloromethane (4×5 ml) with use of a centrifuge to speed up the separation of the aqueous and dichloromethane phases. After addition of 0.85 g of Bu_4NClO_4, the extract was diluted to 25 ml with dichloromethane, and a differential-pulse polarogram was recorded.

In the 'product 2' sample, where β-carotene concentrations are very high, the polarograms are well defined and equivalent to that in Fig. 3(*b*). In the 'product 3' and 'product 1' feed samples, resolution from neighbouring peaks can be achieved and the expected peak from oxidation of β-carotene is observed at +0.5–+0.6 V *versus* the Ag–AgCl (Fig. 5). In the example of the 'effluent 1' sample [Fig. 6(*a*], the β-carotene levels are low and near the detection limit, whereas for the 'effluent 2' sample, the β-carotene concentration is below the detection limit [Fig. 6(*b*)]. However, in all instances, excellent agreement is obtained with the spectrophotometric method. Consequently, it is confirmed that the simple and direct method can be used for the determination of β-carotene in these commercially important samples without the need for separation procedures other than those introduced *via* the solvent-extraction step.

Of course, if samples at naturally occurring β-carotene levels were being examined, where many compounds at much higher concentrations than β-carotene would be present, chromatographic methods with amperometric detection, as described in ref. 14, would almost certainly be required to achieve adequate resolution from overlapping peaks that could arise from the presence of compounds having similar oxidation (reduction) potentials to β-carotene.

In contrast to naturally occurring matrices, the sample we have been interested in, β-carotene, is present at very elevated levels and is a major constituent. In this sense, it may, therefore, be surprising that no significant interference has been encountered in the analytical procedure.

Differential-pulse Voltammetry at a Glassy Carbon Electrode and with Bu_4NBF_4 Electrolyte

In a production plant environment, analytical procedures requiring mercury, as used with the technique of polarography, may not be considered to be suitable from the aspect of occupational health. Consequently, differential-pulse voltammetry at a glassy carbon electrode was examined as an alternative to polarography at a dropping-mercury electrode. As shown in Fig. 7, well-defined curves and linear calibration curves can be obtained at the glassy carbon electrode, and data essentially indistinguishable from those obtained at the mercury electrode are observed for all samples. Use of a glassy carbon electrode for asymmetric detection after chromatographic separation obviously also would be preferred in a liquid chromatography–electrochemical detection method. Similarly, replacement of a 0.1 mol dm^{-3} Bu_4NClO_4 by 0.1 mol dm^{-3} Bu_4NBF_4 was examined and also found to be equally suitable for the determination of β-carotene. Perchlorate electrolytes are often regarded as potentially explosive materials, and the use of tetrafluoroborate electrolyte as an

alternative may, therefore, be preferred. Fortunately, the peak potentials and characteristics of the voltammetric curves obtained at carbon, platinum or mercury electrodes with either perchlorate or tetrafluoroborate electrolytes are essentially the same as described in detail for those at the dropping-mercury electrode, with 0.1 mol dm^{-3} Bu_4NClO_4 as the electrolyte, so that the occupationally safer alternatives are also viable.

Conclusions

A simple voltammetric procedure for determining β-carotene, involving extraction from brine into dichloromethane, followed by direct determination in dichloromethane with 0.1 mol dm^{-3} Bu_4NClO_4 or 0.1 mol dm^{-3} Bu_4NBF_4 as the electrolyte, has been shown to be applicable to solutions relevant to the production of β-carotene from marine microalgae and phytoplankton. Equivalent results to those of methods based on the well-established spectrophotometric procedure are obtained, and the method should be useful for monitoring important stages of plant production of β-carotene. Equivalent and equally useful voltammetric methods could also probably be developed for other components in the increasingly important field of the determination of carotenoids and porphyrins in foods and natural products.

We thank Betatene Ltd. for the supply of the β-carotene samples.

References

1 Morrison, R. T., and Boyd, R. N., *Organic Chemistry*, Allyn and Bacon, Boston, MA, 4th edn., 1983, p. 1153.
2 Walton, H. F., and Reyes, J., *Modern Chemical Analysis and Instrumentation*, Marcel Dekker, New York, 1973.
3 Crompton, T. R., *Determination of Organic Substances in Water*, Wiley Interscience, Chichester, UK, 1985, vol. 2, p. 498.
4 Abaychi, J. K., and Riley, J. P., *Anal. Chim. Acta*, 1979, **107**, 1.
5 Beyermann, K., *Organic Trace Analysis*, Ellis Horwood, Chichester, UK, 1985, p. 235.
6 Hoskins, L. C., and Alexander, V., *Anal. Chem.*, 1977, **49**, 695.
7 Takahashi, R., *Rev. Polarogr.*, 1961, **9**, 247.
8 Takahashi, R., and Tachi, I., *Agric. Biol. Chem.*, 1962, **26**, 771, 777.
9 Takahashi, R., and Tachi, I., *Abh. Dtsch. Akad. Wiss. Berlin, Kl. Med.*, 1966, 589.
10 Kuta, E. J., *Science*, 1964, **144**, 1130.
11 Kuta, E. J., and Yu, M., *Lipids*, 1967, **2**, 411.
12 Mairanovsky, V. G., Engovatov, A. A., and Samokhvalov, G. I., *Zh. Org. Khim.*, 1970, **6**, 632.
13 Mairanovsky, V. G., Engovatov, A. A., Ioffe, N. T., and Samokhvalov, G. I., *J. Electroanal. Chem.*, 1975, **66**, 123.
14 Argneessens, R., Nangniot, P., Lacroix, J. P., and Muri, D., *Bull. Rech. Agron. Gembloux*, 1989, **24**, 85; *Chem. Abstr.*, 1989, **111**, 132701z.
15 *Official Methods of Analysis of the Association of Official Analytical Chemists*, ed. Williams, S., AOAC, Washington, DC, 14th edn., 1984, Nos. 43014–43023, p. 834.

Paper 1/03684J
Received July 19, 1991
Accepted November 11, 1991

Monitoring and Assay of Water Treatment Additives by Alternating Current Tensammetry and Voltammetry: Scope and Limitations

Pierre M. Bersier*
Central Analytical Laboratory, Ciba-Geigy Ltd., Basle, Switzerland
William Neagle and David Clark
Ciba-Geigy Industrial Chemicals, Trafford Park, Manchester, UK

The alternating current (a.c.) tensammetric behaviour of different commercially available water treatment additives is described. Possibilities and limitations of their routine determination by a.c. tensammetry at low levels (0.5–10 ppm) in different aqueous media are discussed. Indirect differential-pulse voltammetry *via* the 12-molybdophosphate derivative allows a classification between phosphino-containing and phosphorus-free water treatment compounds. Practical examples are given.

Keywords: *Water additives; routine determination; alternating current tensammetry; voltammetry*

The whole spectrum of industry, manufacturing and engineering, textiles and chemicals, food and drinks, even leisure and service industries, depend on pure water. Pure water is, however, not widely or readily available. It often has to be chemically treated or obtained from sea-water in limited amounts.

World-wide efforts to develop chemicals for water treatment are being made. These chemicals are essential for modern industry and desalination technology for controlling problems such as: (*i*) scaling: scaling is a build-up of solid material formed on the inner surface of boilers, for instance, when the concentration of the impurities in the water used exceeds their solubility limit and precipitation occurs;[1] (*ii*) microbiological fouling: fouling is the deposition of materials, normally in suspension, onto heat-transfer or other surfaces such as boilers; and (*iii*) corrosion: corrosion is the destruction of a metal by electrochemical reaction with its environment.[1] These problems must be dealt with in a safe and environmentally sound manner.[2]

The need to control the concentration of water treatment chemicals and to control operating costs make it desirable to use cost-effective water treatment products that can be applied with minimum operator involvement.

Chemicals used in non-precipitation programmes are either: (*i*) chelants, forming complexes with calcium and magnesium;[1] or (*ii*) sequestrants (solubilizing agents), which, in the same way as chelants, keep calcium and iron in solution, but are less corrosive.[1]

These formulations typically contain phosphonates, poly(acrylates), poly(methacrylates), poly(maleates) and polymeric dispersants. Operating at threshold levels as opposed to the stoichiometric reaction of chelant reaction programmes, the polymers and phosphonates function primarily by altering or distorting the crystalline structure of hardness precipitates. The new technology eliminates corrosion problems associated with chelants and the excessive precipitation common with phosphate treatments.

Typical sequestering compounds include aminotri(methylenephosphonic acid) or NTP (Wayplex NTP) and hydroxyethylenediphosphonic acid (HEDPA) (see ref. 3). Poly(acrylates) and poly(methacrylates) play leading roles in todays most advanced treatment programmes.[2] Belasol, for instance, was developed to meet the needs of the oil industry. It ensures that sea-water pumped through permeable rock to push the oil up will not leave impurities behind which would clog the rock and block oil recovery.[2] Belgarde EV, on the other hand, is a liquid polymer scale control additive based on an entirely new branch of poly(maleic acid) chemistry.[2]

A factor that is common to all the compounds used is that their monitoring and the control of their concentration is difficult owing to the low levels encountered. In some instances this has led to their being blended with low levels of heavy metal ions as markers.[1]

Analytical Methods

Commonly used methods for determining phosphonate-containing additives are reported to be difficult, time consuming and plagued by interferences.[3]

A rapid method based on the ultraviolet (UV)-catalysed oxidation of the phosphonate moiety to orthophosphate has been reported. The phosphate compound is determined as β-12-molybdophosphate by UV absorption at 700 nm.[3,4] This method is, however, not specific for the intact phosphonate additive and additives as such. For the assay of some additives without a phosphonate moiety, fluorescence has been proposed.[4] This method, although very sensitive, is not specific for the intact additive.

Poly(acrylates) and poly(methacrylates) are highly surface-active and hence have a strong influence on the differential capacity of the electrical double layer at the mercury–water interface.[5–8] They exhibit strong alternating current (a.c.) tensammetric signals. The a.c. tensammogram of a poly(acrylic acid) such as PAA-1 is shown in Fig. 1 (*cf.* Table 1).

Pospisil and Kuta studied the behaviour of maleic acid at a mercury electrode by a.c. polarography[9] and its influence on the electrocapillary curve.[10] The present study shows that the direct a.c. tensammetric assay of poly(maleic compounds) is feasible.

This paper discusses the possibilities and limitations of a.c. tensammetry for the direct assay and monitoring of selected modified phosphinocarboxylic acids (PCA-1, PCA-2, PCA-3 and HPA, *cf.* Table 1). A.c. tensammetry is also applicable to poly(acrylic acids) (PAA-1–PAA-5, *cf.* Table 1) and poly(maleic acids) (PMA-1, PMA-2, *cf.* Table 1), additives which contain no phosphinate groups, *cf.* Table 1.

Experimental

Apparatus

A.c. tensammetric measurements were carried out with a Metrohm Polarecord 506 in conjunction with a Metrohm VA 633 multielectrode stand, using a hanging mercury drop as the working electrode.

* Present address: Gstaltenrainweg 61, 4125-Riehen, Switzerland.

For the indirect differential-pulse voltammetric measurements of the β-12-molybdophosphate, a Polarecord 506 or 626 or an Amel Model 471 Multipolarograph and a dropping mercury electrode as the working electrode were used.

A platinum wire was used as the counter electrode and a saturated calomel electrode as the reference electrode. The latter was connected to the cell by means of a double salt–agar bridge.

All tensammetric and voltammetric measurements were made at room temperature (23 ± 0.5 °C), in de-aerated solutions.

Reagents and Equipment

The additives studied, which are summarized in Table 1, were all of the purest grade available. All other chemicals were of analytical-reagent grade and were used as received.

Generic structures of the three groups of water treatment additive (I, II and III) examined in this work are given in Table 2.

The chemical composition of the model waters, *viz.*, Ca-50, Ca-300, an artificial sea-water formulated according to DIN 50900[11] and an artificial oil-loaded formation water, is given in Tables 3–5.

Sep-Pak C_{18} cartridges (Waters), when used for the assay of water treatment additives in polluted sea-water, were activated with 5 ml of methanol and washed with 10 ml of doubly distilled water.

Direct a.c. tensammetric assays were performed by adding the stock solution or sample solution to the appropriate supporting electrolyte.

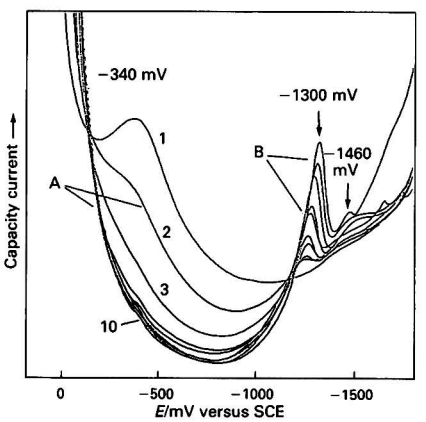

Fig. 1 A.c. tensammograms of poly(acrylic acid), PAA-1, recorded in this laboratory. Supporting electrolyte: model water Ca-300–0.12 mol dm^{-3} sodium perchlorate, pH 4.4. Working electrode, hanging mercury drop. Applied alternating voltage, 15 mV (root mean square) at 75 Hz. Curve 1, supporting electrolyte; 2, 1; 3, 2; 4, 4; 5, 10; 6, 20; 7, 50; 8, 100; 9, 200; and 10, 500 mg l^{-1} of PAA-1. A, Rest current depression; and B, desorption peaks

Procedure

For the a.c. tensammetric assay, the following experimental procedure was applied. Stock solutions of each additive were prepared by dissolving approximately 150 mg of the additive of known concentration in 10 ml of doubly distilled water. For the indirect voltammetric determination of phosphonate-containing additives *via* β-12-molybdophosphate, the UV-catalysed oxidation of the phosphino group to orthophosphate was performed in a glass cell with a thermostatically controlled heating mantle connected to a Lauda water-bath, using a high-pressure 125 W Hg tube. To 2 ml aliquots of the sample were added 1 ml of 1 mol dm^{-3} NaOH, 1 ml of concentrated H_2SO_4 and 1 g of ammonium peroxydisulfate, and the volume was made up to 20 ml with doubly distilled water. The pH of this solution is about 7. The solution was irradiated for 20 min at 70 °C. The irradiated sample was then transferred quanti-

Table 2 Generic structures of the three groups of water treatment additive (I, II and III) examined (*cf.* Table 1)

Group I: *Phosphinocarboxylic acids*—

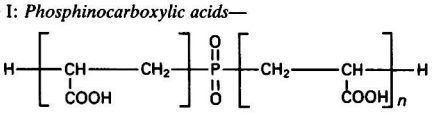

Group II: *Poly(acrylic acids)*—

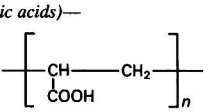

Group III: *Poly(maleic acids)*—

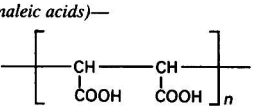

Table 1 General and a.c. tensammetric data for the water treatment additives examined

Compound		Group	Relative molecular mass	Lower detection limit (ppm)	Linear range (ppm)
PCA-1	(I)	Phosphinocarboxylic acid	≈3000	1	1–10
PCA-2		Phosphinocarboxylic acid	≈2700	1	—
PCA-3		Phosphinocarboxylic acid	≈700	1	1–10
PAA-1	(II)	Poly(acrylic acid)	≈2000	1	1–600
PAA-2		Poly(acrylic acid)	≈5000	1	—
PAA-3		Poly(acrylic acid)	≈4500	1	—
PAA-4		Poly(acrylic acid)	≈2000	1	—
PAA-5		Poly(acrylic acid)	≈3000	1	—
PMA-1	(III)	Poly(maleic acid)	≈700	1	1–(50)
PMA-2		Poly(maleic acid)	500–550	1	—
PMA-2		Poly(maleic acid)	≈500	1	1–600
PMA-2		Poly(maleic acid)	≈1250	1	1–60
TCA	(IV)	Triazinecarboxylic acid	≈470	0.1	0.1–20
HPA		Hydroxyphosphonocarboxylic acid	156	10	10–50
P(MA/ME)		Maleic acid–ethylacrylate copolymer	800–850	1	1–10
P(MA/SSA)		Maleic acid–styrene-sulfonic acid copolymer	≈1500	1	—

Table 3 Composition of Ca-50 and Ca-300 model waters

	Concentration/mmol dm^{-3}				
Water	SO_4^{2-}	HCO_3^-	Ca^{2+}	Mg^{2+}	Cl^-
Ca-50	0.4	0.3	0.5	0.5	1.1
Ca-300	0.4	6	3.0	3.0	6.1

Table 4 Composition of artificial sea-water[11,12]

Constituent	Amount present*/g
NaCl	28
$MgSO_4 \cdot 7H_2O$	7
$MgCl_2 \cdot 6H_2O$	5
$CaCl_2 \cdot 6H_2O$	2.4
$NaHCO_3$	0.2

* In 985 ml of distilled water.

Table 5 Composition of artificial oil-loaded formation water (density, 1.029 g cm^{-3}; pH, 5.5; and ionic strength, 0.77 mol dm^{-3}). The water is prepared by shaking artificial Gullfaks formation water with Gullfaks crude oil (50 + 50, v/v) for 24 h at ambient temperature

Constituent	Concentration/mg l^{-1}
Na^+	14 570
K^+	330
Ca^{2+}	1 040
Mg^{2+}	305
Sr^{2+}	260
Ba^{2+}	50
Cl^-	25 600
HCO_3^-	400
CO_3^{2-}	0
SO_4^{2-}	0
Total dissolved solids:	42 555

tatively into a 50 ml calibrated flask and made up to the mark with doubly distilled water. To a 4 ml aliquot of this solution were added 4 ml of acetone and 2 ml of a solution containing 30 g of $Na_2MoO_4 \cdot 2H_2O$, 24 g of tartaric acid and 90 ml of HCl (32%) per litre, and the solution was transferred into the polarographic cell. After de-aeration with pure nitrogen (99.998%) for 10 min, the voltammograms were recorded in the differential-pulse mode.

The exact experimental conditions are given in the figure legends.

Results and Discussion

Quantitative Determinations

Typical a.c. tensammograms of the different classes of additive (*cf.* Table 1) are illustrated in Fig. 2.

The four additives, as shown in Fig. 2, were measured under identical experimental conditions. For a practical assay, however, the optimum conditions for each class and compound must be established.

Variation in the concentration of the surface-active compound affects the depth of the depression of the current of the pure supporting electrolyte (curve 1 in Fig. 1) in addition to the change in the height and the position of the desorption peaks (*cf.* Fig. 1). Both effects can be exploited for the quantification of water treatment additives.

Tensammetric waves frequently behave differently to faradaic processes (*cf.* refs. 5–8, and references cited therein). A characteristic of polarographic and voltammetric techniques is the broad linear dependence over six or more decades. It is therefore much broader than that of most other instrumental methods. In tensammetry the dependence of the value of the measured capacity current on the concentration of the surfactant generally has a non-linear character. Hence a linear

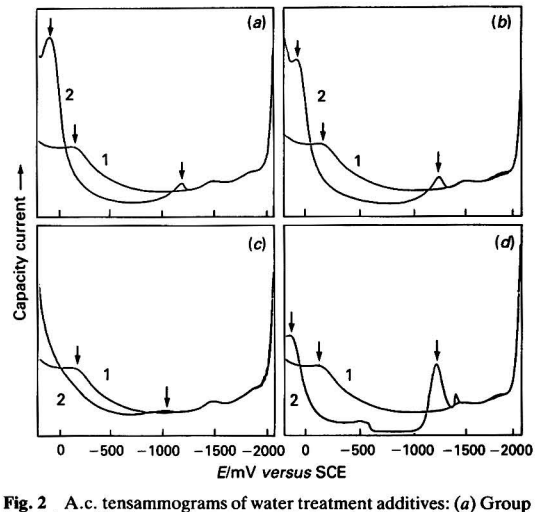

Fig. 2 A.c. tensammograms of water treatment additives: (*a*) Group I, PCA-1; (*b*) Group II, PAA-1; (*c*) Group III, PMA-1; and (*d*) Group IV, TCA. Curve 1: supporting electrolyte, 0.9 N lithium sulfate, pH 4; curve 2: additive concentration, 1.5×10^{-5} mol dm^{-3} (*cf.* Table 4)

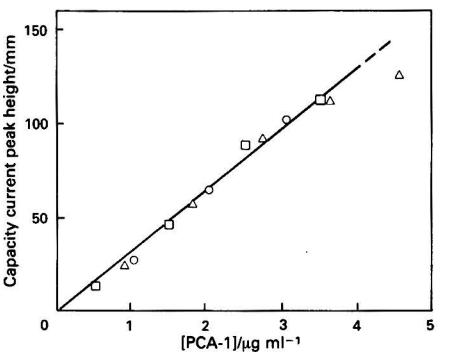

Fig. 3 Calibration graph for the determination of PCA-1 ('as is'), measured in 0.1 mol dm^{-3} sodium fluoride, pH 11. Different symbols indicate replicate measurements

dependence between the measured signal height (depression of the current of the supporting electrolyte) or the height of the desorption peaks, respectively, is observed only at comparably low concentrations and over a narrow concentration range (Fig. 3).

The calibration graphs obtained under the experimental conditions exhibit linear ranges that depend on the compound under study and are therefore a characteristic of each additive. The linear ranges observed are summarized in Table 1. At low concentrations the standard additions method can be applied for the quantitative determination of the water treatment additives, provided that the sum of the analyte present after addition of the reference substance still falls within the linear part of the graph. For quantitative determination in low concentration ranges, the depression of the rest current (*cf.* Fig. 1) was exploited in most instances. The lowest detection limits are in the range 0.1–1 ppm (*cf.* Table 1).

At higher additive concentrations, a dependence of the peak potential (E_p) on the logarithm of the additive concentration (log *c*) is observed in most instances (Fig. 4).

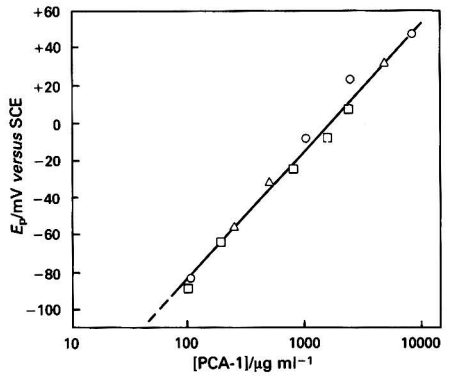

Fig. 4 Peak potential (E_p) *versus* log of the PCA-1 concentration. The first desorption peak is exploited for quantitative assay. Different symbols indicate replicate measurements

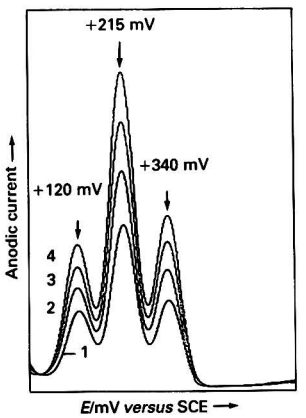

Fig. 5 Differential-pulse voltammograms of β-12-molybdophosphate (procedure according to Fogg and co-workers.[13,14] Curve 1, sample after UV-catalysed oxidation; and curves 2–4, sample after standard additions of phosphate (equivalent phosphate concentrations = 3.07, 6.08 and 9.03 μg ml^{-1} of polarographic solution)

Table 6 Comparison of differential-pulse voltammetric and spectrophotometric results for the determination of the phosphorus content of selected commercial water treatment additives after UV-catalysed oxidation of the phosphinate or phosphonate moiety to orthophosphate

	Phosphorus (%)	
Sample	Polarographic assay	Spectrophotometric assay
PCA-1	0.92	1.02
	0.97	0.98
	0.98	—
PCA-2	0.98	0.93
	0.76	0.77
PCA-3	2.54	2.41
	2.67	2.21
HPA	9.4	11.16
	9.3	11.08
	9.1	—

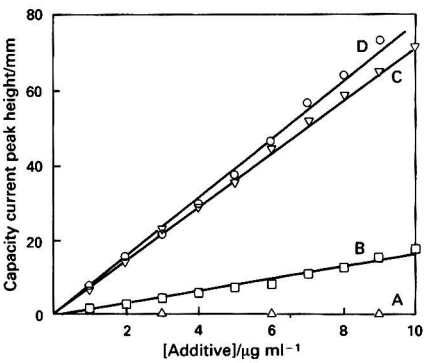

Fig. 6 Influence of the relative molecular mass of phosphinocarboxylic acid additives on the slope of the peak height. A, HPA; B, PAC-3; C, PCA-2; and D, PCA-1

Classification of the Different Additives

A serious shortcoming of tensammetry and of all electrochemical methods in general is their limited specificity and selectivity.

The difficulties in determining surfactants in mixtures and interference problems are certainly among the drawbacks hindering the use of tensammetry as a viable analytical technique. The potential of the tensammetric peaks must differ by at least 0.2–0.3 V. The concentration of the most strongly adsorbed component must be such that the coverage of the electrode surface is less than 100%. Otherwise, only the peak of the most strongly adsorbed compound will be detected on the tensammograms.[5–8]

A direct differentiation between the four classes of water treatment additive (I–IV, *cf.* Fig. 2 and Table 1), *viz.*, (I): additives with phosphino groups; (II): without phosphino groups; (III): poly(maleic acids) (*cf.* Table 2); and (IV): miscellaneous, in the concentration range of interest [0.1(1)–10 ppm] is not possible with the a.c. tensammetric procedure described here. The UV and voltammetric determination of the phosphino group, however, allows a preliminary classification between group I and groups II and III.

The voltammetric wave of β-12-molybdophosphate observed at a glassy carbon electrode (*cf.* Fig. 5) has been used as the basis of a method for determining orthophosphate.[13,14] Hence, voltammetry can serve as an alternative method to spectrophotometry for the determination of phosphate. Good agreement was found between phosphate concentrations determined by voltammetry and data obtained by a spectrophotometric method,[14] as shown in Table 6.

The advantage of the electroanalytical methods used here is that both the voltammetric and the a.c. tensammetric assays can be carried out with the same instrument (a polarograph).

Qualitative Determination Based on Tensammetric Measurements

The shape and peak potentials of the tensammetric waves depend on the nature of the compound studied and, therefore, can, in some instances, give qualitative information. Jehring[8] showed that with increasing relative molecular mass (M_r) (1000, 3000, 5000, 20 000) the peak potential of poly(ethylene glycols) moves progressively towards more negative values. The shift is a linear function of the reciprocal average M_r. Resolved peaks are obtained. The peak width decreases with increasing M_r.

Bagdasarov *et al.*[15] observed that the slope of the plot of capacity current *versus* concentration increased with increasing length of the hydrocarbon chain, for instance from C_8 to C_{12} (*cf.* Fig. 2 in ref. 15). Distinct differences between the slope of the measured capacity current (i_c) (depression of the

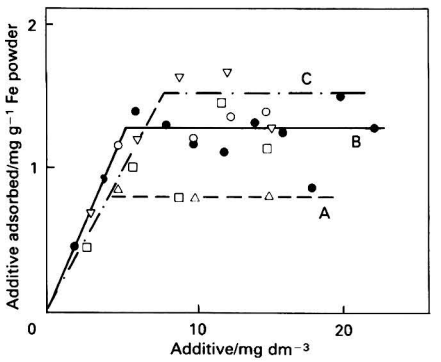

Fig. 7 Adsorption of a water treatment additive onto the surface of iron powder as a function of the amount of additive. Medium: model water Ca-50 containing 4 g l^{-1} of Fe (20 h at 40 °C). □, pH 5.5 de-aerated solution; ○, pH 7.5 de-aerated solution; ●, pH 7.5 aerated solution; ▽, pH 9.5 de-aerated solution; and △, pure water, pH 7.5. A, 0.79; B, 1.21/1.26; and C, 1.53 mg g^{-1} of Fe

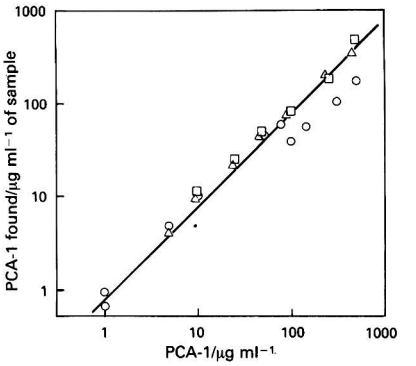

Fig. 8 Recovery of PCA-1 added to artificial sea-water (○, □) and artificial formation water (△). Measured by the proposed a.c. tensammetric procedure

rest current or the peak height, respectively) and the M_r of different phosphonate-containing additives of group I are observed (Fig. 6).

Hence, for the phosphinocarboxylic acids HPA (average $M_r \approx 160$), PAC-3 (average $M_r = 700$) PCA-2 (average $M_r = 2700$) and PAC-1 (average $M_r = 3000$), provided that the amount of phosphonate present is known (the determination is carried out with the indirect procedure *via* β-12-molybdophosphate described above), the slope of a graph of i_c *versus* c furnishes qualitative information on the additive present, as is revealed by an inspection of Fig. 6. A distinction between the phosphinocarboxylic acids containing PCA-1 and PCA-2 with an average M_r of 3000 and 2700, respectively, is, however, not possible, as shown in Fig. 6.

In practical applications, such as monitoring, not all of these compounds are present in a mixture. Hence, tensammetric measurements should permit both their determination down to fairly low levels and, for phosphinocarboxylic acids, with greatly different M_r values, their qualitative determination/identification.

Applications

In addition to the examples mentioned above, the following examples serve to illustrate the possible applications of the a.c. tensammetric techniques to the routine practical analysis of water treatment additives.

Tensammetric determination of additives in the presence of iron (powder) performed on model waters

Experiments run in the presence of iron powder (4 g per litre of model water Ca-50, for instance) showed no direct influence of iron or iron ions on the tensammetric assay of the additive examined. Changes in the concentration of the additive at the ppm level, owing to adsorption onto the surface of the iron powder, could be followed in de-aerated and aerated media. Hence the determination of the amount of an additive adsorbed on a surface and the thickness of the adsorbed layer can be monitored as a function of the given experimental conditions, such as temperature, composition, pH of the bath and time. The adsorption of an additive onto the surface of iron powder as a function of the amount of the additive is shown in Fig. 7.

Determination of scale inhibitors in oil-loaded artificial sea-water and oil-loaded artificial formation water

Concentrations of 0.5–400 ppm (range tested) of the scale inhibitor PCA-1 could be determined in oil-loaded artificial sea-water and formation water (for details of the composition of these waters see Tables 4 and 5) in the presence of a de-emulsifier (100 and 200 ppm) by a.c. tensammetry. The assay was performed in 0.1 mol dm^{-3} NaF, pH 11, supporting electrolyte, after separation and accumulation on a Sep-Pak C_{18} cartridge with or without prior extraction of the oil with CCl_4, using the procedure described by Gruenfeld.[16] A hanging mercury drop electrode was used as the working electrode. In pure 0.1 mol dm^{-3} NaF, pH 11, a linear relationship between the height of the desorption peak and the additive/inhibitor concentration was found in the range 0.5–5 ppm. In the range 100–9000 ppm, a linear (E_p *versus* log c) dependence was observed.

Recoveries of PCA-1 added to oil-loaded artificial formation water and artificial sea-water are illustrated in Fig. 8.

Conclusions

A.c. tensammetry, combining high sensitivity with good precision, appears to constitute a very convenient electrochemical procedure for the assay of water treatment additives, which represent a particularly important group of compounds in modern technology. It is therefore a valuable alternative to the methods commonly used.

However, the practical analytical chemist, who is interested in the potential applications of tensammetric techniques, should be familiar with the variability of these techniques towards medium effects. The type and concentration of electrolyte may influence the wave shape and position far more than faradaic processes (*cf.* refs. 5–8). As stressed by Bond,[17] extreme care and commonsense must, therefore, be employed in using tensammetric techniques in routine analysis.

The skillful technical assistance of H. G. Wenzel and J.-P. Worch is gratefully acknowledged.

References

1 Sendelbach, M. G., *Chem. Eng.*, 1988, August, 127.
2 Sykes, S., *Ciba-Geigy J.*, 1988, **3**, 10.
3 Hach's Water Analysis Handbook, Hach, Loveland, CO, Phosphonates. Range: 0–20 mg l^{-1}. Persulfate/UV Oxidation Method for Water, pp. 2-234–2-236.
4 Clark, D., unpublished work.
5 Bersier, P. M., and Bersier, J., *Analyst*, 1988, **113**, 3.
6 Kalvoda, R., *Pure Appl. Chem.*, 1987, **59**, 715.
7 Kalvoda, R., and Parsons, R., *Electrochem. Res. Dev.*, (Proc. UNESCO Forum, 1984, Publ. 1985; *Chem. Abstr.*, **105**, 69015n).

8 Jehring, H., *Elektrosorptionsanalyse mit der Wechselstrompolarographie*, Akademie Verlag, Berlin, 1974.
9 Pospisil, L., and Kuta, J., *Collect. Czech. Chem. Commun.*, 1968, **33**, 3040.
10 Pospisil, L., and Kuta, J., *Collect. Czech. Chem. Commun.*, 1969, **34**, 3047.
11 Deutsche Industrie Norm (DIN) 50900, November, 1960.
12 *Römpp Chemie Lexikon*, eds. Falbe, J., and Regitz, M., Georg Thieme, Stuttgart, 1991, vol. M-PK, p. 2669.
13 Fogg, A. G., and Bsebsu, N. K., *Analyst*, 1981, **106**, 369.
14 Fogg, A. G., Bsebsu, N. K., and Birch, B. J., *Talanta*, 1981, **28**, 473, and references cited therein.
15 Bagdasarov, K. N., Lokshina, G. A., Sadimenko, L. P., and Sokolov, V. P., *Zh. Anal. Khim.*, 1986, **41**, 171.
16 Gruenfeld, M., *Environ. Sci. Technol.*, 1973, **7**, 636.
17 Bond, A. M., *Modern Polarographic Methods in Analytical Chemistry*, Marcel Dekker, New York, 1980.

Paper 1/01516H
Received April 2, 1991
Accepted December 13, 1991

Rapid, High-purity Chemical Separation of Molybdenum From Iron Meteorites for Isotopic Analysis by Using Thermal Ionization Mass Spectrometry

Qi-Lu and Akimasa Masuda
Department of Chemistry, Faculty of Science, The University of Tokyo, Hongo 7-3-1, Bunkyo-ku, Tokyo 113, Japan

A chemical procedure has been developed, which combines both solvent extraction and anion exchange, so that microgram amounts of Mo can be cleanly, rapidly and efficiently separated from gram amounts of iron meteorites. Particular attention was directed to the complete separation of Mo from Zr and Ru. The isotopic abundance ratios of Mo can subsequently be determined with high accuracy by using thermal ionization mass spectrometry. The experiments indicate that the behaviour of Mo during solvent extraction and anion exchange is considerably different from that reported previously. In particular, it was found that there is a very narrow range of HCl concentrations within which it is possible to separate Mo from Fe by solvent extraction. The reproducibility and recovery of the method were examined by using inductively coupled plasma atomic emission spectrometry.

Keywords: *Molybdenum; solvent extraction; ion exchange; iron meteorite*

Molybdenum is a very interesting element as its seven stable isotopes reflect several effects related to nuclear physics. Investigations on the isotopic abundances of Mo in meteoritic samples can supply important information not only on the nucleosynthesis process of the early solar system but also on the decay of extinct radioisotopes of the elements adjacent in atomic number to Mo.[1–5] However, for reasons discussed in the literature,[5] few isotopic studies of Mo have been performed successfully in either terrestrial or meteoritic situations. At present, information on the subject of Mo isotopes, particularly in meteorites, is limited. For these reasons, a fundamental study on the chemical and isotopic analysis of Mo in molybdenites has recently been carried out by using thermal ionization mass spectrometry (TIMS).[5] In this connection, an efficient and clean chemical separation method to extract microgram amounts of Mo from gram amounts of iron meteorites was developed for the analysis of Mo isotopes with high accuracy.

Basically, the choice of chemical separation procedure was made according to the concentrations of the primary chemical constituents of the iron meteorites[6] and from previous work.[5] It is known that the mean concentrations of Fe and Ni in different types of iron meteorite are about 91 and 8%, respectively, and that the concentration of Cu is about 0.1–0.01%. Kraus *et al.*[7] have studied the anion-exchange behaviour of Mo^{VI} with a strongly basic quaternary amine anion-exchange resin in HCl–HF mixtures, and Murthy[1] and Wetherill[8] have applied this method to the separation of Mo from iron meteorites. Unfortunately, this method is unsatisfactory for the analysis of the isotopes of Mo in iron meteorites.[9] Under the analytical conditions used, Zr and Ru could not be separated from Mo completely; in addition, the separation method is time consuming.

Qureshi *et al.*[10] have carried out a systematic survey of the solvent extraction of many elements in HCl, HNO_3 and $HClO_4$ at various concentrations by using the bis(2-ethylhexyl) hydrogen phosphate (HDEHP)–cyclohexane system, but few studies on the separation of Mo from a matrix such as Fe by use of this system have been reported.

Therefore, in order to establish a suitable method for the isotopic study of Mo in cosmochemistry, the chemical separation of Fe, Zr, Mo and Ru by solvent extraction with the HDEHP–cyclohexane system and the anion exchange of Fe, Ni, Cu, Zr, Mo and Ru under different analytical conditions have been examined. In this work, particular attention was directed to the complete separation of Mo from Zr and Ru, as some isotopes of Zr and Ru produce isobaric interferences on the measurement of the isotope ratios of Mo. By using the analytical conditions described here, greatly improved separation and recovery of microgram amounts of Mo from gram amounts of iron meteorites can be achieved for the isotopic analysis of Mo with high accuracy.

Experimental

Reagents

The water, and the acids HF, HCl, HNO_3 and $HClO_4$ used in the analyses were purified by sub-boiling distillation. The following chemical reagents and materials were used as received: ammonia solution (containing less than 0.005 ppm of Mo), HDEHP and cyclohexane (high-performance liquid chromatography grade). Standard solutions for atomic absorption spectrometry (Aldrich, St. Louis, MO, USA), 1 mg ml^{-1} were used for Fe, Ni, Cu, Mo, Zr and Ru. The anion-exchange resin AG 1-X8, 100–200 mesh, in the chloride form, was used.

Apparatus

An inductively coupled plasma atomic emission spectrometer (ICPS-5000, Shimadzu, Kyoto, Japan) was used as the detector for the solvent extraction and anion-exchange studies. An inductively coupled plasma mass spectrometer (PlasmaQuad, VG Elemental, Winsford, Cheshire, UK) was used to determine the concentrations of Mo in iron meteorites. Samples were dissolved by means of a microwave oven (MCD-81, CEM, Matthews, NC, USA). Isotopic abundances of Mo were measured with a thermal ionization mass spectrometer (VG Sector 54-30) with a single Faraday detector.

Digestion of Iron Meteorites

An accurately weighed amount (2–5 g) of the iron meteorite was placed in a 120 ml poly(tetrafluoroethylene) (PTFE) vessel and approximately 10 ml of 6 mol dm^{-3} HCl were added. The vessel was then sealed and heated in a microwave oven for about 20 min at a power of 2, 4, 5, 10 or 15%. After cooling, the vessel was opened and the clear solution was poured into a beaker. The residue was subjected to the above

procedure several times until it was completely dissolved. The resulting solution was used for chemical separation.

Solvent Extraction of Mo

The experiments were carried out in an air-conditioned room at 21 ± 1 °C. The HDEHP–cyclohexane system was selected for the separation of Mo from Fe, Ni, Cu and other elements in iron meteorites. Generally, after dissolution of the iron meteorites, Mo ions in HCl probably exist as various types of complexes of Mo^{VI}. Molybdenum in the hexavalent state is usually stable; however, as it tends to hydrolyse and form an isopoly or heteropoly acid, its solvent extraction behaviour is complicated and a quantitative treatment of the extraction equilibria is not always possible. Considering that iron meteorites can be dissolved readily in 6 mol dm^{-1} HCl, it was decided to investigate the effect of the HCl concentration on the extraction of the relevant elements. Normally, Zr ions are considered to be strongly partitioned into the organic phase as the Zr^{IV} ion is a small and highly charged ion which forms a stable complex with HDEHP. Hence in subsequent work, the separation of Mo from Zr has to be performed. In order to achieve this, the back-extraction of Mo only was used.

On the basis of the above studies, the procedure adopted for iron meteorites was as follows. (1) Following the dissolution of the iron meteorite, the solution was mixed with 25 ml of 0.75 mol dm^{-3} HDEHP in cyclohexane in a 50 ml separating funnel. After shaking for 5 min, the aqueous phase was removed when separation of the immiscible phases was complete, and the organic phase was washed with three 25 ml portions of 5 mol dm^{-3} $HClO_4$ and then with two 25 ml portions of 10 mol dm^{-3} HNO_3. (2) For the back-extraction of Mo, 5 ml of 10 mol dm^{-3} HNO_3 in 3% H_2O_2 were added to the organic phase and the mixture was shaken for about 5 min. The aqueous phase was transferred into a PTFE beaker and the back-extraction process was repeated. The aqueous phase was then evaporated to dryness at low temperature (about 70 °C) and the residue was dissolved in 1 mol dm^{-3} HF–0.01 mol dm^{-3} HCl for further purification by means of anion exchange.

Anion Exchange of Mo

Further purification of Mo was undertaken by using an anion-exchange method after the solvent extraction. The following procedure was developed as a result of this study. The anion-exchange resin (AG 1 X-8, 100–200 mesh) was prepared by washing successively with concentrated HCl, water, concentrated ammonia solution, water, concentrated HNO_3 and finally 6 mol dm^{-3} HCl (the final 6 mol dm^{-3} HCl stage was repeated). The resin thus prepared was placed in a 0.5 ml PTFE column for the meteoritic samples and in a 15 ml PTFE column for investigating the analytical conditions as a slurry in 1 mol dm^{-3} HF–0.01 mol dm^{-3} HCl. The end of the column was plugged with PTFE wool to prevent outflow of the resin. Before loading the Mo sample, extracted from the iron meteorite, onto a pre-treated 0.5 ml column, the anion-exchange resin was equilibrated with 0.01 mol dm^{-3} HCl–1.0 mol dm^{-3} HF by washing it with 3 ml of this solution. Then, 1 ml of 6 mol dm^{-3} HCl was added to remove any Zr present. The Mo-containing fraction was subsequently collected by passing 2.0 ml of 7 mol dm^{-3} HNO_3 through the column. For the 15 ml column, a synthetic solution was eluted by using different eluting solutions; the details are presented in the following section.

Results and Discussion

Solvent Extraction of Mo

The solvent extraction behaviour of Mo, Fe, Zr and Ru at various concentrations of HCl with the HDEHP–cyclohexane system is shown in Fig. 1. It can be seen that HCl has a marked effect on the extraction characteristics of Fe, only a small effect on Mo and Ru and no effect on Zr. Regardless of the concentration of HCl, the separation of Mo from the main matrix elements (*e.g.*, Fe, Ni, Cu) of the iron meteorites is not possible. When the HCl concentration is about 6 mol dm^{-3}, Zr (100%) and Mo (>95%) will be extracted into the HDEHP–

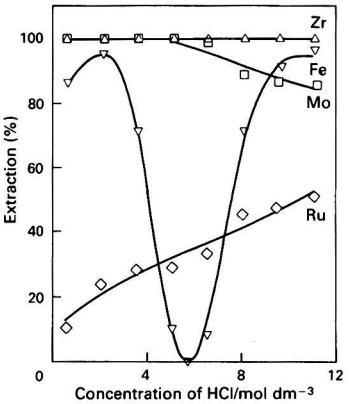

Fig. 1 Solvent extraction of Fe, Zr, Mo and Ru with the 0.75 mol dm^{-3} HDEHP–cyclohexane system in different concentrations of HCl. The data are shown as percentages of each of these elements found in the aqueous phase compared with the total concentration of that element

Table 1 Recovery of Mo and the effect of Fe by using solvent extraction with the HDEHP–cyclohexane system. Data were obtained by ICP–AES

Sample	Mo found in back-extract (%)	Fe found in a series of aqueous phase washings (ppm) 1	2	3
1. 1.00 g (iron meteorite)	88	421	7.3	—*
2. 1.01 g (Fe, 99.99%)	97	273	1.6	—*
3. 1.32 g (Fe, 99.99%)	97	458	9.5	—*
4. No Fe	100			
5. No Fe	99			
6. No Fe	95			
7. No Fe	99			

* Below the detection limit (<50 ppb).

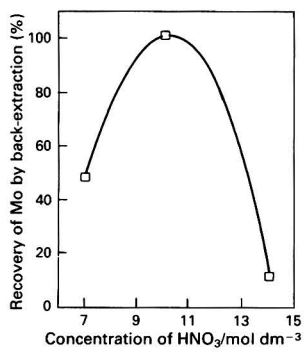

Fig. 4 Comparison of the elution behaviour of Mo in A, 1 mol dm^{-3} HCl; and B, 7 mol dm^{-3} HNO_3

cyclohexane phase, whereas all of the Fe remains in the aqueous phase at this very narrow range of HCl concentration. The data thus obtained are not in agreement with those available in the literature,[10] and these findings are of particular importance in achieving the chemical separation of not only Mo from Fe, but also Fe from the elements under consideration. Therefore, the solvent extraction of Mo from iron meteorites could be performed immediately after dissolution of the iron meteorite in 6 mol dm^{-3} HCl without the need for any other time-consuming chemical treatment. Inductively coupled plasma atomic emission spectrometry (ICP–AES) was used to measure the Fe present as a contaminant on the surface of the container; the Fe can be removed by washing the organic phase several times with $HClO_4$ or HNO_3, as shown in Table 1.

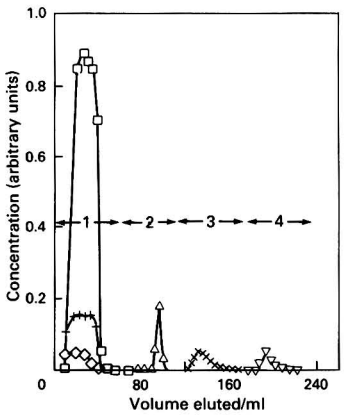

Fig. 2 Effect of concentration of HNO_3 on the back-extraction of Mo from the HDEHP–cyclohexane phase

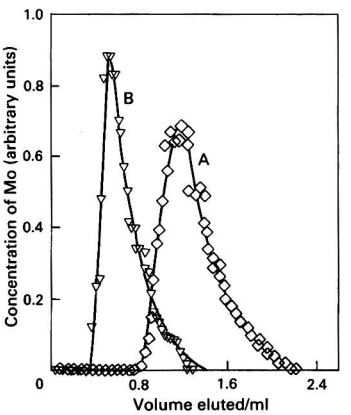

Fig. 3 Study of the elution behaviour of a synthetic solution containing Fe, Ni, Cu, Mo, Zr and Ru by passing the following solutions through a 15 ml column: 1, 1 mol dm^{-3} HF–0.01 mol dm^{-3} HCl; 2, 6 mol dm^{-3} HCl; 3, 1 mol dm^{-3} HCl; and 4, 14 mol dm^{-3} HNO_3. □, Fe; +, Ni; ◇, Cu; △, Mo; ×, Zr; and ▽, Ru

Table 2 Elemental abundances of Mo in iron meteorites. The results were obtained by ICP–MS

Sample	Concentration of Mo (ppm)
Canyon Diablo	6.0
Hardesty	22.7
Odessa	15.6

Under the same conditions, Ru was partly and Zr completely extracted into the organic phase. Ruthenium can be removed by washing the organic phase with $HClO_4$ or HNO_3. In the back-extraction of Mo by use of 10 mol dm^{-3} HNO_3 in 3% H_2O_2, because Zr cannot be reduced to a low valence state, only Mo is back-extracted into the aqueous phase at this stage. The back-extraction of Mo in solutions of 3% H_2O_2 with 7, 10 and 14 mol dm^{-3} HNO_3, respectively, is shown in Fig. 2. The results suggest that the optimum back-extraction of Mo is obtained in an aqueous phase of 10 mol dm^{-3} HNO_3.

The recovery of Mo separated by solvent extraction with the HDEHP–cyclohexane system is shown in Table 1. A 0.50 mg amount of Mo was taken as a tracer in all seven experiments, and there was no Fe in the last three samples. It can be seen that no significant matrix effect of Fe was found in the separation of Mo. It should be noted that for back-extraction using 5 ml of 10 mol dm^{-3} HNO_3–3% H_2O_2, more than 75 and 22% of the Mo could be back-extracted in the first and second back-extractions, respectively. The whole separation process requires only about 1 h.

Anion Exchange of Mo

Although the solvent extraction method is capable of extracting Mo from iron meteorites, it is still necessary to remove isotopes of Zr (^{92}Zr, ^{94}Zr and ^{96}Zr) and Ru (^{96}Ru, ^{98}Ru and ^{100}Ru), which might affect the accuracy of the isotopic analysis of Mo (^{92}Mo, ^{94}Mo, ^{96}Mo, ^{98}Mo and ^{100}Mo). An anion-exchange method was used for removing these isobaric interferences.

It was found that earlier work[1,8] on the measurement of Mo isotopes could be seriously affected by isotopes of Zr under the separation conditions used. In the present study, an improvement was made. In order to demonstrate the reliability of the results obtained in this work, a solution containing 1 mg each of Cu, Zr, Mo and Ru, 3.5 mg of Ni and 25 mg of Fe in 25 ml of 1.0 mol dm^{-3} HF–0.01 mol dm^{-3} HCl was passed through a 15 ml PTFE column, which had been treated as described above for the 0.5 ml column. After removal of Fe, Ni and Cu with about 50 ml of 1.0 mol dm^{-3} HF–0.01 mol dm^{-3} HCl, Zr was removed by passing 20 ml of 6 mol dm^{-3} HCl through the column. Then, about 40 ml of 1 mol dm^{-3} HCl were added and the eluate fraction was collected for the determination of Mo. Finally, the column was eluted with about 40 ml of 7 mol dm^{-3} HNO_3 and this fraction was reserved for the determination of Ru. Aliquots of 4 ml were collected with an automatic fraction collector and the concentrations of these elements in the fractions were determined by ICP–AES. The experimental curves are presented in Fig. 3.

Table 3 Mo isotope ratios in several iron meteorites. All isotope ratios are normalized to $^{94}Mo/^{98}Mo = 0.3802$ by exponential law. Errors given are one standard error of the mean

Sample	$^{92}Mo/^{98}Mo$	$^{95}Mo/^{98}Mo$	$^{96}Mo/^{98}Mo$	$^{97}Mo/^{98}Mo$	$^{100}Mo/^{98}Mo$
Odessa	0.607961 ± 0.000054	0.656051 ± 0.000050	0.688046 ± 0.000070	0.394967 ± 0.000039	0.400134 ± 0.000054
Canyon Diablo	0.608082 ± 0.000047	0.655930 ± 0.000043	0.688156 ± 0.000044	0.394930 ± 0.000024	0.400135 ± 0.000034
Hardesty	0.607900 ± 0.000067	0.655954 ± 0.000051	0.688156 ± 0.000056	0.394897 ± 0.000032	0.400333 ± 0.000042
Molybdenite (Colarado, USA)	0.607924 ± 0.000041	0.655994 ± 0.000016	0.688155 ± 0.000040	0.394937 ± 0.000022	0.400134 ± 0.000016
Standard (MoO_3, 99.999%)	0.607926 ± 0.000013	0.655964 ± 0.000013	0.688146 ± 0.000011	0.394947 ± 0.000007	0.400129 ± 0.000012

As Ru can only be eluted with concentrated HNO_3, no atomic interferences from Zr and Ru isotopes were found in the solution taken for the isotopic analysis of Mo, when monitored by inductively coupled plasma mass spectrometry (ICP–MS).

This result shows that for a synthetic solution, the separation of Zr, Mo and Ru can be achieved and the removal of Fe, Ni and Cu is also possible. However, for iron meteorites, it was found that the reproducibility and recovery of Zr, Mo and Ru were poor. This might be attributed to the effects of bulk matrix elements of the solution resulting from the use of gram amounts of the iron meteorite, which is necessary for extracting at least 20 μg of Mo for the accurate analysis of the seven isotopes of Mo by using a thermal ionization mass spectrometer with a single Faraday detector.[4] Further, according to the literature,[1,8] and from our own experience, before loading the Mo sample onto a larger column the solution obtained from the dissolution of the iron meteorite must be evaporated to dryness at low temperature (about 70 °C) and redissolved, which requires several days.

Therefore, for additional purification of Mo extracted from iron meteorites after solvent extraction, a small PTFE column (0.5 ml) was used, as the purity and amount of the Mo sample obtained following solvent extraction was greatly improved. The elution curves of microgram amounts of Mo in 1 mol dm^{-3} HCl and 7 mol dm^{-3} HNO_3 are shown in Fig. 4. The data were obtained by ICP–AES by measuring the eluate dropwise (the 0.5 ml column was connected to the ICP–AES instrument). The use of 7 mol dm^{-3} HNO_3 rather than 1 mol dm^{-3} HCl is preferred because the chloride salt used for TIMS often generates more molecular and polyatomic interferences than the nitrate salt.

Application

The abundances of Mo in a number of iron meteorites were determined by using ICP–MS. The isotopic abundances of Mo in several iron meteorites were determined by TIMS by use of the single collector method. Details of the TIMS technique have been described previously.[5] The concentrations of Mo in three iron meteorites (Odessa, Canyon Diablo and Hardesty) and the isotopic abundances of Mo in the same three iron meteorites, a molybdenite sample and a standard sample (MoO_3, 99.999%; Aldrich) are shown in Tables 2 and 3. The data obtained in this work for the elemental abundances of Mo in the Canyon Diablo sample show good agreement with the value reported by Murthy[1] (6.3 ppm). However, for the isotopic abundances of Mo in the Canyon Diablo sample, the data obtained in this work are different from those reported by Murthy. In the work of Murthy, the analytical error for the Mo isotope ratios was taken to be ±0.6% of each ratio. In our previous work the standard Mo isotopic data from repeated analyses for seven runs varied by about ±0.4 parts in 10^4. The small differences in the isotopic abundances of Mo among various samples are thought to be evidence of some nuclear effects of the early solar system; these will be discussed elsewhere.

Conclusion

The results obtained in this work indicate that the proposed chemical procedure could afford a rapid and highly efficient method not ony to extract microgram amounts of Mo from gram amounts of iron meteorites but also to separate Mo from Zr and Ru for the analysis of Mo isotopes with high accuracy. Moreover, by carrying out an additional back-extraction for Zr after back-extracting Mo, the former can be removed from the organic phase. Hence isotopic investigations of not only Mo but also Zr and Ru in iron meteorites can be carried out easily in comparison with the traditional ion-exchange method, as the isotopes of Zr and Ru have very similar nuclear backgrounds to Mo in terms of cosmochemistry. Further, the procedure would be applicable in nuclear chemistry and nuclear physics, because some isotopes of Zr, Mo and Ru are important products of the neutron-induced and spontaneous fission of U.

References

1 Murthy, V. R., *Geochim. Cosmochim. Acta*, 1963, **27**, 1171.
2 Burbige, E. M., Burbige, G. R., Fowler, W. A., and Hoyle, F., *Rev., Mod. Phys.*, 1957, **29**, 547.
3 Crouch, E. A., and Tuplin, T. A., *Nature (London)*, 1964, **202**, 1282.
4 Howard, W. M., Meyer, B. S., and Woosley, S. E., *Astrophys. J.*, 1991, **373**, L5.
5 Lu, Q., and Masuda, A., *J. Am. Soc. Mass Spectrom.*, 1992, **3**, 10.
6 Buchald, V. F., *Handbook of Iron Meteorites*, University of California Press, CA, 1975.
7 Kraus, K. A., Nelson, F., and Moore, G., E., *J. Am. Chem. Soc.*, 1955, **77**, 3972.
8 Wetherill, G. W., *J. Geophys. Res.*, 1964, **69**, 4403.
9 Lu, Q., and Masuda, A., *Meteoritics*, 1991, **26**, 367.
10 Qureshi, I. H., McClendon, L. T., and Lafleur, P. D., *Radiochim. Acta*, 1969, **12**, 107.

Paper 1/05022B
Received October 1, 1991
Accepted November 14, 1991

Determination of Trace Amounts of Copper With Extraction–Photoacoustic Spectrometry

Y. Deng and M. Ye
The Centre of Analysis and Testing, Wuhan University, Wuhan, Hubei 430072, People's Republic of China

A sensitive method for the determination of copper in aqueous solution by pulsed laser-induced photoacoustic spectrometry after extraction is described. The copper is chelated with 1,5-diphenylcarbazide in chloroform and extracted into the chloroform phase. The optimum extraction conditions were found experimentally. By using the stepwise dilution method, the minimum absorbance that could be measured was 8.5×10^{-6} at 6.2 mJ per pulse; this corresponds to 6.9×10^{-3} μg l^{-1} of copper in chloroform. The relative standard deviation for ten measurements of an absorbance of 7.8×10^{-3} at 0.7 mJ is 1.5%. Application of the method to the determination of copper in biological samples is also described. The results obtained were compared with those given by atomic absorption spectrometry.

Keywords: *Extraction; photoacoustic spectrometry; copper determination; 1,5-diphenylcarbazide*

The ultra-high sensitivity of photoacoustic (PA) measurements for liquid samples has been demonstrated.[1–3] In recent years, the PA determination of trace amounts of several solutes, such as cobalt, holmium, neodymium, benzene and cyclohexane, has been reported, and detection limits of 1×10^{-7}–1×10^{-8} cm^{-1} were reached.[4–6] The determination of 1×10^{-4} μg l^{-1} of cobalt by extraction–PA spectrometry has also been described.[7]

Copper is a common element that occurs widely in organisms as a necessary trace element possessing specific physiological functions. The determination of trace amounts of copper in biological material is receiving increasing attention in nutrition, and in medicinal and physiological studies.

1,5-Diphenylcarbazide (DPC) is a reagent mainly used for the selective colorimetric determination of chromium(VI). Recently, the use of this reagent for the colorimetric determination of copper in basic medium by extracting the metal into chloroform as the Cu–DPC chelate was reported.[8] However, no detailed studies of the extraction conditions were carried out.

This paper describes the determination of sub-nanomolar amounts of copper in aqueous solution by PA measurement after extraction of the metal with DPC into chloroform. It is also demonstrated that the proposed method can be used for the determination of copper in biological samples such as grass carp and pig kidney.

Experimental

Apparatus

A schematic diagram of the PA measurement system used is shown in Fig. 1. The excitation beam was the frequency-doubled (532 nm) output of an Nd:YAG laser (YG 581, Quantel) operating at 10 Hz with a duration of 8 ns. The power incident into the PA cell was monitored by a laser energy/power meter (LPE-1A, Chinese Academy of Sciences). The beam radius, determined by an aperture, was 2 mm, unless stated otherwise. The PA cell for liquid PA measurements was laboratory-built and is shown schematically in Fig. 2. It was constructed by using a fused-quartz cuvette and two PZT-5H discs, which were fixed separately onto the outside walls of the cell. In order to enhance the PA signal response, the PZT discs were connected in series. In some experiments, a post-cell mirror was used for back-reflecting the pump light so that it passed through the sample again along the incident direction [Fig. 2(*b*)]. The cell with the post-cell mirror will be referred to as cell A, and the cell without the post-cell mirror as cell B.

The PA signal was amplified ten-fold with a preamplifier (M115, PAR), from which the output was fed into a boxcar averager (M162/165, PAR) with a 20 μs aperture and 28% delay. A dual-pen *x*–*y* recorder was used to record the PA and power signals synchronously. A spectrophotometer (UV-240, Shimadzu) with a 1 cm cuvette was used for the absorbance measurements.

Reagents

A stock solution of copper(II) (1.0 mg ml^{-1} in 1 mol dm^{-3} HCl) was prepared from high-purity copper wire. Working

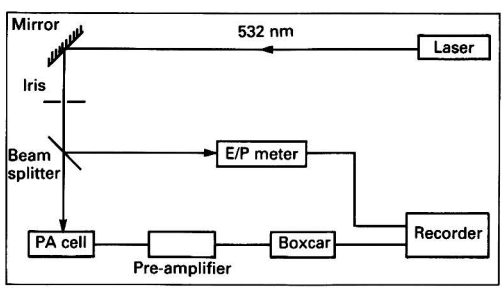

Fig. 1 Schematic diagram of the PA measurement set-up

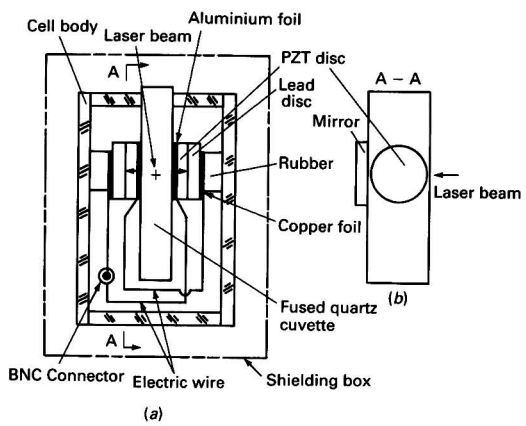

Fig. 2 PA cell for liquid samples

solutions of copper at the ng l^{-1} level were prepared daily by appropriate dilution of the stock solution with water or the desired buffer solution.

Analytical-reagent grade DPC was purified by three recrystallizations from absolute ethanol, after which white crystals of DPC were obtained. A stock solution of DPC in chloroform (0.1%) was prepared by dissolving 100 mg of DPC in 3 ml of hot absolute ethanol and diluting to 100 ml with chloroform. The solution was stored in a brown flask. The DPC extractant used was obtained by further diluting the stock solution with chloroform.

All other chemicals used were of analytical-reagent grade. Doubly distilled water was used throughout.

Prior to solvent extraction, the buffer solution was extracted three times with chloroform containing DPC and then washed three times with chloroform to remove all the extractable impurities.

Procedure

Under optimum extraction conditions, an aliquot of an aqueous solution containing 10–80 ng of copper was transferred into a 60 ml separating funnel and buffer solution of the desired pH was added so that the final volume of the aqueous phase was 20 ml. The solution was then shaken vigorously with 5 ml of chloroform containing 0.02% DPC for 3 min, after which the mixture was allowed to stand for 20 min so that the two phases could separate. After extraction, an aliquot of the extract (about 1.4 ml) was placed directly in the PA cell from the funnel for PA measurement.

In preparing the absorption curve and for carrying out the experiments into the effect of pH, a solution containing microgram levels of copper was extracted and the absorbance measurements were performed with a spectrophotometer.

Treatment of the Samples

A known amount of the fresh sample (pig kidney, grass carp) was dried at 80 °C in an air oven for 8 h and then ground into a powder. A 1 g amount of the dried powder was digested with a mixture of nitric acid and hydrogen peroxide in a flask. After the organic matter had been destroyed, the residue was dissolved in 50 ml of 0.1 mol dm^{-3} HCl, transferred into a 100 ml calibrated flask and diluted to the mark with water. The sample solutions thus prepared were used for the determination of copper.

Results and Discussion

Extraction of Copper(II) With DPC

The reaction of copper(II) with DPC in basic aqueous solution forms a brown chelate which can be extracted into chloroform; in addition, copper(II) in basic aqueous solution is also directly extractable as the Cu–DPC chelate by using chloroform containing DPC. The extraction was performed in various buffer systems, such as phosphate, tris(hydroxymethyl)-methylamine–hydrochloric acid and ammonium chloride–ammonia. It was found that the ammonium chloride buffer was superior to the other buffers examined for the extraction of copper with chloroform containing DPC. The dependence of the absorbance of the extract on pH is shown in Fig. 3; a pH of 8.6 was chosen.

The effect of varying the DPC concentration over the range 0.002–0.1% on the degree of extraction, for 80 ng of copper in 20 ml of ammonium chloride buffer solution with 5 ml of DPC solution in chloroform, was examined. The degree of extraction was found to be constant; hence, a DPC concentration of 0.02% was used as the optimum. Similar studies revealed that a shaking time of 1 min was sufficient to achieve quantitative extraction. Hence, for extracting less than 80 ng of copper in an aqueous phase volume of 20 ml, the optimum extraction

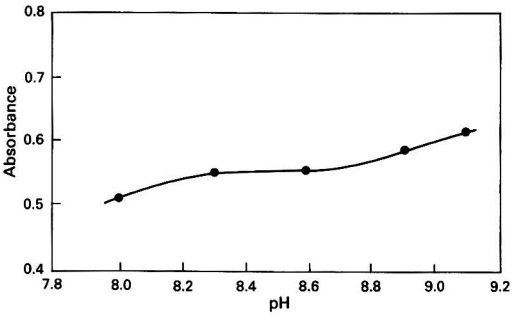

Fig. 3 Effect of pH on the absorbance of the extract. The extraction was carried out in 10 ml of 0.1 mol dm^{-3} NH_3–NH_4Cl buffer containing 4 μg of Cu^{II} with 10 ml of 0.1% DPC in chloroform

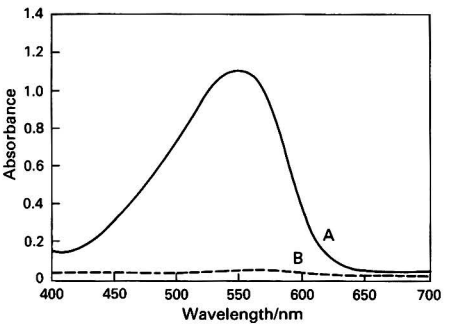

Fig. 4 Absorption spectra of the copper chelate and the DPC reagent blank. A, Cu–DPC chelate against reagent blank; and B, DPC in chloroform against solvent

conditions are as follows: sufficient 0.01 mol dm^{-3} ammonium chloride buffer of pH 8.6 to bring the final volume of the aqueous phase to 20 ml; 5 ml of 0.02% DPC in chloroform; shaking time, 3 min.

Interference experiments were carried out under the conditions described above. Except for cobalt and nickel, none of the elements examined, *i.e.*, Fe^{III}, Cr^{III}, Mn^{II}, Zn^{II}, Cd^{II}, Hg^{II}, Mg^{II} and Cr^{VI}, produced an extractable coloured chelate.

Chelate of Copper With DPC

The absorption spectra of the Cu–DPC chelate and of the reagent blank in chloroform are shown in Fig. 4. The wavelength of the absorption peak of the chelate at 545 nm closely matches that of the pump beam (532 nm) used here. The molar absorptivity of the Cu–DPC chelate in chloroform was found to be 7.8×10^4 l mol^{-1} cm^{-1} at 532 nm, whereas the absorbance of the DPC extractant at the same wavelength was negligible. Hence, this provides a low blank value in the absorption measurements, which is important for highly sensitive pulsed PA measurements. However, DPC is easily oxidized by air to produce a pink compound, which causes the blank to increase. Therefore, it was noted that careful purification of the extractant to obtain a sufficiently constant and low background is a prerequisite for highly sensitive analysis with the pulsed PA method.

The colour system, after extraction, was found to be stable for at least 2 h. However, a gradual decrease in the PA signal was observed during irradiation with the pulsed laser. Curve A in Fig. 5 represents the situation in which the concentration of the chelate is slightly high; the PA signal decreases exponen-

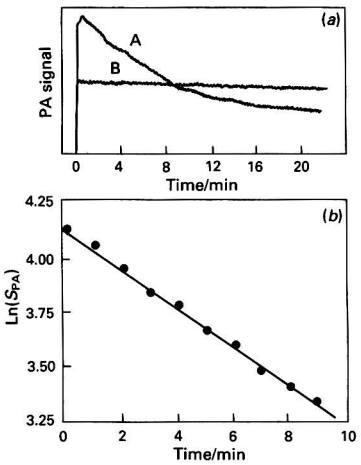

Fig. 5 (*a*) Stability curve for the extracted Cu–DPC chelate during irradiation with a pulsed laser. Pulsed energy: 6.2 mJ. A, Absorbance = 4.4×10^{-2}; and B, absorbance = 1.9×10^{-4}. (*b*) Variation of $\ln(S_{PA})$ with irradiation time for curve A

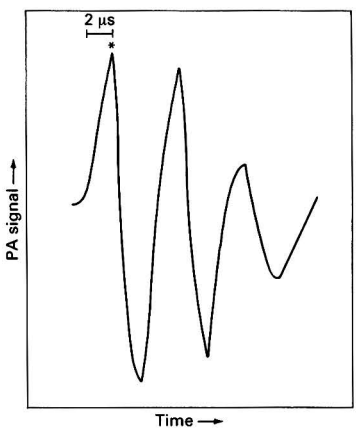

Fig. 6 PA signal generated from pulsed excitation of the Cu–DPC chelate. For details, see text

tially with irradiation time at 6.2 mJ per pulse. However, no decay of the PA signal is apparent at a low concentration of the chelate during the same irradiation time (curve B). In practice, an irradiation time of 1–2 min is sufficient for a single PA measurement. The deviation in the detection caused by the decay of the PA signal due to laser light irradiation is negligible, particularly for a weak absorbance or a low laser energy irradiation.

PA Measurement

The pulsed PA waveform of the extract is shown in Fig. 6. The magnitude of the peak marked with an asterisk is directly proportional to the absorbance of the extract at a constant incident radiation power. It was observed that the waveforms were the same with both cell A and cell B. However, there is an almost 50% enhancement of the magnitude of the PA signal for cell A compared with cell B.

It is known that the magnitude of the PA signal is linearly dependent on the pulsed energy. In order to increase the sensitivity for trace analysis, the pulsed laser energy applied

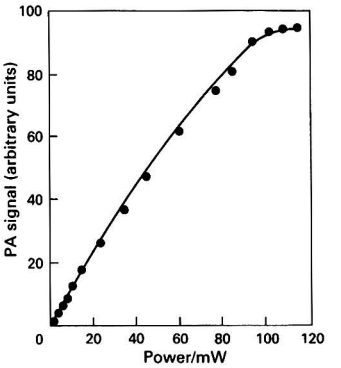

Fig. 7 Dependence of the magnitude of the PA signal on the incident laser power

Table 1 Application of the proposed method to the determination of copper in biological samples and comparison of the results obtained with those given by AAS

	Cu found/μg g^{-1}	
Sample*	Proposed method†	AAS
Pig kidney	25.0	26.5
Grass carp	6.93	7.50

* Dried powder.
† Average of three determinations.

should be as high as possible. However, a high pulsed energy will always induce many non-linear effects such as photodissociation and breakdown. The optimum pulsed energy value is that which not only maintains high sensitivity for PA detection, but also allows Beer's law to be obeyed over the concentration range to be examined. The graph of PA signal intensity *versus* incident laser power is shown in Fig. 7. By using cell A, the optimum energy value found experimentally was about 6.5 mJ per pulse in a 3 mm beam radius for an absorbance of 0.04.

The minimum absorbance that could be measured, which was obtained by using a series of solutions prepared by stepwise dilution of the Cu–DPC chelate with chloroform, was 8.5×10^{-6} at 6.2 mJ per pulse. This corresponds to 6.9×10^{-3} μg l^{-1} of copper in chloroform solution. The relative standard deviation for ten replicate measurements of a chloroform solution of the chelate with an absorbance of 7.8×10^{-3} was 1.5% at 0.7 mJ per pulse. Because of the high content of copper in the biological samples examined here, a calibration graph was constructed in the range 0.04–0.4 μg l^{-1} of copper in aqueous solution. The detection limit, defined as a signal-to-noise ratio of 3 at 1.9 mJ per pulse, was 0.022 μg l^{-1} in aqueous solution.

Applications of the Method

The proposed method was applied to the determination of trace amounts of copper in pig kidney and fish flesh (grass carp).

The results obtained with the proposed method were compared with those given by atomic absorption spectrometry (AAS) and are shown in Table 1.

The relative standard deviation for six replicate extraction–PA measurements of 0.4 ml of a prepared solution was 7.8% for the grass carp sample. The recovery of copper from a sample (fish) was found to be 98.5% by extraction and PA measurement.

Conclusion

A sensitive method for the determination of copper, based on extraction and PA spectrometry, has been developed. The combination of PA measurement and separation by extraction considerably improves the selectivity of the PA measurement; further, the use of an organic solvent enhances the magnitude of the PA signal. The proposed method allows a Cu–DPC extract with an absorbance of 8.5×10^{-6} to be detected, and can also be applied to the determination of copper in biological samples containing little or no cobalt and nickel.

This project was supported by the National Natural Science Foundation of China.

References

1 Lahmann, W., Ludewig, H., and Welling, H., *Anal. Chem.*, 1977, **49**, 549.
2 Oda, S., Sawada, T., and Kamada, H., *Anal. Chem.*, 1978, **50**, 865.
3 Kitamori, T., Fujii, M., Sawada, T., and Gohshi, Y., *J. Appl. Phys.*, 1985, **58**, 268.
4 Yan, H., Deng, Y., and Zeng, Y., *Chem. J. Chin. Univ.*, 1988, **4**, 25.
5 Yan, H., Deng, Y., and Zeng, Y., *Kexue Tongbao* (*Engl. Transl.*), 1989, **34**, 790.
6 Zuo, B., Deng, Y., and Zeng, Y., *Chem. J. Chin. Univ.*, 1990, **11**, 15.
7 Kitamori, T., Suzuki, K., Sawada, T., Gohshi, Y., and Motojima, K., *Anal. Chem.*, 1986, **58**, 2275.
8 Huang, X., *Fenxi Huaxue*, 1990, **18**, 304.

Paper 1/04514H
Received August 29, 1991
Accepted December 4, 1991

Simultaneous Determination of Acetylsalicylic Acid and Its Major Metabolites in Human Serum by Second-derivative Synchronous Fluorescence Spectrometry

Dimitrios G. Konstantianos and Pinelopi C. Ioannou*
Laboratory of Analytical Chemistry, Department of Chemistry, University of Athens, University Campus, Kouponia, Athens 15771, Greece

A method is described for the simultaneous determination of acetylsalicylic, salicylic, gentisic and salicyluric acids (ASA, SA, GA and SU, respectively) in serum, based on their native fluorescence. The ASA–SA–GA–SU-containing serum samples are extracted with chloroform–1% acetic acid solution; ASA and SA are determined in the organic phase, and GA and SU in the aqueous phase, after removal of protein with trichloroacetic acid, at pH 5.0 and 11.6, respectively. The ASA–SA and GA–SU–SA mixtures are resolved using second-derivative fluorescence spectrometry and the appropriate empirical equations involving the effect of each acid on the signal of the other. Recoveries from sera spiked with ASA (1.0–10 μg ml^{-1}), SA (25–50 μg ml^{-1}), GA (0.05–0.2 μg ml^{-1}) and SU (1.0–5.0 μg ml^{-1}) ranged from 100 to 104% (mean 101%), from 93 to 99% (mean 97%), from 94 to 104% (mean 99%) and from 94 to 107% (mean 98%), respectively.

Keywords: *Second-derivative synchronous fluorescence spectrometry; acetylsalicylic acid; metabolites; human serum*

Monitoring of salicylates has been a field of active investigation for more than 45 years.[1] This is due to the widespread and frequent use of salicylic acid (SA) derivatives, especially the acetylated form, aspirin (ASA), for a variety of medical conditions.

Determination of salicylates in biological fluids is of interest both in emergency and routine testing[2–4] and in pharmacokinetic investigations, as ASA and its major metabolites in the body, such as SA, gentisic acid (GA) and salicyluric acid (SU), have all been reported to show different pharmacological effects.[5] Of the techniques used for determining salicylates, high-performance liquid chromatography (HPLC) is preferred for pharmacokinetic investigations because of the required level of specificity, sensitivity and simplicity. However, most of the HPLC methods proposed either fail to quantify ASA or fail to prevent its hydrolysis during sample preparation.[6–8] Only a few methods provide a complete analysis for ASA and its major metabolites.[9–11] Non-chromatographic methods for determining salicylates in biological fluids[2,3] generally lack specificity, although this can be improved by using different techniques of sample preparation and/or different spectral characteristics.

Synchronous scanning derivative fluorescence spectrometry, which combines high sensitivity with improved selectivity, compared with conventional fluorescence spectrometry,[12] is a very useful tool for resolving multicomponent mixtures without prior separation. Muñoz de la Peña *et al.*[13] determined SA and SU in urine by first-derivative fluorescence spectrometry following extraction into diethyl ether and back-extraction of SA and SU into an appropriate buffer solution. Salinas *et al.*[14] improved the method to include GA; ASA cannot be determined by this method, and the ratios of metabolites examined do not cover their ratios in human urine found during pharmacokinetic studies by other methods.[9,15,16] Recently, we reported a method for the simultaneous determination of ASA and SA in serum and pharmaceuticals by second-derivative synchronous fluorescence spectrometry (SDSFS).[17] This study represents an improvement of the method to include SU and GA, hence allowing the simultaneous determination of ASA and its major metabolites (SA, GA and SU) in a single serum sample.

By using the method described here, ASA and SA were determined in the organic phase after simple extraction of the sample with chloroform–1% acetic acid; GA and SU were determined in the aqueous phase, after removal of proteins by treatment with trichloroacetic acid, so as to avoid interference from serum components and to liberate GA and SU, which are strongly bound to serum albumin. Mixtures of ASA–SA, GA–SU, SU–SA, GA–SA and GA–SU–SA were resolved by SDSFS. The proposed method was applied successfully to the determination of ASA, SA, GA and SU in serum samples. The analysis time for all the compounds was less than 15 min. Studies on samples containing various concomitantly administered drugs were performed in order to demonstrate the specificity of the proposed method.

Experimental

Apparatus

A Model 512 fluorescence spectrometer (Perkin-Elmer, Norwalk, CT, USA), equipped with a 150 W xenon arc lamp and a magnetic stirrer under the cell holder, was used. All measurements took place in a standard 10 mm (pathlength) quartz cell, thermostatically controlled at 25.0 ± 0.5 °C. Excitation and emission monochromators were locked together and scanned simultaneously with a constant difference $\Delta\lambda = \lambda_{em} - \lambda_{ex}$. The scan speed and response time of the spectrometer were set at 4 nm s^{-1} and 'Fast' mode, respectively.

The digital read-out unit of the spectrometer was interfaced with an Amstrad CPC-6128 microcomputer (Brentwood, UK) for spectral acquisition, calculations of the spectrum derivatives and automatic evaluation and presentation of the analytical signals, with use of laboratory-made software.[17] Smoothed and derivative spectra were defined by using the Savitzky–Golay method.[18]

Reagents

Spectroscopic-quality grade chloroform (Merck, Darmstadt, Germany) was used to make up 1% v/v acetic acid in chloroform. Henceforth, this mixture will be referred to as 'mixed solvent'. Stock solutions of ASA and SA (Fluka, Buchs, Switzerland) containing 4.00 and 2.00 mg ml^{-1}, respectively, were prepared in the mixed solvent. The stock

* To whom correspondence should be addressed.

solution of ASA was prepared daily, whereas the stock solution of SA was stable for at least 1 year at room temperature.

Aqueous stock solutions of ASA, SA, GA and SU (Sigma, St. Louis, MO, USA), containing 1.00, 0.50, 1.00 and 1.00 mg ml^{-1}, respectively, were prepared in distilled, de-ionized water. The stock solution of ASA was prepared daily, whereas the stock solution of SA was stable for at least 1 month at room temperature. Stock solutions of GA and SU were stable for 1 week at 4 °C.

A stock solution of bovine albumin (Sigma), containing 100 mg ml^{-1}, was prepared in distilled, de-ionized water daily. Phosphate buffers (0.05 mol dm^{-3}) of pH 7.2 and 11.6 were prepared; 10 mol dm^{-3} NaOH was used for pH adjustment. A 16% m/v solution of trichloroacetic acid in chloroform was used for deproteinization.

Procedures and Calculations

Sample preparation

Sample preparation and all measurement steps are summarized in Scheme 1.

Place 0.50 ml of serum containing 0.50–20.0 μg of ASA, 50–100 μg of SA, 0.025–0.4 μg of GA and 1.0–5.0 μg of SU into a test-tube. Add 2.00 ml of the mixed solvent, sonicate the mixture for 1 min and centrifuge for 3 min at 1500*g*. Use the organic phase for ASA and SA determination, and the upper aqueous phase for GA and SU determination.

Transfer 0.40 ml of the aqueous layer into another test-tube. Add 0.12 ml of trichloroacetic solution, sonicate for 2 min and centrifuge for 3 min at 1500*g*. Use the clear supernatant solution for GA and SU determination.

Determination of ASA and SA

Transfer 1.00 ml (0.50 ml for higher concentrations of SA) of the organic phase into the cell, add mixed solvent to a total volume of 2.00 ml and start the stirrer. Obtain the synchronous fluorescence spectra by scanning both monochromators simultaneously at a constant difference $\Delta\lambda$ = 60 nm (λ_{ex} = 240–290 nm) and $\Delta\lambda$ = 130 nm (λ_{ex} = 290–320 nm) for ASA and SA, respectively. (Hereafter, all wavelengths referring to synchronous spectra are taken to be equal to those of the corresponding excitation wavelengths.) Evaluate the second-derivative signal of ASA, ΔI_{ASA}, within the spectral range 260–290 nm, and the signal of SA, ΔI_{SA}, within the spectral range 310–344 nm. Calculate the concentration of SA in the extract, c_{SA} (μg ml^{-1}), from the calibration graph for SA in the mixed solvent (c_{SA} is required for the subsequent determination of ASA). Calculate the total concentration of SA in serum, $c_{SA(serum)}$, from a calibration graph obtained with control serum standards spiked with SA (concentration range 40–200 μg) and treated similarly.

Calculate the total concentration of ASA in serum, $c_{ASA(serum)}$ (μg ml^{-1}), by using eqn. (1). This equation, and eqns. (2)–(6), were reported in previous work.[17]

$$c_{ASA(serum)} = 1.05df\left[\frac{\Delta I_{ASA}}{S_{ASA}(1.008 - 0.017c_{SA})} + 0.157c_{SA} + 0.013\right] \quad (1)$$

where df is the actual dilution factor (8 or 16), and S_{ASA} is the slope of the calibration graph for ASA in the mixed solvent.

Determination of GA and SU

For the determination of GA, transfer 0.30 ml of the clear supernatant solution into the cell, add 1.70 ml of buffer solution (pH 7.2) and start the stirrer. Obtain the synchronous fluorescence spectra by scanning both monochromators simultaneously at a constant difference $\Delta\lambda$ = 120 nm (λ_{ex} = 250–390 nm). Evaluate the analytical signal of GA, ΔI_{GA}, and that of the interferent, $\Delta I_{int,1}$, within the spectral ranges 320–360 and 264–304 nm, respectively. Correct ΔI_{GA} with respect to the signal of the interferent $\Delta I_{int,1}$, by using eqn. (2). Calculate the concentration of GA in serum from a calibration graph obtained with control serum standards spiked with GA (concentration range 0.1–2.4 μg ml^{-1}).

For the determination of SU, place 0.03 ml of 10 mol dm^{-3} NaOH in the same cell to bring the pH to 11.6. Obtain the synchronous fluorescence spectra by scanning both monochromators simultaneously at a constant difference of $\Delta\lambda$ = 70 nm (λ_{ex} = 250–290 nm). Evaluate the analytical signal of SU, ΔI_{SU}, and that of the interferent, $\Delta I_{int,2}$, within the spectral ranges 320–356 and 260–300 nm, respectively. Correct ΔI_{SU} with respect to the signal of the interferent, $\Delta I_{int,2}$, by using eqn. (2):

$$\Delta I_{GA\text{ or }SU(corr)} = df\,\Delta I_{GA\text{ or }SU}\left(0.348\log\frac{\Delta I_{GA\text{ or }SU}}{\Delta I_{int\,1\text{ or }2}} + 0.760\right) \quad (2)$$

where df is the dilution factor (6.67). Calculate the concentration of SU in serum from a calibration graph obtained with control serum standards spiked with SU (concentration range 0.4–8.0 μg ml^{-1}).

All instrumental parameters are summarized in Table 1.

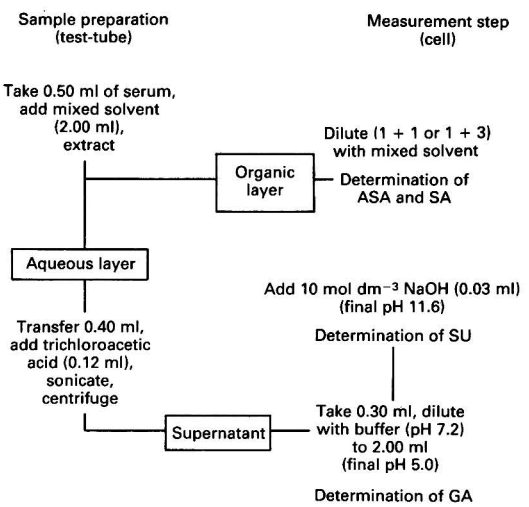

Scheme 1 Determination of ASA, SA, GA and SU in a single serum sample

Table 1 Instrumental parameters for the determination of ASA, SA, GA and SU

Parameter	Compound			
	ASA	SA	GA	SU
Slit-width/ex, em (nm)	20, 20	20, 20	10, 20	10, 20
$\Delta\lambda$/nm	60	130	120	70
Savitzky–Golay filter size/points	9	9	11	11
Synchronous spectrum scanning range/λ_{ex} (nm)	240–320	290–370	250–390	250–390
ΔI evaluation range/λ_{ex} (nm)	260–290 (ΔI_{ASA})	310–344 (ΔI_{SA})	320–360 (ΔI_{GA})	320–356 (ΔI_{SU})
ΔI evaluation range for interference/λ_{ex} (nm)	—	—	264–304 ($\Delta I_{int,1}$)	272–312 ($\Delta I_{int,2}$)

Results and Discussion

The simultaneous determination of ASA and SA by SDSFS has been reported previously.[17] The measurement was performed in chloroform–1% acetic acid solution ('mixed solvent') in order to avoid hydrolysis of ASA, and to make use of the different fluorescence properties of ASA and SA in this solvent.

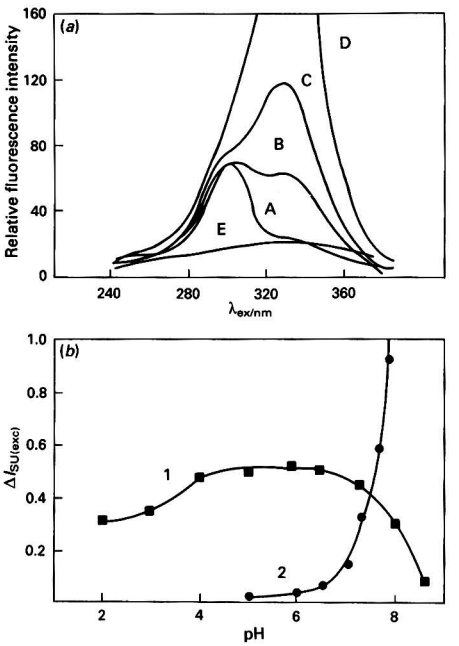

Fig. 1 Effect of pH (*a*) on the excitation spectrum (λ_{em} = 400 nm) of SU (pH: A, 5.0; B, 7.3; C, 8.2; D, 8.9; and E, blank) and (*b*) on the second-derivative signals of the excitation spectra: λ_{ex} = 300 nm (1) and 332 nm (2)

The optimum wavelength differences, Δλ, for the synchronous scanning were found to be 60 nm for ASA and 130 nm for SA. The determination was performed by evaluating the second-derivative signals within the spectral ranges 260–290 nm for ASA and 310–344 for SA (see Table 1). Empirical eqn. (1) for calculating the concentration of ASA at a given concentration of SA was proposed in order to overcome the influence of SA on the determination of ASA.

For the determination of these compounds in serum a single extraction into mixed solvent was proposed.

In this paper, the method was extended to the determination of GA and SU in ASA–SA–GA–SU mixtures. As the extractibility of GA and SU into chloroform has been reported to be poor,[19] the possibility of separating an ASA–SA–GA–SU mixture into ASA–SA and GA–SU mixtures was studied. It was found that the use of mixed solvent instead of chloroform causes a slight increase in the extractibility of GA. However, the extraction of GA and SU from albumin solutions or serum into mixed solvent was negligible, owing to their strong binding with albumin. Hence, by a simple extraction with the mixed solvent, ASA and SA are transferred into the organic phase, while GA and SU remain in the aqueous phase. It should be noted that whereas extraction of ASA from albumin solutions or serum is almost quantitative, SA is extracted only as an unbound fraction[16] (of about 30% of the total amount of SA in serum). The bound fraction of SA is liberated from serum albumin after deproteinization. Therefore, GA and SU have to be separated in the serum supernatant phase as GA–SU–SA mixtures.

For separating binary or ternary mixtures of GA, SU and SA, the SDSFS technique was used in combination with the dependence of the fluorescence properties of the three compounds on the pH. As has been reported previously by Salinas *et al.*,[14] at pH >11.0, the only fluorescent species are SU (λ_{ex} = 332 nm, λ_{em} = 400 nm) and SA (λ_{ex} = 300 nm, λ_{em} = 400 nm), whereas at pH <6.0 only GA (λ_{ex} = 324 nm, λ_{em} = 444 nm) and SA (λ_{ex} = 300 nm, λ_{em} = 400 nm) exhibit fluorescence. A pH of 6.0 and of 11.6 for the determination of GA and SU, respectively, was therefore proposed. However, a detailed study on the influence of SU on the analytical signal of GA showed significant interference from SU, especially at

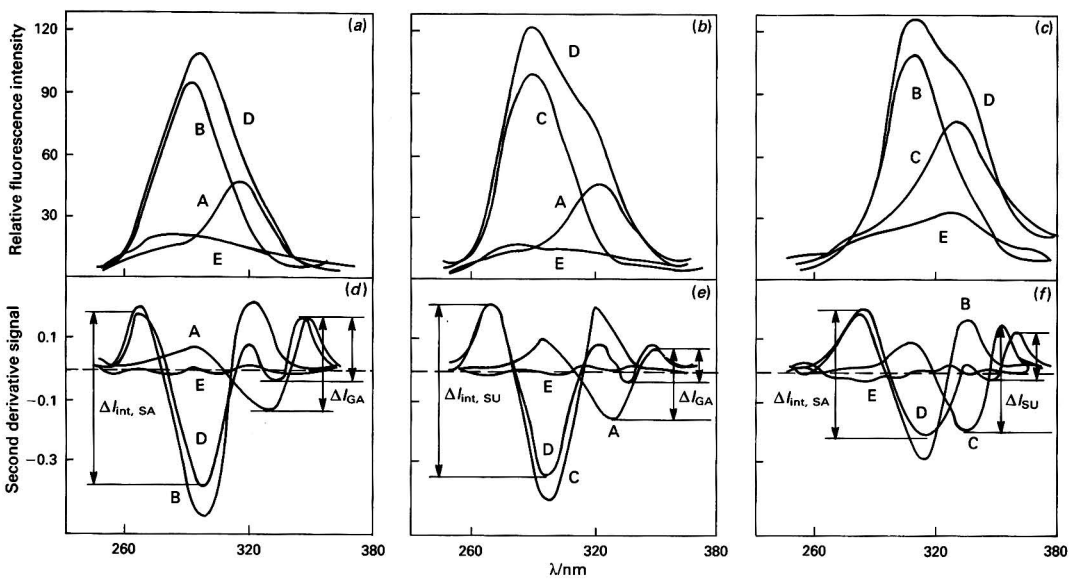

Fig. 2 Synchronous fluorescence spectra [(*a*)–(*c*)] of A, GA; B, SA; C, SU; D, GA–SA (*a*); GA–SU (*b*); and SU–SA (*c*) mixtures, and E, a blank; and their second-derivative spectra [(*d*)–(*f*)]. (*a*): c_{GA} = 0.030 μg ml^{-1}, c_{SA} = 0.15 μg ml^{-1} (Δλ = 120 nm, sensitivity 10, pH = 5.0). (*b*) c_{GA} = 0.025 μg ml^{-1}, c_{SU} = 1.00 μg ml^{-1} (Δλ = 120 nm, sensitivity 10, pH = 5.0). (*c*): c_{SU} = 0.060 μg ml^{-1}, c_{SA} = 0.48 μg ml^{-1} (Δλ = 70 nm, sensitivity 10, pH = 11.6)

high SU : GA ratios. The influence is caused by the existence of a second excitation maximum of SU (λ_{ex} = 300 nm) at 4 < pH < 8 [Fig. 1(*a*)], which results in negative errors when GA is determined by the SDSFS technique at the optimum difference ($\Delta\lambda$ = 120 nm). The influence of pH on the second-derivative excitation signal of SU, $\Delta I_{SU(exc)}$, at two maxima is shown in Fig. 1(*b*). An optimum pH of 5.0 was selected for the determination of GA, where the $\Delta I_{SU(exc)}$ signal at λ_{ex} = 300 nm is almost constant (pH = 4–6), and the $\Delta I_{SU(exc)}$ signal at λ_{ex} = 332 nm is the lowest.

The optimum pH of 5.0 for the determination of GA was obtained by addition of 0.05 mol dm^{-3} phosphate buffer of pH 7.2 to the acidified supernatant phase (after deproteinization with trichloroacetic acid). For the determination of SU, a pH of 11.6 was selected, where the fluorescence intensity of GA is negligible. The signals of SA and SU at pH 5.0 and 11.6 are referred to as interference signals, $\Delta I_{int,1}$ and $\Delta I_{int,2}$, respectively.

Comparison of Spectra

The synchronous spectra and their corresponding second derivatives obtained for GA, SU, SA and GA–SA, GA–SU and SU–SA mixtures, at the optimum pH for the determination of GA and SU, are shown in Fig. 2.

As can be seen from Fig. 2, the combination of synchronous and derivative fluorescence techniques results in adequate resolution of the mixtures. However, the vicinity of large SA and/or SU bands to the band of GA, and the vicinity of the SA band to the band of SU, resulted in a decrease of ΔI_{GA} [Fig. 2(*d*) and (*e*), curve C] and ΔI_{SU} signals [Fig. 2(*f*) curve C], compared with the pure solutions (curves A). This decrease, which is purely a mathematical artifact, inevitably results in a loss of ΔI_{GA} and ΔI_{SU} signals in the presence of a large excess of SA and/or SU, which must be taken into account. The absence of any quenching effect has been confirmed by the fact that the spectral bands of the mixtures are equivalent to the sum of their individual bands.

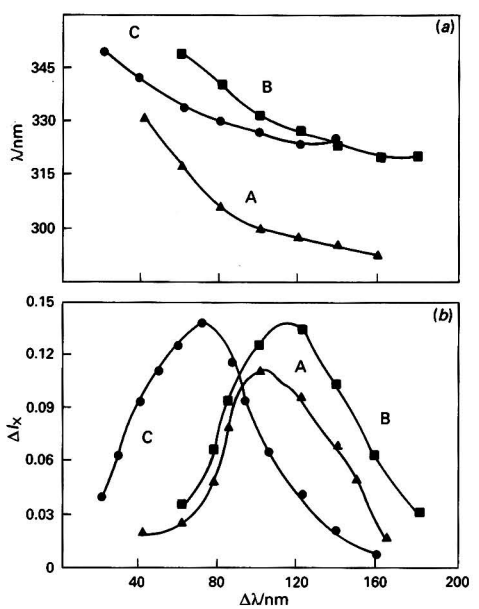

Fig. 3 Effects of $\Delta\lambda$ on the second-derivative synchronous spectra of A, SA; B, GA; and C, SU. (*a*) Effect on the wavelength corresponding to the minimum of the second-derivative peaks; and (*b*) effect on the analytical signals

Selection of $\Delta\lambda$ for Synchronous Scanning

In order to select the optimum wavelength difference between excitation and emission monochromators ($\Delta\lambda$) for the determination of GA and SU with SA by SDSFS, a wide range of $\Delta\lambda$ values (20–240 nm) was examined. The position of the minimum of the second-derivative spectrum and the signal for GA and SU as functions of $\Delta\lambda$ are shown in Fig. 3(*a*) and (*b*), respectively.

As optimum wavelength intervals for GA and SU, $\Delta\lambda$ values of 120 and of 70 nm, respectively, were selected, so as to minimize the spectral interference caused by each compound in the mixture and to minimize the loss of sensitivity.

The same experiment for ASA and SA in the mixed solvent has been reported previously.[16]

Other Instrumental Parameters

For recording the synchronous spectra, a scan speed of 4 nm s^{-1} and a 'Fast' response time were selected. The sampling rate was defined to be 1 point every 4 nm. For the calculation of the second derivatives of the synchronous fluorescence spectra of GA and SU by the Savitzky–Golay method,[18] filter sizes of 11 and 11 points, respectively, were selected.

General Analytical Characteristics

The linear concentration ranges were 0.003–6.50 and 0.006–10.5 μg ml^{-1} for GA and SU, respectively. Pearson's correlation coefficients[20] (*r*) for the calibration graphs were 0.9998 and 0.9992 for GA and SU, respectively. The detection limits obtained by SDSFS, defined as three times the standard deviation of the lowest concentration, were 0.001 and 0.002 μg ml^{-1} for GA and SU, respectively. In order to test the precision of the method, three series of samples, covering the ranges of interest for GA (0.050, 0.50 and 5.00 μg ml^{-1}) and for SU (0.090, 0.80 and 7.00 μg ml^{-1}) were analysed, and the corresponding relative standard deviations (RSDs) (n = 10) were found to be 3.2, 1.5 and 1.5% for GA, and 3.8, 2.3 and 2.0% for SU.

Determination of GA and SU in Binary or Ternary Mixtures with SA

In order to apply the SDSFS technique to the simultaneous determination of GA and SU in binary or ternary mixtures with SA, a detailed study on the influence of the signal for each acid on the analytical signal of the other was performed.

The effect of the analytical signal for SA and SU on the analytical signal for GA (curves A and C), and the effect of the

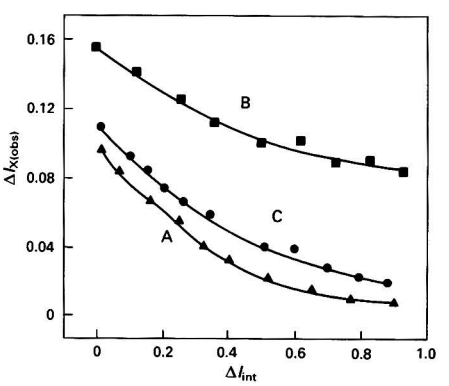

Fig. 4 Effect of the signals of SA and SU as interferences (ΔI_{int}) on the analytical signal [$\Delta I_{X(obs)}$] of GA (A and B) and SU (C)

Table 2 Determination of 0.050 μg ml^{-1} of GA in the presence of an excess of SA in aqueous solutions

SA : GA mass ratio	GA found*/μg ml^{-1}		Recovery ± SD (%)	
	Uncorrected†	Corrected‡	Uncorrected	Corrected
1 : 1	0.040	0.050	80 ± 14	100 ± 2
2 : 1	0.035	0.050	70 ± 11	100 ± 3
4 : 1	0.031	0.050	62 ± 5	100 ± 3
6 : 1	0.028	0.051	56 ± 15	102 ± 3
8 : 1	0.022	0.050	44 ± 2	100 ± 5
10 : 1	0.016	0.048	32 ± 8	96 ± 1
12 : 1	0.018	0.050	36 ± 2	100 ± 3
14 : 1	0.013	0.045	26 ± 6	90 ± 5
16 : 1	0.010	0.049	20 ± 2	98 ± 6
			Mean	98 ± 4

* Average of three measurements.
† Without using correction equation.
‡ After using correction eqns. (3) and (6).

Table 3 Determination of 0.050 μg ml^{-1} of GA in the presence of excess of SU in aqueous solutions

SU : GA mass ratio	GA found*/μg ml^{-1}		Recovery ± SD (%)	
	Uncorrected†	Corrected‡	Uncorrected	Corrected
10 : 1	0.045	0.051	90 ± 8	102 ± 1
20 : 1	0.042	0.050	84 ± 9	100 ± 6
30 : 1	0.036	0.048	72 ± 9	96 ± 3
40 : 1	0.035	0.049	70 ± 4	98 ± 3
50 : 1	0.034	0.051	68 ± 4	102 ± 2
60 : 1	0.036	0.051	72 ± 12	102 ± 6
70 : 1	0.035	0.052	70 ± 9	104 ± 5
80 : 1	0.029	0.046	58 ± 6	91 ± 5
			Mean	99 ± 4

* Average of four determinations.
† Without using correction equation.
‡ After using correction eqns. (4) and (6).

Table 4 Determination of 0.050 μg ml^{-1} of SU in the presence of excess of SA in aqueous solutions

SA : SU mass ratio	SU found*/μg ml^{-1}		Recovery ± SD (%)	
	Uncorrected†	Corrected‡	Uncorrected	Corrected
2 : 1	0.039	0.050	78 ± 5	100 ± 3
4 : 1	0.033	0.050	66 ± 6	100 ± 4
6 : 1	0.028	0.051	56 ± 6	102 ± 4
8 : 1	0.024	0.050	48 ± 4	100 ± 2
10 : 1	0.020	0.051	40 ± 1	102 ± 1
12 : 1	0.019	0.049	38 ± 4	98 ± 1
16 : 1	0.010	0.049	20 ± 2	98 ± 5
20 : 1	0.012	0.051	24 ± 8	102 ± 5
			Mean	100 ± 2

* Average of four measurements.
† Without using correction equation.
‡ After using correction eqns. (5) and (6).

Table 5 Determination of GA and SU in synthetic GA–SU–SA mixtures

SA : SU : GA mass ratio	Concentration/μg ml^{-1}					
	Added		Found*		Recovery (%)	
	GA	SU	GA	SU	GA	SU
7 : 5 : 1	0.050	0.250	0.048	0.240	99.0	96.0
5 : 3 : 1	0.080	0.240	0.087	0.230	108.8	95.8
3 : 5 : 1	0.080	0.400	0.078	0.416	97.5	104.0
2 : 10 : 1	0.050	0.500	0.049	0.485	98.0	97.0
				Mean	100.8	98.2

* Average of three measurements, using eqns. (3) and (6).

analytical signal for SA on the analytical signal for SU (curve B), obtained by SDSFS at $\Delta\lambda$ = 120 nm and $\Delta\lambda$ = 70 nm, respectively, is shown in Fig. 4.

The analytical signals for GA and SU in the presence of the SA and/or SU (for GA) signal, obtained by SDSFS, decreased considerably with an increase in the SA or SU signal. It was found that this decrease, expressed as a correction factor for the analyte in the presence of the interferent, $CF_{\text{anal(int)}}$ (*i.e.*, the ratio of the signal for GA or SU in pure solutions, ΔI_{corr}, to its signal in the presence of the interferent, ΔI_{obs}), is linearly related to the ratio of the observed signal for the analyte ΔI_{GA} or ΔI_{SU} to the signal for the interferent ΔI_{SA} and/or ΔI_{SU}, according to the equations:

$$CF_{\text{GA(SA)}} = 0.348(\pm 0.005) \log \frac{\Delta I_{\text{GA}}}{\Delta I_{\text{SA}}} + 0.760(\pm 0.023) \quad (r = 0.999) \quad (3)$$

$$CF_{\text{GA(SU)}} = 0.253(\pm 0.024) \log \frac{\Delta I_{\text{GA}}}{\Delta I_{\text{SU}}} + 0.905(\pm 0.028) \quad (r = 0.993) \quad (4)$$

$$CF_{\text{SU(SA)}} = 0.356(\pm 0.012) \log \frac{\Delta I_{\text{SU}}}{\Delta I_{\text{SA}}} + 0.776(\pm 0.028) \quad (r = 0.998) \quad (5)$$

The corrected (true) signal in each instance is given by the equation:

$$\Delta I_{\text{corr}} = \Delta I_{\text{obs}} CF_{\text{anal(int)}} \quad (6)$$

Each of the eqns. (3), (4) and (5) is the mean of three equations obtained at three different concentrations of GA (0.050, 0.40 and 3.00 μg ml^{-1}) and at three different concentrations of SU (0.080, 0.50 and 5.00 μg ml^{-1}), at increasing signals for the interferents, SA and/or SU.

Results for the determination of GA and SU in synthetic GA–SA, GA–SU and SU–SA mixtures, calculated from the calibration graphs with and without use of the appropriate correcting equations are summarized in Tables 2–4. As can be seen from these tables, by using the appropriate correcting equations, GA could be determined in the presence of up to a 16-fold excess of SA, or up to an 80-fold excess of SU, and SU could be determined in the presence of up to a 20-fold excess of SA. At higher excess of the interferent the signal for the analyte ΔI_{obs} is completely hidden.

As can be seen from eqns. (3) and (5), the influence of the signal for SA on the signals for GA and SU is similar even though they were obtained at different $\Delta\lambda$ (120 and 70 nm, respectively), and at different pH (5.0 and 11.6, respectively). Table 5 summarizes the results obtained for synthetic GA–SU–SA mixtures at ratios expected in serum samples.[5,15]

The corrected signals for GA in ternary mixtures were calculated without using eqn. (4) because the influence of the signal for SU, with respect to the influence of the signal for SA, is negligible. The concentrations of GA and SU in SA–GA–SU mixtures can be calculated from eqn. (2), which is a combination of eqns. (3) and (6), and from the appropriate calibration graph.

Serum Samples

Serum samples or albumin solutions containing GA and SU gave signals smaller than those obtained with aqueous standard solutions, owing to some type of binding with precipitated proteins. As has been found, the maximum recovery of GA and SU was obtained when a chloroform solution of trichloroacetic acid was used to precipitate proteins, and the mixture was sonicated for 2 min.

Recovery experiments on albumin solutions containing GA or SU at several albumin and component concentrations gave

Table 6 Determination of quaternary mixtures of ASA, SA, GA and SU in synthetic serum mixtures

Serum concentration/μg ml^{-1}				Concentration found*/μg ml^{-1}				Recovery ± SD (%)			
ASA	SA	GA	SU	ASA	SA	GA	SU	ASA	SA	GA	SU
10.0	35.0	0.05	1.0	10.4	34.0	0.049	0.94	104 ± 2	97 ± 1	98 ± 2	94 ± 4
5.0	50.0	0.10	2.0	5.0	47.8	0.097	1.89	100 ± 2	96 ± 2	97 ± 2	94 ± 4
10.0	40.0	0.20	3.0	10.1	39.5	0.207	3.22	101 ± 3	99 ± 1	104 ± 1	107 ± 2
1.0	30.0	0.20	3.0	1.0	28.0	0.202	2.89	100 ± 1	93 ± 1	101 ± 1	96 ± 2
—	25.0	0.10	5.0	—	24.7	0.094	5.02	—	99 ± 2	94 ± 2	100 ± 1
							Mean	101.2	96.8	98.8	98.2

* Average of three measurements.

values of 70.5 ± 0.9% ($n = 5$) and 73.4 ± 3.1% ($n = 6$) for GA and SU, respectively. It was also found that the recoveries of GA and SU are not dependent on albumin concentrations in the range 2–5%.

Recovery data for ASA–SA–GA–SU synthetic mixtures added to serum are shown in Table 6. The selected concentrations for quaternary mixtures are typical for ASA–SA–GA–SU levels in serum, during the first 6 h, from a typical subject, following an oral dose of 650 mg of aspirin.[5,15]

Interference Studies

The determination of SA, ASA and its major metabolites GA and SU is not affected by endogenous substances usually found in the sera of healthy subjects. Interference from other drugs was studied by analysing synthetic mixtures of ASA, SA, GA and SU in serum where amounts of the drug under examination had been added. None of the drugs tested (antipyrine, ibuprofen, amilorid, imipramine, amitriptyline, indomethacin, amoxycillin, levodopa, caffeine, naproxen, carbamazepine, phenacetin, chlorpromazine, theophylline and dithranol) interferes with the determination of ASA, SA, GA and SU at concentrations higher than those achieved therapeutically.

Conclusions

The proposed method is the first non-chromatographic method for the simultaneous determination of ASA, SA, GA and SU in a single serum sample.

The ASA–SA and GA–SU–SA mixtures in a wide range of ratios are resolved by using SDSFS and the appropriate equations, which involve the influence of each acid on the analytical signal of the other. These empirical equations are not instrument dependent and can be used without knowing the concentration of the analytes or the interferents.

The proposed scheme, which incorporates an extraction step for the separation and determination of ASA and SA, thus minimizing hydrolysis of ASA, and a single deproteinization step for the determination of GA and SU, might appear complex. However, the total analysis time (including separation, deproteinization and measurement) does not exceed 15 min. The usual analysis time for all four components by HPLC methods varies between 25 and 35 min.

The proposed method is fairly sensitive and specific for all four compounds and can be used for pharmacokinetic studies of aspirin in serum as an alternative to the HPLC technique. In addition, the method can be applied to the determination of SA, GA and SU in urine. The optimum conditions for this determination are under investigation.

References

1 Stewart, M. J., and Watson, I. D., *Ann. Clin. Biochem.*, 1987, **24**, 1552.
2 Trinder, P., *Biochem. J.*, 1954, **55**, 301.
3 Kang, E. S., Todd, T. A., Capaci, M. T., Schwenzer, K., and Jabbow, J. T., *Clin. Chem. (Winston-Salem, N.C.)*, 1983, **29**, 1012.
4 Ram, N. G., and Mohebullah, Z., *Clin. Chem. (Winston-Salem, N.C.)*, 1990, **36**, 1690.
5 Rumble, R. H., and Roberts, M. S., *J. Chromatogr.*, 1981, **225**, 252.
6 Terweij-Groen, T., Vahlkamp, T., and Krak, C., *J. Chromatogr.*, 1978, **145**, 115.
7 Peng, J. W., Gadalla, A. F., Smith, W., Reng, A., and Chiou, W. L., *J. Pharm. Sci.*, 1978, **67**, 710.
8 Blair, D., Rumack, B. H., and Peterson, R. G., *Clin. Chem. (Winston-Salem, N.C.)*, 1978, **24**, 1543.
9 Mays, D. C., Sharp, D. E., Beach, C. A., Ketshaw, R. A., and Bianchine, J. R., *J. Chromatogr.*, 1984, **311**, 301.
10 Ogunbona, F. A., *J. Chromatogr.*, 1986, **377**, 471.
11 O'Kruk, R. J., Adams, M. A., and Philp, R. B., *J. Chromatogr.*, 1985, **310**, 343.
12 Rubio, S., Gomez-Hens, A., and Valcárcel, M., *Talanta*, 1986, **33**, 633.
13 Muñoz de la Peña, A., Salinas, F., and Durán-Merás, I., *Anal. Chem.*, 1988, **60**, 2493.
14 Salinas, F., Muñoz de la Peña, A., Durán-Merás, I., and Soledad Durán, M., *Analyst*, 1990, **115**, 1007.
15 Reile, U., *J. Chromatogr.*, 1983, **272**, 325.
16 Amick, E. N., and Mason, W. D., *Anal. Lett.*, 1979, **12**, 629.
17 Konstantianos, D. G., Ioannou, P. C., and Efstathiou, C. E., *Analyst*, 1991, **116**, 373.
18 Savitzky, A., and Golay, M. J. E., *Anal. Chem.*, 1964, **36**, 1927.
19 Bakar, S. K., and Niazi, S., *J. Pharm. Sci.*, 1983, **72**, 1020.
20 Miller, J. C., and Miller, J. N., in *Statistics for Analytical Chemistry*, eds., Chalmers, R. A., and Masson, M., Ellis Horwood, Chichester, 2nd edn., 1988, pp. 85–90.

Paper 1/04277G
Received August 15, 1991
Accepted October 23, 1991

Simultaneous Determination of Atmospheric Nitric Acid and Nitrous Acid by Reduction With Hydrazine and Ascorbic Acid With Chemiluminescence Detection

Yukio Kanda and Masafumi Taira
National Laboratory for High Energy Physics, Oho, Tsukuba, Ibaraki-ken 305, Japan

A continuous-flow system for the simultaneous determination of atmospheric HNO_3 and HNO_2 has been developed that consists of two sets of dual-channel flow systems: one is for the measurement of total HNO_3–HNO_2 and the other is for the measurement of HNO_2. Nitric acid and HNO_2 are continuously stripped from the atmosphere into an NaOH solution by drawing the air sample and the solution through a glass coil. The nitrate is reduced with hydrazine sulfate in the presence of Cu^{II} to nitrite, which is then reduced to NO with ascorbic acid solution, and the NO is detected by a chemiluminescence NO_x analyser. This measurement system can also be used to determine HNO_2, thus giving the total concentration of HNO_3 and HNO_2. The measurement system without the hydrazine reduction procedure determines HNO_2 alone. The concentration of HNO_3 is determined by the difference between the two measurements. Of the common pollutants, NO_2 and peroxyacetyl nitrate showed positive interferences. In order to correct for these positive interferences, each of the measurement systems utilizes a dual flow system and a dual-channel NO_x analyser.

Keywords: *Flow system; gaseous nitric acid and nitrous acid; hydrazine and ascorbic acid reduction; chemiluminescence NO_x analyser*

Atmospheric gaseous HNO_3 has received considerable attention because of its role as a major sink for nitrogen oxides in photochemical air pollution[1] and its contribution to the acidity of precipitation.[2,3]

Most analytical methods for the determination of gaseous HNO_3 are based on collection of HNO_3, extraction of nitrate by a suitable solvent and subsequent analysis by colorimetry or ion chromatography. A variety of collection techniques have been developed including the use of a nylon filter,[4,5] an NaCl-impregnated filter[6,7] and diffusion denuder tubes coated with sodium carbonate.[8–10] A tungstic acid denuder technique was also developed in which the collected HNO_3 is thermally decomposed to NO and the NO is detected by a chemiluminescence NO_x analyser.[11] The methods combined with these techniques produce average or integrated HNO_3 concentrations.

A specific and direct method has been reported by Tuazon *et al.*,[12] which uses a 1 km folded path cell coupled to a Fourier transform spectrometer. Although this method may be the best approach because of its selectivity and capability of continuous monitoring, it requires complex instrumentation and its detection limit of about 5 ppb is often above ambient HNO_3 levels. A chemiluminescence method for continuous monitoring of HNO_3 has been developed by Joseph and Spicer,[13] using a modified commercial NO_x analyser and a nylon filter. This method measures HNO_3 as the difference between total NO_x including HNO_3 determined directly and the NO_x determined after selective removal of HNO_3 on a nylon filter. The detection limit of the technique (0.8 ppb) is sufficient for studies in urban areas, but more sensitive techniques are required for studies in non-urban areas.

We have recently developed a chemiluminescence method for the continuous monitoring of ambient gaseous HNO_2.[14] The method is based on collection of HNO_2 by concurrently drawing the air and scrubbing solution through a glass coil, and the subsequent reduction of nitrite to NO by ascorbic acid followed by detection with a chemiluminescence NO_x analyser. The sensitivity of the method is a function of the ratio of sampling flow rate to carrier gas flow rate of sweeping the evolved NO into an NO_x analyser. This permits readily the highly sensitive measurement of HNO_2. The advantage of the technique led us to apply it to the continuous monitoring of gaseous HNO_3.

Several chemiluminescence methods based on the direct reduction of nitrate to NO have been developed for the determination of trace amounts of nitrates in aqueous samples using reducing agents such as iron(II)–molybdate[15,16] and vanadium(III).[17] These methods require highly acidic conditions and/or operation at a relatively high temperature (80–100 °C).

The method described here consists of two steps for the reduction of nitrate to NO. Nitrates are reduced to nitrites with hydrazine sulfate under mild alkaline conditions in the presence of Cu^{II} at a temperature in the range 30–50 °C and the nitrites are then reduced to NO with ascorbic acid under moderately acidic conditions. The measurement systems with and without the hydrazine reduction procedure determine total HNO_3–HNO_2 and HNO_2, respectively, and HNO_3 is calculated from the difference. This paper describes the results of investigations on the reduction of nitrate by hydrazine and some preliminary results of ambient measurements.

Experimental

Choice of Reductant

Many reducing agents have been used for the spectrophotometric determination of nitrate based on the reduction of nitrate to nitrite followed by diazotization–coupling reactions. These include hydrazine sulfate,[18–20] titanium(III) chloride,[21] amalgamated zinc,[22] cadmium,[23,24] amalgamated cadmium,[25] copper-coated cadmium,[24,26–28] and copper-coated cadmium–silver.[24,28] Of these reducing agents, copper-coated cadmium is the most widely used. It was therefore decided to investigate the application of the copper-coated cadmium reduction technique to a continuous monitoring system for gaseous HNO_3. A reduction coil was made from 1.2 mm i.d. poly(tetrafluoroethylene) (PTFE) tubing. A cadmium wire (diameter 1 mm, length 50 cm) was inserted into the tubing and was treated with dilute copper sulfate solution. The quantitative reduction of nitrate to nitrite was obtained with a stream of 5×10^{-3} mol dm^{-3} ethylenediaminetetraacetic acid (EDTA) in borate buffer of pH 8 at flow rates ranging from 0.15 to 0.30 ml min^{-1}. However, the reducing power deteriorated with use because of contact with air bubbles accidentally introduced into the coil, and the reproducible

regeneration of the reductant was difficult. A homogeneous reduction procedure appears to be more suitable for a continuous-flow system. In this study, alkaline hydrazine solution was therefore used for the reduction of nitrate to nitrite.

Reagents

All chemicals used were of analytical-reagent grade from Wako Chemical Industries. Reagent solutions were prepared with high-purity water from a Millipore Milli-Q purification system. Stock standard solutions containing 100 mg l^{-1} of nitrate-N and 100 mg l^{-1} of nitrite-N were prepared in water from potassium nitrate and sodium nitrite dried at 110 °C, respectively. Working standard solutions were prepared in 0.05 mol dm^{-3} NaOH by appropriate dilution of the respective stock standard solutions. Stock solutions of 0.1 mol dm^{-3} hydrazine and 0.01 mol dm^{-3} Cu^{II} were prepared by dissolving $N_2H_4 \cdot H_2SO_4$ and $CuSO_4 \cdot 5H_2O$ in water, respectively. A 0.2 mol dm^{-3} ascorbic acid solution was prepared in 0.1 mol dm^{-3} H_2SO_4.

Standard gas sources were the same as those used previously.[14] They included a diffusion tube device for HNO_3, a continuous generation system for HNO_2 and a cylinder gas mixture for NO. The carrier gas was room air freed of NO_x compounds by passage through a cobalt(III) oxide coated denuder.

Apparatus

A schematic diagram of the measurement system is shown in Fig. 1. The system consists of two sets of dual-channel flow systems. One is for total HNO_3–HNO_2 measurement and the other for HNO_2 measurement. The system for total HNO_3–HNO_2 is identical with that for HNO_2 except that it includes reaction coils for the reduction of nitrate to nitrite. In each system the second channel measures the interference effects from NO_2 and peroxyacetyl nitrate (PAN).

Gaseous HNO_3 and HNO_2 were stripped from the air sample into the solution by concurrently drawing the air and scrubbing solution through a glass stripping coil. The reaction coil for the reduction of nitrate to nitrite by hydrazine was made from a 1 m length of 0.68 mm i.d. PTFE tubing and was immersed in a constant temperature water-bath. A gas–liquid separating coil, made from microporous PTFE tubing, was used for the reduction of nitrite to NO and the successive scrubbing of NO. Details of the stripping and gas–liquid separating coils have been described elsewhere.[14] Air sample and carrier gas flow rates were controlled by calibrated mass flow controllers (SEC-410, Stec Corp.). Constant and continuous supplies of reagent solutions were delivered by four- and two-channel peristaltic pumps (Gilson Minipuls-2, Gilson Medical Electronics). Measurements of HNO_3, HNO_2, and NO were made with Monitor Labs Model 8840 NO_x analysers. The instrument is a dual-channel monitor with two reaction chambers and two photomultiplier tubes. In the measurements of ambient HNO_3 and HNO_2, the NO_x flow line in the instrument was modified to lead directly to the reaction chamber by by-passing the converter to measure simultaneously the NO from the dual flow system.

Ambient Measurement

The experimental conditions for measurements of ambient HNO_3 and HNO_2 were: sampling flow rate, 2.0 l min^{-1}; scrubbing solution, 0.10 ml min^{-1} of 0.05 mol dm^{-3} NaOH; reduction of nitrate to nitrite, 0.10 ml min^{-1} of 2.0×10^{-3} mol dm^{-3} hydrazine–1.6×10^{-5} mol dm^{-3} Cu^{II} at 30 °C; reduction of nitrite to NO, 0.10 ml min^{-1} of 0.2 mol dm^{-3} ascorbic acid in 0.1 mol dm^{-3} H_2SO_4; purging flow rate, 0.29 l min^{-1} in the total HNO_3–HNO_2 system and 0.35 l min^{-1} in the HNO_2 system.

Results and Discussion

Optimization of the Conditions for the Reduction With Hydrazine

The effects of several parameters on the reduction of nitrate to nitrite by hydrazine were investigated. The parameters were:

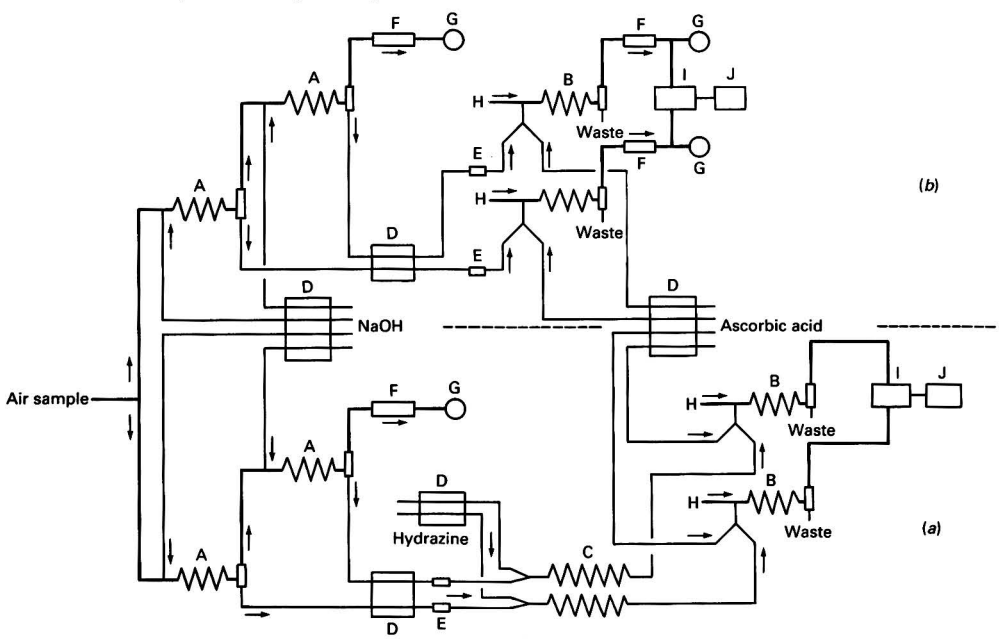

Fig. 1 Schematic diagram of the measurement systems for (*a*) HNO_3–HNO_2 and (*b*) HNO_2. A, Stripping coil; B, gas–liquid separating coil; C, reaction coil; D, peristaltic pump; E, de-bubbler; F, mass flow controller; G, air pump; H, clean air input; I, NO_x analyser; and J, recorder

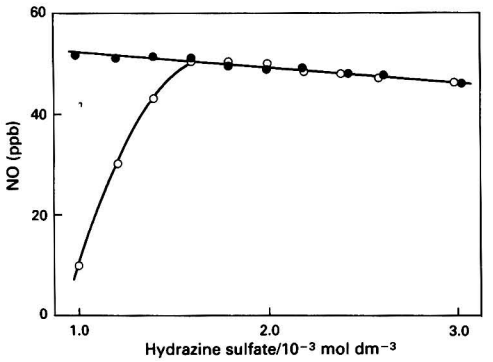

Fig. 2 Effect of hydrazine concentration on the reduction of nitrate (open symbols) and nitrite (closed symbols). Nitrate and nitrite concentration, 0.2 μg ml^{-1} in 0.05 mol dm^{-3} NaOH; Cu^{II} in hydrazine solution, 1.6×10^{-5} mol dm^{-3}; pumping rate, 0.10 ml min^{-1}; ascorbic acid, 0.2 mol dm^{-3} in 0.1 mol dm^{-3} H_2SO_4; and temperature, 30 °C

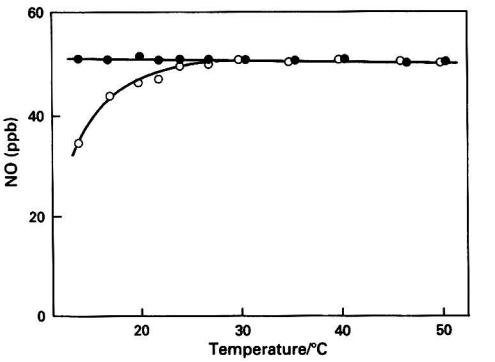

Fig. 3 Effect of temperature on the reduction of nitrate (open symbols) and nitrite (closed symbols). Nitrate and nitrite concentration, 0.2 μg ml^{-1} in 0.05 mol dm^{-3} NaOH; hydrazine, 2.0×10^{-3} mol dm^{-3} containing 1.6×10^{-5} mol dm^{-3} Cu^{II}; ascorbic acid, 0.2 mol dm^{-3} in 0.1 mol dm^{-3} H_2SO_4; and flow rate, 0.10 ml min^{-1}

NaOH, hydrazine and Cu^{II} concentrations, reaction time and temperature. Previous work[14] showed that nitrites can be quantitatively reduced to NO with acidic ascorbic acid. The effects were therefore evaluated by determining the NO evolved by the subsequent reduction by ascorbic acid of the nitrite produced. Measurements were performed by varying one parameter over a range of values while holding the others constant, using nitrate and nitrite standard solutions, and a 1 m length of reaction coil.

Effect of NaOH concentration

For assessment of the effect of the NaOH concentration on the reduction of nitrate to nitrite, each of a series of 0.2 μg ml^{-1} nitrate–N standard solutions prepared in different concentrations of NaOH and a 2.0×10^{-3} mol dm^{-3} hydrazine solution containing 1.6×10^{-5} mol dm^{-3} Cu^{II} were separately pumped into the reaction coil at the same flow rate of 0.10 ml min^{-1}. The mixed solution was then introduced into the gas–liquid separating coil, together with a 0.1 ml min^{-1} flow of a 0.2 mol dm^{-3} ascorbic acid solution, and the NO evolved from the coil was measured. The maximum reduction efficiency was obtained when the NaOH concentration was between 0.02 and 0.16 mol dm^{-3}. A 0.05 mol dm^{-3} NaOH solution was chosen as the scrubbing solution.

Effect of hydrazine concentration

As shown in Fig. 2, the yield of NO from nitrate steadily increased with hydrazine concentration and became equal to that from nitrite at 1.6×10^{-3} mol dm^{-3}. At higher concentrations, the yield of NO from both nitrate and nitrite showed a slight decrease, which apparently indicates that nitrite produced by reduction of nitrate is simultaneously being further reduced. The magnitude of the decrease in the NO yield caused by this over-reduction was about 20.7% at 3.0×10^{-3} mol dm^{-3} hydrazine.

Effect of Cu^{II} concentration

Mullin and Riley[18] have reported that reduction with hydrazine requires a small amount of Cu^{II} to catalyse the reaction. In order to determine the effect of Cu^{II} concentration on the reduction of nitrate to nitrite, a 0.2 μg ml^{-1} nitrate-N solution and each of a series of 2.0×10^{-3} mol dm^{-3} hydrazine solutions containing different amounts of Cu^{II} were separately pumped into the reaction coil at the same flow rate of 0.10 ml min^{-1}, and the NO evolved by the subsequent reduction by ascorbic acid was measured. The results showed that the system requires more than 1.4×10^{-5} mol dm^{-3} Cu^{II} for the quantitative reduction of nitrate and that the reduction is not affected by Cu^{II} concentrations up to 3.0×10^{-5} mol dm^{-3}.

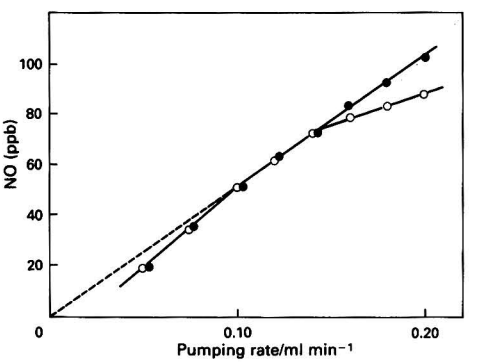

Fig. 4 Effect of reaction time on the reduction of nitrate (open symbols) and nitrite (closed symbols). The reaction time is the residence time of the reaction mixture in the coil, which is inversely proportional to the pumping rate. In this system, a 0.10 ml min^{-1} pumping rate corresponds to a residence time of 2 min

Effect of temperature

Kamphake *et al.*[19] reported that the reduction of nitrate and nitrite with hydrazine was very sensitive to temperature; a quantitative reduction of nitrate to nitrite was obtained in a very narrow temperature range of 35–38 °C and increasing the temperature led to rapid reduction of nitrite. As shown in Fig. 3, however, the influence of temperature was not so significant in the present system. The yield of NO from nitrate became equal to that from nitrite at 30 °C and remained almost constant up to 50 °C.

Effect of time

Another important parameter is reduction time. Measurement of the effect of time was carried out by varying the residence time of the reaction mixture in the coil, in practice, by varying the pumping rates of the reagent solutions using a fixed length of coil. Each of a series of standard solutions of 0.2 μg ml^{-1} of nitrate-N and 0.2 μg ml^{-1} of nitrite-N, and a 2.0×10^{-3} mol dm^{-3} hydrazine–1.6×10^{-5} mol dm^{-3} Cu^{II} solution were separately pumped into a 1 m length of coil at the same rates ranging from 0.05 to 0.20 ml min^{-1}, corresponding to residence times of approximately 4–1 min. The results are shown in Fig. 4.

If the reduction of nitrate to nitrite proceeds quantitatively in the residence times examined, a linear relationship should be obtained between the yield of NO and the pumping rate of

the reagent solutions when the evolved NO is purged at a fixed rate. Fig. 4 indicates that at a pumping rate in the range 0.10–0.14 ml min^{-1} the reduction of nitrate to nitrite is quantitative; below 0.10 ml min^{-1} over-reduction of nitrate occurs and above 0.14 ml min^{-1} the reduction of nitrate to nitrite is not quantitative because of the insufficient reaction time.

Collection of HNO_3 and HNO_2

The collection efficiency of the stripping coil for gaseous HNO_3 and HNO_2 was determined by monitoring the respective standard gas flows upstream and downstream of the coil with an NO_x analyser. Measurements were carried out by varying the sampling rate from 0.5 to 4.0 l min^{-1}, while pumping a 0.05 mol dm^{-3} NaOH solution into the coil at a fixed rate of 0.10 ml min^{-1}. The collection of HNO_3 and HNO_2 was found to be quantitative at sampling rates up to 3.0 l min^{-1} for both HNO_3 and HNO_2.

Interferences

Of the common air pollutants concomitant with HNO_2 and HNO_3, NO_2 and PAN yield nitrate and/or nitrite ions in alkaline solution and, hence, would produce positive interferences.

$$2NO_2 + 2OH^- \rightarrow NO_2^- + NO_3^- + H_2O \quad (1)$$

$$CH_3C(O)OONO_2 + 2OH^- \rightarrow CH_3COO^- + NO_2^- + O_2 + H_2O \quad (2)$$

A previous study[14] on the interference of NO_2 and PAN with the measurement of HNO_2, in which 5×10^{-3} mol dm^{-3} Na_2CO_3 was used as the scrubbing solution, revealed that NO_2 and PAN produce only a 0.7 and 1.9% positive interference, respectively. Peroxyacetyl nitrate decomposes in alkaline solutions to yield only nitrite ion, whereas NO_2 yields equimolar amounts of nitrite and nitrate ions. Hence the effect of the interference from NO_2 on the total HNO_3–HNO_2 measurement system is twice that on the HNO_2 measurement system; it is estimated to be 1.4%. This was confirmed by interference experiments using a scrubbing solution of 0.05 mol dm^{-3} NaOH. In order to correct for these interferences, both the total HNO_3–HNO_2 and HNO_2 measurement systems were made up of two equivalent flow systems with two stripping coils connected in series. The interfering effects were measured with the respective second flow system.

Sensitivity and Calibration Graphs

As demonstrated in the previous paper,[14] the analytical sensitivity of the technique, expressed as the slope of the straight line calibration graph, is proportional to the ratio of sampling flow rate to purging flow rate of the NO produced by chemical reduction and is given by

$$m = (q_s/q_p)\eta_1\eta_2\eta_3$$

where q_s is the sampling flow rate, q_p is the purging flow rate, η_1 is the collection efficiency of gaseous HNO_3 or HNO_2, η_2 is the yield of NO_2^- from reduction with hydrazine (= 1.0 for the HNO_2 measurement system) and η_3 is the yield of NO from reduction with ascorbic acid. In the present study, η_1 was greater than 0.99 for both HNO_3 and HNO_2, η_2 was 0.86 and η_3 was greater than 0.99.

The equation obviously shows that high sensitivity can be obtained when the sampling flow rate is high and the purging flow rate is low; however, a high sampling flow rate results in a decrease in the collection efficiency and a low purging flow rate is limited by the sample flow rate demanded by the NO_x monitor. In order to check the analytical performance and linearity of the systems, the calibration graphs were generated by using a sampling flow rate of 2.0 l min^{-1} and a purging flow rate of 0.29 l min^{-1}. Plotting the NO in the total HNO_3–HNO_2 measurement system against HNO_3 concentration in the range 6.5–26.5 ppb gave a linear calibration with a slope of 5.88 and a correlation coefficient of 0.998, which was the same, within statistical variation, as that obtained for HNO_2 in the range 2.1–20.5 ppb. A slope of 6.85 was obtained for the calibration graph for HNO_2 in the HNO_2 measurement system. These slopes were in good agreement with the values of 5.94 and 6.90 expected from the equation for the sensitivity when the sampling flow rate is 2.0 l min^{-1} and the purging flow rate is 0.29 l min^{-1}.

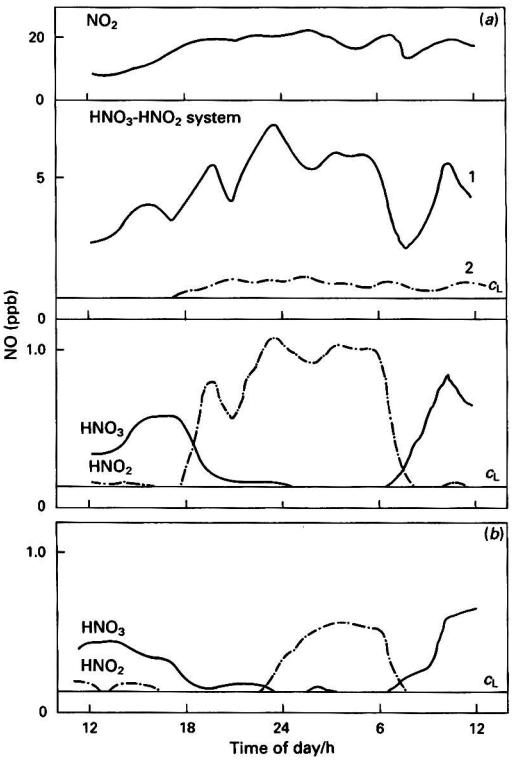

Fig. 5 Ambient HNO_3 and HNO_2 measured in Tsukuba: (*a*) June 17–18, 1991; curve 1, first channel − second channel; and curve 2, second channel; and (*b*) June 20–21, 1991. c_L indicates the limit of detection

In practice, it is desirable that the calibration graphs for the total HNO_3–HNO_2 and HNO_2 measurement systems have the same slope in order to simplify the calculation of the HNO_3 concentration, which is determined by subtracting the value for HNO_2 from that for total HNO_3–HNO_2. The above equation for the sensitivity clearly indicates that a coincidence of the slopes of the calibration graphs for the two measurement systems can easily be obtained by setting the purging flow rate in the HNO_2 system at a rate of $1/\eta_2$ (1.16 in this system) times that in the total HNO_3–HNO_2 system.

The limit of detection was calculated to be approximately 0.13 ppb, using $k = 3$ in the equation $c_L = ks_B/m$,[29] where s_B is the standard deviation of the blank and m is the slope of the calibration graph.

Ambient Measurement

In order to assess the performance of the system, air was sampled at a rural site, Tsukuba, located approximately 60 km north-east of Tokyo. After removal of nitrate particles by

passage through a PTFE filter, the air stream was divided equally between the two measurement systems.

Typical time profiles for gaseous HNO_3 and HNO_2 obtained with a single continuous 24 h measurement are shown in Fig. 5. The concentrations of HNO_3 and HNO_2 showed very characteristic diurnal profiles; the HNO_3 concentration exhibited a maximum during the day and a much lower (sometimes below the detection limit) level at night. In contrast, the HNO_2 level built up during the night and decayed rapidly after sunrise. During this study, the NO_2 concentrations measured were in the range 4–23 ppb and the measurement of PAN was not carried out. In the measurement of total HNO_3–HNO_2 on June 17–18, 1991, as shown in Fig. 5(*a*), the maximum contribution of NO_2 to the NO evolved from the second channel was about 1.5 ppb, which corresponds to 0.13 ppb of HNO_3 and 0.13 ppb of HNO_2. In the measurement of HNO_2, no observable amount of NO was evolved from the flow system of the second channel.

The proposed method has been demonstrated to be a sensitive technique for the continuous monitoring of HNO_3 and HNO_2. The accuracy is, however, affected by artefact formation of HNO_3 caused by the separation of gaseous and particulate nitrates. As the proposed method cannot discriminate between gaseous and particulate nitrates, it is necessary to remove particulate nitrates from the air stream prior to the measurement of gaseous HNO_3. Although a PTFE filter was used in this study, the removal of particulate nitrate on a filter is known to result in the loss of particulate nitrate and generation of artifact HNO_3 by the reaction between H_2SO_4 aerosols and deposited nitrate salts.[7,30,31] This problem appears to be solved by use of the diffusion denuder technique, which is capable of separating gases from particles without particle–particle interactions. A continuous sampling technique based on the principle of the diffusion denuder is currently under development in this laboratory.

References

1 Spicer, C. W., *Environ. Sci. Technol.*, 1983, **17**, 112.
2 Galloway, J. N., and Likens, G. E., *Atmos. Environ.*, 1981, **15**, 1081.
3 Durham, J. L., Overton, J. H., and Aneja, V. P., *Atmos. Environ.*, 1981, **15**, 1059.
4 Appel, B. R., Wall, S. M., Tokiwa, Y., and Haik, M., *Atmos. Environ.*, 1980, **14**, 549.
5 Shaw, R. W., Jr., Steven, R. K., and Bowermaster, J., *Atmos. Environ.*, 1982, **16**, 845.
6 Okita, T., Morimoto, S., and Izawa, M., *Atmos. Environ.*, 1976, **10**, 1085.
7 Forrest, J., Tanner, R. L., Spandau, D., D'Ottario, T., and Newman, L., *Atmos. Environ.*, 1980, **14**, 137.
8 Forrest, J., Spandau, D. J., Tanner, R. L., and Newman, L., *Atmos. Environ.*, 1982, **16**, 1473.
9 Levin, E. E., and Hansen, K. A., *Anal. Chem.*, 1984, **56**, 842.
10 Ferm, M., *Atmos. Environ.*, 1986, **20**, 1193.
11 Braman, R. S., Shelly, J. J., and McClenney, W. A., *Anal. Chem.*, 1982, **54**, 358.
12 Tuazon, E. C., Graham, R. A., Winer, A. M., Easton, R. R., Pitts, J. N., Jr., and Hanst, P. L., *Atmos. Environ.*, 1978, **12**, 865.
13 Joseph, D. W., and Spicer, C. W., *Anal. Chem.*, 1978, **50**, 1400.
14 Kanda, Y., and Taira, M., *Anal. Chem.*, 1990, **62**, 2084.
15 Cox, R. D., *Anal. Chem.*, 1980, **52**, 332.
16 Yoshizumi, K., Aoki, K., Matsuoka, T., and Asakura, S., *Anal. Chem.*, 1985, **57**, 737.
17 Braman, R. S., and Hendrix, S. A., *Anal. Chem.*, 1989, **61**, 2715.
18 Mullin, J. B., and Riley, J. P., *Anal. Chim. Acta*, 1955, **12**, 464.
19 Kamphake, L. J., Hannah, S. A., and Cohen, J. M., *Water Res.*, 1967, **1**, 205.
20 Madsen, B. C., *Anal. Chim. Acta*, 1981, **124**, 437.
21 Al-Wehaid, A., and Townshend, A., *Anal. Chim. Acta*, 1986, **186**, 289.
22 Bajic, S. J., and Jaselskis, B., *Talanta*, 1985, **32**, 115.
23 Margeson, J. H., Suggs, J. C., and Midgett, H. V., *Anal. Chem.*, 1980, **52**, 1955.
24 Koupparis, M. A., Walczak, K. M., and Malmstadt, H. V., *Anal. Chim. Acta*, 1982, **142**, 119.
25 Morris, A. W., and Riley, J. P., *Anal. Chim. Acta*, 1963, **29**, 272.
26 Anderson, L., *Anal. Chim. Acta*, 1979, **110**, 123.
27 Gine, M. F., Reis, B. F., Zagatto, A. E. G., Krug, F. J., and Jacintho, A. O., *Anal. Chim. Acta*, 1983, **155**, 131.
28 Willis, R. B., *Anal. Chem.*, 1980, **52**, 1376.
29 Long, G. L., and Winefordner, J. D., *Anal. Chem.*, 1983, **55**, 712A.
30 Harker, A. B., Richards, L. W., and Clark, W. E., *Atmos. Environ.*, 1977, **11**, 87.
31 Appel, B. R., and Tokiwa, Y., *Atmos. Environ.*, 1981, **15**, 1087.

Paper 1/05189J
Received October 14, 1991
Accepted December 2, 1991

Application of Dowex-2 Loaded With Sulfonephthalein Dyes to the Preconcentration of Copper(II) and Cadmium(II)

Ajai Kumar Singh and Surendra Kumar Dhingra
Department of Chemistry, Indian Institute of Technology, New Delhi-110 016, India

Dowex-2 loaded with sulfonephthalein dyes, *viz.*, Pyrocatechol Violet (PV) and Xylenol Orange (XO), was prepared and investigated for the preconcentration of Cu^{II} and Cd^{II} prior to their determination by flame atomic absorption spectrometry. At pH 7.0–8.0, 1 g of the resin sorbs 23–26 mg of PV or XO. Copper(II) ($\geq$ 0.01 ppm) is sorbed quantitatively at pH 5.0–10.0 and 6.0–10.0 by the PV- and XO-loaded resin, respectively. The corresponding pH ranges for maximum sorption of Cd^{II} ($\geq$0.01 ppm) are 9.5–10.0 and 8.0–10.0. Copper and Cd were desorbed quantitatively with 1 mol dm^{-3} HCl and 1 mol dm^{-3} HNO_3, respectively. The metal ion sorbing capacity of the two resins was found to be $\leq$100 μg of metal per 100 mg of resin. The sorption decreases when the concentration of NaCl exceeds 0.1 mol dm^{-3}. The applicability of both resins to the preconcentration of Cu and Cd prior to their determination by flame atomic absorption spectrometry was demonstrated by analysing Yamuna river water samples for the two ions (relative standard deviation = 4.8–5.7%).

Keywords: *Sulfonephthalein dye; Dowex-2; preconcentration; copper(II); cadmium(II)*

There is continued interest among analytical chemists in the development of chelating polymeric resins,[1] which can provide more flexible working conditions together with good stability and a high capacity for metal ions. This is because such resins can be used for preconcentration purposes in trace metal analysis, particularly for water systems. Several types of chelating reagent have been loaded on a polymeric matrix in order to prepare such resins,[2–7] either by forming a covalent bond between the reagent and the matrix or by an ion-exchange/π–π interaction. The systems prepared by ion exchange involve an anionic group which does not participate in chelation, *e.g.*, a sulfonate group. The main advantage of an ion exchange based sorption system is the ease with which the active part can be varied, without recourse to the often difficult and time-consuming procedures needed for covalently linking the reagent to the skeleton of the resin. However, such systems do not always exhibit very good stability. If ion exchange were to be supported by π-π dispersion forces between the reagent and the polymer matrix, the stability would be improved.

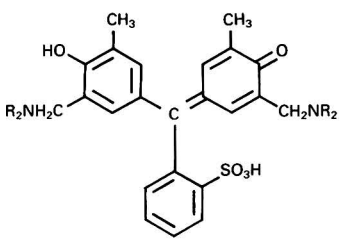

R = $-CH_2COOH$

XO

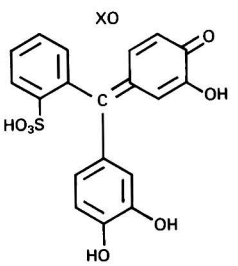

PV

Therefore, the loading of sulfonephthalein dyes, by ion exchange, on a polymeric matrix having π-electron systems might result in a more stable chelating resin. In this work, Pyrocatechol Violet (PV) and Xylenol Orange (XO), which have a conjugated π-electron system and a sulfonate group, were immobilized on the anion-exchange polystyrene-based resin Dowex-2 and the resulting chelating polymers were investigated for the preconcentration of Cu^{II} and Cd^{II} prior to their determination by flame atomic absorption spectrometry (AAS). In order to demonstrate the utility of these resins, Cu^{II} and Cd^{II} present in river water samples were preconcentrated and then determined by AAS.

Experimental

Apparatus and Reagents

Atomic absorption spectrometric measurements were made with a Pye Unicam SP 191 atomic absorption spectrometer, using an air–acetylene flame (air and acetylene flow rates, 4 and 1 dm^3 min^{-1}, respectively). The pH measurements were made on an Elico Model LI 120 digital pH meter. Spectrophotometric measurements were made on a Perkin-Elmer Lambda-3 ultraviolet/visible spectrophotometer.

The stock solutions (0.01 mol dm^{-3}) of Cu^{II} and Cd^{II} were prepared by dissolving appropriate amounts of analytical-reagent grade copper(II) sulfate and cadmium(II) chloride, respectively, in doubly distilled water acidified with a small amount of the corresponding acid and standardized[8] before use. The pH adjustments were made with 0.01–1.0 mol dm^{-3} HCl and NaOH. In some instances, hexamine buffer was also employed for adjusting the pH to about 6.0. The anion-exchange resin Dowex-2 (moderately basic, chloride form, 8% cross-linked) (200–400 mesh) was obtained from Sigma.

Pyrocatechol Violet [BDH (now Merck)] was recrystallized from a 10% v/v ethanol–water mixture before use. Xylenol Orange (BDH) was used as received. All other reagents used were of analytical-reagent grade. The glassware used was soaked in 5% HNO_3 for 1 week before use and cleaned with doubly distilled water. The water samples from the Yamuna river (near the Okhla industrial area, New Delhi, India) were collected in clean polyethylene bottles and concentrated HNO_3 (2 cm^3 per dm^3 of water) was added to each sample immediately after its collection.

Procedure for Regenerating Dowex-2

Dowex-2 (2 g) was equilibrated with 6 mol dm^{-3} HCl (20 cm^3) for 3 h and then washed successively with water (50 cm^3), ammonia solution (40 cm^3) and water until the filtrate was colourless towards phenolphthalein. The resin was finally washed with methanol, dried and stored in a desiccator *in vacuo*.

Procedure for Loading PV on Dowex-2

Dowex-2 (100 mg) was mixed with 20 cm^3 of a solution of PV (0.6 mmol dm^{-3}). After adjusting the pH to 7.5–8.0, the mixture was shaken on a mechanical shaker for 8 h. The resin was then filtered, washed successively with water and methanol, dried and stored *in vacuo*.

Procedure for Loading XO on Dowex-2

Dowex-2 (300 mg) was mixed with 75 cm^3 of XO (0.14 mmol dm^{-3}). After adjusting the pH to 7.0–7.5, the mixture was shaken for 3 h. The resin was subsequently filtered, washed successively with water and methanol, dried and stored *in vacuo*.

Recommended Procedure for Preconcentration and Determination of Cd

A mixture containing 100 mg of PV-loaded chelating resin and 25 cm^3 of a solution containing not more than 2 μg cm^{-3} of Cd^{II} was taken and its pH was adjusted to 9.5–10.0 with 0.1 mol dm^{-3} NaOH. The mixture was equilibrated for 20 min on a mechanical shaker after which the resin was filtered and washed with 20 cm^3 of water. Cadmium(II) ions were desorbed by treating the resin with two 2.5 cm^3 aliquots of 0.05 mol dm^{-3} HNO_3. The acidic solution containing desorbed Cd^{II} was aspirated into an air–acetylene flame for measurement of the absorption at 228.8 nm. The absorbance values were corrected for the blank and read from a previously constructed calibration graph.

The same procedure was used for the XO-loaded Dowex-2, except that the working conditions were as follows: volume of Cd^{II} solution, 40 cm^3; pH, 8.0–8.7; shaking time, 10 min; and desorbing solution, 10 cm^3 of 1 mol dm^{-3} HNO_3.

Recommended Procedure for Preconcentration and Determination of Cu

The pH of a mixture containing 100 mg of PV-loaded chelating resin and 25 cm^3 of a solution containing not more than 2 μg cm^{-3} of Cu was adjusted to 6.0 with hexamine buffer. The mixture was equilibrated for 30 min on a mechanical shaker after which the resin was filtered and washed with 20 cm^3 of water. Copper(II) ions were desorbed by equilibrating the resin with two 2.0 cm^3 aliquots of 1 mol dm^{-3} HCl for 1 h. The acidic solution containing desorbed Cu^{II} was aspirated into an air–acetylene flame for measurement of the absorption at 324.8 nm. The absorbance values were corrected for the blank and read from a previously constructed calibration graph.

The same procedure was used for the XO-loaded resin, except that the pH was adjusted to 9.0 with 0.1 mol dm^{-3} NaOH and the concentration of Cu^{II} in the solution was not more than 4 μg cm^{-3}.

Results and Discussion

Pyrocatechol Violet and XO are among the most versatile chelating agents capable of forming complexes with a variety of metal ions. Both can be sorbed on Dowex-2 apparently by exchange of the Cl^- ion of the resin matrix with the sulfonate group attached to the dyes and by means of π-π dispersion forces arising from the aromatic nature of the resin and the reagent. The sorption of the two dyes on Dowex-2 was monitored spectrophotometrically at the maximum wavelength of absorption and was found to be pH dependent. At pH 7.0–8.0, maximum sorption is obtained if the resin is equilibrated for 2 and 7 h with XO and PV, respectively. Longer shaking times, however, do not adversely affect the sorption process. One gram of resin was found to sorb 25.7 mg of XO or 23 mg of PV. By using the batch method, both chelating resins were investigated for the preconcentration of Cu^{II} and Cd^{II}.

Optimum Conditions for Sorption

The sorption of Cu^{II} and Cd^{II} on PV- and XO-loaded resins was studied at different pH values, keeping the other parameters constant. Optimum pH values for maximum and constant sorption of the two metal ions are given in Table 1; pH values above 10.0 were not investigated because the mixtures became turbid. Hexamine buffer was found to be suitable for adjusting the pH to about 6.0 for Cu^{II}. Sorption of both metal ions on PV- and XO-loaded Dowex-2 was studied by varying the equilibration time from 5 to 60 min. The optimum amounts of Cu^{II} and Cd^{II} sorbed on 100 mg of each of the two resins are also given in Table 1. Copper(II) and Cd^{II} (10 μg each) were first sorbed on 100 mg of PV- or XO-loaded Dowex-2 and then desorbed by using the recommended procedure. The average percentage recovery of three experiments was determined and the values are given in Table 1.

Effect of NaCl on Sorption

Sorption of both metal ions decreases slowly when the concentration of NaCl is increased beyond 0.1 mol dm^{-3}. In the presence of 0.2, 0.4 and 0.6 mol dm^{-3} NaCl, the sorption was found to be 86, 81 and 74%, respectively, for both ions.

Limit of Preconcentration

The two metal ions can be collected effectively (94–97%) on either of the two chelating resins from their solutions having a concentration of the order of 0.01 ppm. Sorption of the two ions was neither quantitative nor reproducible at lower concentrations.

Desorption of Metal Ions From the Resins

The desorption of Cd from both resins was instantaneous with 1 mol dm^{-3} HNO_3. However, in order to desorb Cu quantitatively, equilibration of the resins with 1 mol dm^{-3} HCl for 1 h on a mechanical shaker is required.

Determination of Cu and Cd in River Water Samples

One gram of PV- or XO-loaded chelating resin was shaken successively with five 100 cm^3 aliquots of a filtered water sample as described in the recommended procedure. The resin was separated by filtration and treated successively with two aliquots of 25 cm^3 of 1 mol dm^{-3} HNO_3 and 1 mol dm^{-3} HCl.

Table 1 Optimum conditions for sorption of metal ions

	PV-loaded resin		XO-loaded resin	
Parameter	Cu^{II}	Cd^{II}	Cu^{II}	Cd^{II}
pH range	5.0–10.0	9.5–10.0	6.0–10.0	8.0–10.0
Equilibration time/min	20	10	30	10
Metal ion sorbed per 100 mg of resin/μg	50.0	62.5	100.0	80.0
Recovery (%)	97.4	98.3	96.7	98.2

Table 2 Determination of Cu and Cd (μg per 100 cm^3) in Yamuna river water samples

		PV-loaded resin				XO-loaded resin			
Sample	Method	Cu	RSD (%)	Cd	RSD (%)	Cu	RSD (%)	Cd	RSD (%)
1	Direct	4.9	5.6	8.0	5.2	5.2	5.4	8.7	5.5
	SA*	5.3	4.8	8.8	4.9	5.6	5.0	8.2	5.3
2	Direct	5.2	5.6	8.1	4.8	4.8	5.7	8.8	5.1
	SA*	5.8	5.0	8.7	4.8	5.3	5.6	8.4	5.2

* SA = Standard additions method.

All the desorption solutions were mixed and the metal ions in the mixture determined by AAS as described above. The results are given in Table 2 and compared with the values obtained by the standard additions method. The relative standard deviation (RSD) for six determinations was calculated. The results are presented in Table 2.

The optimum pH range for the sorption of Cu^{II} is wider than that for Cd^{II}. Dowex-2 loaded with PV offers a better pH range for the collection of Cu than either XO-loaded Dowex-2 or the other known preconcentration systems.[1] This is a significant advantage. Sorption of Cd on the resins prepared in this work is much faster than on other commonly used ion-exchange and chelating resins.[1] Dowex-2 loaded with XO has a greater sorbing capacity than the PV-modified system. Recoveries are comparable to those obtained[1] for ion exchangers, other chelating resins, polyurethane foam and polystyrene beads. The greater compatability between the size of the hydrated Cd^{II} ion and the pores of the resins prepared in this work is probably responsible for the greater sorption of this ion compared with Cu^{II}. The instantaneous desorption of Cd^{II} is another advantage of these modified resins. They are comparable to other functionalized resins[1] in terms of the lower limit of preconcentration. For the analysis of river water, the performances of the direct and standard additions methods are similar, although the latter gives higher results and a lower RSD than the former. The discharge of industrial effluent into the river at a site very close to that at which the sampling was performed is probably responsible for the high Cu and Cd contents of the water samples analysed in this work.

Financial support of this work from the Council of Scientific and Industrial Research (India) is gratefully acknowledged.

References

1 Kantipuly, C., Katragadda, S., Chow, A., and Gesser, H. D., *Talanta*, 1990, **37**, 491.
2 Nakayama, M., Chikuma, M., Tanaka, H., and Tanaka, T., *Talanta*, 1982, **29**, 503, and references cited therein.
3 Pesavento, M., Profumo, A., and Biesuz, R., *Talanta*, 1988, **35**, 431.
4 Chwastowska, J., and Kosiarska, E., *Talanta*, 1988, **35**, 439.
5 Brajter, K., Olbrych-Sleszynska, E., and Staskiewicz, M., *Talanta*, 1988, **35**, 65.
6 Singh, A. K., and Kumar, T. G. S., *Microchem. J.*, 1989, **40**, 197.
7 Mendez, R., and Pillai, V. N. S., *Analyst*, 1990, **115**, 213.
8 Vogel, A. I., *A Text-Book of Qualitative Inorganic Analysis*, Longman, London, 3rd edn., 1973.

Paper 1/00702E
Received February 14, 1991
Accepted November 6, 1991

Use of Hydrous Iron(III) Oxide in a Concentration Step for the Determination of Trace Amounts of Organophosphorus Compounds in Aqueous Solutions

Toshitaka Hori and Masahito Sugiyama*
Department of Chemistry, College of Liberal Arts and Sciences, Kyoto University, Kyoto 606, Japan

Adsorption onto hydrous iron oxide (HIO) was compared as a function of pH for a variety of organophosphorus compounds (OPs), including phosphate esters of ethanolamine, hydroxyamino acids and sugars, phosphonates with methyl and aminoethyl substituents, and nucleotides. The percentage adsorption *versus* pH curves could be classified into four types according to an empirical rule, *viz.*, that the adsorptivity of OPs depended primarily on the number of unsubstituted P–O moieties in the tetrahedral structure around the P atom of the compound. The rule predicted that a large group of OPs containing more than three unsubstituted P–O moieties should be collected quantitatively by HIO from waters of pH 5.0–6.5. The OPs collected by adsorption onto HIO did not show appreciable degradation during storage for at least 2 weeks. In addition, they could be released from the HIO by using pentane-2,4-dione [acetylacetone (Hacac)] so that they entered a small-volume aqueous phase which was derived from the HIO by the following reaction: $Fe_2O_3 \cdot nH_2O \cdot$ (OPs) + 6Hacac $\rightarrow$ 2Fe(acac)$_3$ + $(n + 3)H_2O$ + (OPs). The whole procedure, involving adsorption of OPs onto HIO from a 1 l water sample, separation of the HIO from water by filtration and release of the OPs from the HIO into a 2.5 ml aqueous phase, realized a 400-fold concentration with efficiencies ranging from 45% (for adenosine-5′-triphosphate) to 92% (for 2-aminoethylphosphonate).

Keywords: *Organophosphorus compounds; adsorption; hydrous iron oxide*

It is known that the use of 4-amino-3-hydroxynaphthalene-1-sulfonic acid as a reducing agent for the Heteropoly Blue method greatly improves the determination of orthophosphate concentrations.[1] The so-called Fiske–Subbarow procedure[1] not only provides reliable analytical results for the phosphate content of blood and urine samples but has also found wide application in the discovery of new types of organophosphorus compounds (OPs),[2,3] many of which are nowadays known to act as cell membrane components, intermediates in energy metabolism and essential constituents of genes.

Ishibashi and Tabushi[4] proposed a method for the sensitive determination of orthophosphate concentrations by a series of procedures involving the adsorption of orthophosphate onto hydrous iron oxide (HIO), the addition of acidic molybdate solution to dissolve the HIO and obtain molybdophosphate, and the measurement of the absorbance of molybdophosphate extracted into butyl acetate. The method has since been used to determine orthophosphate concentrations down to 1×10^{-8} mol dm^{-3}; orthophosphate is found in the hydrosphere as an essential nutrient for micro-organisms.[5] Owing to the difficulty in designing an automated procedure, however, the method of Ishibashi and Tabushi[4] has now been replaced by that of Murphy and Riley,[6] which is based on the formation of heteropoly blue with the use of ascorbic acid and antimonyl tartrate. Nevertheless, the former method revealed that HIO can adsorb some OPs in addition to orthophosphate,[7] although systematic adsorption studies on a large group of OPs have not yet been performed.

Hori *et al.*[8] measured the percentage adsorption onto HIO of a selection of oxophosphorus compounds, such as hypophosphite (H_2PO_2), dimethylphosphate [$(MeO)_2PO_2$], phosphonate (HPO_3), monomethylphosphate ($MeOPO_3$), α- and β-glycerophosphates (α- and β-glyOPO_3, respectively), orthophosphate (PO_4), pyrophosphate (P_2O_7) and triphosphate (P_3O_{10}), each of which was dissolved in buffer solutions with various pH values. It was found[8] that the shape of the percentage adsorption *versus* pH curves (adsorption curves) that were obtained appeared to reflect the structural characteristics of the phosphorus molecules tested. It was suggested that when the structural formula (and hence the number of P–O moieties free of any substituents) of a given phosphorus compound was known, its adsorption curve could be predicted. In addition, it also seemed possible that measurement of the adsorption curve of an unknown phosphorus compound, even at a concentration as low as 1×10^{-8} mol dm^{-3}, could allow the structural characteristics of the compound to be ascertained from the shape of the curve.

In the present paper, the characteristics of the adsorption curves measured for 13 types of OPs are reported. As was anticipated, it is shown here that the adsorption of these OPs, all of which are biologically important and have a fairly sophisticated molecular structure, was primarily governed by the number of free P–O moieties and was scarcely affected by the bulk of the substituent groups and the oxidation state of the P atoms. A procedure for releasing OPs adsorbed onto an HIO matrix into a small-volume water phase is proposed, from which a concentration method for the analysis of a group of OPs dissolved in water at submicromolar concentrations was developed.

Experimental

Reagents

A solution of 100 mg ml^{-1} of Fe in 5 mol dm^{-3} HCl was prepared by dissolving $FeCl_3 \cdot 6H_2O$ in a calculated amount of HCl and diluting with water. If the $FeCl_3 \cdot 6H_2O$ reagent contained more than 0.002 mol-% of PO_4 as impurities, it was purified according to the procedure of Dodson *et al.*[9] before use.

Toluene, chloroform and pentane-2,4-dione [acetylacetone (Hacac)] were all commercially available products of guaranteed-reagent grade, and were used after washing them with water.

The standard materials used for preparing the OP stock solutions are listed in Table 1 together with the abbreviations adopted and the content of various impurities such as PO_4, AMP and ADP. The level of PO_4 impurities, and the AMP impurities in ADP and also the ADP in ATP, were determined chromatographically under the conditions given in

* To whom correspondence should be addressed.

Table 1 Standard materials used for preparing OP stock solutions

OP standard material	Abbreviation	OP stock solution/mmol dm^{-3}	Impurities found (mol-%)
Monomethylphosphonic acid	$MePO_3$	10	PO_4, 0.14
O-Phosphorylethanolamine	PEA	10	PO_4, 0.78
2-Aminoethylphosphonic acid	2-AEP	10	PO_4, 0.76
(±)-1-Aminoethylphosphonic acid	1-AEP	10	PO_4, 0.18
D-Fructose-1-phosphate, sodium salt	F-1-P	10	PO_4, 1.70
D-Fructose-6-phosphate, disodium salt	F-6-P	10	PO_4, 1.18
α-D-Glucose-1-phosphate, disodium salt	G-1-P	10	PO_4, 1.20
D-Fructose-1,6-diphosphate, tetrasodium salt	F-1, 6-P	5	PO_4, 0.67
O-Phospho-DL-threonine	P-Thr	10	PO_4, 0.47
O-Phospho-L-serine	P-Ser	10	PO_4, 0.24
Adenosine-5′-monophosphoric acid	AMP	10	PO_4, 0.031; ADP, 17
Adenosine-5′-diphosphate, disodium salt	ADP	5	PO_4, 2.28; AMP, 7
Adenosine-5′-triphosphate, disodium salt	ATP	3	PO_4, 0.78; ADP, 2

Table 2 High-performance liquid chromatography conditions used for OP analysis

OPs analysed*	Separation column	Eluent buffer and flow rate	Method of detection†	Ref.
HPO_3, α-glyOPO_3, β-glyOPO_3, $MeOPO_3$, $MePO_3$, F-1-P, F-6-P, G-1-P	TSKgel-IC Anion-SW, 5 cm × 4.6 mm i.d.	1 mmol dm^{-3} tartaric acid solution of pH 3.35, 1.5 ml min^{-1}	COND	This work
P_2O_7, F-1, 6-P	Shim-pac IC-A2, 10 cm × 4.6 mm i.d.	0.75 mmol dm^{-3} potassium hydrogen phthalate solution of pH 4.2, 1.5 ml min^{-1}	COND	This work
AMP, ADP, ATP	Finepak SIL C_{18}, 25 cm × 4.6 mm i.d.	30 mmol dm^{-3} KH_2PO_4 containing 3 mmol dm^{-3} Bu_4NBr and 8% v/v EtOH, 1 ml min^{-1}	ABS (254 nm)	10
PEA, 1-AEP, 2-AEP, P-Ser, P-Thr	TSKgel IEX-215LI, 7.5 cm × 7.5 mm i.d.	67 mmol dm^{-3} citric acid solution of pH 2.80 containing 0.2 mol dm^{-3} LiCl, 0.5 ml min^{-1}	ABS (570 nm)	11

* Simultaneous separation of the groups of OPs was not necessarily successful, but the individual OP could always be separated from its possible moiety derived through hydrolytic decomposition and from PO_4.

† COND and ABS denote the measurements of conductivity and absorbance, respectively.

Table 2. Stock solutions of the OPs were obtained by dissolving the corresponding standard materials in water or dilute NaOH solution and were standardized spectrophotometrically against an orthophosphate standard solution, after being converted into orthophosphate by incineration with $HClO_4$. This was followed by correction for the PO_4, AMP and ADP impurities. These solutions were freshly prepared every 2 weeks and stored in polyethylene bottles at 1 °C.

The stock solutions of P_2O_7, HPO_3, $MeOPO_3$, and α- and β-glyOPO_3 and the buffer solutions of HOAc–NaOAc (pH 4.0–5.9), 2-(*N*-morpholino)ethanesulfonic acid–NaOH (pH 6.0–7.0), *N*-2-hydroxyethylpiperazine-*N*′-2-ethanesulfonic acid–NaOH (pH 7.1–8.2) and NH_3–NH_4Cl (pH 8.3–10.2) were prepared as described previously.[8]

A 0.5 mol dm^{-3} acetate buffer solution (pH 6.0), 1 l of which contained 20 g of NaOH and 29 ml of glacial acetic acid, was also prepared.

Measurements of Adsorption Curves for Various OPs

Unless stated otherwise, the procedures and conditions used were the same as those reported previously.[8] Briefly, 30 μmol of each OP were equilibrated with a fixed amount of HIO (5 mg as Fe) in a 100 ml aliquot of 0.01 mol dm^{-3} buffer solution adjusted to the desired pH, and the percentage adsorption was calculated from the amount of OP found in the HIO and the amount used initially. The adsorption curves thus obtained are shown in Fig. 1.

Apparatus

A Shimadzu 6A high-performance liquid chromatograph was used for the analysis of OPs, and the conditions employed are summarized in Table 2.

A Taiyo EP-1 mechanical shaker, a Kokusan H-103N centrifuge and a Shimadzu UV-200 spectrophotometer were also used.

Results and Discussion

Characterization and Classification of the Adsorption Curves by the Molecular Structure of OPs

It was previously reported that the adsorption curves for the nine oxophosphorus compounds can be classified into four types as follows.[8]

(*i*) The first type of adsorption curve was observed with PO_4 (curve 1 in Fig. 1). The adsorption of PO_4 was quantitative from pH 4.0 to 8.5 after which it started to decrease with a further increase of pH, so that no adsorption was observed above pH 11. From the adsorption curve, the $pH_{\frac{1}{2}}$ value (*i.e.*, the pH at which half of the PO_4 is adsorbed) could be determined as 9.5. This curve can be used as a convenient reference for the classification of the other eight OPs. (*ii*) Adsorption curves of the second type were observed with $MeOPO_3$, α- and β-glyOPO_3, and HPO_3 (curve 2 in Fig. 1). It can be seen from Fig. 1 that compounds with one less P–O moiety than PO_4, owing to substitution, commonly have an adsorption curve that recedes into the acidic region by

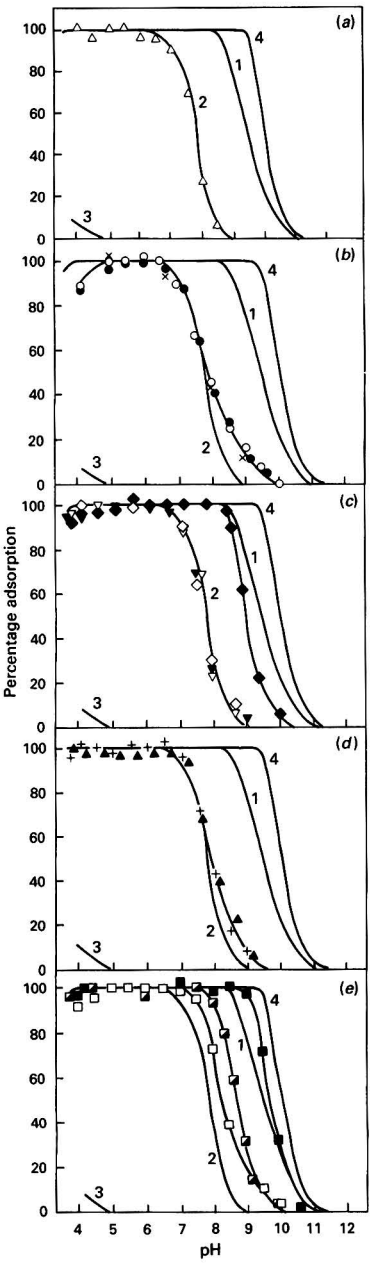

Fig. 1 Classification of the adsorption curves of 13 types of OPs, with reference to the representative curves measured for PO_4 (curve 1), $MeOPO_3$ (curve 2), $(MeO)_2PO_2$ or H_2PO_2 (curve 3), and P_2O_7 or P_3O_{10} (curve 4). (*a*) △, $MePO_3$. (*b*) ○, PEA; ●, 2-AEP; and ×, 1-AEP. (*c*) ◇, F-1-P; ▽, F-6-P; ▼, G-1-P; and ◆ F-1, 6-P. (*d*) +, P-Thr; and ▲, P-Ser. (*e*) □, AMP; ◪, ADP; and ■, ATP

approximately 1.5 pH unit compared with curve 1. It is also noteworthy that the curve depended little on the nature of the substituent groups or the oxidation state of the P atoms in the compounds tested. (*iii*) The third type was observed with $(MeO)_2PO_2$ and H_2PO_2 (curve 3). These compounds have two less P–O moieties than PO_4 and show no appreciable tendency to be adsorbed. (*iv*) The fourth type of adsorption is illustrated by curve 4, and was found with P_2O_7 and P_3O_{10}. The adsorption curve for both compounds extends towards the alkaline region by 0.5 pH unit compared with curve 1, indicating that they were adsorbed more strongly than PO_4 (curve 1) against the increasing concentration of hydroxide ions which might compete for the adsorption sites on HIO. Such stronger adsorption was consistent with the larger numbers of P–O moieties in P_2O_7 and P_3O_{10} than in PO_4.

The adsorption curves measured for the 13 OPs are summarized in Fig. 1, and each is superimposed on the four types of typical adsorption curves (curves 1–4).

Fig. 1(*a*) shows that the adsorption curve for $MePO_3$ accords well with curve 2.

The adsorption curves for PEA, 1-AEP and 2-AEP, OPs which commonly have amine groups as the substituents, are compared in Fig. 1(*b*). Among these OPs, the number of free P–O moieties is the same and, as expected, the adsorption curves closely resemble each other. The fact that these three OPs have very similar adsorption behaviour indicates that neither the position of the amine residue (*cf.* 1-AEP and 2-AEP) nor the oxidation state of the P atoms (*cf.* 1-AEP and PEA) plays a significant part in the adsorption phenomenon. The slight deviations of these adsorption curves from curve 2 are attributable to the amine groups, *i.e.*, below pH 5 the positive charge on the amine groups acts to suppress adsorption onto the positively charged surface of HIO, whereas at pH 7.5–9.5 the positive charge on the amines actually facilitates adsorption onto the negatively charged HIO. On the basis of these findings, it is expected that a group of aminoalkyl phosphates and phosphonates could be collected by HIO from solutions with pH values between 5.0 and 6.5.

Sugar phosphates such as F-1-P, F-6-P, G-1-P and F-1,6-P exhibit adsorption curves similar to that shown in Fig. 1(*c*). The curves for the first three of these OPs are in good accord with curve 2, suggesting again that the bulk and chemical nature of these sugar-substituents had little effect on the adsorption curve. In contrast, the curve for F-1, 6-P appears in a more alkaline region (by 1.5 pH unit) than those for the other three compounds. This is due to a pair of PO_3 groups, each of which is bonded to C_1- and C_6-carbons in the fructose skeleton. Although the detailed mechanisms of the adsorption of these compounds are not known, the adsorption curves of sugar monophosphates and diphosphates are thus different. Nevertheless, all these sugar phosphates can be collected on HIO in the pH range 4.0–6.8.

By using P-Ser and P-Thr, the effect of the amino acid substituents of OPs was examined. As shown in Fig. 1(*d*), the effects of the amino acid substituents were small and the adsorption curves for both P-Ser and P-Thr were identical with that of $MeOPO_3$, except for a slight deviation appearing above pH 7. As mentioned above [Fig. 1(*b*)], this deviation is caused by the amine groups of the amino acid substituents. Hence, it appears that OPs possessing amino acid substituents could be collected by HIO from waters at pH 4.0–6.5.

By using AMP, ADP and ATP as representative examples, adsorption curves for nucleotides were obtained and the results are shown in Fig. 1(*e*). It can be seen that AMP, which is formally regarded as a monosubstituted compound of PO_4, is adsorbed more favourably than $MeOPO_3$ (curve 2). Hence, the adenosine group appears to have a role in facilitating the adsorption of the AMP molecule. It can also be seen that ADP is adsorbed more favourably than AMP owing to the presence of a P_2O_6 group. Similarly, the effect of the P_3O_9 group is seen in the adsorption of ATP. Among the nucleotides studied here, ATP was adsorbed most favourably, but this was still slightly less than for P_2O_7 or P_3O_{10} (curve 4). The polyphosphates and their derivatives can therefore be differentiated by their adsorption curves. It can be expected that various OPs belonging to this group could be collected simultaneously by HIO at pH 4–7.

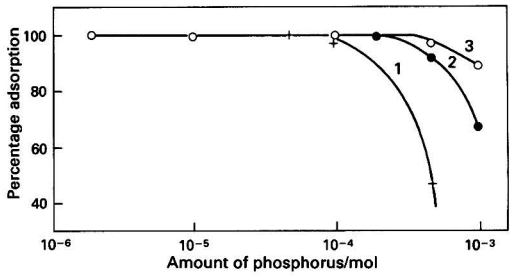

Fig. 2 Maximum amounts of PO_4 collected by 100 (curve 1), 200 (curve 2) and 300 mg of Fe in HIO (curve 3). For each experimental run, a series of 1 l solutions of pH 6.0 impregnated with increasing amounts of PO_4 were treated

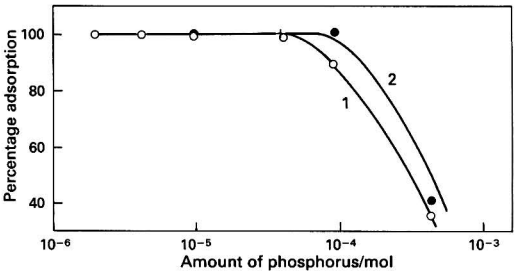

Fig. 3 Collection of HPO_3 (curve 1) and P_2O_7 (curve 2) using 100 mg of Fe. Other conditions as in Fig. 2

Amount of HIO Needed for Collecting OPs

From the results presented above, it can be seen that OPs with adsorption curves of type (*i*), (*ii*) or (*iv*) could be collected from waters of pH 5.0–6.5, leaving behind OPs of type (*iii*).

The amount of HIO necessary to collect OPs from 1 l of water was determined for various OP concentrations. The results are shown in Fig. 2, where the amounts of HIO are indicated in terms of the mass of Fe. It can be seen from Fig. 2 that 100, 200 and 300 mg of Fe can collect up to 50, 100 and 150 μmol of PO_4, respectively, at pH 6.0. However, it should be noted that after adsorbing the maximum amounts of PO_4, HIO becomes colloidal and cannot be filtered, leading to serious clogging of the membrane filters. In order to avoid this problem, it is recommended that, for instance, 100 mg (1.8 mmol) of Fe should be used to collect 30 μmol of PO_4.

Similar experiments were performed using HPO_3 and P_2O_7, and it was found that 100 mg of Fe can collect 30 μmol of HPO_3 and 15 μmol of P_2O_7 (Fig. 3) without the formation of non-filtrable colloids. The Fe : P atomic ratio of 60, which is calculated as the ratio of the amount of Fe required to that of P in the OPs to be collected, was found to be a convenient measure of the HIO necessary for collecting a certain amount of OP.

Procedure for Concentrating OPs From Water Using HIO (HIO Procedure)

Preparation of the HIO suspension

A 1 ml aliquot of the 100 mg ml^{-1} Fe solution was taken in a 50 ml centrifuge tube and mixed with 20 ml of 1 mol dm^{-3} NH_3 solution. The HIO thus formed was washed twice with 20 ml of 0.5 mol dm^{-3} acetate buffer (pH 6.0), centrifuged for further washing and then dispersed into 20 ml of pure water by vigorous shaking.

Adsorption of OPs

With magnetic stirring, the HIO suspension was added to a 1 l water sample, the pH of which had been brought to approximately 6.0 by the addition of 20 ml of 0.5 mol dm^{-3} acetate buffer. After allowing to stand for 2 h, the HIO was collected by filtration and washed with pure water. It was then air-dried to produce flakes. The still wet HIO flakes were transferred into a glass-stoppered 10 ml centrifuge tube using a spatula.

Release of OPs from HIO

To the 10 ml centrifuge tube containing the HIO flakes were added 2 ml of Hacac. The mixture was shaken for 1 h at 20–30 °C; the HIO flakes turned to a reddish emulsion and finally to blood-red $Fe(acac)_3$ which was extracted with 3 ml of toluene. After discarding the toluene extract, the remaining lower phase was mixed with a further 2 ml of Hacac and shaken for 12 h at 20–30 °C, followed by washing twice with 2 ml of toluene and once with 2 ml of chloroform. Washing with chloroform also facilitated the changeover of the aqueous phase from the bottom layer to the top layer, into which the OPs were released. The approximately 1.2 ml of aqueous phase thus obtained were transferred into a vial and made up to 2.5 ml by adding the washings of the centrifuge tube. When polyphosphates or their analogues were involved, the final aqueous phase was slightly coloured owing to the inclusion of trace amounts of Fe, otherwise it was colourless.

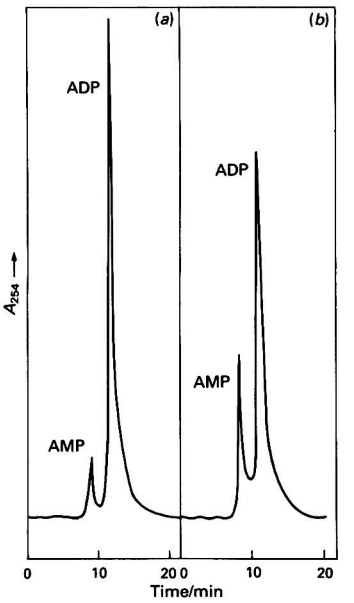

Fig. 4 Recovery of ADP with the HIO procedure. A 2.5 ml aliquot of a 0.479 mmol dm^{-3} ADP standard solution was diluted to 1 l and returned to a 2.5 ml sample by the HIO procedure. (*a*) Before and (*b*) after the HIO procedure; 20 μl aliquots of the ADP solution were chromatographed under the conditions given in Table 2

Recovery of OPs With the HIO Procedure

Phosphonates such as $MePO_3$, 1-AEP and 2-AEP do not undergo hydrolytic decomposition, whereas the other OPs have a greater or lesser tendency to undergo degradation and liberate PO_4. By comparing the contents of OPs before and after the HIO procedure, the percentage recovery of each OP

Table 3 Recovery of OPs and some inorganic oxophosphorus compounds with the HIO procedure

Compound*	Recovery (%) (min–max)†	Recovery after storage‡ (%)	Compound*	Recovery (%) (min–max)†	Recovery after storage‡ (%)
α-glyOPO$_3$	73.8–79.4	74.6	F-1-P	82.2–84.0	81.1
β-glyOPO$_3$	78.7–79.5	—	F-6-P	73.0–77.8	—
PEA	85.1–88.1	85.2	G-1-P	75.7–82.8	—
HPO$_3$	87.9–96.6	88.5	G-6-P	87.0–90.8	—
P-Ser	85.8–92.3	—	PO$_4$	90.0–96.8	92.5
P-Thr	84.4–92.0	78.2	P$_2$O$_7$	60.0–61.9	—
1-AEP	87.0–90.4	88.3	AMP	83.7–90.7	—
2-AEP	80.3–92.2	—	ADP	67–77	—
MePO$_3$	84.3–92.8	—	F-1,6-P	92–96	—
MeOPO$_3$	64.3–77.9	62.6	ATP	45–60	—

* OPs (1–3 μmol) were treated according to the HIO procedure.
† The minimum and maximum values of triplicate experiments are indicated.
‡ The HIO with adsorbed OPs was stored for 2 weeks at 1 °C and then treated with Hacac to release the OPs (for details see text).

was evaluated. The OP concentrations were determined chromatographically under the conditions shown in Table 2.

The typical chromatograms recorded for the ADP standard solution before (*a*) and after (*b*) the HIO procedure are compared in Fig. 4. The peaks appearing at 8.4 and 12.0 min are due to AMP and ADP, respectively. It can be seen that ADP is recovered with an efficiency of 72%.

The efficiencies thus evaluated for the individual OPs are summarized in Table 3. The OPs examined here were recovered with efficiencies ranging from 45% (for ATP) to 92% (for 2-AEP). Because of their resistance to hydrolytic degradation, relatively low efficiencies were observed for ATP and ADP. It can also be seen from Table 3 that the recoveries evaluated with and without storage of OPs on HIO flakes under cold conditions (1 °C) showed good agreement within experimental error. The method therefore appears to offer a safe and convenient procedure for the compact storage of OPs adsorbed onto HIO rather than as bulky solutions.

At each of three different concentrations, *viz.*, 1×10^{-7}, 5×10^{-8} and 1×10^{-8} mol dm^{-3}, five (1 l) standard solutions of 1-AEP, which was taken as a representative OP, were treated by the HIO procedure and then analysed by high-performance liquid chromatography. The mean and standard deviation of the recoveries were found to be 89.3 ± 2.8, 91.5 ± 6.4 and 86 ± 18% at the respective concentrations. From these values the precision (relative standard deviation) of the proposed method was calculated to be 3.1 and 7.0% at concentrations of 1×10^{-7} and 5×10^{-8} mol dm^{-3}, respectively, and the limit of detection (signal-to-noise ratio = 5) to be 1×10^{-8} mol dm^{-3}.

The authors thank Dr. F. Yamamoto of Kyoto University and Dr. T. Okada of Shizuoka University for their helpful suggestions in optimizing the conditions for high-performance liquid chomatography. This research was carried out under financial support (No. 01540474) from the Ministry of Education, Science and Culture, Japan.

References

1 Fiske, C. H., and Subbarow, Y., *J. Biol. Chem.*, 1925, **66**, 375.
2 Pontis, H. G., and Leloir, L. F., in *Analytical Chemistry of Phosphorus Compounds*, ed. Halmann, H., Wiley-Interscience, New York, 1971, pp. 617–658.
3 Fiske, C. H., and Subbarow, Y., *J. Biol. Chem.*, 1929, **81**, 629.
4 Ishibashi, M., and Tabushi, M., *Bunseki Kagaku*, 1959, **8**, 588.
5 Fujinaga, T., and Hori, T., *Environmental Chemistry on Lake Biwa*, Japan Society for the Promotion of Sciences, Tokyo, 1982.
6 Murphy, J., and Riley, J. P., *Anal. Chim. Acta*, 1962, **27**, 31.
7 Ishibashi, M., and Tabushi, M., *Bunseki Kagaku*, 1957, **6**, 7.
8 Hori, T., Moriguchi, M., Sasaki, M., Kitagawa, S., and Munakata, M., *Anal. Chim. Acta*, 1985, **173**, 299.
9 Dodson, R. W., Forney, G. J., and Swift, E. H., *J. Am. Chem. Soc.*, 1936, **58**, 2573.
10 Pennings, E. J. M., and van Kemper, G. M. J., *J. Chromatogr.*, 1979, **176**, 478.
11 Hori, T., and Kihara, S., *Fresenius' Z. Anal. Chem.*, 1988, **330**, 627.

Paper 1/04648I
Received September 6, 1991
Accepted December 6, 1991

Denuder Tube Preconcentration and Detection of Gaseous Ammonia Using a Coated Quartz Piezoelectric Crystal

Zulfiqur Ali, C. L. Paul Thomas and John F. Alder*
Department of Instrumentation and Analytical Science, UMIST, P.O. Box 88, Manchester M60 1QD, UK
Geoffrey B. Marshall†
National Power Technology and Environmental Centre, Kelvin Avenue, Leatherhead, Surrey KT22 7SE, UK

The feasibility of using a cylindrical denuder tube for sampling gaseous ammonia, followed by detection with a piezoelectric quartz crystal, was investigated. Gaseous ammonia was sampled with a tungsten oxide-coated cylindrical denuder tube and then thermally desorbed onto a piezoelectric quartz crystal coated with pyridoxine hydrochloride–Antarox CO-880. A linear calibration graph of peak area response *versus* ammonia concentration sampled was obtained for ammonia concentrations between 3.1 and 8.2 μg l^{-1}. A concentration of 29 ng l^{-1} of ammonia in air was detected with a signal-to-background ratio of 14:1 by achieving an enrichment ratio of 900 with the tungsten oxide denuder tube.

Keywords: *Ammonia; piezoelectric crystal; denuder tube; preconcentration*

Ammonia is one of the most important trace gases in the atmosphere and is the only one that is basic. It is water-soluble and can react with aerosols, thus influencing atmospheric acidity. Most ammonia emissions are released into the atmosphere by biological processes, primarily through the decomposition of organic matter.[1] The main industrial source is from fertilizer and ammonia production plants.[2]

In determining the precise role of ammonia in the atmosphere, it is important to distinguish free ammonia from ammonium particulates. Filtration techniques have been used for separation of the gaseous phase from particulates, although their use can cause errors by the introduction of artefacts. For instance, an over-estimation of the ammonia concentration can be obtained by release of ammonia from ammonium nitrate on the filter-paper. Equally, an under-estimation can be obtained by reaction of gaseous ammonia with acids deposited on the filter.

Denuder tubes have been shown to be effective for the separation of gases from particles, and their theory and application for the determination of gaseous species have been reviewed.[3,4] Air is drawn under conditions of laminar flow through a tube coated with a selective adsorbent. Gaseous species diffuse to the collection surfaces. Particulates, having much lower diffusion velocities, cannot migrate to the walls and hence pass through unabsorbed and do not contribute to the final measurement. Gormley and Kennedy[5] have derived a solution describing diffusion from a stream flowing through a cylindrical tube:

$$\frac{c}{c_0} = 0.819 \exp(14.6272\Delta) + 0.0976 \exp(-82.22\Delta) + 0.01896 \exp(-212\Delta) \quad (1)$$

where c is the mean concentration of gas leaving the tube, and c_0 is the gas concentration entering the tube.

$$\Delta = \frac{\pi D l}{4F} \quad (2)$$

where D is the diffusion coefficient of the target gas in air, l is the length of coated tube, and F is the flow rate.

For $\Delta \geq 0.05$ only the first term in eq. (1) is significant.

$$c \simeq 0.819\, c_0 \exp(-14.6272\Delta) \quad (3)$$

The gas flow is, therefore, depleted by diffusion of the gaseous component to the walls, where it is adsorbed. The particulate phase, being heavier, passes through the tube.

An oxalic acid-coated denuder tube has been used for the determination of free ammonia in ambient air.[6,7] The method described requires washing the sorbed ammonia from the tube and determining it by potentiometry with an ammonia-sensitive probe. A tungsten oxide-coated denuder tube has also been used for sampling ammonia, which was then thermally desorbed and determined by means of a chemiluminescence nitrogen detector.[8] Hlavay and Guilbault[9] have used a pyridoxine hydrochloride-coated piezoelectric quartz crystal for the detection of ammonia. Pyridoxine hydrochloride reversibly adds ammonia to the phenolic 3-OH:

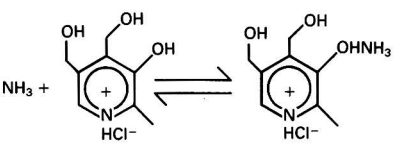

A reported frequency change of 1190 Hz for 1 ppm of ammonia in air was obtained, while Moody *et al.*[10] extended the useful lifetime of the detector by supporting the pyridoxine hydrochloride in a nonyl phenoxypolyethoxylate matrix of high relative molecular mass (Antarox CO-880). This was, however, at the expense of decreased sensitivity. Antarox CO-880 did not itself adsorb ammonia.

The present paper describes the application of a tungsten oxide-coated denuder tube to the collection of gaseous ammonia, which is subsequently thermally desorbed and detected by a pyridoxine hydrochloride–Antarox CO-880 coated, 14.9 MHz piezoelectric quartz crystal. The frequency responses of the piezoelectric quartz crystal detector to various concentrations of ammonia were measured.

Experimental

Piezoelectric Quartz Crystal Oscillator

The piezoelectric quartz crystals used were 14.9 MHz, fundamental mode, AT-cut with 3.8 mm diameter circular gold electrodes, on both sides of the 8 mm diameter quartz slab, supplied by Cathodeon Crystals, Cambridge, UK. The reference and detector crystals were made part of two pre-fabricated crystal oscillator circuits (Cathodeon Crystal)

* To whom correspondence should be addressed.

† Present address: Chemistry Department, Birkbeck College, 20 Gordon Square, London WC1H 0PP, UK.

powered from a 5 V d.c. power supply. The oscillator outputs were mixed in the exclusive-OR gates of a 74LS86 operational amplifier (RS Components, Corby, Northamptonshire, UK), and a low-pass filter was used to select the difference frequency, which was passed to a 120 MHz range, 0.01 Hz resolution digital frequency counter (Philips PM6671; Philips, Cambridge, UK), equipped with a digital-to-analogue converter. The sensor crystal was housed in a double-impinger type cell with a swept volume of 0.7 ml, sample gas being injected perpendicular to each face of the coated crystal.

Ammonia Determination

A continuous-gas flow regime was used for the determination of ammonia. Cylinder air (dried over silica gel) was used as the carrier gas. Poly(tetrafluoroethylene) (PTFE) tubing (6.5 mm o.d., Omnifit, Cambridge, UK) was used for all supply and waste lines. Gas flows were controlled by needle valves and were measured by rotameters calibrated against a soap-film bubble meter.

Low concentrations of ammonia in air were produced by two-stage dilution of a 100 ppm ammonia-in-air standard mixture (BOC Special Gases, London, UK). A four-way valve (Omnifit) was used to switch from the reference air flow to the sampling flow. A flow rate of 20 ml min^{-1} was maintained in the piezoelectric quartz crystal detector cell by means of a needle valve.

Pyridoxine hydrochloride–Antarox CO-880 coated piezoelectric quartz crystals were prepared by brush-coating a 1 + 1 (v/v) mixture of 0.02% m/v pyridoxine hydrochloride in 50% v/v aqueous ethanol and a 0.2% m/v solution of Antarox CO-880 in acetone. The coated quartz crystals were then kept in an oven at 80 °C for 2 h and allowed to cool in a desiccator.

Preparation of Tungsten Oxide Denuder Tube

Quartz tubes were coated with tungsten oxide by using a modification of the procedure described by Braman *et al.*[8] The quartz tubing (3 mm i.d., 5 mm o.d., 35 cm length) was prepared for coating by first washing with benzene and then with 50% sodium hydroxide solution. The tubes were then treated with 40% m/v hydrofluoric acid before being finally rinsed with high-purity water and dried in an oven at 150 °C for 2 h. Flow rates of less than 1 l min^{-1} were used for much of the gas sampling work. A 10 cm subduction zone was made by pipetting a solution of trimethylsilane in dichloromethane to the 10 cm mark, draining and then washing with high-purity water and drying at 150 °C for 2 h.

The denuder tubes were coated by means of the apparatus shown in Fig. 1. The quartz tube to be coated was connected between two Swagelok T unions with 0.25–0.125 in reducing PTFE ferrules. Tungsten wire (0.5 mm o.d.; Goodfellow Metals, Cambridge, UK) was spot-welded to stainless-steel rods (0.125 in o.d.) at each end. Several welds were necessary to achieve a mechanically strong join between the wire and rod. The stainless-steel rods and tungsten wire were threaded through the denuder tube and the T union compression fittings. A gas-tight seal was formed by using the PTFE reducing ferrule (Phase Separations, Deeside Industrial Estate, Clwyd, UK).

The denuder tube was evacuated to 267-400 Pa with a rotary vacuum pump. The tungsten wire was heated to approximately 1000 °C by passing through it a current (a.c.) of 12 A. Heating the tungsten wire caused expansion, and the tension was maintained by carefully pulling the stainless-steel rods with insulated pliers. The current was controlled by a variable transformer to provide a slow coating rate. A light coating of the blue oxide was obtained after passage of 12 A for 30 min; a heavier coating was obtained after 2 h. Denuder tubes coated rapidly at higher currents resulted in mechanically less stable coatings. The blue tungsten(IV) oxide was obtained by heating the tube to 350 °C at a pressure of approximately 650 Pa. The denuder tube was heated with a Kanthal resistance wire heater (Scientific Wire Co., London, UK). The resistance wire was wrapped around the quartz tube and held in place with hose clips at both ends. The temperature of the denuder tube was monitored by placing in the tube a thermocouple connected to two strands of Kanthal wire, with output to a digital thermometer.

Chemiluminescence Nitrogen Detector

A chemiluminescence nitrogen detector (Monitor Laboratories, Model 8440E) was used to characterize the tungsten oxide denuder tubes. Operation of the detector was based on the chemiluminescence reaction between nitrogen oxide and ozone. The nitrogen oxide and ozone reaction yielded stable nitrogen dioxide, primarily in the electronic ground state. A small fraction of the reaction yielded excited nitrogen dioxide, which emitted an infrared/visible continuum with a maximum intensity at approximately 1.1 μm.[11] Determination of ammonia was achieved by chemically converting the sample into nitrogen oxide in a stainless-steel converter at 850 °C, prior to its entry into the reaction cell. The instrument was calibrated against standard nitrogen oxide mixtures (BOC Special Gases) and calibrated for ammonia by passing standard ammonia–air mixture into the converter.

Characterization of the Tungsten Oxide Denuder Tube

The collection efficiency of the tungsten oxide denuder tube was established by measuring the decrease in the steady-state signal, when the denuder tube was inserted between the standard ammonia sample stream and the chemiluminescence nitrogen detector. Desorption of the adsorbed ammonia was carried out by heating the denuder tube from ambient temperature to 350 °C, with a desorption time of 1 min. The recovery efficiency was measured by dividing the area under

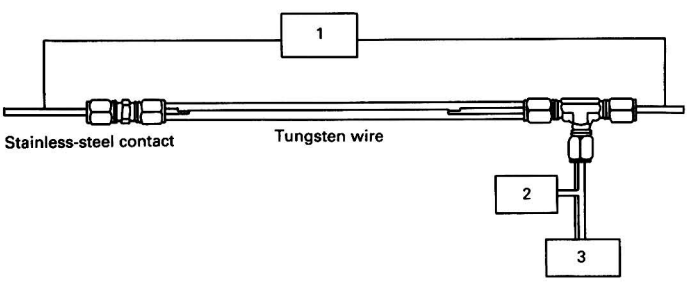

Fig. 1 Apparatus used for coating the denuder tubes with tungsten oxide. For details, see text. 1, A.c. voltage controller; 2, Pirani vacuum gauge; and 3, rotary vacuum pump

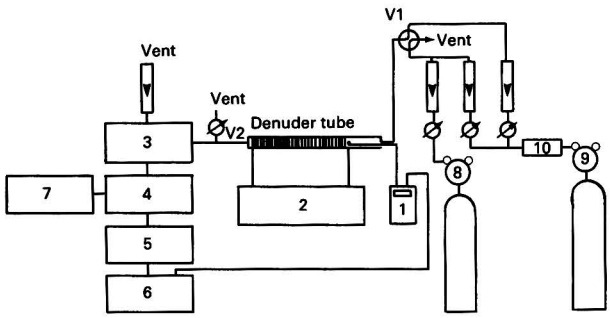

Fig. 2 Apparatus for the preconcentration of ammonia on the denuder tube, and subsequent desorption onto the piezoelectric crystal detector. 1, Digital thermometer; 2, a.c. voltage controller; 3, piezoelectric crystal detector cell; 4, oscillator; 5, frequency counter; 6, chart recorder; 7, power supply; B, ammonia, 100 ppm in air; 9, air; and 10, drying tube

the thermal desorption peak by the area under the collection profile. This ratio corresponds to the mass of ammonia desorbed from the denuder tube divided by the mass sorbed from the air stream.

The linearity of response of the denuder system for ammonia detection was measured by introducing known mixtures of increasing ammonia concentration into the tungsten oxide denuder tube. Ammonia standards were prepared by dilution of standard 100 ppm ammonia-in-air mixtures. The adsorption capacity of the denuder was ascertained by subjecting it to an ammonia concentration of 60 μg m^{-3} in air at a flow rate of 100 ml min^{-1}, noting the time taken for breakthrough to the NO_x detector.

Sampling and Detection of Gaseous Ammonia by Denuder Tubes and Piezoelectric Quartz Crystals

A schematic diagram of the system used to sample and detect gaseous ammonia is shown in Fig. 2. Low ammonia concentrations were generated from permeation tubes, prepared in the laboratory, having typical permeation rates of 180 ng min^{-1} at a temperature of 28 °C. Standard ammonia gas streams were routed to the tungsten oxide denuder tube through a four-way valve V1. The collected ammonia was thermally desorbed into a dry air stream. Detection of ammonia was carried out by an AT-cut 14.9 MHz piezoelectric crystal coated with pyridoxine hydrochloride–Antarox CO-880.

Results and Discussion

The effect of temperature on the preparation of the denuder tube, and the desorption temperature, were examined. Tungsten oxide denuder tubes subjected to a desorption temperature of 500 °C showed degradation in response with successive sampling cycles, using chemiluminescence nitrogen detection. Desorption products included nitrogen oxide, nitrogen dioxide and ammonia. Tungsten oxide denuder tubes subjected to temperatures of less than 350 °C gave ammonia as the only desorption product, and 11 successive sampling and analysis cycles of a 3 ppm ammonia standard gas stream resulted in peak heights with a relative standard deviation of 3%. The collection and recovery efficiencies were found to be 97 and 96%, respectively. The linearity of quantitative adsorption of ammonia by the tungsten oxide denuder tube was demonstrated over ammonia mass loadings of 0.2–3.3 μg, with a correlation coefficient of 0.998. These results show that the tungsten oxide denuder tube is capable of reproducible and quantitative sampling of ammonia. Ammonia thermally desorbs at a temperature near to that where degradation of the denuder occurs. The reliability of the technique is, therefore, dependent on accurate temperature control.

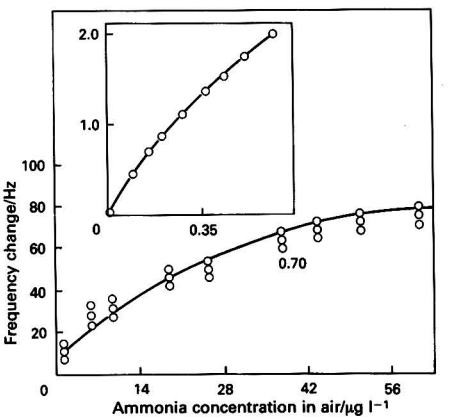

Fig. 3 Calibration graph for the coated piezoelectric crystal detector over the range 0.7–63 μg l^{-1} (1–90 ppm) of ammonia. The inset shows the calibration in the range 0–0.7 μg l^{-1} (0–1 ppm) of ammonia obtained at a different time

Fig. 3 shows the response curve for the direct exposure of the piezoelectric crystal to increasing concentrations of ammonia in dry air. The sensitivity obtained is lower than that reported by Hlavay and Guilbault.[9] A linear change in frequency with sorbed mass is expected for low mass loadings on the piezoelectric crystal,[12–15] hence the response curve will represent the ammonia sorption isotherm. The curve is similar to a Langmuir isotherm, and this is a reasonable model for a surface such as pyridoxine hydrochloride with clearly identifiable active sites.

Thermal desorption cycles of the tungsten oxide denuder tube, without added ammonia, resulted in frequency decreases of the sensor piezoelectric quartz crystal. The frequency decreases were thought to be as a result of an elevation in the temperature of the piezoelectric quartz crystal and expansion of the desorption gas volume. The effects could be decreased by increasing the desorption gas flow rate. A plot of this blank peak area *versus* desorption gas flow rate (Fig. 4) showed an exponential decrease of the peak with increasing desorption volume flow. A compromise high-desorption flow will, however, result in increased dilution of the desorbed analyte. A desorption flow rate of 100 ml min^{-1}, which minimized the peak, but maintained practical sensitivity, was used for all further studies.

The linearity of response of the piezoelectric quartz crystal denuder system for ammonia sampling and detection was tested by exposing the tungsten oxide denuder to ammonia concentrations between 3.1 and 8.2 μg l^{-1}. A linear plot of

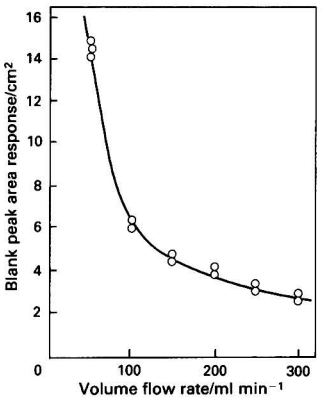

Fig. 4 Plot of coated piezoelectric crystal blank response peak area *versus* air flow rate through the denuder tube

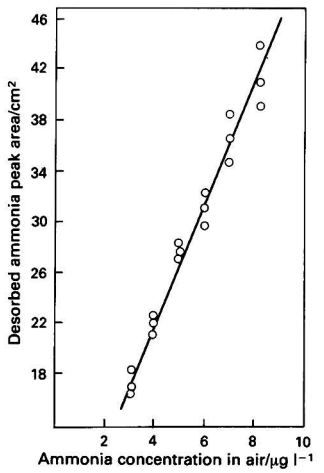

Fig. 5 Plot of ammonia response peak area from the coated piezoelectric crystal *versus* concentration of ammonia sampled in the denuder tube. The correlation coefficient of the straight line is 0.97; the ordinate axis intercept is 7.1

peak area response *versus* concentration of ammonia is shown in Fig. 5. The linearity of response of the piezoelectric quartz crystal/denuder system was further tested by varying the exposure times of a 6.1 μg l^{-1} ammonia gas stream to a tungsten oxide denuder tube. Exposure times of between 30 and 210 s resulted in 0.3–2.1 μg calculated ammonia mass loadings. A least-squares fit analysis of the peak area response *versus* calculated mass loading yielded a straight line between 0.6 and 2.1 μg, with a slope of 25 cm^2 μg^{-1} and with a *y*-axis intercept of -2.0 cm^2 μg^{-1}. The correlation coefficient for the straight line was 0.99. Below 1 μg of ammonia, the line curved towards the origin. The adsorption capacity was calculated to be 2.9 μg of ammonia, which compares favourably with a value of 2.5 μg in earlier work[16], when using the same method, and with 3 μg from breakthrough studies.

Ammonia thermal-desorption profiles show the initial blank response followed by the ammonia peak. The tailing of the analyte peak increased with the mass of ammonia exposed. Such tailing could be due to a number of factors. The collection surface of the tungsten oxide denuder tube is not homogeneous, and the adsorption sites will have a range of binding energies, resulting in tailing of the desorption peak.

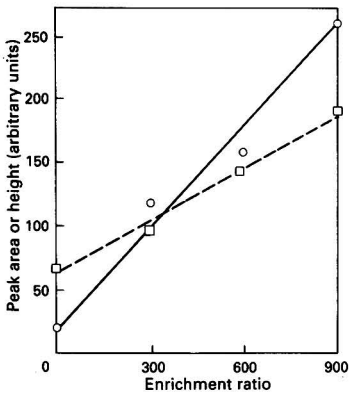

Fig. 6 Plots of peak height (□) and peak area (○) for the coated piezoelectric crystal response *versus* enrichment ratio calculated for the tungsten oxide-coated denuder tube

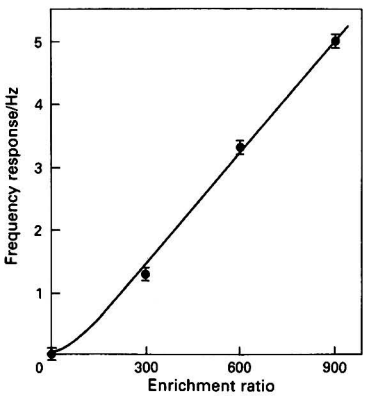

Fig. 7 Plot of frequency response *versus* enrichment ratio

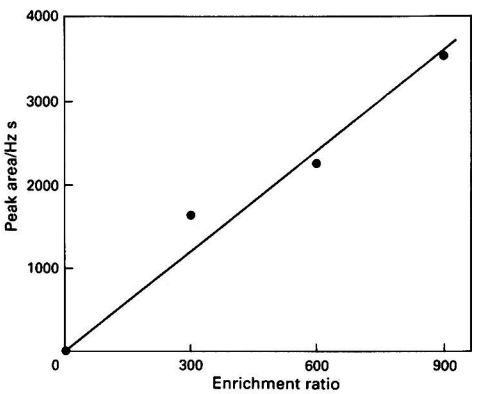

Fig. 8 Plot of integrated peak area *versus* enrichment ratio

Diffusional broadening and adsorptive retardation by the sampling lines and fittings could also lead to tailing.

Preconcentration of the Analyte

The denuder tube, in addition to separating gaseous ammonia from particulates, also serves to preconcentrate the analyte and hence increase the sensitivity of the system. The extent of

preconcentration is determined by the enrichment ratio (ER), defined as the ratio of the concentration of ammonia in the desorbed gas (c_D) to that in the ambient air [c_0; see eqn. (3)]. If the denuder tube preconcentrator is exposed until it is saturated, a significant part of the sample can be lost, but the ER is optimized. If the sampling time is restricted such that breakthrough does not occur, higher sampling efficiency, but lower enrichment ratios, are observed.

A study was carried out to illustrate the improvement in sensitivity of the system with an increase in the enrichment ratio. An ammonia-in-air concentration of 29 ng l^{-1} was passed over the tungsten oxide denuder tube for times sufficient to yield enrichment ratios of 300, 600 and 900. The data obtained are shown in Figs. 6–8 as plots of peak frequency response and integrated area response for the blanks and three enrichment ratios. It is clear that this procedure significantly enhances the over-all sensitivity of the determination.

Conclusions

The feasibility of using a tungsten oxide denuder tube preconcentrator with a pyridoxine hydrochloride–Antarox CO-880 coated piezoelectric quartz crystal for the sampling and detection of ammonia has been demonstrated. Analysis for low concentrations of ammonia can be carried out if high enrichment ratios are used. The enrichment ratios could be further increased by increasing the adsorption capacity of the denuder tubes by using an annular denuder, which would also permit much shorter sampling times. The use of denuder preconcentrators thus leads to the significant advantage of being able to desorb the sampled vapour in dry carrier gas, hence overcoming the effect of relative humidity on the piezoelectric crystal. Although the temperature pulse has an effect on the piezoelectric crystal, it can be minimized and useful sensitivity can be achieved. The data in Figs. 6–8 represent a signal-to-background ratio of about 14:1 in integrated area terms, with an enrichment ratio of 900 for an ammonia concentration of 29 ng l^{-1}, which represents a limit of detection of the order of 6.5 ng l^{-1} of ammonia.

The effect of interfering species on this technique has not been studied in this work. Previously published data indicate that alkylamines, nitrogen dioxide, peroxyacetyl nitrate and nitric acid adsorb into denuder tubes with tungsten(VI) oxide coatings.[3] However, none of these species in the gas phase has been reported as adsorbing onto coatings of pyridoxine hydrochloride, and hence the second-stage selectivity of the piezoelectric crystal detector should minimize their action. It is also expected that aerosol and particulate interference will be minimal.

The authors are grateful to SERC and the then CEGB for support of Z. A. under the CASE scheme. The contribution of G. B. M. is published by permission of National Power plc.

References

1 Bujisman, E., Moss, H. F., and Asman, W. A. H. *Atmos. Environ.*, 1987, **21**, 1009.
2 Dawson, G. A., *J. Geophys. Res.*, 1977, **82**, 3125.
3 Ali, Z., Thomas, C. L. P., and Alder, J. F., *Analyst*, 1989, **114**, 759.
4 Murphy, D. M., and Faheg, D. W., *Anal. Chem.*, 1987, **59**, 2753.
5 Gormley, P. G., and Kennedy, M., *Proc. R. Ir. Acad., Sect. A.*, 1949, **52A**, 103.
6 Ferm, M., *Atmos. Environ.*, 1979, **13**, 1385.
7 Dimmock, N. A., and Marshall, G. B., *Anal. Chim. Acta*, 1986, **185**, 159.
8 Braman, R. S., Shelley, T. J., and McClenny, W. A., *Anal. Chem.*, 1982, **54**, 365.
9 Hlavay, J., and Guilbault, G. G., *Anal. Chem.*, 1978, **50**, 1044.
10 Moody, G. J., Thomas, J. D. R., and Yarmo, M. A., *Anal. Chim. Acta*, 1983, **155**, 225.
11 Clyne, M. A. A., Thrush, B. A., and Wayne, R. P., *Discuss. Faraday Soc.*, 1964, **60**, 359.
12 Sauerbrey, G. Z., *Z. Phys. Chem. (Leipzig)*, 1959, **155**, 206.
13 Miller, J. G., and Bolef, D. I., *J. Appl. Phys.*, 1968, **139**, 5815.
14 Lu, C. S., *J. Vac. Sci. Technol.*, 1975, **12**, 578.
15 Cumpson, P. J., and Seah, M. P., *Meas. Sci. Technol.*, 1990, **1**, 544.
16 Ali, Z., PhD Thesis, UMIST, University of Manchester, 1989.

Paper 0/05024E
Received May 23, 1991
Accepted November 5, 1991

Automated Gravimetric Management of Solutions
Part 1. High-performance Microcomputer-controlled Gravimetric Burette

Ildenise B. S. Cunha and Celio Pasquini*
Instituto de Química, Universidade Estadual de Campinas, Caixa Postal 6154, CEP 13081, Campinas, São Paulo, Brazil

A versatile gravimetric burette and the necessary interface that allows it to be controlled by an IBM-PC microcomputer are described. The burette employs an electronic balance that holds three 30 ml flasks. The flasks are used for delivering different titrants or standard solutions and are connected to the sensor through the bottom of the balance. The addition of the solution is controlled by poly(tetrafluoroethylene) electromechanical valves housed inside the unit. The flasks can be refilled automatically from larger reservoirs placed outside the case. Solution level sensors are used to realize automatic refill when necessary. The mass delivered from the flasks is read by the computer through an RS232C interface. The burette can, when driven by the appropriate software, perform potentiometric, biamperometric and spectrophotometric titrations, standard additions procedures and the preparation of standard solutions.

Keywords: *Gravimetric burette; titration; standard additions; automated titration*

The gravimetric addition of a solution in titration procedures has been described in the literature.[1–5] The advantages of such an approach to titrant addition are always emphasized: for example, it is claimed that gravimetric additions do not require any calibration of the glassware, and are free from errors caused by solution viscosity and by contraction/dilatation of the volume caused by a change in the ambient temperature. Moreover, additional advantages are provided by the use of modern electronic balances: for example, rapid weighing, absence of moving parts that can be affected by mechanical stress, and the balance frequently has a standard RS232 interface providing prompt communication with microcomputers.

In addition to these advantages the potential of the gravimetric approach has not yet been fully exploited. In fact, the gravimetric manipulation of solutions in the laboratory could lead to more precise and reliable results. On the other hand, there is a need for a versatile, cost effective, gravimetric apparatus to deal with the variety of analytical procedures that demand solution management.

Some of the instruments described previously do not guard against air currents which can affect the mass measurement. Therefore, high sensitivity balances cannot be used.[1,3,4] The instruments described also employ a large reservoir (and sometimes a control valve) placed on the balance plate. As the load on the balance is high, the usable sensitivity is only 0.01 g in those less expensive balances which can handle, for example, only 100 g with a sensitivity of 1 mg.

Previously described instruments do not allow the simultaneous use of more than one solution in the same gravimetric addition unit. The use of more than one solution with only one balance would improve the cost to benefit ratio of constructing the unit and at the same time would extend its ability to perform, for example, a back-titration, and simple or multiple standard additions procedures.

This paper describes a versatile microcomputer-controlled gravimetric burette that extends the application of such units and allows for the use of more than one solution per balance which can operate with a higher sensitivity.

* To whom correspondence should be addressed.

Experimental

Gravimetric Burette

The gravimetric burette is depicted in Fig. 1. The unit was constructed using a metallic frame 50 cm high, 25 cm wide and 25 cm deep. Three sides of the metallic frame were closed with metallic sheets and the front was closed with an acrylic sheet that can be lifted if access to the flasks inside the unit is desired. The metallic frame has a platform on which an Acatec Model BCM 1003 electronic balance with capacitive sensor was placed. The balance can operate with a sensitivity of 1 mg (maximum load 100 g) or 10 mg (maximum load 1000 g). At the top of the case there is a small metallic door through which it is possible to reach the balance plate. A metallic rod was connected to the sensor through a hole in the base of the balance case. At the end of the rod, an acrylic plate sustains three 30 ml polyethylene flasks held on the plate by inner plastic screws. At the base of the flasks a hole of 0.1 mm diameter was drilled for admission of air during solution delivery. The outlet of the flasks contains a 2.0 cm long, 1.6 mm o.d., 1.2 mm i.d., glass tube, to which is attached a 1.5 mm i.d. Tygon tube. The length of the Tygon tube is twice the distance between the glass tube and the three-way valves (NResearch Model 161TO31) to which the tubes are connected to the common port. The normally closed outlets of the valves are connected to poly(tetrafluoroethylene) (PTFE) tubes (20 cm × 0.9 mm i.d.). These tubes are taken out from the metallic case through small holes drilled in the front acrylic sheet and are used for solution delivery. The normally open outlets of the valves are connected to two-way valves (NResearch Model 161TO11) placed outside the case. These valves are connected to 1 l solution reservoirs placed on the outside of the case. The manifold used to couple the solution reservoir to the flasks inside the burette case is shown in Fig. 2. When any of the two-way valves is turned on the stock solution is delivered to the respective burette flask. When any of the three-way valves is turned on the solution present in the respective flask is delivered outside the case, through the PTFE tube. The mass, delivered during the period in which the valve is kept on, is monitored by the computer.

Around the small glass tube fitted at the outlet of each inner flask there is an infrared opto-switch (PCST-2103). The switches are used to detect when a flask is empty, requiring immediate action by the computer to turn on the respective two-way valve to refill the flask. The refill operation is

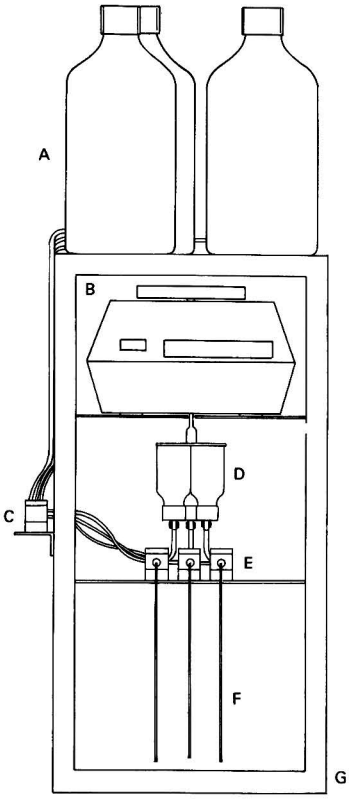

Fig. 1 Proposed gravimetric burette. A, External solution reservoir flasks; B, electronic balance; C, two-way electromechanical valves; D, internal flasks; E, three-way electromechanical valves; F, solution outlet; and G, metallic case

performed by switching the respective two-way valve on and by following the increase in the mass of the whole set of inner flasks. For the flasks used, a maximum mass increase of 20 g is allowed before the valve is switched off, stopping the operation. Therefore, no sensor for the 'full' status is required. The time spent on this operation can be reduced if a nitrogen pressure is applied to the external stock solution reservoir.

Interface and Electronic Circuits

The communication of the balance with the microcomputer (DICOM, IBM-PC XT compatible, 640 kbyte RAM, Winchester of 20 Mbyte and Floppy of 360 kbyte, Display CGA-monochrome) is made at 9600 bits s^{-1} using the serial RS232 interface present in both the balance and computer. The balance sends a string containing the mass reading every 0.3 s.

The control of the gravimetric unit is effected by using the asynchronous interface described previously.[6] The interface communicates with the microcomputer through a user port based on the CI 8255.[7] The card, containing the user port, is plugged into an extension slot inside the microcomputer. Two handshake signals (strobe and acknowledge), the ground line and the eight parallel data lines are exchanged between the computer user port and the interface.

A circuit diagram of the interface employed for control of the burette and for data acquisition is shown in Fig. 3. The CI 74LS373 (I) is used as an address decoder and up to eight electronic devices can be accessed.[6] Two of the addresses (254 and 253 corresponding to bit 0 and 1) are used for a dynamic

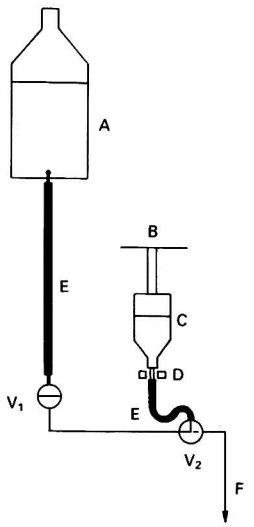

Fig. 2 Manifold to connect the external reservoir flasks to the internal burette flasks. A, External reservoir flask; B, balance support; C, burette flask; D, opto-switch; E, Tygon tube; F, burette outlet; V1, two-way valve; and V2, three-way valve

analogue-to-digital converter based on an 8 bit DA (ZN428) and an 8 bit AD (ZN448).[8] The address line 251 (bit 2) is connected to another 74LS373 (III) used as an 8 bit latch. Six of the output lines are used to source the base current to 2222N transistors, used as switches for the electromechanical valves.

Address line 243 (bit 3) is used to enable another CI 74LS373 (II), used to input the logic state of the three level sensors. A circuit diagram of the optical sensors is shown in Fig. 4. The average change in the voltage at the collector of the opto-transistor is 2.0 V (from 6.0 to 4.0 V). This change is caused mainly by the difference in the refractive index between the full and the empty glass tube. Therefore, approximately the same change is observed for coloured solutions such as 0.01 mol dm^{-3} $KMnO_4$ and 0.1 mol dm^{-3} $K_2Cr_2O_7$. The reference voltage for the 741 comparators is set to the middle of the range, about 5.0 V. When the level of liquid in the flask is above the limit the TTL logic level at the comparator output is high. The existence of a low level signs the 'flask empty' condition.

Analogue signals to be monitored are passed through an analogue input pre-conditioning stage. This stage (which is not shown in Fig. 3) is based on two OP07 operational amplifiers and is designed to provide a high versatility in terms of the dynamic range and polarity of the signal to be followed. The first OP07 can supply a positive or negative gain to the signal. Its output is sent to the next stage which will sum a positive or negative offset voltage[9] to change a bipolar signal to a positive only signal which can be followed by the dynamic analogue-to-digital converter, shown in Fig. 3.

Main Software to Control the Gravimetric Burette

General use software to drive the user card and the interface, and for reading the dynamic analogue-to-digital converter, has been described previously.[7,8] In addition to this software, a number of QUICKBASIC 4.5 sub-programs were written specifically to control the gravimetric unit. These sub-programs are shown in the Appendix.

Five sub-programs are necessary to control the gravimetric burette. The SUB valveon(nv%) and SUB valveoff(nv%) are used to open or close, respectively, any of the six valves present in the gravimetric unit; nv% is the valve number (1–6). The sub-program SUB fillburette(n%,ma) is used to fill

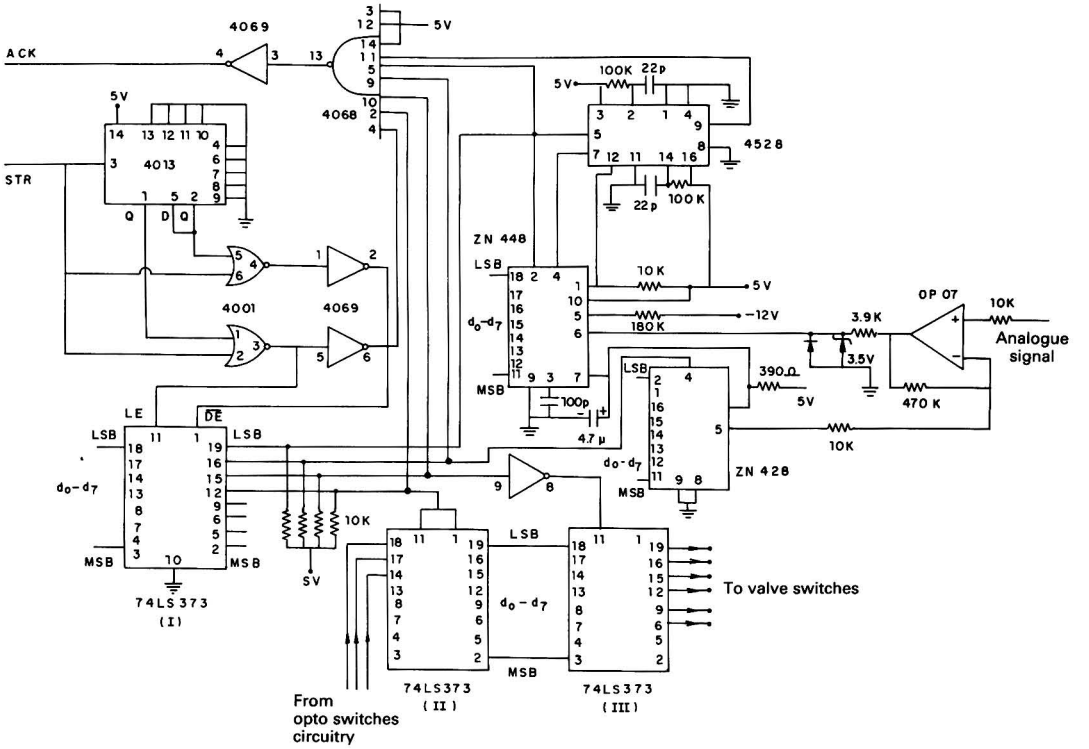

Fig. 3 Electronic circuit diagram of the interface employed for control of the burette and data acquisition

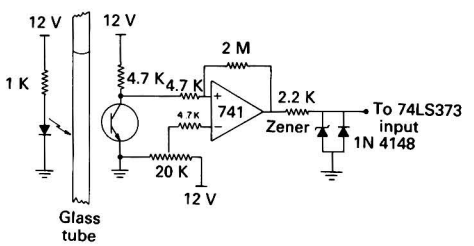

Fig. 4 Electronic circuit diagram for solution level detection

the burette flask n% (1–3). The flask n% will be empty to the optical sensor level and then refilled until a mass change equal to ma is observed. If the flask is already empty the refill operation is executed directly.

The sub-program SUB addtime(n%,t,madd) can be used to deliver the solution present in flask n% (1–3) for a fixed time interval t (in seconds). The sub-program checks if the flask is not empty and, in that situation, the SUB fillburette(n%,ma) is automatically called. The mass actually added is returned in the variable madd. The SUB addmass(n%,m, madd) is used to deliver a mass approximately equal to m from the flask n%; it also checks for the level of the solution. Again the added mass is returned in madd. The SUB readbalance(stb,flaginst-%,mass) is used to read the balance through the RS232 serial interface. Mass is the variable containing the mass reading, stb is the value for the reading stability test. If two consecutive readings agree in between this value the sub-program is exited and the flaginst% is set to 0. If more than ten readings are made the last value is returned in the 'mass' variable and the flaginst% is set to 1, indicating that the balance is unstable.

The above set of sub-programs are sufficient for the implementation of most of the titration or standard additions procedures.

Results and Discussion

The gravimetric burette was evaluated for its accuracy in transferring mass from the burette flask to the reaction flask outside the case. The burette flasks were filled with water and the sensitivity of the balance was set to 1 mg. The mass was transferred to a previously weighed glass flask. The mass transferred was determined with an analytical balance with a sensitivity of 0.1 mg. The values of mass accessed by the microcomputer from the burette balance(mt) were compared with those obtained with the analytical balance(mr). Results for 120 comparisons (ten trials for each delivery time interval: 0.5, 2.0, 5.0 and 10 s, for each burette flask) showed that the differences (mt − mr) were never higher than +0.002 g or lower than −0.002 g. The mt values are related to the mr values by the equation:

$$mt = (-8.17 \times 10^{-4} \pm 0.34) + (0.9989 \pm 1.2 \times 10^{-3})mr$$

the correlation coefficient is 0.99998 and the error of the estimate is 9.6×10^{-4} g. No systematic proportional or constant error between the two sets of measurements could be detected at the 95% confidence level.[10]

The flow rate of the gravimetric burette changes slightly as a function of the height of the liquid column inside the flasks. The change is not significant and does not alter the true measurement of the mass transferred. At the level of the bench the flow rate for a diluted aqueous solution is about 3.0 ml min^{-1}, if the manifold described under Experimental is employed. If it is necessary, an increase in the flow rate can be achieved by placing the case higher than the level of the bench or by using larger bore tubing to assemble the manifold.

The potentiometric titration curve for the titration of 5 ml of 0.01 mol dm^{-3} Fe^{II} solution with 0.001667 mol kg^{-1} $K_2Cr_2O_7$ solution, monitored by using a Pt electrode and an Ag–AgCl reference electrode, is shown in Fig. 5. The end-point was found using the second-derivative method. Note that the

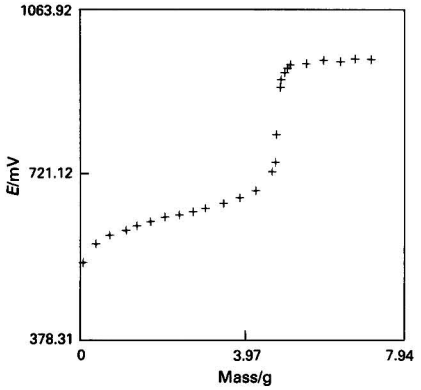

Fig. 5 Potentiometric titration curve obtained using the prototype gravimetric burette. Titrant, 1.667×10^{-3} mol kg^{-1} $K_2Cr_2O_7$; titrand, 0.01 mol dm^{-3} Fe^{II} solution

driven software is capable of slowing down the mass added near the end-point, permitting an increase in the precision of the determination. A sensitivity of 1 mg was employed in the burette balance in carrying out such titrations. The average of ten determinations and the standard deviation were (1.007 ± 0.007) $\times 10^{-2}$ mol dm^{-3}. The precision is good considering the small (5 ml) sample volume titrated.

The gravimetric burette described here presents some advantages over previously described instruments. The unit is isolated from air currents, allowing the use of more sensitive balances. The same balance can be used with more than one flask, improving the cost to benefit ratio of constructing the unit. The total load of the accessories (support + empty flasks) is about 45 g. Therefore, it is possible to use high sensitivity balances in the construction of the burette. Refill of the burette is achievable and is performed automatically by the control program. The flasks do not need to be removed from the unit. Therefore, the over-all performance of the instrument is improved as factors affecting the weighing precision, such as a change in the condition of the tube connecting the flask to the valve, are not present.[3] The tube is always 'relaxed' as is necessary for good precision in mass transference.[3] The gravimetric unit can also be used to implement a totally gravimetric approach to a given analytical procedure. The mass of the sample (liquid or solid) can be found using the same balance of the unit, gaining access to the balance plate through the door at the top of the case. In so doing, it is important to keep the total load on the balance below the higher limit for the selected sensitivity.

Although three flasks were used in the prototype described here, it is possible to add more flasks to the unit. By using a sensitivity of 0.01 g, the total mass of the support plus flasks can be as high as 1000 g.

The atmosphere in the case can be kept inert (free of oxygen, for example) by maintaining a slight positive pressure of nitrogen. An inert atmosphere can be useful if one wishes to use the burette to perform standard additions in polarographic determinations, for example.

If compared with the modern volumetric addition units commercially available, the gravimetric unit can offer the same performance at low cost per individual solution. No moving parts are present and less care need be expended in keeping the instrument in working order. One disadvantage of the gravimetric approach is, perhaps, that it does not enable the continuous addition of titrant to be performed when the reaction is sufficiently fast to permit the use of this type of procedure. However, a quasi-continuous procedure with rapid gravimetric additions followed by reading of the mass and potential without any stability test is being evaluated for use in routine determinations.

Finally, more complex titration procedures requiring the addition of more than one reagent, back-titrations and multiple standard additions (as are necessary for the generalized standard additions methods[11]) can be carried out by using the proposed gravimetric burette driven by the appropriate software. These applications of the gravimetric burette in routine laboratory tasks will be described in a subsequent paper.

APPENDIX

LISTING 1 Main QUICKBASIC 4.5 Sub-programs to Control the Gravimetric Burette

```
' The following constant values associated with the
' interface control and addresses of the devices
' should be declared in the main module of the program.
' The following sub-programs assume that the user card has
' been initialized and that the asynchronous interface is in
' step. For details of the interface and user card operation
' see refs. 6–8.

CONST contr% = 1003, pa% = 1000, pb% = 1001, pc% = 1002

CONST ohstr% = 3, olstr% = 2, ihstr% = 5, ilstr% = 4

CONST iack% = 32, oack% = 128, hill% = 255

CONST adc% = 254, dac% = 253, vadd% = 251, senadd% = 247

CONST iof% = 1          ' enables/disables 1/0, 1 = enabled,
                        ' 0 = disabled

CONST tmax = 400        ' time in seconds necessary to empty a
                        ' full burette flask

COMMON SHARED dout%,ma,stb

' initialization of the user card (see ref. 7)
```

```
OUT contr%,193: OUT pa%,hill%: OUT pb%,ohstr%

' the following sub-programs are necessary to control the
' gravimetric
' burette and to perform analytical procedures


SUB fillburette(n%,ma)                  ' fill the burette n% (1<n%<4)

    empty% = 2 (n%-1)
       nr% = n% + 3

   CALL readinter(247,di%)              ' checks for level sensor state
      IF (di% AND empty%) = 0 THEN GOSUB fill : EXIT SUB
' flask is empty
            CALL valveon(n%)            ' flask is being emptied
                                        ' flask is not empty
   WHILE (di% AND empty%) > 0           ' waiting for an empty flask
      CALL readinter(247,di%)
   WEND
      CALL valveoff(n%)
       GOSUB fill
   EXIT SUB

 fill:
        CALL readbalance(flaginst%,mass,stb)
         mi=mass


           CALL valveon(nr%)
        WHILE ABS(mass-mi) < ma
        CALL readbalance(flaginst%,mass,stb)
        WEND
           CALL valveoff(nr%)
 RETURN

END SUB

SUB addtime(n%,t,madd)   ' delivers solution from burette n%
                         ' during the
                         ' time interval t (s). Returns madd,
                         ' the true added mass
      told = t
   IF t > tmax THEN EXIT SUB
   CALL readbalance(flaginst%,mass,stb)
     mi = mass: maddi = 0
     empty% = 2 (n%-1): ti=TIMER
     CALL valveon(n%)
   WHILE (TIMER - ti) < t
      CALL readinter(247,di%)
       IF di% AND empty% = 0 THEN
        CALL valveoff(n%)
        CALL readbalance(flaginst%,mass, stb)
        maddi = ABS(mass - mi)
              dt = TIMER - ti: t = t - dt
        CALL fillburette(n%,ma%)
        CALL readbalance(flaginst%,mass,stb)
        mi = mass
            ti = TIMER
        CALL valveon(n%)
       END IF
   WEND
      CALL valveoff(n%)
      CALL readbalance(flaginst%,mass,stb)
      madd = maddi + ABS(mass - mi)
        t = told
END SUB

SUB addmass(n%,m,madd)                  ' adds solution from burette n%
                                        ' until the mass m is
                                        ' approximately added. Returns
                                        ' madd, the true mass added
```

```
        mold = m
      IF m > ma% THEN EXIT SUB
        CALL readbalance (flaginst%,mass,stb)
        mi = mass: empty% = 2 (n%-1): maddi = 0
        CALL valveon(n%)
  WHILE ABS(mass - mi) < m
        CALL readinter(247,di%)
        CALL readbalance(flaginst%,mass,stb)
    IF di% AND empty% = 0 THEN
        CALL valveoff(n%)
        CALL readbalance(flaginst%,mass,stb)
          maddi = ABS(mass-mi): m = m - maddi
        CALL fillburette(n%,ma%)
        CALL readbalance(flaginst%,mass,stb)
          mi = mass
        CALL valveon(n%)
    ENDIF
  WEND
        CALL valveoff(n%)
        CALL readbalance(flaginst%,mass,stb)
        madd = maddi + ABS(mass - mi)
          m = mold
END SUB


SUB readbalance(flaginst%,mass,stb)     ' reads the balance
                                        ' through RS232 in COM2
        IF iof% = 0 THEN EXIT SUB

            OPEN "COM2: 9600,N,7,2,RS,DSO" FOR INPUT AS #1
            n=0: mass1=0: mass2= 2*stb

DO UNTIL n > 10 OR ABS(mass2 - mass1) =< stb
            GOSUB readmass
             mass1 = mass

            GOSUB readmass
             mass2 = mass
            n=n+1
LOOP
        IF n > 10 then flaginst% = 1 ELSE IF n =< 10 THEN
flaginst% = 0
        dout% = dout% and 191
        CALL outda(251,do%)
        CLOSE #1

EXIT SUB

  readmass:
        INPUT #1, mass$
        mass = VAL(mass$)
  RETURN

END SUB


SUB valveon(nv%)                        ' turns the valve nv% on
        IF nv%>6 OR nv%<1 THEN EXIT SUB
        dout% = dout% OR (2 (nv%-1))
    CALL outda(251,dout%)
END SUB


SUB valveoff(nv%)               ' turns the valve nv% off
        IF nv% > 6 OR nv% < 1 THEN EXIT SUB
        dout% = dout% AND (255-(2 (nv%-1)))
        CALL outda(251,dout%)
END SUB


SUB outda(ad%,bytetosend%)              ' used for output data to
                                        ' the interface
```

```
    IF iof% = 0 THEN EXIT SUB
      OUT pb%,ohstr%
          OUT pa%,ad%
        OUT pb%,olstr%
    WHILE (INP(pc%) AND oack% = 0) : WEND
        OUT pb%,ohstr%
      OUT pa%,bytetosend%
        OUT pb%,olstr%
    WHILE (INP(pc%) AND oack% = 0) : WEND
        OUT pb%,ohstr%
      OUT pa%,hil%
END SUB


SUB readinter(ad%,di%)                  ' for input data from the
                                        ' interface. This sub-program
                                        ' can access the sensor state
                                        ' and the ADC converted value
    IF iof% = 0 THEN EXIT SUB
    OUT pb%,ohstr%
        OUT pa%,ad%
      OUT pb%,olstr%
      WHILE (INP(pc%) AND oack%) = 0: WEND
      OUT pb%,ohstr%
          OUT pb%,ihstr%
        OUT pb%,ilstr%
    WHILE (INP(pc%) AND iack%) = 0: WEND
        di% = INP(pa%)
END SUB
```

References

1 Tamberg, T., *Fresenius' Z. Anal. Chem.*, 1978, **291**, 124.
2 Luft, L., *Talanta*, 1980, **27**, 221.
3 Kratochvil, B., and Nolan, J. E., *Anal. Chem.*, 1984, **56**, 586.
4 Chipperfield, J. R., and Webster, D. E., *Anal. Chim. Acta*, 1987, **197**, 373.
5 Mak, W. C., and Tse, R. S., *J. Chem. Educ.*, 1991, **68**, A95.
6 Souza, P. S., and Pasquini, C., *Lab. Micro*, 1990, **9**, 77.
7 Malcolme-Lawes, D. J., *Lab. Micro.*, 1987, **6**, 16.
8 Malcolme-Lawes, D. J., *Lab. Micro.*, 1987, **6**, 122.
9 Horowitz, P., and Hill, W., *The Art of Electronics*, Cambridge University Press, Cambridge, 8th edn., 1987.
10 Eckshlager, K., *Errors, Measurements and Results in Chemical Analysis*, Van Nostrand Reinhold, London, 1972, p. 144.
11 Saxberg, B. E. H., and Kowalski, B. R., *Anal. Chem.*, 1979, **51**, 1031.

Paper 1/04873B
Received September 23, 1991
Accepted December 2, 1991

Colorimetric Determination of Iron(II) and Iron(III) in Glass*

Elizabeth W. Baumann
Westinghouse Savannah River Co., Savannah River Site, Aiken, SC 29808, USA

A simple method to determine relative amounts of Fe^{II} and Fe^{III} was developed for the analysis of glass containing nuclear waste. The pulverized glass sample was dissolved in a sulfuric acid–hydrofluoric acid mixture with ammonium metavanadate added to preserve the Fe^{II} content. The V^{V}–V^{IV} couple, which is strongly acid-dependent, caused the Fe^{II} to be oxidized to Fe^{III} in the highly acidic dissolution and then to be regenerated when the solution was adjusted to pH 5 for formation of the magenta Fe^{II}–Ferrozine complex. Boric acid was added to complex the fluoride and permit regeneration of Fe^{II}, otherwise Fe^{III} would be stabilized as a fluoride complex. The Fe^{II} content was determined from the absorbance at 562 nm, and total Fe was determined from the absorbance of the same solution after ascorbic acid had been added to reduce Fe^{III} to Fe^{II}. The relative standard deviation was 5%, and the range was 3–97% for Fe^{II} in total Fe. The method was validated by analysing a glass frit spiked with ammonium iron(II) sulfate and/or ammonium iron(III) sulfate solutions. The method is applicable to glasses (or minerals) that contain more than about 5% total Fe.

Keywords: *Glass analysis; iron(II) determination; iron(III) determination; iron in glass; Ferrozine*

At the Savannah River Site, a process has been developed for incorporating defence nuclear waste in a glass matrix for disposal. In this process, the redox state in the glass melter is an important process control parameter. If the mixture of the glass frit and waste in the glass melter is too reducing, nickel sulfide and other metals may precipitate within the melter.[1] If the mixture is too oxidizing, the durability of the glass product is affected.[2]

A recognized indicator of redox conditions in systems such as glasses and minerals is provided by the Fe^{III}–Fe^{II} couple, which is reversible and responsive to redox conditions. Hence the relative amounts of Fe^{II} and Fe^{III} will define the redox state. A simple and reliable procedure for this determination was needed for routine process control analysis of the radioactive glass product.

The determination of both Fe^{II} and Fe^{III} in a sample is challenging because Fe^{II} may be converted into Fe^{III} through inadvertent oxidation prior to the final analytical measurement. A non-destructive method such as Mössbauer spectroscopy[3] was attractive for this application, but the technique is not suited to routine analyses because of the long data collection time, sophistication, and limited sensitivity for low concentrations of either oxidation state. Many colorimetric methods have been described, in which differentiation between oxidation states is accomplished with chromogens specific for either the Fe^{II} or Fe^{III} ion.[4–9]

For colorimetric methods the sample must be dissolved, which can provide an opportunity for significant oxidation of Fe^{II} to occur. Iron(II) is readily oxidizable in the acidic fluoride medium common to most glass dissolutions. Techniques for rapid dissolution and/or inert environments have been recommended.[5–9] Chemical stabilization by vanadate has also been used.[4]

This paper describes the development and application of a simple and rapid method suitable for the remote routine analysis of glass that contains nuclear waste.[10] The method has been used successfully for comparison studies with Mössbauer determinations[3] and in other studies,[11] but has never been fully described in the literature. This paper describes the method and its validation.

* This paper was prepared in connection with work done under Contract No. DE-AC09-89SR18035 with the US Department of Energy.

Experimental

Description of the Method

Features

The procedure combined several features to provide an integrated method for the reliable determination of Fe^{II} and Fe^{III}.

The glass sample, in a polystyrene vial, was dissolved in sulfuric–hydrofluoric acid as described by Jones *et al.*[5] The mixture was not heated, except for the heat generated by the dissolution reaction. Because of the preservation of Fe^{II} by vanadate, discussed below, no inert gas blanket or protection from air was required.

Iron(II) was preserved by taking advantage of the acid dependence of the V^{V}–V^{IV} couple, as described by Wilson[4] and illustrated by the reversible equation:

$$V^{5+} + Fe^{2+} \underset{\text{pH 5 buffer}}{\overset{\text{acid dissolution}}{\rightleftharpoons}} V^{4+} + Fe^{3+}$$

In a strongly acidic solution such as the dissolution mixture, V^{V} is a strong oxidizing agent and quantitatively oxidizes Fe^{II} to Fe^{III}, producing V^{IV}. The oxidation potential is substantially reduced at pH 5, and Fe^{II} is regenerated from the V^{IV} preservative.

Ferrozine (Hatch) was used as the chromogen because of its rapid colour formation, stability and selectivity.[12] The complex has a broad peak with a maximum absorbance at 562 nm and a molar absorptivity of about 28 000 l mol^{-1} cm^{-1}.

Because this application required that only the relative amounts of Fe^{II} and Fe^{III} be determined, volumes were not closely controlled. Measurements of Fe^{II} and total Fe were made on the same solution before and after addition of solid ascorbic acid. The procedure can easily be made quantitative if desired with controlled volumes and use of standards.

Procedure

The stepwise analytical procedure, which assumes about 10% total Fe in the sample, is as follows.

(1) Pulverize the glass to a free-flowing powder (mesh size was not determined) in a Brinkmann vibratory mill with an agate container and balls; avoid using Fe-bearing components. Keep the time for pulverization to a minimum to avoid possible oxidation of the Fe^{II} in the glass.

(2) Weigh, to 0.1 mg, 10–30 mg of the pulverized sample into a polystyrene vial (typically 1 in diameter and 3 in high).

(3) Add 100 μl of 0.85 mol dm^{-3} ammonium metavanadate solution (0.3 g of NH_4VO_3 dissolved in 1 ml of concentrated H_2SO_4 + 2 ml of H_2O).

(4) Add 500 μl of concentrated (95–98%) sulfuric acid (H_2SO_4).

(5) After swirling to slurry the glass into the mixture, cautiously add, dropwise, 1000 μl of concentrated (48–51%) hydrofluoric acid (HF). The solution will heat up and effervesce as the glass dissolves.

(6) When dissolution is complete, add 20 ml of saturated boric acid solution (about 6.5 g of H_3BO_3 in 100 ml of H_2O).

(7) Transfer an aliquot (typically 200 μl) containing 20–50 μg of total Fe into a second container.

(8) Add 20 ml of buffered Ferrozine solution {prepared by diluting the following to 1000 ml: 50 ml of pH 5 buffer [270 g of sodium acetate trihydrate ($CH_3COONa \cdot 3H_2O$) and 60 ml of glacial acetic acid (CH_3COOH) diluted to 1000 ml] and 50 ml of 1% Ferrozine [3-(2-pyridyl)-5,6-bis(4-phenylsulfonic acid)-1,2,4-triazine] (1 g of Ferrozine dissolved in 100 ml of H_2O)}.

(9) After 10 min, measure the absorbance of the solution in a 1 cm cuvette at a wavelength of 562 nm to determine the Fe^{II} content.

(10) Dissolve about 5 mg of solid ascorbic acid ($C_6H_8O_6$) in the remaining solution and allow the colour to develop for about 2 mins.

(11) Measure the absorbance at 562 nm to determine the total Fe content.

Matched 0.01 mol dm^{-3} ammonium iron(II) sulfate and ammonium iron(III) sulfate solutions were prepared for the validation studies. These solutions were made up in 0.1 mol dm^{-3} sulfuric acid to help retard the oxidation of Fe^{II}.

Comments

The aliquots of the dissolved glass, which contain concentrated acids, should be kept as small as is reasonable and must not exceed the capacity of the buffer added. A pH of 5–9 is essential for proper colour formation.

Table 1 Composition of glass frit 165[13]

Component	Content (% m/m)
SiO_2	68
B_2O_3	10
Na_2O	13
Li_2O	7
MgO	1
ZrO_2	1

Also, in order to ensure quantitative preservation of the Fe^{II}, the vanadate should be approximately equivalent to the Fe^{II} expected in the sample. A large excess of vanadate causes the generation of excess of Fe^{II} and drifting readings, as discussed later.

Because Ferrozine detects very small concentrations of Fe, trace amounts of Fe in the reagents or apparatus may cause high blanks, high results or irreproducible results. Vials and pipette tips should not be reused.

Results and Discussion

Validation of the Method

Glass standards with known Fe^{II} and Fe^{III} contents cannot be reliably prepared. Therefore, validation of the method was carried out by analysing ammonium iron(II) sulfate and ammonium iron(III) sulfate solutions spiked into an Fe-free glass frit. The composition of the frit, which was also used in other aspects of the glass programme,[13] is given in Table 1.

The Fe^{II} and/or Fe^{III} solutions and the spiked glass frit were used to study the recovery of Fe^{II}. The typical results, presented in Table 2, demonstrate the effectiveness of the addition of vanadate in preserving Fe^{II}.

Further confirmation that the recovery of Fe^{II} was improved by including vanadate in the procedure is provided by the results shown in Table 3. Experimental glass samples were analysed both with and without the addition of vanadate. All samples without vanadate showed a negative bias.

The results presented in Table 4 show that the addition of vanadate preserved the Fe^{II} in the H_2SO_4–HF solutions used for dissolution for at least 5 d. These samples were stored in closed vials in air. These observations agree with those of Wilson,[4] who reported that it was possible to leave dissolved samples in air for up to 72 h to attain dissolution, without loss of Fe^{II}.

Precision, Accuracy and Range

The Fe^{II} : Fe^{III} ratios obtained using the proposed method were compared with those obtained with Mössbauer spectroscopy by Karraker[3] and by Hunter *et al.*[11] The ratios determined with the two methods agreed well.

Precision and accuracy values are given in Table 5. The relative standard deviation was less than 5% for three or more determinations. The relative accuracy, from the ammonium iron(II) sulfate and ammonium iron(III) sulfate spike studies, is also calculated to be 5%.

The range of the method is judged to be from 3 to 97% Fe^{II} in total Fe. One limitation lies in establishing the magnitude of the blank value. It is shown in Table 2 that the results for individual ammonium iron(II) and ammonium iron(III) salts were within 3% of the values expected for the pure salts.

Table 2 Validation with ammonium iron(II) sulfate and ammonium iron(III) sulfate solutions

Spike	Frit	Vanadate	Fe^{II} in total Fe (%)		Reagents added*
			Expected	Found	
Fe^{II}	No	Yes	100	96.5	None
Fe^{III}	No	Yes	0	2.0	None
1:1†	No	Yes	50	49.2	None
1:1	No	No	50	48.1	None
1:2	No	No	33	32.0	None
1:1	No	Yes	50	51.5	H_2SO_4, HF, H_3BO_3
1:1	No	No	50	44.7	H_2SO_4, HF, H_3BO_3
1:2	No	No	33	28.6	H_2SO_4, HF, H_3BO_3
1:1	Yes	Yes	50	48.1	H_2SO_4, HF, H_3BO_3
1:1	Yes	No	50	41.9	H_2SO_4, HF, H_3BO_3
1:2	Yes	No	33	28.1	H_2SO_4, HF, H_3BO_3

* In addition to buffered Ferrozine and ascorbic acid for colour formation.
† Mixtures are Fe^{II} : Fe^{III}.

Table 3 Analysis of glass samples with and without the addition of vanadate

Glass No.	Fe^{II} in total Fe (%) With vanadate	Fe^{II} in total Fe (%) Without vanadate	Relative bias (%)
1	76.9	63.4	−17
2	32.0	28.1	−12
3	12.5	6.1	−51
4	52.4	42.2	−19
5	32.4	28.1	−13
6	43.8	39.4	−10
7	51.0	46.5	−9
8	90.3	79.5	−12

Table 4 Effect of time on glass dissolution

Sample	Vanadate	Time since dissolution	Fe^{II} in total Fe (%)
Fe^{II} : Fe^{III} (1 : 1) with glass frit	Yes	0	48.1
	Yes	1 d in air	50.2
	Yes	5 d in air	52.6
Glass No. 1	No	0	63.4
	No	2 h in air	49.3
Glass No. 9	Yes	0	18.3
	Yes	2 d in air	18.1
Glass No. 10	No	0	16.0
	No	2 h under N_2	16.0

Table 5 Precision of measurements

Set	Fe^{II} in total Fe (%) Results	Mean	Standard deviation
1	17.2		
	20.8		
	17.6		
	18.5*	18.5	±1.6
2	18.3		
	18.9		
	19.1	18.8	±0.4
3	17.6		
	18.8		
	18.3	18.2	±0.6
	Average:	18.5	±0.9

* Analysed 2 d later.

The effect of other redox-sensitive elements on the method was not systematically studied. Ferrozine itself has few interferences, but the effect of other oxidizable species on the method is open to question. The experimental glasses analysed here contained formate, uranium, manganese and nickel.

Limitations of the Method

The method has proved to be satisfactory for the analysis of glass samples that contain >5% Fe.[3,11] However, limitations have been encountered as discussed below.

Control of vanadate concentration

Vanadate affects the kinetics of the formation of the Fe^{II}–Ferrozine complex. Although complete colour formation in the absence of vanadate was rapid, in the presence of vanadate about 10 min were needed for full colour development. Further, a significant excess of vanadate led to drifting readings and excessive colour formation.

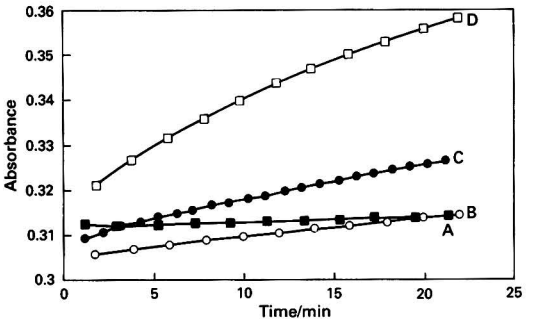

Fig. 1 Effect of vanadate on colour development. Vanadate to Fe ratio: A, 0; B, 0.5; C, 1.2; and D, 5. Ammonium iron(II) and ammonium iron(III) sulfate, 10×10^{-6} mol dm^{-3}

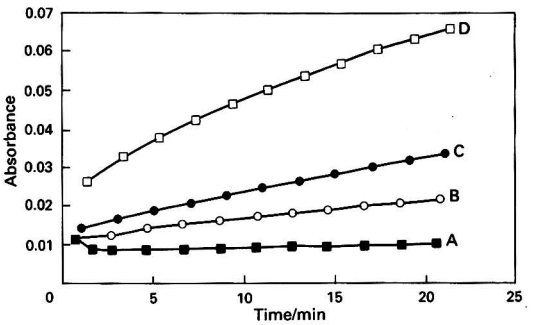

Fig. 2 Effect of vanadate on colour development. Vanadate to Fe ratio: A, 0; B, 0.5; C, 1.2; and D, 5.0. Ammonium iron(III) sulfate, 20×10^{-6} mol dm^{-3}

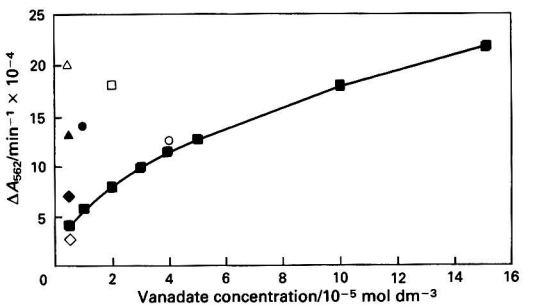

Fig. 3 Effect of vanadate concentration on rate of colour development. Total dilution of matrix [(initial volume × final volume)/aliquot]: △, 31; □, 62; ●, 125; ▲, 125 and 62; ◆, 250; ◇, 500; and ○, 2000. Line shown without matrix

The kinetic effect, and also the effect of excess of vanadate, on colour formation is shown in Fig. 1. The solution contained 1×10^{-5} mol dm^{-3} Fe^{II} and 1×10^{-5} mol dm^{-3} Fe^{III}. The rate of colour development increased as the proportion of vanadate relative to Fe was increased beyond equivalence. The absorbance continued to increase beyond that corresponding to the Fe^{II} in the original solution.

The V^{IV} and the Ferrozine in solution apparently slowly drive the reduction of Fe^{III} to Fe^{II}, with formation of the Fe^{II}–Ferrozine complex and the abnormal absorbances observed. This action is illustrated in Fig. 2 where the original

solution contained Fe^{III} only. The rate of colour generation increased with the amount of vanadate in the system.

Effect of glass dissolution mixture

The glass dissolution mixture consists of H_2SO_4, HF, H_3BO_3 and sometimes acid neutralizers such as NaOH or CH_3COONa at significantly higher concentrations than the Fe^{II} sought. The presence of too much of this matrix affected colour development. It was found that the method worked satisfactorily for the application described here, which involved a nominal total dilution {TD = [(initial volume) × (final volume)]/(aliquot volume)} of 1000–2000. For glasses with lower Fe concentrations, larger aliquots had to be used to attain the required sensitivity.

Absorbance values continuously drifted upward at TDs below about 500.

This behaviour is illustrated in Fig. 3, which compares the rate of colour formation in water and in dissolution mixtures at various TDs. The vanadate and Fe concentrations were approximately equal at 1×10^{-5} mol dm^{-3}.

The drifting phenomenon was attributed to an unidentified component from the dissolution matrix solution, which reduces Fe^{III}. This drift at lower TDs limits the applicability of the method.

The information in this paper was developed during the course of work done under Contract No. DE-AC09-89SR18035 with the US Department of Energy.

References

1 *The Treatment and Handling of Radioactive Wastes*, eds. Blasewitz, A. G., Davis, J. M., and Smith, M. R., Battelle Press, Columbus, OH, 1983.
2 Jantzen, C. M., and Plodinec, M. J., *J. Non-Cryst. Solids*, 1984, **67**, 207.
3 Karraker, D. G., *Adv. Ceram. Mater.*, 1988, **3**, 337.
4 Wilson, A. D., *Analyst*, 1960, **85**, 823.
5 Jones, D. R., IV, Jansheski, W. C., and Goldman, D. S., *Anal. Chem.*, 1981, **53**, 923.
6 Begheijn, L. T., *Analyst*, 1979, **104**, 1055.
7 Abe, S., Saito, T., and Suda, M., *Anal. Chim. Acta*, 1986, **181**, 203.
8 Fritz, S. F., and Popp, R. K., *Am. Miner.*, 1985, **70**, 961.
9 Close, W. P., and Tillman, J. F., *Glass Technol.*, 1969, **10**, 134.
10 Baumann, E. W., Coleman, C. J., Karraker, D. G., and Scott, W. E., 194th National Meeting of the American Chemical Society, New Orleans, LA, September 1987; Abstract ANYL-175, American Chemical Society, Washington, DC, 1987; and US Department of Energy Report DP-MS-87-18, Aiken, SC, 1987.
11 Hunter, R. T., Edge, M., Kalivretenos, A., Brewer, K. M., Brock, N. A., Hawkes, A. E., and Fanning, J. C., *J. Am. Ceram. Soc.*, 1989, **72**, 943.
12 Stookey, L. L., *Anal. Chem.*, 1970, **42**, 779.
13 Soper, P. D., Walker, D. D., Plodinec, M. J., Roberts, G. J., and Lightner, L. F., *Am. Ceram. Soc. Bull.*, 1983, **62**, 1013.

Paper 1/05379E
Received October 22, 1991
Accepted December 18, 1991

Conductimetric and Spectrophotometric Determination of the Volatile Acidity of Wines by Flow Injection*

Flávio Guimarães Barros and Matthieu Tubinot
Instituto de Química, Universidade Estadual de Campinas, CP 6154, 13081 Campinas, São Paulo, Brazil

Usual methods for the determination of the volatile acidity of wines are relatively slow, as about 40 min are necessary to perform one analysis. In this work, a method was developed which provides results in a much shorter time. About 60 analyses can be performed in 1 h. The conductimetric analysis consists of the injection of the wine sample into a de-ionized water stream which then flows past a poly(tetrafluoroethylene) membrane separator. The acetic acid diffuses through the membrane into another water stream that passes through a conductivity cell. The spectrophotometric method is similar. The acetic acid diffuses into a stream of Bromocresol Purple solution, at pH 7.0, which passes through a flow cell in a spectrophotometer set at 540 nm. For comparison, analyses were also carried out by the method of Jaulmes.

Keywords: *Flow injection; volatile acidity; wine; conductimetry; spectrophotometry*

Fonzès-Diacon and Jaulmes[1] defined volatile acidity for wines as: 'The volatile acidity is the assembly of the fatty acids of the acetic series that are in the wine. The lactic and succinic acids and also carbonic acid and the free and combined sulfurous anhydride are excluded from the volatile acidity'. The most recent official definitions are usually very close to this concept.

The known methods for the determination of volatile acidity are based on distillation processes. Among these methods the more usual ones are those of Duclaux,[2] Ferré,[3] Jaulmes[4] and the Cash-Still method.[5] All these involve distillation and are slow, in addition to being subject to a variety of errors.

The first method is essentially an ordinary distillation whereas the other three are steam distillations. The method of Jaulmes, however, involves use of a column containing a helicoidal band of inox (stainless steel) screen to avoid distillation of non-volatile acids such as succinic and lactic acids. In all these methods the distilled acid is titrated with standard NaOH solution, after which it is necessary to carry out a titration with I_2 to determine the concentration of SO_2 that must be subtracted from the result obtained in the NaOH titration.

Flow injection (FI),[6] which is essentially the introduction of a sample into a solution stream continuously passing through a detector, is a very important methodological innovation in analytical chemistry, which is customarily characterized by simple chemical processes, low-cost apparatus, easy manipulation and ability in yielding results that are usually of good quality. The use of an FI system, with a gas-diffusion membrane,[7] to separate volatile acids from wine, allows very good quality results in a rapid process. About 60 (spectrophotometric) or 80 (conductimetric) samples can be analysed in 1 h.

Similar systems have been used previously to determine the volatile acidity of vinegars[8] and spoilt beer.[9]

Experimental

Materials

A standard solution of approximately 1% m/v of acetic acid (analytical-reagent grade) was prepared and titrated. Solutions of 0.02, 0.04, 0.06, 0.08 and 0.10% m/v in acetic acid were obtained from this solution by dilutions to 100.0 ml.

Bromocresol Purple (BCP) solution (1×10^{-4} mol dm^{-3}). Prepared by dissolving 0.27 g of BCP in 10 ml of ethanol, the volume being diluted to 500 ml with water; 50 ml of this solution were diluted to 500 ml to obtain the working solution. The pH was adjusted to 7.0 by dropwise addition of dilute NaOH solution. In order to avoid absorption of CO_2 from the air, the BCP solution was kept in a bottle protected by a tube containing $CaCl_2$–NaOH–$CaCl_2$ (respite). The solution was pumped to the FI system by another tube.

Water used in the experiments was always boiled (degassed) and de-ionized.

Apparatus

Peristaltic pump. Ismatec mp13 GJ4.

Conductimeter. Micronal Model B-331, connected to a chart recorder.

Spectrophotometer. Single-beam Carl Zeiss Model PM2D set at 540 nm, connected to a chart recorder.

Gas diffusion cell. This cell has been described previously[10] and is similar to that of van der Linden.[7]

Conductimetric cell. This has been described previously.[10]

Sampling valve. This has been described previously.[11]

Volatile acidity is expressed, in this work, as mass (g) of acetic acid in 100 ml of solution (wine).

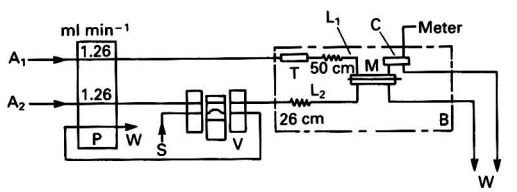

Fig. 1 Conductimetric FI manifold: T, ion-exchange resin column; P, peristaltic pump; S, sample inlet; V, sampling valve system; B, water-bath; M, diffusion cell; C, conductance flow cell; W, waste; and A_1 and A_2, de-ionized water streams

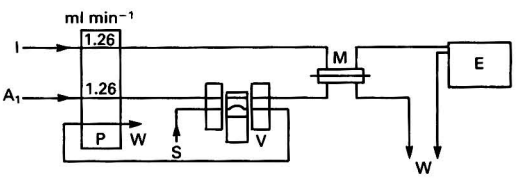

Fig. 2 Spectrophotometric FI manifold: P, peristaltic pump; S, sampling inlet; V, sampling valve system; M, diffusion cell; E, spectrophotometer; W, waste; A_1, de-ionized water stream; and I, BCP solution stream

* From the M.Sc. Thesis of F. G. B.

† To whom correspondence should be addressed.

Methods

Conductimetric

A schematic flow diagram for the conductimetric method is shown in Fig. 1. The injected sample (S), de-gassed wine, is combined with the de-ionized water carrier stream (A_1), pumped at a flow rate of 1.26 ml min^{-1}, and is passed through the coil L_2 kept in a temperature-controlled bath. In the diffusion cell (M), acetic acid and other volatile components of the wine diffuse into another de-ionized and de-gassed water stream, which passes through the conductimetric cell (C). In order to guarantee de-ionization of the water stream A_2, an additional ion-exchange resin treatment is carried out in a column (T) introduced into the system. The temperature control of the streams A_1 and A_2 is performed in the coils L_1 and L_2. The diffusion (M) and conductimetric cells (C) are also temperature controlled by the bath B, which is simply a circulating tap water-bath. The temperature (25 °C) was kept constant within ±0.5 °C or less during the entire day.

Spectrophotometric

The flow system used for the spectrophotometric analysis is shown in Fig. 2. It is similar to that used for the conductimetric analysis. The ion-exchange column and water-bath are not necessary, and the detector is a spectrophotometer set at 540 nm. The stream A_2 carries the BCP (1×10^{-4} mol dm^{-3}) solution.

Results and Discussion

Flow rates of the donor and acceptor streams were adjusted at 1.26 ml min^{-1} as a function of the height of the signal, relative standard deviations and frequency of analysis. The same situation was found to be adequate for the spectrophotometric and conductimetric methods.

The optimum concentration for BCP was found to be 1×10^{-4} mol dm^{-3}, at 540 nm, with the pH of the acceptor stream adjusted to 7.0. Other acid–base indicators were tested, such as Bromothymol Blue in an aqueous solution adjusted to pH 8.0. However, the results obtained were invariably higher than expected.

In both the spectrophotometric and conductimetric methods, many different sampling loops (the volume of the loop is the volume of sample injected by the valve), of various materials, volumes and internal diameters were tested, as retention of acetic acid on the walls of the loops was observed. This phenomenon was responsible for an increase in the peak height of the decreasing calibration graph.[8] As a complete study of the materials, sizes and diameters of the loops would be an exhaustive task, an empirical selection was made. However, special attention had to be paid to the choice of the size and material of the sampling loops for initiating either of the two methods.

In this work, it was empirically established that either a polyethylene loop (volume 120 µl; 0.8 mm i.d.) or a poly(tetrafluoroethylene) (PTFE) (volume 62 µl; 0.9 mm i.d.) can be used in the conductimetric method without significant interference from retained acetic acid. For the spectrophotometric method, a polyethylene loop (volume 240 µl; 1.6 mm i.d.) afforded the best results.

In order to minimize the influence of the retention of the acetic acid in the loop, air was passed through it after each sampling.

Carbon dioxide must be eliminated from samples before performing the analysis, as the gas diffuses through the PTFE micro-porous membrane, enhancing the resulting signal. This elimination is easily performed by subjecting the wine sample to low pressure, for about 10 min, with a water aspirator vacuum pump.

As wines usually contain SO_2 and sulfite it is necessary to oxidize these species to sulfate. Some drops (about 5) of H_2O_2, 0.5 volumes in about 10 ml of sample, are sufficient. The H_2O_2 must not be more concentrated than this, otherwise ethanol will be oxidized to acetic acid, with a consequent increase in the values obtained.

A typical FI profile for the conductimetric method is shown in Fig. 3. The FI profile for the spectrophotometric method can be seen in Fig. 4. The calibration graphs that correspond to these profiles are shown in Fig. 5. Five wines were analysed by each method, four being the same wines in both instances.

The measurements of the concentrations can be obtained graphically or by fitting first- and second-order equations for the spectrophotometric and conductimetric methods, respectively, by using an electronic calculator. The non-linearity of the calibration graphs in the conductimetric procedure can be

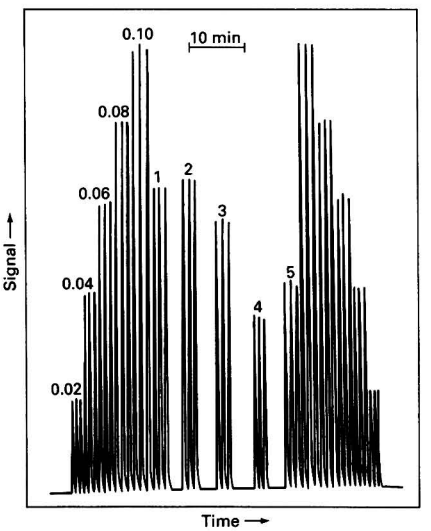

Fig. 3 Calibration and sample runs for the determination of volatile acidity (conductimetric system). From left to right: triplicate signals for acetic acid standards (0.02, 0.04, 0.06, 0.08 and 0.10 g of acetic acid per 100 ml of solution); triplicate signals for wines; standards in the reverse order. Polyethylene sampling loop, 120 µl (0.8 mm i.d.)

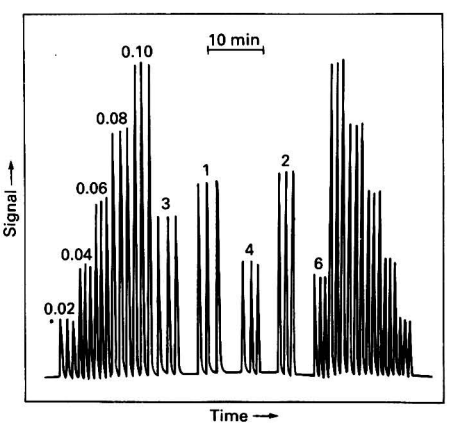

Fig. 4 Calibration and sample runs for the determination of volatile acidity (spectrophotometric system). From left to right: triplicate signals for acetic acid standards (0.02, 0.04, 0.06, 0.08 and 0.10 g of acetic acid per 100 ml of solution); triplicate signals for wines; standards in the reverse order. Polyethylene loop (240 µl; 1.6 mm i.d.)

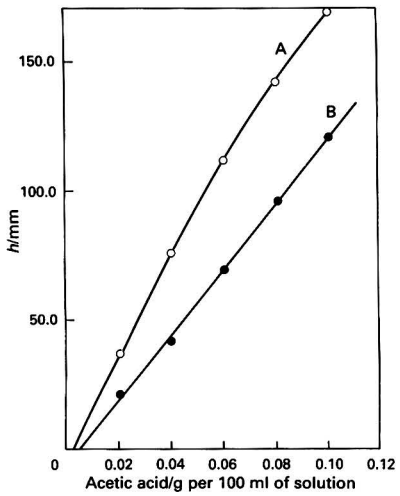

Fig. 5 Calibration graphs for the determination of volatile acidity. Details as in Figs. 3 and 4. h = Peak height in millimetres. A, Conductimetric and B, spectrophotometric system

Table 1 Volatile acidity of wines (g dl^{-1} acetic acid in wine) determined by the conductimetric and spectrophotometric FI systems and the method of Jaulmes[4]

	Conductimetric		Spectrophotometric	
Sample	Lo_1* $\sigma = \pm 0.002$§ (% m/v)	Lo_2†	Lo_3‡ $\sigma = \pm 0.002$ (% m/v)	Jaulmes $\pm\sigma$ (% m/v)
1(R)¶	0.063	0.064	0.063	0.067 ± 0.004
2(R)	0.065	0.064	0.066	0.064 ± 0.004
3(R)	0.055	0.055	0.052	0.055 ± 0.004
4(W)‖	0.034	0.033	0.038	0.037 ± 0.002
5(W)	0.041	0.042	—	0.048 ± 0.003
6(R)	—	—	0.035	0.034 ± 0.002

* Lo_1 = Loop 1, volume = 120 µl, i.d. = 0.8 mm, polyethylene.
† Lo_2 = Loop 2, volume = 62 µl, i.d. = 0.9 mm, PTFE.
‡ Lo_3 = Loop 3, volume = 240 µl, i.d. = 1.6 mm, polyethylene.
§ σ = Estimates of standard deviation.
¶ (R) = Red wine.
‖ (W) = White wine.

explained by the fact that acetic acid is a weak electrolyte and, as a consequence, conductivity is not linearly related to concentration. In the spectrophotometric method, deviations from linearity, as a consequence of the limitations of Beer's law, were observed only above an acetic acid concentration of 0.12% m/v, which is outside the working range.

In Table 1, the values for the volatile acidity obtained by the FI conductimetric and spectrophotometric methods, and also by the known method of Jaulmes[4] are reported.

The statistical t-test[9] was used to compare the results obtained by the proposed methods and also by the method of Jaulmes[4] (Table 2). Except for the t value (2.75, t_3 in Table 2), obtained when comparing the FI conductimetric result for sample 5 with the Jaulmes result, which is close to the tabulated limit (2.776),[12] no significant differences were observed between results at the 95% confidence level.

Table 2 Comparison between values obtained by the FI conductimetric, FI spectrophotometric and Jaulmes methods, using the statistical Student's t-test. Tabulated t value for the degree of freedom (v) 4 is 2.776 ($\alpha = 0.05$); $v = n_1 + n_2 - 2$ and $n_1 = n_2 = 3$ in this instance

Sample	t_1*	t_2†	t_3‡	t_4§	t_5¶	t_6‖
1(R)	0.50	0.00	1.26	0.50	0.95	1.26
2(R)	0.50	0.50	0.32	1.00	0.00	0.32
3(R)	0.00	1.50	0.00	1.50	0.00	0.95
4(W)	0.50	2.00	1.50	2.50	2.00	0.50
5(W)	0.50	—	2.75	—	2.35	—
6(R)	—	—	—	—	—	0.50

* t_i (i = 1–6) is the calculated Student's t values: t_1 = Lo_1 *versus* Lo_2.
† t_2 = Lo_1 *versus* Lo_3.
‡ t_3 = Lo_1 *versus* Jaulmes.
§ t_4 = Lo_2 *versus* Lo_3.
¶ t_5 = Lo_2 *versus* Jaulmes.
‖ t_6 = Lo_3 *versus* Jaulmes.

Comparing operationally the spectrophotometric and conductimetric methods, the former appears to be simpler as it is not necessary to control the temperature of the detector or to use an ion-exchange resin column in the flow system. However, the conductimetric method allows a slightly more rapid sampling rate (about 80 h^{-1}) than the spectrophotometric (about 60 h^{-1}) method.

The authors are grateful to Fundação de Amparo à Pesquisa do Estado de São Paulo, FAPESP, and to Conselho Nacional de Desenvolvimento Científico et Technológico, CNPq, for financial support. The authors also thank Professor Roy E. Bruns for the English revision of the manuscript.

References

1 Fonzès-Diacon, and Jaulmes, P., *Bull. Pharm. Sud-Est*, 1930, **34**, 170.
2 Duclaux, E., *Ann. Chim. Phys.*, 1874, **2**, 289.
3 Ferré, L., *Ann. Falsif. Fraudes*, 1930, **23**, 323.
4 Jaulmes, P., *Bull. Soc. Chim. Fr.*, 1937, **4**, 157.
5 *Official Methods of Analysis of the Association of Official Analytical Chemists*, ed., Horowitz, W., 11th edn., 1970, sect. 11036–11039, p. 187.
6 Růžička, J., and Hansen, E. H., in *Chemical Analysis*, ed. Winefordner, J. D., Wiley, New York, 1988, vol. 62, and references cited therein.
7 van der Linden, W. E., *Anal. Chim. Acta*, 1983, **151**, 359.
8 Tubino, M., and Barros, F. G., *J. Assoc. Off. Anal. Chem.*, 1991, **74**, 346.
9 Williams, J. G., Holmes, M., and Porter, D. G., *J. Autom. Chem.*, 1982, **4**, 176.
10 Pasquini, C., and Faria, L. C., *Anal. Chim. Acta*, 1987, **193**, 19.
11 Tubino, M., and Barros, F. G., *Quím. Nova*, 1991, **14**, 49.
12 Eckschlager, K., *Errors, Measurements and Results in Chemical Analysis*, ed., Chalmers, R. A., Van Nostrand Reinhold, New York, 1972, pp. 107–112.

Paper 1/03543F
Received July 12, 1991
Accepted November 6, 1991

Determination of Mercury(II) by Its Inhibitory Effect on the Enzymic Reaction of Ethanol Oxidation Using Flow Injection

M. Jesús Almendral Parra, Angel Alonso Mateos, Cándido Garcia de María and Leonor G. Rozas
Departamento de Química Analítica, Nutrición y Bromatología. Facultad de Química, Universidad de Salamanca, 37008, Salamanca, Spain

A flow injection procedure is described for the determination of Hg^{2+}, based on its non-competitive inhibition of the catalytic effect of alcohol dehydrogenase on the oxidation of ethanol by the coenzyme nicotinamide adenine dinucleotide. Mercury can be determined within the range 0.5–20 ppm with a relative standard deviation of 1–1.5% and at a sampling rate of 120–150 h^{-1}. Only Ag^{+} was observed to interfere.

Keywords: *Mercury(II); enzymic determination; flow injection; inhibition reaction*

Among kinetic analytical methods, in the past few decades enzymic reactions have acquired considerable importance in analytical chemistry; this is essentially because of the great selectivity (sometimes specificity) of enzymes as catalysts for a given reaction.

In some instances, enzymic activity increases or decreases owing to the presence of substances, mainly inorganic ions, that bind to the enzyme or to the substrate. This effect, both inhibitory and activating, has been exploited in analytical chemistry as a sensitive and selective method for the determination of numerous species; work in this field is of interest, both from the clinical and toxicological viewpoints.[1–5]

Also of importance is the potential of this type of determination in view of its application to the determination of metal ions at trace levels. Apart from the work of Baum and Czok[6] on the determination of Mg, that of Townshend and co-workers[7–12] is also of interest; these workers offered the first reports on the inhibition of the enzyme alcohol dehydrogenase by heavy metals.

$$NAD^{+} + C_2H_5OH \rightleftharpoons NADH + CH_3CHO + H^{+} \quad (1)$$

The optimum catalysis for the oxidation of ethanol occurs at pH 8.7, and at pH 5.5–6.5 for the reverse reaction. The determination of ethanol and acetaldehyde in different types of sample, with use of this reaction as a basis, has been the subject of several studies involving flow injection (FI).[13–15]

The present paper reports on the results obtained in the study of the inhibitory effect of Hg^{2+} on this reaction [eqn. (1)] by use of the FI technique, with a view to developing a procedure for the determination of Hg, which can be used in routine analysis. The technique was found to offer noteworthy advantages, with respect to selectivity, incubation times and sampling rate, over other procedures described for this type of determination.[7,9]

Experimental

Apparatus

A Gilson 2HP4 Minipuls peristaltic pump (Worthington, OH, USA), a rotatory injection valve of poly(tetrafluoroethylene) (PTFE) (Tecator L-100-1; Herndon, VA, USA) with six ports (three for inflow and three for outflow), and PTFE tubing of 0.5 and 0.7 mm i.d. with normalized Rheodyne tube endings (Cotati, CA, USA), were used. Linear and T-shaped connectors were made of Perspex, the T connectors being constructed with internal diameters of 0.7 and 1.0 mm.

A Unicam 1800 UV/visible Spectrophotometer, equipped with a Unicam AR-25 linear recorder and a flow cell of 38 μl and 10 mm optical pathlength in Suprasil I quartz glass (Hellma, Jamaica, NY, USA), was also used.

Reagents

Lyophilized alcohol dehydrogenase (*E.C.* 1.1.1.1). Solutions were prepared by diluting suitable amounts of the enzyme (Boehringer, Mannheim, Germany) in pyrophosphate buffer solution (pH range 7–9) containing gelatin (10 mg dl^{-1}) and ammonium sulfate (0.4 g dl^{-1}) as stabilizers.

Nicotinamide adenine dinucleotide (*NAD+*) *oxidoreductase*. This enzyme (Boehringer), at a purity of 100% was prepared in pyrophosphate buffer solution in the pH range 7.8–9.

Pyrophosphate buffer solution. Prepared from 33.4545 g of sodium pyrophosphate, 8.3647 g of semicarbazide hydrochloride, 1.5768 g of glycine, 8.7660 g of sodium chloride and 1 mol dm^{-3} sodium hydroxide (as necessary to adjust the pH to the working conditions), all in 1 l of solution.

Ethanol. Solutions, at various concentrations between 55 and 2000 ppm, were prepared from the chromatographic reagent.

Standard solutions (at 100 ppm) of Hg^{2+}, Ag^{+}, Cu^{2+}, Pb^{2+} and Zn^{2+} were prepared from analytical-reagent grade chemicals by dissolution in distilled water with a few drops of HNO_3. More dilute solutions were prepared immediately before use by appropriate dilution of the standard solutions.

Adsorption of metal ions onto glass walls

Both mercury and silver are adsorbed by glass, which could lead to errors in the determination of low concentrations of these elements. These errors can be minimized by leaving the solution in contact with the glass for as short a time as possible or by inducing saturation by maintaining a solution of equal concentration in the vessel over a certain period of time (12 h).

Procedure

In the FI scheme depicted in Fig. 1, distilled water is introduced into the carrier channel C_1, while a solution of ethanol (500 or 1000 ppm) in pyrophosphate buffer, pH 8.7, is introduced through the confluence channel C_2. The resulting solution is made to merge at a second merging point with a third solution, circulating through carrier channel C_3 formed from a mixture of enzyme (20 mg dl^{-1} or 40 mg dl^{-1}) and coenzyme (48 mg dl^{-1} or 80 mg dl^{-1}), keeping the flow rate for all solutions constant at 1 ml min^{-1}. Mercury solutions are injected (126 μl) into channel C_1. After mixing and reaction in reactor R_2 (1.25 m), the signal corresponding to the absorbance at 340 nm is recorded. Both reactors R_1 and R_2 should be thermostatically controlled in glass tubes containing water at 25 °C. The reagents circulating through C_1, C_2 and C_3 are thermostatically controlled in a water-bath at the same temperature.

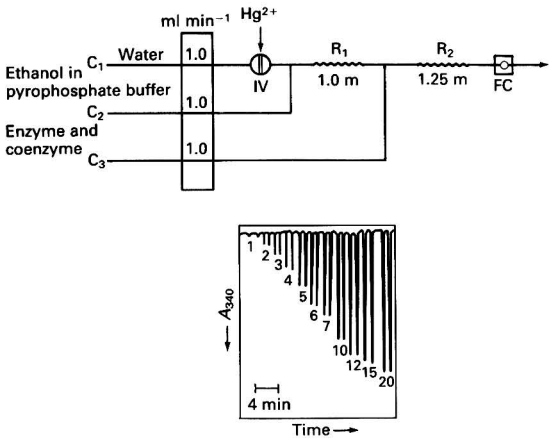

Fig. 1 FI system of optimum confluence for the determination of mercury by continuous flow (IV = injection valve and FC = flow cell) and analytical signal obtained for different concentrations of mercury (ppm)

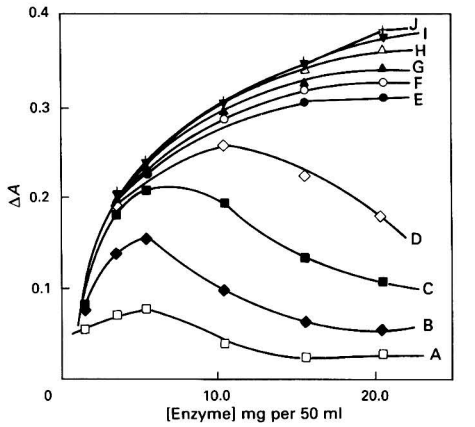

Fig. 2 Effect of concentration of enzyme for different concentrations of Hg^{II}. Ethanol, 393 ppm in pyrophosphate buffer; coenzyme, 48 mg dl^{-1}; pH, 8.7; and concentration of enzyme variable between 2 and 40 mg dl^{-1}. Mercury concentrations: A, 2.0; B, 3.0; C, 4.0; D, 5.0; E, 6.0; F, 7.0; G, 8.0; H, 10.0; I, 12.5; and J, 15.0 ppm

Results and Discussion

Design of the Flow System

The proposed flow system is shown in Fig. 1.

Solutions of Hg^{II} are introduced directly into the carrier channel containing distilled water and are made to merge with the solution of ethanol in pyrophosphate buffer in reactor R_1 and then with the solution of enzyme, coenzyme and pyrophosphate in reactor R_2. In the absence of Hg^{II}, the confluence of the three channels gives rise to a constant signal for reduced nicotinamide adenine dinucleotide (NADH), which is measured at 340 nm, induced by the oxidative enzymic conversion of ethanol into acetaldehyde in the presence of alcohol dehydrogenase. In the presence of Hg^{II}, the inhibitory effect of this species on the reaction brings about a decrease in the constant signal obtained, which is modified when the concentration of Hg^{II} injected decreases (Fig. 1).

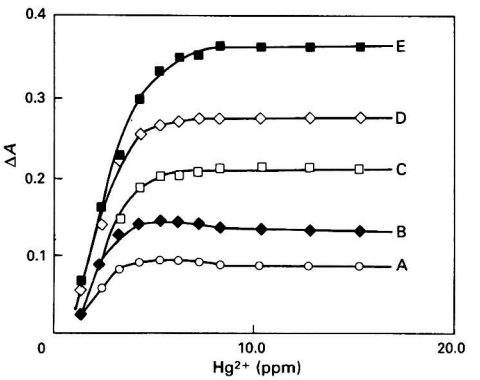

Fig. 3 Variation of increase in absorbance as a function of Hg^{II} concentration for different concentrations of ethanol. Enzyme, 20 mg dl^{-1}; coenzyme, 48 mg dl^{-1} of pyrophosphate buffer; and pH, 8.7. Ethanol concentration: A, 55; B, 118; C, 196; D, 300; and E, 500 ppm

Study of Variables

The effect of the following experimental variables on the efficiency of the inhibition was investigated within the indicated ranges: pH (7–9), concentrations of coenzyme (16.0–80.0 mg dl^{-1}), enzyme (4.0–40.0 mg dl^{-1}), ethanol (55–1000 ppm) and Hg (1–15 mg l^{-1}), length of reactor R_2 (0.5–3.0 m), injection volume (50–500 μl) and flow rates (0.5–2.0 ml min^{-1}).

The reaction will occur with greater sensitivity under the optimum conditions of the enzymic reaction, *i.e.*, at pH 8.7. This pH was accordingly chosen as the optimum value for later studies.

At a given concentration of Hg^{II} (approximately 7 ppm) and as the concentration of coenzyme rises, an increase occurs in the analytical signal ($\triangle A$). This indicates that the inhibitory effect increases in absolute values as the rate of the non-inhibited reaction increases. Additionally, for Hg concentrations below 7 ppm a decrease is observed in the signal as the concentration of coenzyme increases, because this increase favours the non-inhibited enzymic reaction, such that the increase in absorbance tends towards zero.

As can be seen in Fig. 2, for Hg^{II} concentrations above 7 ppm, on increasing the concentration of enzyme in the solution, the value of the analytical signal ($\triangle A$) also increases, which shows that the inhibitory effect becomes more pronounced (in absolute terms) as the rate of the non-inhibited reaction increases.

For each concentration of enzyme studied, a point is reached at which the increase in absorbance becomes independent of the concentration of Hg in the solution, indicating that the reaction kinetics tend towards zero order with respect to this parameter, *i.e.*, the number of active sites blocked is virtually constant, having reached an equilibrium.

For Hg concentrations below 7 ppm it can be seen that the increase in absorbance *versus* the concentration of inhibitor is not uniform, showing that, in order to obtain the maximum analytical signal (maximum inhibition), there must be an optimum concentration of inhibitor in each instance.

The slowing in the increase in absorbance, as from a given value of enzyme concentration, can be attributed to a steadily decreasing relative blockage of the active sites. This type of behaviour is consistent with a non-competitive inhibition, as was expected. This led to the choice of enzyme concentrations as a function of the Hg^{II} concentrations in the particular sample to be analysed.

The analytical signal $\triangle A$ reaches a constant value that is independent of the concentration of Hg in solution for each substrate concentration studied (Fig. 3).

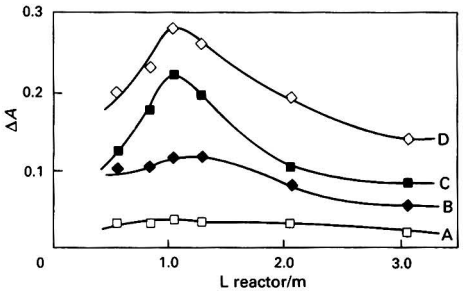

Fig. 4 Effect of reactor length for different concentrations of mercury. Enzyme, 40 mg dl^{-1}; coenzyme, 80 mg dl^{-1}; pH, 8.7; and ethanol concentration, 1000 ppm. Concentration of Hg^{II}: A, 2.0; B, 4.0; C, 5.0; and D, 6.0 ppm

The value of the inhibitory (Hg) concentration at which the maximum rate of reaction is achieved depends on the concentration of substrate and increases parallel to the increase in the latter concentration. For lower amounts of Hg^{II}, the reaction rate is proportional to the concentration of inhibitor.

In general, throughout the concentration range of Hg^{II} studied, ΔA increases parallel to the increase in substrate concentration, tending toward constant values. This shows that in each instance there is a point after which inhibition does not progress, which is the type of behaviour expected for non-competitive inhibition. The possibility of carrying out determinations of Hg at concentrations below 1 ppm prompted a study of the effect of the concentration of ethanol for lower values of enzyme (10 mg dl^{-1}) and coenzyme (24 mg dl^{-1}), a zone which, as mentioned earlier, had been observed to be more favourable for this. In no instance was a detectable analytical signal observed for Hg concentrations below 0.5 ppm.

The results obtained led to the use of the corresponding calibrations with substrate concentrations always as a function of the concentration range of Hg^{II} in the samples to be analysed.

Reactor length

For a reaction characterized by slow kinetics, reactor length, in general, increases in parallel with the residence time. However, as the reactor length is increased, dispersion also increases such that it is necessary to reach a compromise between both parameters in order to improve the sensitivity of the determination.

The results obtained (Fig. 4) point to the following: with respect to the analytical signal, this increases until an optimum length is reached because the time of reaction also increases. Thereafter, a decrease in the signal is observed, because of the predominance of physical dispersion over the reaction kinetics. These results, to a certain extent, differ from those expected, according to the literature concerning this type of reaction when carried out by classical methods.[12] In all the procedures used for the determination of metal ions, based on the inhibitory effect of enzymic reactions, long incubation times are required, thus making such determinations tedious and time consuming; this can be avoided by the flow system proposed here.

Volume of sample injected

This can affect both the magnitude of the signal and its shape. The results indicate, as expected, that the larger the volume injected, the larger the bandwidth, leading to reduced sampling rates. Moreover, on increasing the injection volume, physical dispersion decreases (less dilution) such that, by keeping the chemical variables of the system constant, the analytical signal is greater. Injection volumes of the order of 126 μl lead to a suitable analytical signal without an excessive consumption of sample and with an adequate sampling rate.

Table 1 Comparison of results

Mercury added/mg l^{-1}	Mercury found/mg l^{-1}* FI method	Dithizone method
2.1	2.1	2.0
5.2	5.3	5.2
7.4	7.5	7.3
10.2	10.1	10.1
14.3	14.4	14.2

* Mean value of three determinations.

Flow rate

This is one of the most important hydrodynamic variables to be considered in an FI determination because it governs the reaction time and the sampling rate. With respect to the analytical signal, this was found to increase with a rise in flow rate; this is logical as dilution is lower. At a certain flow rate, a tendency to reach a given constant value, due to the dilution occurring in the confluence points, is observed (1.0 ml min^{-1}).

Calibration and Determination Limits

When the concentration of Hg is lower than 8 ppm, the following is advised for use in the carrier channel C_1: de-ionized water, introducing into channel C_2: ethanol 500 ppm, and in C_3 a solution of enzyme (20 mg dl^{-1}) and coenzyme (48 mg dl^{-1}), keeping the flow rate at 1 ml min^{-1}. A helical reactor of 1.25 m and an injection volume of 126 μl are employed.

When the concentration of Hg is above 8 ppm, it is necessary to modify the concentrations of the different species, the best results being obtained when the determination is carried out under the following conditions.

De-ionized water is introduced through channel C_1 while the carrier channels C_2 and C_3 are used to introduce ethanol (1000 ppm) and a solution of enzyme (40 mg dl^{-1}) and coenzyme (80 mg dl^{-1}), respectively. The other physical and hydrodynamic characteristics of the system are kept constant.

Under these conditions it is possible to determine concentrations of Hg between 0.5 and 20.0 mg l^{-1}, the detection limit being 0.5 mg l^{-1}.

The precision of the procedure was measured by analysis of ten aliquots, each containing 5 ppm of Hg for the first calibration and 8 ppm for the second, relative standard deviations of 1.1 and 1.4%, respectively, being obtained. Under the proposed conditions it was possible to carry out between 120 and 150 determinations per hour.

The results obtained were compared with those of the standard dithizone method[16] and are summarized in Table 1. The values obtained by the proposed method can be seen to be in good agreement with those of the standard method.

Selectivity of the Procedure

There are many metal ions that, in principle, might also act as inhibitors of the enzymic reaction. In this sense, Ag, Cd, Cu, Zn and Pb ions; at different concentrations; have been described as inhibitors.

For this study, into the flow system designed as ideal for the determination of Hg, solutions of different elements were introduced at concentrations ranging from 1 to 100 ppm.

The Ag ion is an important source of interference because its inhibitory effect on the enzymic reaction is similar to that of Hg for low concentrations of Ag, being slightly lower for concentrations above 4 ppm.

For the other species studied (Cd, Cu, Zn and Pb), no inhibition reaction was observed to occur, even at concentrations of 100 ppm.

The different behaviour shown by these elements in FI shows that, compared with classical methods, this technique, owing to its kinetic characteristics (shorter times), could be a method of kinetic differentiation. The fact that the above-mentioned species, which interfere in the classical procedure, are not a source of interference here indicates that, in enzymic processes of this type, there is an authentic selection based on kinetic parameters, although other parameters cannot be ruled out.

Conclusion

The possibility of working with inhibition reactions in continuous-flow systems has been demonstrated. Although the sensitivity of the procedure is poorer than that of the discontinuous method, because one is working with shorter reaction times (unfavourable kinetic conditions for the interfering reactions), the selectivity of the method is considerably improved.

References

1 Keller, H., *Naturwissenschaften*, 1965, **39**, 109.
2 Giang, P. A., and Hall, S. A., *Anal. Chem.*, 1951, **23**, 1830.
3 Kramer, D. N., and Gamson, R. M., *Anal. Chem.*, 1957, **29**, 21A.
4 Hobom, G., and Zollner, N., *Z. Physiol. Chem.*, 1964, **335**, 117.
5 Goldstein, J. L., and Swain, T., *Physiol. Chem.*, 1965, **4**, 185.
6 Baum, P., and Czok, R., *Biochem. Z.*, 1959, **332**, 121.
7 Townshend, A., and Vaughan, A., *Talanta*, 1970, **17**, 289.
8 Townshend, A., and Vaughan, A., *Talanta*, 1969, **16**, 929.
9 Mealor, D., and Townshend, A., *Talanta*, 1968, **15**, 747.
10 Mealor, D., and Townshend, A., *Talanta*, 1968, **15**, 1371.
11 Mealor, D., and Townshend, A., *Talanta*, 1968, **15**, 1477.
12 Townshend, A., and Vaughan, A., *Talanta*, 1970, **17**, 299.
13 Ruz, J., Luque de Castro, M. D., and Valcárcel, M., *Analyst*, 1987, **112**, 259.
14 Fernández, A., Luque de Castro, M. D., and Valcárcel, M., *Fresenius' Z. Anal. Chem.*, 1987, **327**, 552.
15 Lázaro, F., Luque de Castro, M. D., and Valcárcel, M., *Anal. Chem.*, 1987, **59**, 1859.
16 Analytical Methods Committee, *Analyst*, 1965, **90**, 515.

Paper 1/02227J
Received May 13, 1991
Accepted October 22, 1991

Determination of *N*-Acetylcysteine in Pharmaceutical Samples by Flow Injection

Concepcion Sánchez-Pedreño, Mª. Isabel Albero, Mª. Soledad Garcia and Vicente Rodenas
Department of Analytical Chemistry, Faculty of Science, University of Murcia, 30071 Murcia, Spain

Two flow injection (FI) methods, involving spectrophotometric detection, are proposed for the determination of *N*-acetylcysteine (NAC). Both methods are based on the formation of a yellow complex between NAC and Pd^{II} in a medium of 1 mol dm^{-3} HCl. In the first method, which is based on the conventional FI technique, NAC is determined over the range 5×10^{-5}–5×10^{-3} mol dm^{-3}, and in the second, in which the doublet-peak FI mode is used, the working range is extended (5×10^{-5}–5×10^{-2} mol dm^{-3}). The FI methods were applied to the determination of NAC in pharmaceutical samples.

Keywords: N-*Acetylcysteine; palladium(II); flow injection; pharmaceutical samples*

N-Acetyl-L-cysteine (NAC) is a biologically active substance with a mucolytic effect,[1] shown to be effective as an antidote in cases of acetaminophen poisoning.[2] In addition, it is useful in the prevention, or reduction, of the side effects of cyclophosphamide treatment in cancer patients.[1] Studies on the stability of NAC in pharmaceuticals have shown that this compound is stable at room temperature.[3,4] *N*-Acetylcysteine has been determined by chromatographic,[5–9] spectrophotometric[10–14] and spectrofluorimetric techniques.[15] It has also recently been determined by kinetic[16,17] and flow injection (FI) methods.[18]

Two simple, fast and inexpensive methods, useful for the routine determination of the drug in pharmaceuticals and based on the reaction of NAC and $PdCl_2$ and involving FI, are described in this paper. The peak height and width are used as quantitative parameters.

Experimental

Apparatus

The FI system consisted of a Gilson HP4 peristaltic pump (Worthington, OH, USA), an Omnifit injection valve (New York, USA), a Hellma 18 μl flow cell (Jamaica, NY, USA) and a Pye Unicam spectrophotometer (Cambridge, UK) as detector. Connecting tubing of 0.5 mm bore, poly(tetrafluoroethylene) (PTFE) tubing and various end-fittings and connectors (Omnifit) were used. For the peak-width measurements, a gradient tube consisting of a Perspex tube of 2 mm i.d. was used.

Reagents

All chemicals were of analytical-reagent grade and the solutions were prepared with doubly distilled water.

Stock NAC solution (0.1 mol dm^{-3}). Prepared by dissolving 1.6319 g of NAC (Merck, Darmstadt, Germany) in 100 ml of water and storing at approximately 4 °C in a dark bottle. Working solutions of NAC were prepared daily by dilution of the stock solution.

Palladium dichloride standard solution (5×10^{-3} mol dm^{-3}). Prepared by dissolving 0.2216 g of $PdCl_2$ (Merck) in 5 ml of water, to which 0.5 ml of concentrated HCl had been added, by warming the mixture in a water-bath. The solution was cooled and diluted with water in a 250 ml calibrated flask, and titrated as described elsewhere.[19]

More dilute solutions were obtained by appropriate dilution with water.

Hydrochloric acid (6 mol dm^{-3}). Prepared by dilution of the concentrated acid.

Britton–Robinson buffer solutions. These covered the pH range 2.00–8.00.

FI Procedures

Use the FI manifold shown in Fig. 1(*a*). Inject 70 μl of NAC solution into 5×10^{-4} mol dm^{-3} $PdCl_2$ in a 1 mol dm^{-3} HCl stream and measure the peak height at 380 nm. Prepare a calibration graph by plotting the peak height (*h*) *versus* NAC concentration over the range 5×10^{-5}–5×10^{-3} mol dm^{-3}.

For the peak-width method, use the FI manifold shown in Fig. 1(*b*). Inject 680 μl of NAC solution, with concentrations between 5×10^{-5} and 5×10^{-2} mol dm^{-3}, into 2×10^{-4} mol dm^{-3} $PdCl_2$ in a 1 mol dm^{-3} HCl stream and monitor the absorbance at 380 nm. Obtain a calibration graph by plotting the time interval between the doublet peaks (Δt) *versus* the logarithm of the NAC concentration (ln *c*).

Determination of NAC in Pharmaceutical Samples

No sample pre-treatment was needed for these analyses. Dissolve an accurately weighed or measured volume of the pharmaceutical sample with water, up to 250 ml, in a calibrated flask. Filter, dilute the filtrate, if necessary, and analyse a suitable aliquot by the FI procedures.

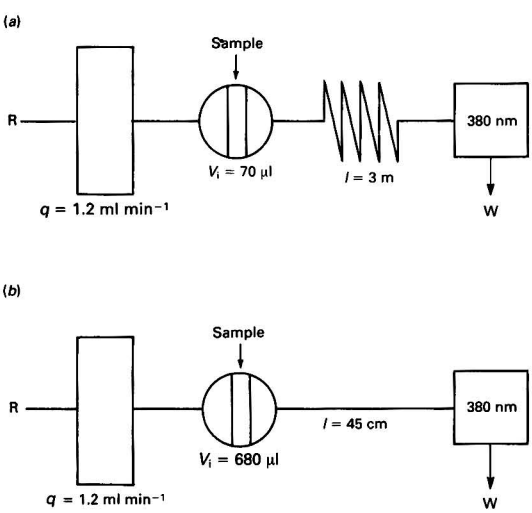

Fig. 1 FI manifolds for the determination of NAC. (*a*) Peak-height method: R = reagent solution, 5×10^{-4} mol dm^{-3} Pd^{II} in 1 mol dm^{-3} HCl. (*b*) Doublet-peak FI mode: R = reagent solution, 2×10^{-4} mol dm^{-3} Pd^{II} in 1 mol dm^{-3} HCl. V_i = volume injected (loop size); l = length of reaction coil; and q = flow rate (pump)

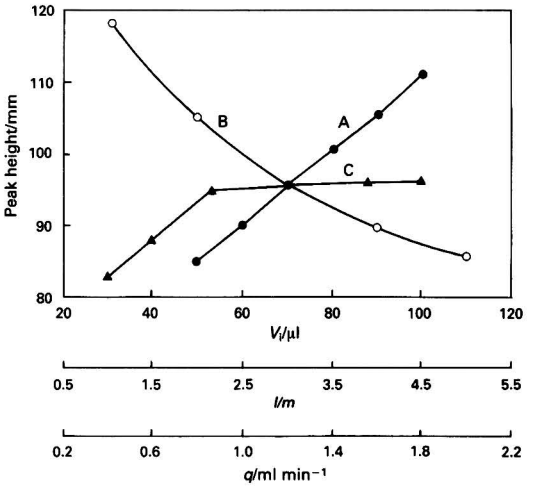

Fig. 2 Effect of: A, loop size (V_i); B, reactor length (l); and C, pumping rate (q), on the peak height. Sample injected, 2×10^{-4} mol dm^{-3} NAC

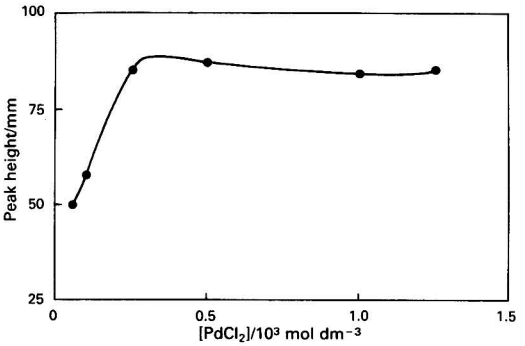

Fig. 3 Effect of Pd^{II} concentration on peak height

Results and Discussion

Palladium(II) chloride reacts with NAC to form a yellow complex.[14] In the acidic medium used in this work, it has been ascertained that the complex has a stoichiometric ratio of NAC:Pd^{II} of 2:1 and a well-defined absorption maximum at 380 nm. The NAC does not absorb at this wavelength, and $PdCl_2$ has a very low absorbance under the same experimental conditions.

The reaction between Pd^{II} and NAC has been adapted in order to develop two spectrophotometric–FI methods for determining the drug.

FI Method

The design of the manifold shown in Fig. 1(*a*) is simple. The sample is injected into the stream of $PdCl_2$ solution in 1 mol dm^{-3} HCl. The Pd^{II} forms the NAC:Pd^{II} complex, the absorbance of which is measured by means of the detector at 380 nm.

In the absence of NAC (blank), a small signal is obtained. This signal is used to pre-adjust the zero absorbance in the detector. The presence of the drug causes an increase in the analytical signal, proportional to its concentration.

The optimization of FI and chemical variables was studied in order to establish an FI method.

Fig. 2 shows the effect of the loop size, the reactor length and the flow rate on the peak height. An increase in loop size produces an increase in peak height (Fig. 2, A); however, at large injected volumes, split peaks were observed. Hence, a loop size of 70 µl was chosen.

The influence of reactor length was studied from the minimum distance possible (injection valve–detector) up to 5 m. The results (Fig. 2, B) showed that the peak height decreases as the reactor length increases. In order to confirm the optimum reactor size, different calibration graphs for NAC with different reactor lengths were produced. A 3 m reactor was selected as this provided the greatest reproducibility.

The effect of flow rate on peak height was studied over the range 0.7–2.3 ml min^{-1}. An increase in the flow rate resulted in an increase in absorbance (Fig. 2, C). However, this effect was lower between 1 and 2.3 ml min^{-1}, and hence a flow rate

From the above, the optimum values for the FI variables were as follows: injected volume, 70 µl; reactor length, 3 m (i.d. 0.5 mm); and pumping rate, 1.3 ml min^{-1}.

It is known that, in neutral or slightly acidic solution, Pd^{II} ions yield coloured complexes with a number of compounds. In strongly acidic solution, however, the reaction is much more specific for compounds containing sulfur,[20] as is found with NAC. For this reason, a strongly acidic medium was selected, the best results being obtained with 1 mol dm^{-3} HCl. The influence of the concentration of Pd^{II} was studied in the range 5×10^{-5}–1.5×10^{-3} mol dm^{-3} and a fixed concentration of NAC of 5×10^{-4} mol dm^{-3}. As can be observed from Fig. 3, constant and maximum values of peak heights are obtained with Pd^{II} concentrations up to 4×10^{-4} mol dm^{-3}. A concentration of 5×10^{-4} mol dm^{-3} $PdCl_2$ was selected, which is sufficient for the total formation of the complex in the range of the calibration graph for NAC determination.

Determination of NAC

With the described manifold and under the optimum experimental conditions (5×10^{-4} mol dm^{-3} $PdCl_2$ and 1 mol dm^{-3} HCl), a calibration graph linear between 5×10^{-5} and 5×10^{-3} mol dm^{-3} NAC was obtained. The regression equation found was $h = 104.9 \times 10^3$[NAC] + 37.6, where h is the peak height in millimetres and [NAC] is expressed in mol dm^{-3}, with a correlation coefficient of 0.9995. The relative standard deviation (RSD) for ten determinations of 4×10^{-4} mol dm^{-3} NAC was 1.4%. The detection limit was 1×10^{-5} mol dm^{-3} NAC and the sampling frequency was 45 h^{-1}.

Doublet-peak FI Mode

The most commonly used quantitative parameter in FI is the peak height. However, it is also possible to obtain useful analytical information from other properties of the response curve, but little use has been made of peak area, although its usefulness in some situations has been demonstrated.[21] The use of peak width as a quantitative parameter in FI was demonstrated by Růžička *et al.*[22] and has been applied by several workers.[23–26]

Doublet peaks are obtained when the operating variables are adjusted so that the injected sample material is in excess over the reagent in the centre of the reaction zone. Tyson[27,28] proposed equations relating the time interval between the peaks and the concentration of the material injected. The major advantage of this FI monitoring mode is the considerable extension of the working concentration range by several orders of magnitude. This increase is originated by the generation of an exponential concentration gradient of the sample and reagent, which is responsible for the appearance of

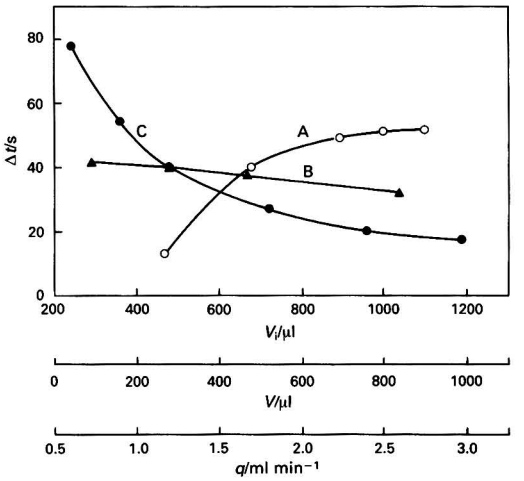

Fig. 4 Variation of Δt with: A, the volume of sample injected (V_i); B, volume of the gradient tube (V); and C, pumping rate (q). Sample injected, 5×10^{-4} mol dm^{-3} NAC

doublet peaks is related to the logarithm of the sample concentration.

One of the problems found in routine analytical determinations is that the analyte concentrations of the sample often do not fall within the limited range of concentration of the calibration graphs. As the routine determination of NAC is the aim of this work, the peak-width (separation between doublets) FI method was applied in order to extend the useful working range for this drug. Hence, a greater loop size and an injected sample concentration greater than the reagent carrier-stream concentration were used, and a short connecting line was introduced to produce the appearance of doublet peaks. A logarithmic relationship between the time interval between the doublet peaks and the concentration of the injected sample was obtained.

The effect of the experimental variables on Δt was studied. The results obtained are shown in Fig. 4. The optimum values for the FI variables are as follows: $q = 1.2$ ml min^{-1}, with which a suitable separation between the peaks without a notable decrease in the sampling frequency is obtained; $V_i = 680$ μl, the large sample volume injected ensures that doublet peaks are obtained; several tubes of 2 mm i.d. and between 0 and 40 cm long were used for the study of the influence of the gradient tube volume on Δt. The distance between the doublet peaks decreases when the volume of the tube increases, as is shown in Fig. 4, B. Hence, a tube of 0.5 mm i.d. with the minimum possible length was used to connect the injection valve and the detector. In this way, maximum separation between the peaks was obtained.

The concentrations of some reagents are decisive. Hence, the optimum concentration of $PdCl_2$ is 2×10^{-4} mol dm^{-3}, which produces well-defined doublet peaks. The acidic medium selected was HCl (1 mol dm^{-3}).

Calibration Graphs

The equation of the calibration graph for the determination of NAC is $\Delta t = 1.5\ln[\text{NAC}] + 31.8$ ($r = 0.9986$), where Δt is expressed in seconds and [NAC] in mol dm^{-3}. The equation is satisfied between 5×10^{-5} and 5×10^{-2} mol dm^{-3} NAC. Therefore, by using the peak width as a quantitative parameter, it is possible to extend the calibration graph for the routine determination of NAC by ten orders of concentration.

The RSD ($n = 10$) for 5×10^{-4} mol dm^{-3} NAC was 3.4%.

Table 1 Effect of various foreign species on the determination of 2×10^{-4} mol dm^{-3} NAC by the two FI methods

Foreign species	Maximum tolerated [species]: [NAC$^-$] molar ratio
SO_4^{2-}, NO_3^-, F^-, $C_2O_4^{2-}$, lactose	200*
CO_3^{2-}, alanine, aspartic acid, arginine, asparagine, valine, glutamine, proline, glycine, lysine, glutamic acid, leucine, saccharin, fructose, glucose, caffeine, tartrate, citrate	100
Phenylalanine, Br^-, maltose	50
Histidine, tryptophan	25
Tyrosine, starch†	10
N,N'-Diacetylcystine	6
Methionine	0.1

* Maximum molar ratio tested.
† Mass ratio.

Table 2 Determination of NAC in pharmaceutical preparations. Composition of samples. Fluimicil: 100 mg NAC, 8 mg saccharin and excipient up to 5 g; Flubiotic: 250 mg amoxycillin (trihydrate), 100 mg NAC, 4 mg saccharin and excipient up to 5 g; Fluimicil ampoules: 300 mg NAC in 3 ml of solution at pH 6.5; Rinofluimucil: 10 mg NAC, 5 mg 2-heptylamine sulfate, 0.125 mg benzalkonium chloride and excipient up to 1 ml

	NAC content		
Trade name*	FI peak-height method	Doublet-peak FI mode	Certified value
Fluimicil	19.9 ± 0.2†	20.5 ± 0.5†	20 mg g^{-1}
Flubiotic	19.8 ± 0.2†	19.6 ± 0.6†	20 mg g^{-1}
Fluimicil ampoules	98.6 ± 0.1‡	98.2 ± 0.4‡	100 mg ml^{-1}
Rinofluimucil	9.7 ± 0.3‡	9.8 ± 0.5‡	10 mg ml^{-1}

* All preparations manufactured by Zambon, Barcelona, Spain.
† mg g^{-1} (± RSD).
‡ mg ml^{-1} (±RSD).

Study of Interferents in Each Method

The effect of foreign species in both FI methods was studied. The results for the determination of 2×10^{-4} mol dm^{-3} NAC are listed in Table 1. The tolerance limit was taken as the concentration causing an error of not more than ±5% in the determination of NAC. As can be seen, the proposed methods are sufficiently selective.

Applications

The two proposed FI methods were applied to the determination of NAC in various pharmaceutical products. No sample pre-treatment was required for the determination of NAC, apart from suitable dilution. The results obtained are presented in Table 2. There are no significant differences between the certified values and those obtained by the two proposed FI methods.

The authors are grateful to the Spanish Dirección General de Investigación Científica y Técnica (DGICYT) (Project 87-0053) for financial support.

References

1 *The Pharmacological Basis of Therapeutics*, eds. Goodman, G. A., Goodman, L. S., Rall, T. W., and Murad, F., Panamericana, Madrid, 7th edn., 1989, p. 911 (in Spanish).

2 Prescott, L. F., Illingworth, R. N., Critchley, J. A., Stewart, M. J., Adam, R. D., and Proudfoot, A. T., *Br. Med. J.*, 1979, **2**, 1097.
3 van Loenen, A. C., de Jong, A., van der Meer, Y. G., and Schwietert, H. R., *Pharm. Weekbl.*, 1985, **120**, 313.
4 Vythg, A., and Timmer, J. G., *Pharm. Weekbl.*, 1985, **120**, 444.
5 Shimada, K., Tanaka, M., and Mambera, T., *Anal. Chim. Acta*, 1983, **147**, 375.
6 Toyo'oka, T., and Imai, K., *J. Chromatogr.*, 1983, **282**, 495.
7 Lewis, P. A., Woodward, A. J., and Maddock, J., *J. Pharm. Sci.*, 1984, **73**, 996.
8 Holdiness, M. R., Morgan, L., Gillen, L., and Harrison, E., *J. Chromatogr., Biomed. Appl.*, 1986, **55**, 99.
9 Johansson, M., and Westerlund, D., *J. Chromatogr.*, 1987, **385**, 343.
10 Raggi, M. A., Cavrini, V., and Di Pietra, A. M., *J. Pharm. Sci.*, 1982, **71**, 1384.
11 Talley, J. R., Magarian, R., and Sommers, E., *Am. J. Hosp. Pharm.*, 1973, **30**, 526.
12 Murty, B. S. R., Kapoor, J. N., and Kim, M. W., *Am. J. Hosp. Pharm.*, 1977, **34**, 305.
13 Groszkowski, S., and Ochocki, Z., *Farm. Pol.*, 1980, **36**, 273.
14 Jovanović, T. S., and Stanković, B. S., *Analyst*, 1989, **114**, 401.
15 Imai, K., Toyo'oka, T., and Watanabe, Y., *Anal. Biochem.*, 1983, **128**, 471.
16 Garcia, M. S., Sánchez-Pedreño, C., and Albero, M. I., *Analyst*, 1990, **115**, 989.
17 Viñas, P., Hernández Córdoba, M., and Sánchez-Pedreño, C., *Analyst*, 1990, **115**, 757.
18 Viñas, P., Sánchez, J., and Hernández, M., *Quim. Anal.*, 1990, **9**, 205.
19 Vogel, A., *Quantitative Inorganic Analysis*, Longman, London, 3rd edn., 1961.
20 Akerfeldt, S., and Lovgren, G., *Anal. Biochem.*, 1964, **8**, 223.
21 Wolf, W. R., and Stewart, V. K., *Anal. Chem.*, 1979, **51**, 1201.
22 Růžička, J., Hansen, E. H., and Mosbaek, H., *Anal. Chim. Acta*, 1977, **92**, 235.
23 Pardue, H. L., and Fields, B., *Anal. Chim. Acta*, 1981, **124**, 39.
24 Olsen, S., Růžička, J., and Hansen, E. H., *Anal. Chim. Acta*, 1982, **136**, 101.
25 Stewart, K., and Rosenfeld, A., *Anal. Chem.*, 1982, **54**, 2368.
26 Tyson, J. F., *Analyst*, 1984, **109**, 319.
27 Tyson, J. F., *Anal. Chim. Acta*, 1986, **179**, 131.
28 Tyson, J. F., *Analyst*, 1987, **112**, 523.

Paper 1/04757D
Received September 13, 1991
Accepted November 19, 1991

BOOK REVIEWS

Chemometrics Tutorials

Edited by D. L. Massart, R. G. Brereton, R. E. Dessy, P. K. Hopke, C. H. Spiegelman and W. Wegscheider. *Collected from Chemometrics and Intelligent Laboratory Systems —An International Journal, Volumes 1–5.* Pp. vii + 427. Elsevier. 1990. Price $66.75; Dfl130.00. ISBN 0-444-88837-3.

This text represents a compilation of tutorial papers that have appeared in the journal *Chemometrics and Intelligent Laboratory Systems* since 1986 and cover the main subject areas of the discipline. For those not familiar with the journal the tutorial papers are for me one of the outstanding features of that publication and the book therefore represents a comprehensive tutorial-type guide to the subject presented by experienced chemometricians. The inevitable independence or stand-alone nature of each tutorial results in the book having little or no co-ordination except for a contents page and a subject index. However, each of the 27 chapters represents a concise and critical review of its particular subject but some overlap between tutorials does occur, especially in the introductory paragraphs. All of the tutorials (Chapter 27 is a review rather than a tutorial) have their own contents list, and are, in general, written in a lucid manner with the use of good worked examples. There is some variation in the level at which each of the tutorials is pitched but for the sections of particular interest to the analyst this will not cause a problem for a novice to the subject. The chapters have been roughly combined into subject groups and a general list of contents is present at the front of the book to guide the reader. I have reviewed the book very much with a bias towards the analytical chemist and so found some chapters of little direct relevance. The early chapters offer an introduction to the use of computers in the laboratory and Chapter 1, on scientific word processing, I found of particular value, with Chapter 2 on LIMS infrastructure being undoubtedly of interest to many analysts. The following five chapters take the reader deeply into expert systems and computer programming describing the Dendral project and the use of PROLOG. This latter subject covered in Chapters 6 and 7 will be of value to those interested in expert systems. For the analytical chemist the real interest in the book starts with Chapters 8–11 on experimental design and optimization with tutorials on ANOVA, factorial design, and simplex with two specific tutorials (Chapters 10 and 11) on applications in HPLC. The next two tutorials (or chapters) address the area of signal processing, whilst Chapter 14 focuses on sampling theory. The final group of chapters (15–26) offer the reader a substantial literature base in multivariate and related methods. These chapters vary in style, length and mathematical regime but cover all the techniques widely used including principal component analysis, correspondence factor analyses and spectral map analysis with Chapter 19 offering a good comparison between these methods. Regression techniques are represented in detail along with projection techniques, with the final few chapters describing the use of multivariate techniques in the area of geoscience. The final chapter is a review of 'fuzzy theory' but it will not assist those readers confused by the extensive subject coverage given in the preceding 26 chapters!

The book represents an excellent source of information for a wide range of chemometric techniques of great relevance to any analytical chemist. However, the text could not be described as easy bed-time reading, but each tutorial, when taken in its own right, represents a complete tutorial on its specific subject area. For the analyst who wishes to see how chemometric techniques might be applicable to his or her work then this collection of tutorials represents a good starting place.

Stephen J. Haswell

Multielement Detection Systems for Spectrochemical Analysis

By Kenneth W. Busch and Marianna A. Busch. *Volume 107 in Chemical Analysis. A Series of Monographs on Analytical Chemistry and Its Applications.* Pp. xxi + 688. Wiley-Interscience. 1990. Price £70.00. ISBN 0-471-81974-3.

Multi-element detection systems for optical spectroscopy have historically been the recipients of considerable research effort. A large variety of instrument systems has appeared, each designed to provide multi-element determinations based on a variety of sources, optics, detectors and spectroscopic principles. The stated purpose of this book is a unified treatment of the fundamental principles necessary for understanding this spectroscopic instrumentation and a comprehensive discussion of modern image detectors. It is intended for the graduate student in analytical spectroscopy and researchers in other disciplines.

The book is divided into three sections. After an introductory chapter, Chapters 2–7 are devoted to the principles of optics, diffraction, spectrographs and spectrometers, and Hadamard and Fourier transform spectroscopy. Chapters 8–11 focus on photographic, photoelectric and solid-state detectors. Finally, Chapters 12–15 take a look at multi-element detection systems. Chapter 12 provides an interesting discussion on the philosophy of instrument development. Chapter 13 then provides a brief overview of atomic emission, absorption and fluorescence spectrometry with consideration of the possible dominant noise sources. Chapters 14 and 15 review various commercial and research detection systems under the heading of transform and non-transform systems, respectively.

The authors have succeeded very nicely in their stated purpose for this book. They have drawn together, in a single text, the many fundamental areas that are necessary for research in the field of analytical spectroscopy. The book is very readable, serves as an excellent reference source for research in the field, and provides numerous historical accounts, which provide an interesting perspective. The principles of optics, diffraction, spectrometers and interference are presented in a very understandable manner without a blizzard of mathematical equations. The review of solid-state detectors and underlying principles is very detailed. Radiation sources are discussed only in the abstract as sources of various limiting noises. The effects of these types of noise are then considered with respect to the instrumental design.

The coverage of transform spectrometric methods is particularly well done. The groundwork is well laid with chapters on interference, masked spectrometers and Fourier transform spectroscopy. Chapter 14 then presents a detailed review of the state-of-the-art and the limitations of the field as based on consideration of signal-to-noise ratios arising from the various sources.

The one weakness I found with the book was in the review of non-transform detector systems (Chapter 15). Compared with the preceding chapter on transform spectrometric systems, the review of non-transform systems seemed rushed and did not provide the same detailed coverage. Of course, non-transform systems cover a much wider field of designs and sources. The same depth of coverage would have made for a longer book (which is already 688 pages). It is regrettable, however, that the authors did not provide a more thorough

evaluation of these systems, especially since they did such a superb job on transform methods. Still, the strengths of this book far outweigh this weakness. It is a welcome addition to any spectroscopists' library.

J. M. Harnly

DECHEMA Corrosion Handbook. Volume 6. Acetic Acid, Alkanols, Benzene and Benzene Homologues, Hydrogen Chloride

Edited by Dieter Behrens. Pp. ix + 368. VCH. 1990. Price DM775.00 and £286.00 (Single volume price); DM645.00 and £238.00 (Subscription price). ISBN 3-527-26657-7 (VCH Verlagsgesellschaft); 0-89573-627-6 (VCH publishers).

Having reviewed earlier volumes in this series, this latest contribution maintains the standards set by the editors. For new readers, the editors' aims are to review the effects of corrosive media on metallic materials, non-metallic inorganic materials, organic materials, and materials with special properties, and to provide answers to the questions designers, corrosion specialists and others want. Considerable detail is given so that questions beyond the behaviour of a material under consideration can be answered, and possible protective measures and the conditions under which a less resistant material will give satisfactory service can be considered.

Volume 6 commences with 175 pages devoted to acetic acid (the remaining sections on alkanols, benzene and benzene homologues, and hydrogen chloride are each around 50 pages long). The interaction of acetic acid, from vinegar to glacial, with different materials is preceded by an interesting and detailed account of the various industrial procedures for preparing acetic acid. I was intrigued to observe that the reference numbers began sequentially but soon numbers above 762 appeared and thus felt the urge to try a minor detective-type investigation. A survey of the 848 references revealed that only two before reference 763 were to work done after 1978. I thus deduced that this chapter was originally written around 1979, and as the latest reference is to 1988, was extended about ten years later, but without altering the original reference numbering. As the later information does not, unlike research papers, modify the earlier conclusions the insertions are either new data or amplify the existing data, and consequently the narrative reads smoothly.

Formic acid, also as a special topic, and the alkanecarboxylic acids (propionic and higher acids) were covered in Volume 4, and hence the account of the carboxylic acids is now complete.

Volume 4 also included the polyols, and now the addition of the monohydric alcohols would make the alkanol story complete, except that methanol is only here mentioned occasionally for comparison: perhaps it will be discussed in a future volume. Here, mainly ethanol, propanol and butanol are described, including air–alcohol mixtures, aqueous mixtures and the addition of small amounts of HCl to the latter to achieve passivation. The effect of these and other mixtures on stress corrosion cracking and on polymers and resins is also reported. The latest references are in 1986.

Hydrochloric acid was reported in Volume 5 and now hydrogen chloride gas completes this story. The value of this chapter, to my mind, is the detail provided for dry hydrogen chloride (gas and liquid), which does not attack many metals and alloys, and the harmful effects of trace amounts of moisture. Under the latter circumstances the need to keep temperatures above the dew-point of the system is stressed, to avoid corrosion. Suitable coatings and linings are also described. As with the acetic acid chapter this one appears to have been written some years ago but then updated with references up to 1989.

The chapter on Benzene and Benzene Homologues is the first in this series dealing with aromatic materials. Pure benzene does not attack most metals, but with technical-grade or crude benzene, particularly if sulfur is present, attack can occur. Benzene is frequently the most aggressive agent of the aromatic hydrocarbons towards organic materials. It is thus useful to learn which resins and other synthetic materials are resistant to, or swell in, benzene and its homologues. Interestingly the earliest reference is 1970 and the latest 1987.

This volume of the DECHEMA Corrosion Handbook is therefore recommended, and necessary if you (or more likely your library) have previous volumes, as it completes the survey of the corrosive effects of acids and alcohols.

T. R. Griffiths

CUMULATIVE AUTHOR INDEX

JANUARY–MAY 1992

FOURTH SYMPOSIUM ON KINETICS IN ANALYTICAL CHEMISTRY (KAC '92)

September 27-30, 1992
Erlangen, Germany

You are cordially invited to participate in the 4th Meeting on Kinetics in Analytical Chemistry (KAC). This conference is intended to continue the series of KAC meetings which started in Cordoba, Spain (1983) and then Preveza, Greece (1986) and Cavtat, Yugoslavia (1989).

The meeting will be particularly important to all scientists involved in kinetic techniques in analytical chemistry and will provide a forum where interesting and useful applications of kinetics can be reported and discussed. In addition to keynote lectures there will be poster sessions and a social programme for delegates and their guests.

The scientific programme will include the following themes:

Kinetic determination of substances because of their catalytic or inhibitory effect
Differential rate methods
Electrochemical methods (e.g., electrocatalysis and chemically modified electrodes)
Flow methods (e.g., flow injection)
Chromatographic methods
Chemical and biochemical sensors
Applications of luminescence
Kinetics in pharmaceutical analysis
Instrumentation
Environmental

Scientific Committee:

Professor K. Cammann (*Munster, Germany*)
Professor U. Nickel (*Erlangen, Germany*)
Professor M. D. Perez-Bendito (*Cordoba, Spain*)
Professor H. A. Mottola (*Stillwater, USA*)
Professor H. L. Pardue (*West Lafayette, USA*)
Professor G. Werner (*Leipzig, Germany*)

Local Organizers:

Professor Dr. U. Nickel (*Erlangen*)
Mrs. B. Thormann (*Erlangen*)

Further information can be obtained from the following address:

Professor Dr. Ulrich Nickel, Institute of Physical and Theoretical Chemistry, Egerlandstrasse 3, D-W-8520 Erlangen, Germany.

Telephone: +49 9131 857334
Telefax: +49 9131 858307

The KAC '92 meeting is held in cooperation with the "Fachgruppe 'Analytische Chemie' in der Gesellshaft Deutscher Chemiker".

The XXVIII Colloquium Spectroscopicum Internationale

will be held in

The University of York, United Kingdom
June 29–July 4, 1993

This traditional biennial conference in analytical spectroscopy will once again provide a forum for atomic, nuclear and molecular spectroscopists worldwide to encourage personal contact and the exchange of experience.

Participants are invited to submit papers for presentation at the XXVIII CSI, dealing with the following topics:

Basic Theory, Techniques and Instrumentation of—

Computer Applications and Chemometrics
Laser Spectroscopy
Atomic Spectroscopy (Emission, Absorption, Fluorescence)
Electron Spectroscopy
Gamma Spectroscopy
Mass Spectrometry (Inorganic and Organic)
Methods of Surface Analysis and Depth Profiling
Molecular Spectroscopy (UV, VIS, IR)
Mössbauer Spectroscopy
Nuclear Magnetic Resonance Spectrometry
Photoacoustic Spectrometry
Raman Spectroscopy
X-ray Spectroscopy

Applications of Spectroscopy in the Analysis of—

Biological Samples
Environmental Samples
Food and Agricultural Products
Geological Materials
Industrial Products
Metals Alloys

PLENARY AND INVITED SPEAKERS

The scientific programme will consist of Plenary and Invited Speakers. To date the following scientists have accepted invitations to present keynote lectures:

Plenary—
M L Gross, *Lincoln, NE*
R E Hester, *York*
C L Wilkins, *Riverside, CA*
J D Winefordner, *Gainesville, FL*

Invited—
F C Adams, *Antwerp*
F V Bright, *Buffalo, NY*
J A Caruso, *Cincinnati, OH*
B T Chait, *New York, NY*
R Donovan, *Edinburgh*
D E Games, *Swansea*
D L Glish, *Oak Ridge, TN*
P Hendra, *Southampton*
F Hillenkamp, *Munster*
J A Holcombe, *Austin, TX*
J Reffner, *Stanford, CT*
B L Sharp, *Loughborough*
M Sigrist, *Zurich*
M Thompson, *London*
J C Vickerman, *Manchester*

PRE- and POST-SYMPOSIA

In connection with the XXVIII CSI a number of symposia and workshops will be organized.

EXHIBITION

The conference will feature an exhibition of the latest instrumentation.

ACCOMMODATION

Accommodation has been reserved on campus and in the halls of residence, although hotel accomodation in York will be available if desired.

SOCIAL PROGRAMME

The scientific programme will be punctuated with memorable social events and excursions of scientific, cultural and tourist interest. The social programme is open to all participants and accompanying persons.

For further information contact—

THE SECRETARIAT XXVIII CSI
Department of Chemistry, Loughborough University of Technology, Loughborough, Leicestershire LE11 3TU, UK.
Telephone: +44 (0) 509 222575; Fax: +44 (0) 0509 233163; Telex: 34319.

FIRST FOLD HERE

THE ANALYST READER ENQUIRY SERVICE
For further information about any of the products featured in the advertisements in this issue, write the appropriate number on the postcard, detach and post.

FOLD HERE

THE ANALYST READER ENQUIRY SERVICE MAY'92

For further information about any of the products featured in the advertisements in this issue, please write the appropriate number in one of the boxes below.
Postage paid if posted in the British Isles but overseas readers must affix a stamp.

PLEASE USE BLOCK CAPITALS LEAVING A SPACE BETWEEN WORDS *Valid 12 months*

1 NAME

2 COMPANY

PLEASE GIVE YOUR BUSINESS ADDRESS IF POSSIBLE. IF NOT, PLEASE TICK HERE ☐

3 STREET

4 TOWN

5 COUNTY
POST CODE

6 COUNTRY

7 DEPARTMENT/
DIVISION

8 YOUR JOB TITLE/
POSITION

9 TELEPHONE NO

OFFICE USE ONLY REC'D PROC'D

FOLD HERE

Postage will be paid by Licensee

Do not affix Postage Stamps if posted in Gt. Britain, Channel Islands, N. Ireland or the Isle of Man

BUSINESS REPLY SERVICE
Licence No. WD 106

Reader Enquiry Service
The Analyst
The Royal Society of Chemistry
Burlington House, Piccadilly
LONDON
W1E 6WF
England

CA SELECTS

Analytical Chemistry

A Selects are a series of current awareness bulletins reporting on the latest research findings, patents, oks and conference proceedings in 238 different subject areas.

blished every two weeks, **CA Selects** will bring you the latest developments in your field – quickly, ncisely and inexpensively – keeping you up to date with the chemical and related scientific literature d saving you hours of time.

here are a huge number of CA Selects available that may be of interest to you – 22 on Analytical hemistry, 5 on Chromatography and 6 on Spectroscopy, as well as many others in related areas!

1992 Price Only £147.00 for 26 issues!

(N.B. Subscriptions run for twelve months from date of order.)

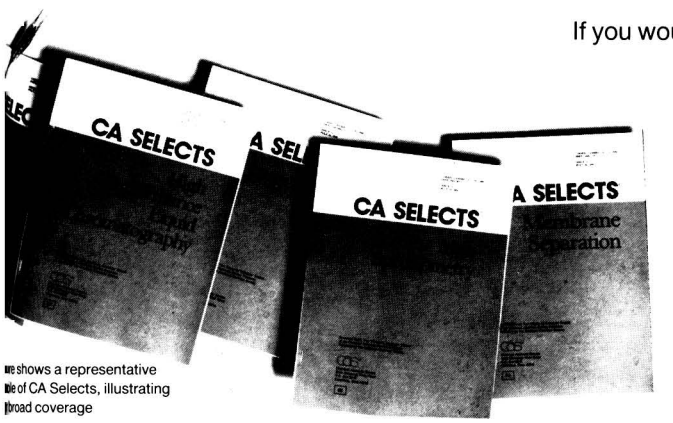

re shows a representative
le of CA Selects, illustrating
broad coverage

If you would like to see sample copies to find out how **CA Selects** can help you, simply complete and return the slip below!

We look forward to hearing from you.

For a complete listing of all **CA Selects**, tick here. ☐ We will send you a copy of our latest catalogue.

ase send me samples of the following
Selects:

_____

_____

_____

_____

_____

Name _____

Position _____

Organisation _____

Address _____

_____

_____

Tel: _____

se return to:

Secretary, Chemical Abstracts Service, Royal Society of Chemistry, Thomas Graham se, Science Park, Milton Road, Cambridge CB4 4WF, United Kingdom
+44(0)223 420066 Fax: +44(0)223 423429
e 006 for further information

CAS®

ROYAL SOCIETY OF CHEMISTRY
Information Services

ANALAO 117(5) 831–932 (1992) May 1992

The Analyst

The Analytical Journal of The Royal Society of Chemistry

CONTENTS

0003-2654(1992)5-Z

Typeset and printed by Black Bear Press Limited, Cambridge, England